Title
Sources of methane and nitrous oxide in California's Central Valley estimated through direct airborne flux and positive matrix factorization source apportionment of ground-based and regional tall tower measurements

Permalink
https://escholarship.org/uc/item/58h2d5dr

Author
Guha, Abhinav

Publication Date
2014

Peer reviewed|Thesis/dissertation

Sources of methane and nitrous oxide in California's Central Valley estimated through direct airborne flux and positive matrix factorization source apportionment of ground-based and regional tall tower measurements

By

Abhinav Guha

A dissertation submitted in partial satisfaction of the

requirements for the degree of

Doctor of Philosophy

in

Environmental Science, Policy, and Management

in the

Graduate Division

of the

University of California, Berkeley

Committee in charge:

Professor Allen H. Goldstein, Chair
Professor Dennis D. Baldocchi
Professor Robert A. Harley
Dr. Marc L. Fischer

Fall, 2014

Sources of methane and nitrous oxide in California's Central Valley estimated through direct airborne flux and positive matrix factorization source apportionment of ground-based and regional tall tower measurements

Abstract

Sources of methane and nitrous oxide in California's Central Valley estimated through direct airborne flux and positive matrix factorization source apportionment of ground-based and regional tall tower measurements

by

Abhinav Guha

Doctor of Philosophy in Environmental Science, Policy, and Management

University of California, Berkeley

Professor Allen H. Goldstein, Chair

Methane (CH_4) and nitrous oxide (N_2O) are two major greenhouse gases that contribute significantly to the increase in anthropogenic radiative-forcing causing perturbations to the earth's climate system. In a watershed moment in the state's history of environmental leadership and commitment, California, in 2006, opted for sharp reductions in their greenhouse gas (GHG) emissions and adopted a long-term approach to address climate change that includes regulation of emissions from individual emitters and source categories. There are large CH_4 and N_2O emissions sources in the state, predominantly in the agricultural and waste management sector. While these two gases account for < 10% of total annual greenhouse gas emissions of the state, large uncertainties exist in their 'bottom-up' accounting in the state GHG inventory. Additionally, an increasing number of 'top-down' studies based on ambient observations point towards underestimation of their emissions in the inventory.

Three intensive field observation campaigns that were spatially and temporally diverse took place between 2010 and 2013 in the Central Valley of California where the largest known sources of CH_4 and N_2O (e.g. agricultural systems and dairies) and potentially significant CH_4 sources (e.g. oil and gas extraction) are located. The CalNex (California Nexus – Research at the Nexus of Air Quality and Climate Change) field campaign during summer 2010 (May 15 – June 30) took place in the urban core of Bakersfield in the southern San Joaquin Valley, a city whose economy is built around agriculture and the oil and gas industry. During summer of 2011, airborne measurements were performed over a large spatial domain, all across and around the Central Valley as part of the CABERNET (California Airborne BVOC Emission Research in Natural Ecosystem Transects) study. Next, a one-year continuous field campaign (WGC 2012-13, June 2012 – August 2013) was conducted at the Walnut Grove tall tower near the Sacramento-San Joaquin River Delta in the Central Valley.

1

Through analysis of these field measurements, this dissertation presents the apportionment of observed CH_4 and N_2O concentration enhancements into major source categories along with direct emissions estimates from airborne observations. We perform high-precision measurements of greenhouse gases using gas analyzers based on absorption spectroscopy, and other source marker volatile organic compounds (VOCs) using state of the art VOC measurement systems (e.g. proton transfer reaction mass spectrometry). We combine these measurements with a statistical source apportionment technique called positive matrix factorization (PMF) to evaluate and investigate the major local sources of CH_4 and N_2O during CalNex and Walnut Grove campaigns. In the CABERNET study, we combine measurements with an airborne approach to a well-established micrometeorological technique (eddy-covariance method) to derive CH_4 fluxes over different source regions in the Central Valley.

In the CalNex experiments, we demonstrate that dairy and livestock remains the largest source sector of non-CO_2 greenhouse gases in the San Joaquin Valley contributing most of the CH_4 and much of the measured N_2O at Bakersfield. Agriculture is observed to provide another major source of N_2O, while vehicle emissions are found to be an insignificant source of N_2O, contrary to the current statewide greenhouse gas inventory which includes vehicles as a major source. Our PMF source apportionment also produces an evaporative/fugitive factor but its relative lack of CH_4 contributions points to removal processes from vented emissions in the surrounding O&G industry and the overwhelming dominance of the dairy CH_4 source.

In the CABERNET experiments, we report enhancements of CH_4 from a number of sources spread across the spatial domain of the Central Valley that improves our understanding of their distribution and relative strengths. We observe large enhancements of CH_4 mixing ratios over the dairy and feedlot intensive regions of Central Valley corresponding with significant flux estimates that are larger than CH_4 emission rates reported in the greenhouse gas inventory. We find evidence of significant CH_4 emissions from fugitive and/or vented sources and cogeneration plants in the oil and gas fields of Kern County, all of which are minor to insignificant CH_4 sources in the current greenhouse gas inventory. The CABERNET campaign represents the first successful implementation of airborne eddy covariance technique for CH_4 flux measurements.

At Walnut Grove, we demonstrate the seasonal and temporal dependence of CH_4 and N_2O sources in the Central Valley. Applying PMF analysis on seasonal GHG-VOC data sets, we again identify dairies and livestock as the dominant source of CH_4. A clear temporal dependence of emissions originating from a wetlands / Delta CH_4 source is observed while CH_4 contributions are also observed from a source originating from upwind urban and natural gas extraction activities. The agricultural soil management source of N_2O has a seasonal dependence coincident with the agricultural growing season (and hence, fertilizer use) accounting for a majority of the N_2O enhancements during spring and summers but being reduced to a negligible source during late fall and winters when manure management N_2O emissions from dairy and livestock dominate the relative distribution. N_2O is absent from the 'urban' source, in contrast to the significant contribution to the statewide N_2O inventory from vehicle emissions.

The application of greenhouse gas source apportionment using VOC tracers as identification tools at two independent sites in the Central Valley over vastly different temporal resolutions provide significant insights into the regional distribution of major CH_4 sources. Direct airborne eddy covariance measurements provide a unique opportunity to constrain CH_4 emissions in the

Central Valley over regional spatial scales that are not directly observable by ground-based methods. Airborne observations provide identification of 'hotspots' and under-inventoried CH_4 sources, while airborne eddy covariance enables quantification of emissions from those area sources that are largely composed of arbitrarily located minor point sources (e.g. dairies and oil fields).

The top-down analysis provides confirmation of the dominance of dairy and livestock source for methane emissions in California. Minor but significant contributions to methane emissions are observed from oil and gas extraction, rice cultivation and wetlands; the estimates for these sectors being either negligible (e.g. wetlands) or highly uncertain (e.g. oil and gas extraction) in the statewide inventories and probably underestimated as a proportion of the total inventory. The top-down analysis also confirms agricultural soil management and dairy and livestock as the two principal sources of N_2O consistent with the inventory, but shows that N_2O contributions attributed to the transportation sector are overestimated in the statewide inventory. These new top down constraints should be used to correct these errors in the current bottom-up inventory, which is a critical step for future assessments of the efficacy of emission reduction regulations. Particularly, measurement techniques like vehicle dynamometer emission calculations (for transportation sources), source-specific short range ground-based inverse dispersion (for dairy and livestock sources), airborne eddy covariance and airborne mass balance approach based emissions estimation (over oil and gas fields) and ground based eddy-covariance (for wetlands and agriculture sector) can be used effectively to generate direct emissions estimates for methane and nitrous oxide that help update and improve the accuracy of the state inventory.

Table of Contents

Table of Figures:

Table of Tables:

Chapter 1: Introduction

1.1   Non carbon dioxide greenhouse gases (GHGs)

The majority of greenhouse gas (GHG) emissions occurring across the globe are that of carbon dioxide which accounts for about 72 % of the total anthropogenic radiative forcing caused by greenhouse gases (2.77 Wm^{-2}) since the pre-industrial era (year 1750) (IPCC, 2007; Montzka et al., 2011). The remaining balance is attributed to non-carbon dioxide (non-CO_2) greenhouse gases such as methane (CH_4; 21 %), nitrous oxide (N_2O, 7 %), and halocarbons (< 1 %). These greenhouse gases have more significant climate change effects than CO_2 on a per-ton basis as these molecules have a higher ability to trap heat in the atmosphere relative to CO_2 described by their Global Warming Potential (GWP). The relatively long atmospheric lifetime of ~ 10 years and large infrared absorption at unique spectral wavelengths gives CH_4 a large GWP of 25 (Forster et al., 2007; Montzka et al., 2011), thus making it a potent greenhouse gas. Anthropogenic global CH_4 emissions are due to agricultural activities like enteric fermentation and manure management in livestock (Owen and Silver, 2014) and rice cultivation (McMillan et al., 2007), energy sector emissions from oil and gas operations and coal mining (USEPA, 2014), waste management (landfills and waste water treatment), and biomass burning (some of which is natural) (Smith et al., 2007; Pacala et al., 2010). N_2O has a much longer persistence in the atmosphere (~ 120 years) which results in a very high GWP of ~ 300 (Montzka et al., 2011). Agriculture is the biggest source of anthropogenic N_2O emissions since the use of synthetic fertilizers and manure leads to microbial N_2O emissions from soil (Crutzen et al., 2007; Galloway et al., 2008). Management of livestock and animal waste is another important agricultural source of N_2O, while industrial processes including fossil fuel combustion have been estimated to account for 15 % of total global anthropogenic N_2O emissions (Denman et al., 2007). Owing to its shorter lifetime than CO_2, reducing CH_4 emissions globally can have a more rapid effect on reduction of climate forcing. On the other hand, reducing N_2O emissions is critical for the long term success of climate change mitigation efforts since N_2O is removed from the atmosphere much more slowly than CH_4 (Montzka et al., 2011).

1.2   California's AB32 law

California was the first state in the nation to adopt an ambitious climate change strategy to reduce its greenhouse gas emissions when, in 2006, the Assembly Bill 32 was passed into a law formally known as the Global Warming Solutions Act of 2006. The legislature identified climate change as a serious threat to the economic well-being, public health and natural resources of the state, particularly reducing the quality and supply of water from the Sierra snowpack, causing rise in sea levels and damage to marine ecosystems, exacerbation of air quality problems, detrimental effects on industries like agriculture, wine, commercial fishing, forestry and strain on

electricity supplies in a warmer environment, besides other effects (AB32, 2006). The law requires the state to adopt regulatory and reformative measures to reduce its greenhouse gas emissions to 1990 levels by the year 2020. Besides this short term target, the noteworthy long-term goal of AB32 is to cut emissions by 80% below 1990 levels by the year 2050.

1.3   California's non-CO$_2$ Greenhouse Gas inventory

The state's main air quality regulatory agency, the California Air Resources Board (ARB), is entrusted with the responsibility and authority to create regulations to achieve the targets defined in AB32. A statewide greenhouse gas emissions inventory (CARB, 2013) is used to report, verify and regulate emissions from greenhouse gas sources. In 2011, CH$_4$ accounted for 32.5 million metric tonnes (MMT) CO$_2$-eq representing 6.2 % of the statewide greenhouse gas emissions, while N$_2$O emissions totaled 6 MMT CO$_2$-eq representing about 3 % of the greenhouse gas emissions inventory (Figures 1.1 a-b). California is the most populous state in the United States, home to one out of eight people who live in the nation with a total of 38 million people. It is also the leading agricultural state accounting for more than half of the fruits produced in the nation, and a major source of milk products and vegetables, in all generating more than \$43 billion in revenue (CASR 2011). Agriculture is the major source of non-CO$_2$ greenhouse gas emissions in the state and in the national inventory (USEPA, 2014). Nationally, CH$_4$ accounts for 9 % of the total greenhouse gas emissions inventory while N$_2$O accounts for 6 % of the emissions. The statewide greenhouse gas inventory differs from the national greenhouse gas inventory in that the CH$_4$ and N$_2$O emissions constitute a lesser fraction of total emissions even though the state's agriculture sector is so prolific. Additionally, there seems to be a discrepancy between the relative strengths in the distribution of major source categories. While CH$_4$ emissions from natural gas and petroleum systems (29 %) is significant in the national inventory, in the state inventory, the industry accounts for a much smaller fraction of less than 10 % (Figure 1.1 a). This is in spite of California being the fourth largest oil producing state in the country. On the other hand, while transportation sector only accounts for 4 % of annual N$_2$O emissions in the national inventory; this sector has a much larger contribution in the statewide N$_2$O inventory (Figure 1.1 b) accounting for 18 % of the total N$_2$O emissions.

1.4   Motivation for Current Research

ARB's accurate knowledge of greenhouse gas sources and statewide emissions is critical to the success of any climate change mitigation strategy under AB32. The greenhouse gas inventory of the ARB is a 'bottom–up' inventory which, in most cases, is based on scaling of spatially and temporally constant emission factors with activity data (e.g. number of cowheads, fertilizer sales data, oil production in barrels per day etc.). A singular emission factor based accounting approach can lead to oversimplification for large area sources with biological pathways. The emission factors for many of these sources have large uncertainties as these sources emit CH$_4$

and N_2O through biological pathways whose production and release mechanisms are inadequately understood (e.g. emissions of N_2O from farmlands) (Guo et al., 2011). Additionally, many of these emissions sources are susceptible to spatial heterogeneity (e.g. CH_4 from landfills), seasonal variability (e.g. CH_4 from wetlands and rice cultivation) or are process-dependent (dry versus wet manure management in dairies) and this adds further uncertainties to the emission factor approach. CH_4 emissions in California occur from a suite of anthropogenic sources that are primarily driven by microbially-mediated pathways like dairy and livestock operations, landfills, waste water treatment and rice cultivation that account for ~ 90 % of total CH_4 emissions (Figure 1.1 a). Emissions from major N_2O sources of agricultural soil management and livestock manure management (Figure 1.1 b) are also controlled by microbial activity that scale to a number of environmental factors like N fertilizer application rate, soil organic matter content, moisture, management practices, meteorological conditions etc. In spite of these variables, the ARB inventory still uses constant emission factors to compute emissions from these N_2O sources.

Recent 'top-down' field studies have shown observational evidence from satellite remote sensing, and in-situ measurements from tall towers and aircrafts that point towards underestimation of the 'true' CH_4 emissions in the 'bottom-up' inventory of California (Zhao et al., 2009; Wunch et al., 2009; Jeong et al., 2012a; Santoni et al., 2012; Peischl et al., 2013). Fugitive, vented and process losses of CH_4 from oil and gas production is a minor source in the current inventory (~ 3 %). However, there is a lack of adequate data from source-specific 'top-down' approaches in order to verify and validate the CH_4 inventory especially in case of emissions from the oil and gas sector. Recently, a spatially resolved oil and gas inventory developed from USEPA emission factors suggests that the ARB GHG inventory is underestimating emissions from the petroleum and natural gas production sector by 3 to 7 times (Jeong et al., 2014). Top-down inverse estimates of N_2O emissions measured in California's Central Valley predict larger emissions than those predicted by satellite-derived global emissions maps (Jeong et al., 2012b). The discrepancy of the non-CO_2 GHG emissions inventory with atmospheric measurements poses an impediment to the successful application of AB32 for regulation and development of comprehensive emissions control strategies. Therefore, this research is motivated by the need for new approaches to quantitatively assess the inventory and understand better the distribution and relative strengths of major and minor CH_4 and N_2O sources across California.

1.5 Overview of this research

In this dissertation, two fixed field site and one airborne measurement campaign were conducted in and around the Central Valley of California to investigate CH_4 and N_2O sources and emissions (Figure 1.2):

1) Bakersfield, California at the southern end of the San Joaquin Valley: California Nexus experiments – Research at the Nexus of Air Quality and Climate Change (CalNex, May 15 – June 30, 2010).

3

2) Eight unique flights covering ~ 10000 km of flight path during California Airborne BVOC Emission Research in Natural Ecosystem Transects (CABERNET, June 2011). The flights were operated from the Naval Postgraduate School airstrip in Marina, California.

3) Walnut Grove tall tower in the Sacramento - San Joaquin River Delta at the southern end of Sacramento valley and northern end of San Joaquin Valley (WGC, June 2012 – August 2013).

In all the aforementioned studies, measurements of greenhouse gases and CO were made using high precision in-situ gas analyzers based on absorption spectroscopy. At CalNex 2010, coincident gas-phase VOC measurements, serving as potential source tracers, were made using a gas chromatograph (GC) with a quadrapole mass selective detector and a flame ionization detector (Gentner et al., 2012). In the CABERNET campaign, a customized Proton Transfer Reaction Mass Spectrometer (PTR-MS), designed to make high frequency measurements of VOCs (10 Hz), was deployed on a Twin Otter aircraft along with greenhouse gas instrumentation (Misztal et al., 2014). For the year-long measurements at WGC, automated in-situ measurement of VOCs was performed using PTR-MS sampling from five different heights while greenhouse gases were sampled from three heights (Figure 4.1; Chapter 4).

In Chapter 2, I combine the half-hourly averaged measurements of greenhouse gases and ~ 50 VOCs in a unified data set and apply the source apportionment technique of positive matrix factorization (PMF) to apportion the major sources of CH_4 and N_2O impacting the measured signals. I find that while the local CH_4 signals are predominantly and expectedly apportioned to a dairy and livestock source, we do not observe any significant CH_4 contributions to the evaporative and fugitive source arising from the local oil and gas industry. I find that N_2O is apportioned into two major sources: the dairy and livestock source and the agricultural and soil management source, which is consistent with the inventory. I find a relative absence of N_2O emissions from the vehicle emission source, a finding which is in direct contrast to its significant contribution assumed in the state inventory.

In Chapter 3, I present CH_4 enhancements above background levels from seven flights and use the simultaneous observations of measured VOCs to identify the contributing sources on the ground. CH_4 enhancements are observed from dairies, landfills, oil and gas fields, natural gas cogeneration plants, rice paddy fields, biomass burning plumes and wetlands. For the first time, CH_4 fluxes are quantified using the airborne eddy covariance technique for a limited number of flight segments that include the dairy and livestock source region, oil and gas fields, and rice cultivation. I proceed to compare these fluxes with estimates from the 'bottom-up' inventory and source-specific measurements.

In Chapter 4, I analyze the Walnut Grove tall tower observations, performing PMF source apportionment on seasonally parsed unified datasets consisting of hourly averaged measurements of greenhouse gases, CO and ~ 10 VOCs over a complete annual cycle. The major sources of CH_4 and N_2O influencing the measured signals are apportioned and their relative contributions over different seasons are compared and contrasted with their distribution in the inventory. Contributions from three major sources of CH_4 are evaluated: a dairy and livestock source, a

wetlands / Delta related source and an urban and oil / gas source. For N_2O, two major sources explain the observed enhancements: an agriculture and soil management source and a dairy and livestock source, although their relative contributions depend vastly on seasonality.

In Chapter 5, I briefly summarize the results from the above-mentioned GHG data measurement and source evaluation campaigns. I pose research questions and propose future directions to bridge the data gap between top-down measurements and the bottom-up official California inventory.

1.6   References

AB32, 2006. California Global Warming Solutions Act summary document. http://www.leginfo.ca.gov/pub/05-06/bill/asm/ab_00010050/ab_32_bill_20060927_chaptered.pdf

CARB (2013), California Greenhouse Gas Inventory for 2000-2012 - by IPCC Category. http://www.arb.ca.gov/cc/inventory/data/data.htm. accessesd on September 23, 2014.

CASR (2011), California Agricultural Statistics Crop Report, 2011. created by California Department of Food and Agriculture, Sacramento, CA and United States Department of Agriculture.Crutzen, P. J., Mosier, a. R., Smith, K. a. and Winiwarter, W.: N_2O release from agro-biofuel production negates global warming reduction by replacing fossil fuels, Atmos. Chem. Phys. Discuss., 7(4), 11191–11205, doi:10.5194/acpd-7-11191-2007, 2007.

Denman, K.L., G. Brasseur, A. Chidthaisong, P. Ciais, P.M. Cox, R.E. Dickinson, D. Hauglustaine, C. Heinze, E. Holland, D. Jacob, U. Lohmann, S Ramachandran, P.L. da Silva Dias, S.C. Wofsy and X. Zhang, 2007: Couplings Between Changes in the Climate System and Biogeochemistry. In: Climate Change 2007: The Physical Science Basis. Contribution of Working Group I to the Fourth Assessment Report of the Intergovernmental Panel on Climate Change [Solomon, S., D. Qin, M. Manning, Z. Chen, M. Marquis, K.B. Averyt, M.Tignor and H.L. Miller (eds.)]. Cambridge University Press, Cambridge, United Kingdom and New York, NY, USA.

Forster, P. ., Ramaswamy, V. ., Artaxo, P. ., Berntsen, T. ., Betts, R. ., Fahey, D. W. ., Haywood, J. ., Lean, J. ., Lowe, D. C. ., Myhre, G. ., Nganga, J. ., Prinn, R. ., Raga, G. ., Schulz, M. . and Dorland, R. V.: 2007: Changes in Atmospheric Constituents and in Radiative Forcing, in Climate Change 2007: The Physical Science Basis. Contribution of Working Group I to the Fourth Assessment Report of the Intergovernmental Panel on Climate Change, edited by S. Solomon, D.

Galloway, J. N., Townsend, A. R., Erisman, J. W., Bekunda, M., Cai, Z., Freney, J. R., Martinelli, L. a, Seitzinger, S. P. and Sutton, M. a: Transformation of the nitrogen cycle: recent trends, questions, and potential solutions., Science, 320(5878), 889–92, doi:10.1126/science.1136674, 2008.

Gentner, D. R., Isaacman, G., Worton, D. R., Chan, A. W. H., Dallmann, T. R., Davis, L., Liu, S., Day, D. A., Russell, L. M., Wilson, K. R., Weber, R., Guha, A. and Harley, R. A.: Elucidating secondary organic aerosol from diesel and gasoline vehicles through detailed characterization of organic carbon emissions, , doi:10.1073/pnas.1212272109/-/DCSupplemental.www.pnas.org/cgi/doi/10.1073/pnas.1212272109, 2012.

Guo, L., Luo, D., Li, C. and Fitzgibbon, M.: Development of Spatial Inventory of Nitrous Oxide Emissions from Agricultural Land Uses in California Using Biogeochemical Modeling, 2011.

IPCC, 2007. Climate Change 2007: Working Group I: The Physical Science Basis. Intergovernmental Panel on Climate Change. Solomon, S., D. Qin, M. Manning, Z. Chen, M. Marquis, K.B. Averyt, M. Tignor and H.L. Miller (eds.) Cambridge University Press, Cambridge, United Kingdom and New York, NY, USA.

Jeong, S., Millstein, D. and Fischer, M. L.: Spatially Explicit Methane Emissions from Petroleum Production and the Natural Gas System in California, 2014.

Jeong, S., Zhao, C., Andrews, A. E., Bianco, L., Wilczak, J. M. and Fischer, M. L.: Seasonal variation of CH 4 emissions from central California, J. Geophys. Res., 117(D11), D11306, doi:10.1029/2011JD016896, 2012a.

Jeong, S., Zhao, C., Andrews, A. E., Dlugokencky, E. J., Sweeney, C., Bianco, L., Wilczak, J. M. and Fischer, M. L.: Seasonal variations in N 2 O emissions from central California, Geophys. Res. Lett., 39(16), n/a–n/a, doi:10.1029/2012GL052307, 2012b.

McMillan, A. M. S., Goulden, M. L. and Tyler, S. C.: Stoichiometry of CH 4 and CO 2 flux in a California rice paddy, J. Geophys. Res., 112(G1), G01008, doi:10.1029/2006JG000198, 2007.

Misztal, P. K., Karl, T., Weber, R., Jonsson, H. H., Guenther, a. B. and Goldstein, a. H.: Airborne flux measurements of biogenic volatile organic compounds over California, Atmos. Chem. Phys. Discuss., 14(6), 7965–8013, doi:10.5194/acpd-14-7965-2014, 2014.

Montzka, S. A., Dlugokencky, E. J. and Butler, J. H.: Non-CO2 greenhouse gases and climate change., Nature, 476(7358), 43–50, doi:10.1038/nature10322, 2011.

Owen, J. J. and Silver, W. L.: Greenhouse gas emissions from dairy manure management: a review of field-based studies., Glob. Chang. Biol., doi:10.1111/gcb.12687, 2014.

Pacala, Stephen W., et al.(2010): Verifying Greenhouse Gas Emissions: Methods to Support International Climate Agreements, The National Academies Press, Washington, DC, 124 pp., 2010.

Peischl, J., Ryerson, T. B., Brioude, J., Aikin, K. C., Andrews, a. E., Atlas, E., Blake, D., Daube, B. C., de Gouw, J. a., Dlugokencky, E., Frost, G. J., Gentner, D. R., Gilman, J. B., Goldstein, a. H., Harley, R. a., Holloway, J. S., Kofler, J., Kuster, W. C., Lang, P. M., Novelli, P. C., Santoni,

G. W., Trainer, M., Wofsy, S. C. and Parrish, D. D.: Quantifying sources of methane using light alkanes in the Los Angeles basin, California, J. Geophys. Res. Atmos., 118(10), 4974–4990, doi:10.1002/jgrd.50413, 2013.

Santoni, G. W.; Xiang, B.; Kort, E. A.; Daube, B.; Andrews, A. E.; Sweeney, C.; Wecht, K.; Peischl, J.; Ryerson, T. B.; Angevine, W. M.; Trainer, M.; Nehrkorn, T.; Eluszkiewicz, J.; Wofsy, S. C. (2012) California's Methane Budget derived from CalNex P-3 Aircraft Observations and the WRF-STILT Lagrangian Transport Model. AGU Fall Meeting 2012, San Francisco, CA.

Smith, P., D. Martino, Z. Cai, D. Gwary, H. Janzen, P. Kumar, B. McCarl, S. Ogle, F. O'Mara, C. Rice, B. Scholes, O. Sirotenko, 2007: Agriculture. In Climate Change 2007: Mitigation. Contribution of Working Group III to the Fourth Assessment Report of the Intergovernmental Panel on Climate Change [B. Metz, O.R. Davidson, P.R. Bosch, R. Dave, L.A. Meyer (eds)], Cambridge University Press, Cambridge, United Kingdom and New York, NY, USA.

USEPA, 2014. Inventory of U.S. Greenhouse Gas Emissions and Sinks 1990-2012, USEPA . http://www.epa.gov/climatechange/ghgemissions/usinventoryreport.html#fullreport

Wunch, D., Wennberg, P. O., Toon, G. C., Keppel-Aleks, G. and Yavin, Y. G.: Emissions of greenhouse gases from a North American megacity, Geophys. Res. Lett., 36(15), L15810, doi:10.1029/2009GL039825, 2009.

Zhao, C., Andrews, A. E., Bianco, L., Eluszkiewicz, J., Hirsch, A., MacDonald, C., Nehrkorn, T. and Fischer, M. L.: Atmospheric inverse estimates of methane emissions from Central California, J. Geophys. Res., 114(D16), D16302, doi:10.1029/2008JD011671, 2009.

1.7   Tables and Figures
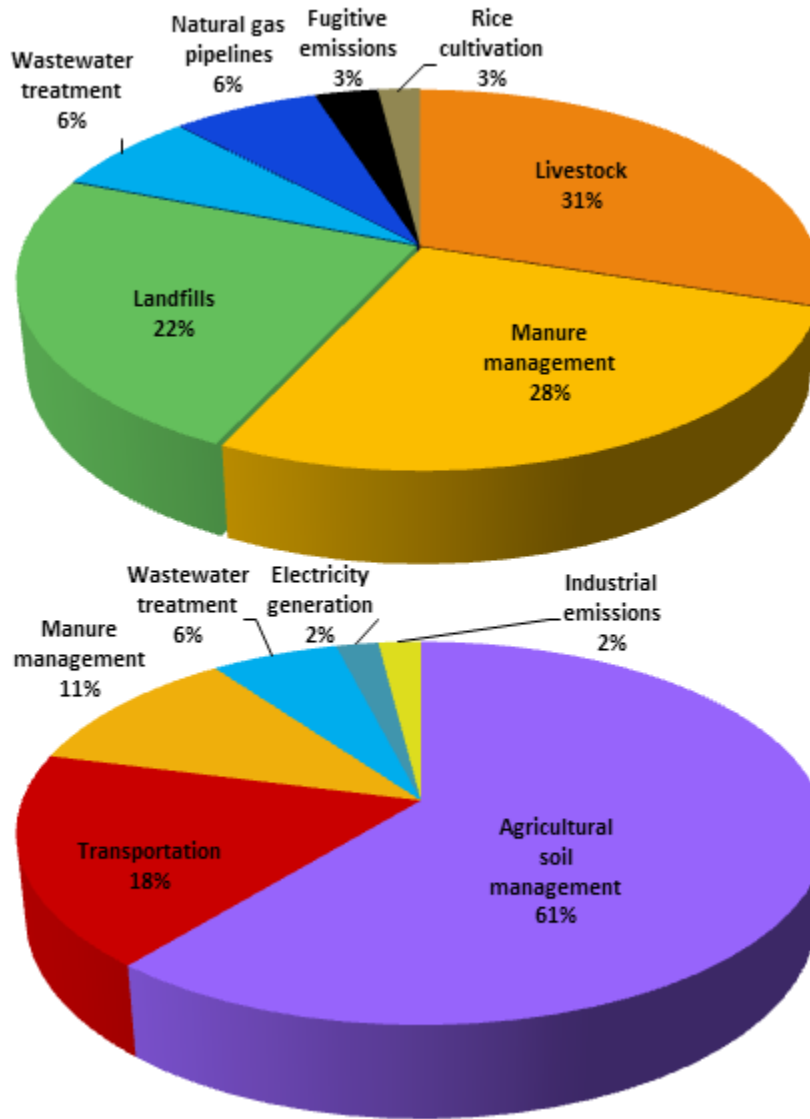
Figure 1.1. 2011 California emissions inventory for (top) methane (CH_4) - 32.5 million ton CO_2eq at GWP = 25; and (bottom) nitrous oxide (N_2O) - 13.4 million ton CO_2eq at GWP = 298. (Source: CARB GHG Inventory Tool, Aug 2013)
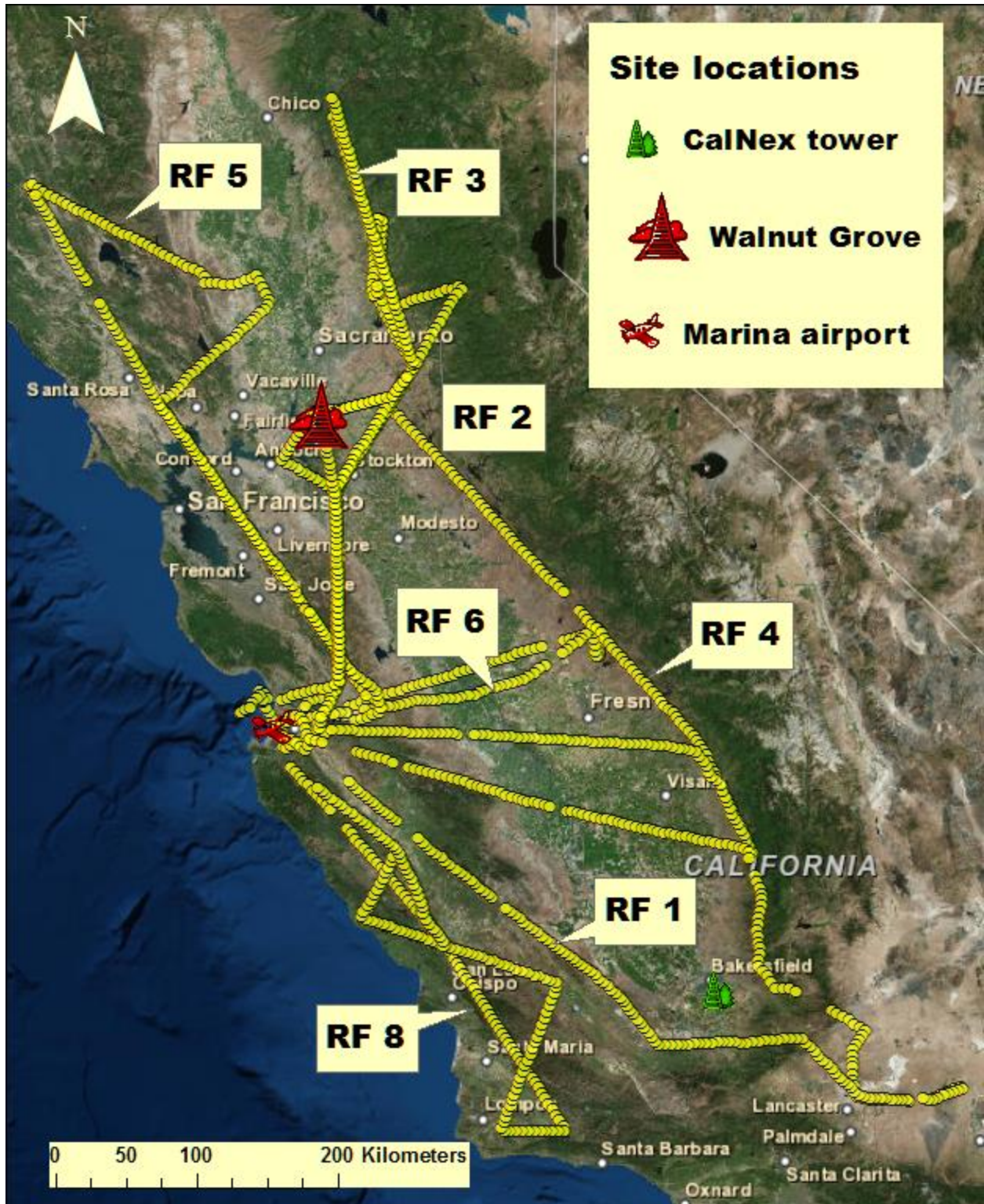
Figure 1.2. Site map showing the geographical location of the CalNex 2010 experiment site in Bakersfield and the Walnut Grove tower experiments in 2012-13. The yellow solid dots track the flight paths of seven unique flights flown during the CABERNET campaign in summer of 2011 over and around the Central valley. The Marina airport marks the origin point of all flights.

9

Chapter 2: Source apportionment of methane and nitrous oxide in California's San Joaquin Valley at CalNex 2010 via positive matrix factorization (PMF)

Abstract

Sources of methane (CH_4) and nitrous oxide (N_2O) were investigated using measurements from a site in southeast Bakersfield as part of the CalNex (California at the Nexus of Air Quality and Climate Change) experiment from May 15th to June 30th, 2010. Typical daily minimum mixing ratios of CH_4 and N_2O were higher than daily averages that were simultaneously observed at a similar latitude background station (NOAA, Mauna Loa) by approximately 70 ppb and 0.5 ppb, respectively. Substantial enhancements of CH_4 and N_2O (hourly averages > 500 ppb and > 7 ppb, respectively) were routinely observed suggesting the presence of large regional sources. Collocated measurements of carbon monoxide (CO) and a range of volatile organic compounds (VOCs) (e.g. straight-chain and branched alkanes, cycloalkanes, chlorinated alkanes, aromatics, alcohols, isoprene, terpenes and ketones) were used with a Positive Matrix Factorization (PMF) source apportionment method to estimate the contribution of regional sources to observed enhancements of CH_4 and N_2O.

The PMF technique provided a "top-down" deconstruction of ambient gas-phase observations into broad source categories, yielding a 7-factor solution. We identified these source factors as emissions from the following sources: evaporative and fugitive; motor vehicles; livestock and dairy; agricultural and soil management; daytime light and temperature driven; non-vehicular urban; and nighttime terpene biogenics and anthropogenics. The dairy and livestock factor accounted for a majority of the CH_4 (70 - 90 %) enhancements during the duration of the experiments. Propagation of uncertainties in the PMF-derived factor profiles and time series from bootstrapping analysis resulted in a 29 % uncertainty in the CH_4 apportionment to this factor. The dairy and livestock factor was also a principal contributor to the daily enhancements of N_2O (60 − 70 %) with an uncertainty of 33 %. Agriculture and soil management accounted for ∼ 20-25 % of N_2O enhancements over the course of a day, not surprisingly, given that organic and synthetic fertilizers are known to be a major source of N_2O. The N_2O attribution to the agriculture and soil management factor had a relatively high uncertainty of 70 %, most likely due to an asynchronous pattern of soil-mediated N_2O emissions from fertilizer usage and collocated biogenic emissions from crops from the surrounding agricultural operations that is difficult for PMF to detect and apportion. The evaporative / fugitive source profile which resembled a mix of petroleum operation and non-tailpipe evaporative gasoline sources did not include a PMF resolved-CH_4 contribution that was significant (< 2 %) compared to the uncertainty in the livestock-associated CH_4 emissions. The vehicle emission source factor broadly matched VOC profiles of on-road exhaust sources. This source factor had no statistically significant detected contribution to the N_2O signals (confidence interval of 3 % of livestock N_2O enhancements) and negligible CH_4 (confidence interval of 4 % of livestock CH_4 enhancements) in the presence of a dominant dairy and livestock factor. The

CalNex PMF study provides a measurement-based assessment of the state CH_4 and N_2O inventories for the southern San Joaquin valley. The state inventory attributes ~ 18% of the total N_2O emissions to the transportation sector. Our PMF analysis directly contradicts the state inventory and demonstrates there were no discernible N_2O emissions from the transportation sector in the region.

2.1   Introduction

Methane (CH_4) and nitrous oxide (N_2O) are the two most significant non-CO_2 greenhouse gases (GHGs) contributing about 50 % and 16 % of the total non-CO_2 GHG radiative forcing (~ 1 W m^{-2}), respectively (Forster et al., 2007). CH_4, with a lifetime of ~ 10 years and Global Warming Potential (GWP) of 25 on a 100-year basis (Forster et al., 2007; Montzka et al., 2011), is emitted by both anthropogenic and natural sources (e.g. wetlands, oceans, termites etc.). Anthropogenic global CH_4 emissions are due to agricultural activities like enteric fermentation in livestock, manure management and rice cultivation (McMillan et al., 2007; Owen and Silver, 2014), energy sector (oil and gas operations and coal mining), waste management (landfills and waste water treatment), and biomass burning (some of which is natural) (Smith et al., 2007; Pacala et al., 2010). N_2O has a higher persistence in the atmosphere (lifetime of ~ 120 years) and stronger infrared radiation absorption characteristics than CH_4 giving it a GWP of 298 (Forster et al., 2007; Montzka et al., 2011). Agriculture is the biggest source of anthropogenic N_2O emissions since the use of synthetic fertilizers and manure leads to microbial N_2O emissions from soil (Crutzen et al., 2007; Galloway et al., 2008). Management of livestock and animal waste is another important agricultural source of N_2O, while industrial processes including fossil fuel combustion have been estimated to account for 15 % of total global anthropogenic N_2O emissions (Denman et al., 2007).

In 2006, the state of California adopted Assembly Bill 32 (AB32) into a law known as the Global Warming Solutions Act, which committed the state to cap and reduce anthropogenic GHG emissions to 1990 levels by 2020. A statewide GHG emission inventory (CARB, 2013) maintained by the Air Resources Board of California (CARB) is used to report, verify and regulate emissions from GHG sources. In 2011, CH_4 accounted for 32.5 million metric tonnes (MMT) CO_2-eq representing 6.2 % of the statewide GHG emissions, while N_2O emissions totaled 6 MMT CO_2-eq representing about 3 % of the GHG emissions inventory (Figures 1.1; Chapter 1). CARB's accurate knowledge of GHG sources and statewide emissions is critical to the success of any climate change mitigation strategy under AB32. CARB's GHG inventory is a "bottom–up" summation of emissions derived from emission factors and activity data. The bottom-up approach is reasonably accurate for estimation and verification of emissions from mobile and point sources (vehicle tailpipes, power plant stacks etc.) where the input variables are well-understood and well-quantified. The main anthropogenic sources of CH_4 in the CARB inventory include ruminant livestock and manure management, landfills, wastewater treatment, fugitive and process losses from oil and gas production and transmission, and rice cultivation while the major N_2O sources are agricultural soil management, livestock manure management and vehicle fuel combustion (CARB, 2013). The emission factors for many of these sources have large uncertainties as they are biological and their production and release mechanisms are inadequately understood thus making these sources unsuitable for direct measurements (e.g.

emissions of N_2O from farmlands). Many of these sources (e.g. CH_4 from landfills) are susceptible to spatial heterogeneity and seasonal variability. Unfortunately, a more detailed understanding of source characteristics is made difficult because CH_4 and N_2O are often emitted from a mix of point and area sources within the same source facility (e.g. dairies in the agricultural sector) making bottom-up estimation uncertain. There is a lack of direct measurement data or "top-down" measurement-based approaches to independently validate seasonal trends and inventory estimates of CH_4 and N_2O in California's Central Valley, which has a mix of several agricultural sources and oil and gas operations, both of which are known major sources of GHGs.

In the recent past, regional emission estimates derived from measurements from a tall tower at Walnut Grove in Central California coupled with inverse dispersion techniques (Fischer et al., 2009) reported underestimation of CH_4 and N_2O emissions especially in the Central Valley. Comparison of regional surface footprints determined from WRF-STILT algorithm between Oct-Dec 2007 indicate posterior CH_4 emissions to be higher than California-specific inventory estimates by 37 ± 21 % (Zhao et al., 2009). Predicted livestock CH_4 emissions are 63 ± 22 % higher than *a priori* estimates. A study over a longer period (Dec 2007 - Nov 2008) at the same tower (Jeong et al., 2012a) generated posterior CH_4 estimates that were 55 - 84 % larger than California-specific prior emissions for a region within 150 km from the tower. For N_2O, inverse estimates for the same sub-regions (using either EDGAR32 and EDGAR42 *a priori* maps) were about twice as much as *a priori* EDGAR inventories (Jeong et al., 2012b). Recent studies have incorporated WRF-STILT inverse analysis on airborne observations across California (Santoni et al., 2012). The authors conclude that CARB CH_4 budget is underestimated by a factor of 1.64 with aircraft-derived emissions from cattle and manure management, landfills, rice, and natural gas infrastructure being around 75 %, 22 %, 460 %, and 430 % more than CARB's current estimates for these categories, respectively. Statistical source footprints of CH_4 emissions generated using FLEXPART-WRF modeling and CalNex-Bakersfield CH_4 concentration data are consistent with locations of dairies in the region (Gentner et al., 2014a). The authors conclude that the majority of CH_4 emissions in the region originate from dairy operations. Scaled-up CH_4 rice cultivation estimates derived from aircraft CH_4 / CO_2 flux ratio observations over rice paddies in the Sacramento Valley during the growing season when emissions are at their strongest (Peischl et al., 2012) are around three times larger than inventory estimates. CH_4 budgets derived for the Los Angeles (LA) basin from aircraft observations (Peischl et al., 2013) and studies involving comparison with CO enhancements and inventory at Mt. Wilson (Wunch et al., 2009; Hsu et al., 2010) indicate higher atmospheric CH_4 emissions in the LA basin than expected from bottom-up accounting.

Recent literature seems to suggest that the CARB bottom-up inventory is underestimating CH_4 and N_2O sources, especially from the livestock sector and perhaps from the oil and gas industry as well. Source apportionment studies of non-CO_2 GHGs over the Central Valley can provide critical information about under-inventoried or unknown sources that seek to bridge the gap between 'bottom-up' and 'top-down' methods. GHG emission inventories can potentially be constrained through simultaneous measurements of GHGs and multiple gas species (VOCs) that are tracers of various source categories. This study provides CH_4 and N_2O source attribution during a six-week study involving a complete suite of continuous GHG and VOC tracer measurements during the CalNex 2010 campaign in Bakersfield, located in the southern part of

the Central Valley (May-June 2010). The objective of this study is to partition the measured CH_4, N_2O and VOC enhancements into statistically unique combinations using Positive Matrix Factorization (PMF) apportionment technique. We classify these combinations as plausible source factors based on our prior knowledge of the chemical origin of mutually co-varying groups of VOC tracers found in each statistical combination. We examine the source categorization using observations from source-specific, ground site and airborne measurements and results from other source apportionment studies. We also compare the relative abundance of CH_4 and N_2O enhancements in each source factor with the CARB inventory estimates in order to assess the accuracy of the inventory. We hypothesize that the PMF analysis will be able to parse the atmospheric observations into unique statistical source combinations that, as an analyst, I will be able to distinguish from each other on the basis of unique VOC source markers and appropriately attribute the CH_4 and N_2O apportioned to each of these factor profiles to a major source category. We then proceed to answer the scientific question if our top down assessment of the CH_4 and N_2O inventory can improve our understanding of the bottom-up CARB inventory in the region.

2.2   Experiment

2.2.1   Field site and meteorology

Measurements were conducted from 19 May to 25 June 2010 at the Bakersfield CalNex supersite (35.3463°N, 118.9654°W) (Figure 2.1) in the southern San Joaquin Valley (SJV) (Ryerson et al., 2013). The SJV represents the southern half of California's Central Valley. It is 60 to 100 km wide, surrounded on three sides by mountains, with the Coastal Ranges to the west, the Sierra Nevada Mountains to the east, and the Tehachapi Mountains to the southeast.

The measurement site was located to the southeast of the Bakersfield urban core in Kern County (Figure 2.1). The east-west Highway 58 is located about 0.8 km to the north; the north-south Highway 99 about 7 km to the west. The city's main waste water treatment plant and its settling ponds are located to the east and south of the site (< 2.5 km), respectively. Numerous dairy and livestock operations are located to the south-southwest of the site at 10 km distance or farther. The metropolitan region has three major oil refineries located within 10 km from the site (two to the northwest; one to the southeast). A majority of Kern County's high-production active oil fields (> 10000 barrels (bbl) per day) (CDC, 2013) are located to the west / northwest and are distant (~ 40 - 100 km). Kern River oilfield (~ 60000 bbl day^{-1}), one of the largest in the country, and Kern Front (~ 11000 bbl day^{-1}) are located about 10-15 km to the north. There are several other oil fields dotted within the urban core (5 - 20 km) which are less productive (< 2000 bbl day^{-1}) or not active (< 100 bbl day^{-1}). The whole region is covered with agricultural farmlands with almonds, grapes, citrus, carrots and pistachios amongst the top commodities by value and acreage (KernAg, 2010).

The meteorology and transport of air masses in the southern SJV is complex and has been addressed previously (Bao et al., 2007; Beaver and Palazoglu, 2009). The wind rose plots (Figure

13

2.2) shown here present a simplified distribution of microscale wind speed and direction at the site, the latter often being non-linear over larger spatial scales. The plots depict broad differences in meteorology during daytime and nighttime. A mesoscale representation of the site meteorology during this study period was evaluated through back-trajectory footprints generated from each hourly sample using FLEXPART Lagrangian transport model with WRF meteorological modeling (Gentner et al., 2014a). The 6-h and 12-h back trajectory footprints are generated on a 4 × 4 km resolution with simulations originating from top of the 18-m tall tower. The site experiences persistent up-valley flows from the north and northwest during afternoons and evenings, usually at high wind speeds. The direction and speed of the flow during the nights is quite variable (Figure 2.2). On some nights, the up-valley flows diminish as night-time inversion forms a stable layer near the ground, and eventually downslope flows off the nearby mountain ranges bring winds from the east and south during late night and early morning periods. On other nights, fast moving northwesterly flows extend in to middle of the night leading to unstable conditions through the night. The daytime flows bring plumes from the upwind metropolitan region (Figures 2.1 and 2.2), as well as regional emissions from sources like dairies and farmlands located further upwind. The slow nighttime flows and stagnant conditions cause local source contributions to be more significant than during daytime, including those from nearby petroleum operations and dairies (Gentner et al., 2014a), and agriculture (Gentner et al., 2014b).

2.2.2   Trace gas measurements and Instrumentation

Ambient air was sampled from the top of a tower 18.7 m a.g.l (above ground level) through Teflon inlet sampling lines with Teflon filters to remove particulate matter from the gas stream. CH_4, CO_2 and H_2O were measured using a Los Gatos Research (LGR Inc., Mountain View, CA) Fast Greenhouse Gas Analyzer (FGGA, Model 907-0010). N_2O and CO were measured by another LGR analyzer (Model 907-0015) with time response of ~ 0.1 to 0.2 Hz. These instruments use off-axis Integrated Cavity Output Spectroscopy (ICOS) (O'Keefe, 1998; Paul et al., 2002; Hendriks et al., 2008; Parameswaran et al., 2009). The FGGA instrument automatically corrects for water vapor dilution and reports CH_4 and CO_2 on a dry (and wet) mole fraction basis. We report dry mole fraction mixing ratios. The FGGA instrument had a 1σ-precision of 1 ppb (for CH_4) and 0.15 ppm (for CO_2) while the N_2O/CO instrument had a 1σ-precision of 0.3 ppb, respectively over short time periods (< 10 s). The instruments were housed at ground level in a thermally insulated temperature controlled 7-foot wide cargo wagon trailer developed by the GHG instrument manufacturers (LGR Inc.). CO was coincidentally measured using another instrument (Teledyne API, USA, Model # M300EU2) with a precision of 0.5 % of reading and output as 1-minute averages. The mixing ratios from the two collocated CO instruments correlated well (r ~ 0.99) and provided a good stability check for the LGR instrumentation. Scaled Teledyne CO data was used to gap-fill the LGR CO data. The coincident gas-phase VOC measurements were made using a gas chromatograph (GC) with a quadrapole mass selective detector and a flame ionization detector (Gentner et al., 2012).

Hourly calibration checks of the three GHGs and CO were performed using near-ambient level scuba tank standards through the entire campaign. During data processing, final

concentrations were generated from the raw data values using scaling factors obtained from comparison of measured and target concentrations during calibration checks. Diurnal plots of measured species are generated from 1-min averages. PMF analyses in the following sections are based on 30-minute averages to match the time resolution of VOC measurements. The meteorological data measured at the top of the tower included relative humidity (RH), temperature (T), and wind speed (WS) and direction (WD).

2.2.3 Positive Matrix Factorization (PMF)

Source apportionment techniques like PMF have been used in the past to apportion ambient concentration datasets into mutually co-varying groups of species. PMF is especially suitable for studies where *a priori* knowledge of number of sources impacting the measurements, chemical nature of source profiles and relative contribution of each source to the concentration time series of a measured compound are unknown or cannot be assumed. PMF has been applied to ambient particulate matter studies (Lee et al., 1999; Kim et al., 2004); in determining sources of atmospheric organic aerosols (OA) (Ulbrich et al., 2009; Slowik et al., 2010; Williams et al., 2010); and in gas phase measurements of VOCs in major metropolitan cities (Brown et al., 2007; Bon et al., 2011). PMF is a receptor-only unmixing model which breaks down a measured data set containing time series of a number of compounds into a mass balance of an arbitrary number of constant source factor profiles (FP) with varying concentrations over the time of the data set (time series *or* TS) (Ulbrich et al., 2009).

In real world ambient scenarios, sources of emissions are often not known or well-understood. PMF technique requires no a priori information about the number or composition of factor profiles or time trends of those profiles. The constraint of non-negativity in PMF ensures that all values in the derived factor profiles and their contributions are constrained to be positive leading to physically meaningful solutions. PMF attributes a measure of experimental uncertainty (or weight) to each input measurement. Data point weights allow the level of influence to be related to the level of confidence the analyst has in the measured data (Hopke, 2000). In this way, problematic data such as outliers, below-detection-limit, or altogether missing data can still be substituted into the model with appropriate weight adjustment (Comero et al., 2009) allowing for a larger input data set, and hence a more robust analysis. PMF results are quantitative; it is possible to obtain chemical composition of sources determined by the model (Comero et al., 2009). PMF is not data-sensitive and can be applied to data sets that are not homogenous and/or require normalization without introducing artifacts.

2.2.4 Mathematical framework of PMF

The PMF model is described in greater detail elsewhere (Paatero and Tapper, 1994; Paatero 1997; Comero et al., 2009; Ulbrich et al., 2009) and we will briefly mention some concepts relevant to the understanding of the analysis carried out in this study. The PMF input parameters involve a $m \times n$ data matrix $\mathbf{X}$ with i rows containing mixing ratios at sampling time t_i and j

columns containing time series of each tracer$_j$. A corresponding uncertainty matrix **S** reports measurement precision (uncertainty) of the signal of each tracer$_j$ at every t_i (s_{ij}). The PMF model can then be resolved as:

$$X_{ij} = \sum_p g_{ip}f_{pj} + e_{ij}$$ (1)

where p refers to the number of contributing factors in the solution as determined by the analyst (discussed below), g_{ij} (mass concentration) are elements of a $m \times p$ matrix **G** whose columns represent the factor time series while f_{ij} (mass fraction) are elements of a $p \times n$ matrix **F** whose rows represent the factor chemical profiles. e_{ij} are the elements of a $m \times n$ matrix **E** containing residuals not fit by the model matrix at each data point.

The PMF algorithm uses a least-squares algorithm to iteratively fit the values of **G** and **F** by minimizing a "a quality of fit" parameter Q (Bon et al., 2011), defined as:

$$Q = \sum_{i=1}^{m}\sum_{j=1}^{n}\left(e_{ij}/s_{ij}\right)^2$$ (2)

In this way, PMF minimizes the sum of squares of error-weighted model-measurement deviations. The theoretical value of Q, denoted by Q-expected (Q_{exp}) can be estimated as:

$$Q_{exp} \equiv (m \times n) - p \times (m + n)$$ (3)

If all the errors have been estimated within the uncertainty of the data points (i.e. $e_{ij}\ s_{ij}^{-1} \sim 1$) and the model fits the data perfectly, then Q should be approximately equal to Q_{exp}.

2.2.5   Data preparation for PMF analysis

For this study, measurements from the FGGA, LGR N2O/CO analyzer and the GC were combined into a unified data set to create matrices **X** and **S**. Only VOCs that are a part of broad chemical composition of nearby sources (like dairies and vehicle emissions) or could potentially serve as source specific tracers (e.g. iso-octane as a tailpipe emissions tracer; isoprene as a biogenic tracer) were included. Isomers were limited (e.g. 2,3-dimethylbutane over 2,2-dimethylbutane) and VOCs with large number of missing values were not included. The input data set represented major chemical families like straight-chain and branched alkanes, cycloalkanes, alkenes, aromatics, alcohols, aldehydes, ketones and chlorinated as well as organosulfur compounds. In all, there were a total of 653 half-hour samples of data covering a period from 22 May to 25 June. Table 2.1 lists all the compounds included in the PMF analysis along with a spectrum of their observed and background concentrations.

PMF analysis resolves the covariance of mixing ratio enhancements and thus characterizes the chemical composition of emissions from various sources. Hence, for this analysis, only

16

enhancements were included in the data set after subtracting local background concentrations from the original signals. Background concentrations were derived as the minima in the time series (0th percentile) for each of the 50 tracers included in the PMF analysis (CH_4, N_2O, CO and 46 VOCs). For VOCs, tracers with a minimum value less than two times the limit of detection (LOD, in ppt) and a maximum value larger than hundred times the LOD were assumed to have a negligible background (0 ppt) (Table 2.1). The 99th percentile for each tracer was treated as the effective-maximum mixing ratio and the upper limit of the range for the "normalization" of time series. Data points representing enhancement values above the 99th percentile are often extreme data points. Such outliers, even if true enhancements, represent isolated and short-duration footprints of high-emission events that are difficult for PMF to reconstruct. In order to maintain the robustness of PMF analysis, outliers were selectively down-weighted by increasing their uncertainty in proportion to the uncertainty of other data points (described below). Finally, the enhancements in each time series were "normalized" by dividing every sample by the normalizing range i.e. the difference in the 99th percentile and background as seen in Equation 4. This process scaled the enhancements in each time series (final data points in **X**) within a range of 0 to 1. This allowed for a consistent scheme to represent tracers with vastly different concentrations (e.g. ppm level of CH_4 vs ppt level of propene) and improve the visual attributes of PMF output plots to follow. Data points denoting zero enhancement (lower limit) were replaced by a very small positive number (i.e. exp(-5)) to avoid 'zeroes' in the data matrix **X**.

$$x_{ij} = \left. \left(Mixing\ ratio_{ij} - Background_j \right) \middle/ \left(Maximum\ mixing\ ratio_j - Background_j \right) \right. \tag{4}$$

For the VOCs, guidelines set forth by (Williams et al., 2010) were adopted to calculate the uncertainty estimates. An analytical uncertainty (AU) of 10 % was used; a limit of detection (LOD) of 1 ppt and a limit of quantification (LOQ) of 2 ppt (Gentner et al., 2012) was used to calculate the total uncertainty for each x_{ij}:

$$s_{ij} \equiv 2 \times LOD, \qquad\qquad\qquad \text{if } x_{ij} \leq \text{LOD}, \tag{5a}$$

$$s_{ij} \equiv LOQ, \qquad\qquad\qquad \text{if LOD} < x_{ij} \leq \text{LOQ}, \tag{5b}$$

$$s_{ij} \equiv \left(\left(AU \times x_{ij} \right)^2 + (LOD)^2 \right)^{0.5}, \qquad \text{if } x_{ij} > \text{LOQ} \tag{5c}$$

In this way, the detection limit dictates the errors for small enhancements (near LOD) while errors for larger enhancements in the time series are tied more to the magnitude of the data value (x_{ij}) itself.

The GHG and CO measurements have high precision and significantly lower detection limits than ambient levels. The relatively low values of GHGs in the uncertainty matrix, compared to VOCs, is substituted with those calculated using a custom approach. The GHG and CO uncertainties are assumed to be proportional to the square root of the data value and an arbitrary scaling factor determined through trial and error in order to produce lower values of $Q\ Q_{exp}^{-1}$:

$$s_{ij} \equiv A \times \left(x_{ij} \right)^{0.5}, \tag{6}$$

where A = 1 (for CH$_4$), 0.25 (for CO$_2$), 0.5 (for CO), 0.1 (for N$_2$O)

This method attributes larger percentage uncertainties to smaller enhancements and hence lesser weight in the final solution and vice versa. This approach leads to an uncertainty matrix that attributes relatively similar percentage errors to both GHGs and VOCs, which should lead to a better fitting of the data in PMF.

Missing values are replaced by geometric mean of the tracer time series and their accompanying uncertainties are set at four times this geometric mean (Polissar et al., 1998) to decreases their weight in the solution. Based on the *a priori* treatment of the entire input data (scaling) and the corresponding outputs of the PMF analysis, a weighting approach (for measurements from different instruments) as used in (Slowik et al., 2010) is not found to be necessary.

2.2.6   PMF source factor analysis

We use the customized software tool (PMF Evaluation Tool v2.04, PET) developed by Ulbrich et al. (2009) in Igor Pro (Wavemetrics Inc., Portland, Oregon) to run PMF, evaluate the outputs and generate statistics. The PET calls the PMF2 algorithm (described in detail in Ulbrich et al., 2009) to solve the bilinear model for a given set of matrices **X** and **S** for different numbers of factors *p* and for different values of FPEAK or SEED (defined and described later). The tool also stores the results for each of these combinations in a user friendly interface that allows simultaneous display of the factor profiles (FP) and time series (TS) of a chosen solution along with residual plots for individual tracers. A procedural description of the PMF analysis performed in this study is provided below. First we describe the approach of how the final number of user-defined factors was chosen; then we explain the outcomes of linear transformations (rotations) of various PMF solutions and finally, how uncertainties in the chosen solution are derived. The standard deviations in the mass fractions of individual tracers in each factor profile and time series of each factor mass is evaluated using a bootstrapping analysis (Norris et al., 2008; Ulbrich et al., 2009) described below. These error estimates are combined and propagated to derive PMF-based uncertainties for each factor's contribution to source-apportioned diurnal enhancements for a specific compound (Section 2.3.2).

Determination of number of PMF factors

In PMF, the choice of modeled factors in the solution is made on the basis of a qualitative judgment and remains the most critical step in the interpretation of results (Ulbrich et al., 2009). A number of metrics aid in this decision making process. One of these is the *Q*-value which represents the total sum of the squares of scaled residuals. If the assumptions of bilinear model are appropriate and the errors in the input data have been properly estimated such that each reproduced data point is fit to within its estimated error value, then, Q/Q_{exp} should be ~ 1. Values of $Q/Q_{exp} >> 1$ indicate underestimation of the errors or inability of the PMF solution to explain a significant portion of the variability in factor profiles as the modeled sum of contributions of the chosen number of factors *p*. Hence, the estimated Q/Q_{exp} is explored as a function of the number

of factors in order to determine the best modeled representation. Addition of factors (increasing *p*) adds more degrees of freedom to enable a better fitting of the data and decreases the value of Q/Q_{exp} and if the decrease is large enough, it implies that the additional factor has explained significantly more of the variation in the data and hence the added factor is real (Paatero and Tapper, 1993). The % decrease in Q/Q_{exp} values or slope of the curve at each step increase in *p* should be used as a criterion in determining the '*best*' number of factors in the solution. One should be careful and wise in not choosing a PMF solution solely based on Q/Q_{exp} values. Choosing too many factors in a PMF solution may make a real factor further dissociate into two or more non-existing sources. This phenomenon is known as *splitting* and discussed by Ulbrich et al. (2009). Hence rejecting a solution involving *splitting* behavior in factors should serve as a criterion while narrowing down on a PMF solution. Additional factors may also be non-unique with contributions from all major classes of compounds thus rendering the apportionment of the factor useless and should be used as a criterion to reject solutions. On the other hand, choosing too few factors will combine sources with different emission characteristics together to produce a single factor and hence yield a solution that will be difficult to interpret (Hopke, 2000). In the end, the ability to interpret a FP and issue it a name of a source category, based on *a priori* knowledge of the chemical compositional profile of the source, remains a qualitative but a necessary step in identification of the final PMF solution. As per P. Paatero (the creator of the PMF technique), this subjectivity is a part of the PMF process and should be reported in scientific publications (Ulbrich et al., 2009).

Figure 2.3 (a) shows the variation of Q/Q_{exp} values with increasing *p* for solutions including up to 10 factors at FPEAK = 0 (discussed below). The Q/Q_{exp} values show a steep decrease from *p* = 1 to 5 (> 10 % drop at each step) but then gradually the decrease becomes steady and is less than 10 % at each step (*p* > 5) indicating the *optimum* solution is at *p* > 5. PMF solutions for all cases in Figure 2.3 (a) (1 to 10 factors) were examined. A 7-factor solution was found to be the most suitable in explaining the variability in the data, yielding factor profiles which are unique and well-distinguishable from each other. The Q/Q_{exp} value at *p* = 7 (FPEAK = 0) is 4.3 which suggests that the errors are either somewhat underestimated, there are a fair number of *weak* data points (e.g. missing and below-detection-limit values) and that the variability in the dataset cannot be modeled better than this due to physical parameters at the site. In this study, the slightly higher Q/Q_{exp} value can be attributed to limitations in the modeling ability which arises due to a lack of strong contrast in the time trends of species during the nighttime as all primary emissions accumulate in a shallow boundary layer and there is minimal chemical processing of the air parcels. The same was observed by Bon et al. (2011) in their Mexico City study.

Besides the chosen 7-factor solution, other PMF solutions have been evaluated, and figures of factor profiles for a 6-factor PMF solution (FPEAK = 0) and an 8-factor PMF solution (FPEAK = 0) are also included (Figures 2.4 and 2.5, respectively). On comparing the FP plots of various PMF solutions, we find that the gray colored factor in Figure 2.4 of the 6-factor solution does not resolve/separate the urban (green) and nighttime biogenics (navy blue) sources seen in the 7-factor solution (Figure 2.6). The chemical profile of this factor seems '*mixed*' with no major contribution from any specific source marker but instead has minor source contributions from almost all the tracers included in the PMF analysis and is thus indistinguishable. On the other hand, the agricultural soil management factor from the 7-factor solution (Figure 2.6) seems to be '*split*' into two separate factors in the 8-factor solution (gray and brown factors in Figure

19

2.5). Neither of the two split factors resembles any particular source category and do not provide any additional insight into the data. The diurnal profiles of the two split factors (not shown) look identical giving further evidence of the "factor splitting" phenomenon.

Rotation of factors

The bilinear PMF analysis has rotational ambiguity and is not mathematically unique. The constraint of non-negativity reduces the rotational freedom in the system but does not generally produce a unique solution. There may be potentially infinite linear transformations, better known as "rotations", that can reduce the rotational freedom by introducing zero values in the factor mass profile (F) and time series (G) and can force the solution to produce an identical fit to the data (Ulbrich et al., 2009), such that:

$$GF = GTT^{-1}F \text{ , where } T = \text{transformation matrix, } T^{-1} = \text{inverse of } T \tag{7}$$

In the PMF2 algorithm, the rotated factor product is allowed to differ slightly from the product of the G and F matrices ($GF \approx GTT^{-1}F$) on account of the non-negative forcing of the matrices in order to produce "distorted" rotations which may lead to a slightly worse but acceptable fit to the data with similar but higher values of Q and potentially yield more physically realistic solutions (Paatero et al., 2002). After the case with the *best* number of factors has been established, a subset of the "distorted" linear transformations of the solution can be explored using the FPEAK parameter. Positive FPEAK values force the routine to add one G column vector to another and subtract the corresponding F row vectors from each other while negative FPEAK values explore the reverse scenario (Paatero, 1997; Hopke, 2000). Zero values in the F and G matrices (no rotations) will limit subtractions in the matrices owing to the non-negativity constraint and thus limit the scope of solutions. Only "rotations" for which the Q-value is not significantly greater than the central case (FPEAK = 0) are considered. Prior literature suggests not considering rotations for a FPEAK case in which the Q/Q_{exp} value shows an increase of 10 % or more above its minimum value (usually $Q_{FPEAK=0}$)(Paatero et al., 2002). The rotation procedure produces, for each FPEAK, new rotated matrices GT and $T^{-1}F$ that represents time series and factors respectively, that may appear to be closer to physically real source profiles than G and F.

A narrow FPEAK range is more appropriate in cases where Q/Q_{exp} value for (*p-1*)-factor solution (FPEAK = 0) is less than 10 % higher than the Q/Q_{exp} value for the corresponding case in the *p*-factor solution. This is true in the current case of 6 versus 7-factor solution (Figure 2.3 a). Figure 2.3 (b) plots the variation in Q/Q_{exp} values with respect to the FPEAK parameter for the 7-factor solution over a range of FPEAKS from -3 to +3 in increments of 0.2 units. Solutions with narrower FPEAK range that give an increase of 1 % over the minimum Q/Q_{exp} value have been investigated for acceptable PMF fits (Ulbrich, 2009). The FPEAK range that meets the 1 % criterion is -1.6 to 0.4 (Figure 2.3 b). The standard deviation over this FPEAK range is the estimated error in mass fraction of each tracer in each of the seven factors. We follow the guidelines in (Paatero et al., 2002; Comero et al., 2009) about behavior of Q/Q_{exp} with change in the FPEAK parameter and determine the physical plausibility of the all the factor profiles at each FPEAK within the shortlisted range and choose the *best* fit to the data at FPEAK = +0.6.

Uncertainty estimates of chosen solution

Bootstrapping in PMF is a quantitative technique that addresses the difficult topic of evaluating the stability and statistical uncertainty in a candidate PMF solution (Norris et al., 2008; Ulbrich et al., 2009). In the bootstrapping procedure, the PET creates a new data set by randomly selecting non-overlapping blocks of consecutive samples. The new data set has the same dimensions as the original data set. PMF is then applied to this new data set. In every run, each bootstrap factor is assigned to a base run factor by comparing the contributions of each factor and assigning it to the one with highest correlation. At the end of the user-specified number of iterations, bootstrapping statistics for all the runs are generated in the PET which include average and 1σ values for each fractional component and sample mass in the FP and TS, respectively. The results of bootstrapping inform the analyst of the robustness of the factor profiles chosen in the base run.

Bootstrapping was applied to the base run (7-factor solution, FPEAK = +0.6, SEED = 0) with 100 runs. The FP of the seven factors with their bootstrapping averages and standard deviation range is plotted in Figure 2.6. The fractional contributions to a source factor from tracers that occur in relatively high proportions in the base run (indicated by colored bars) is quite similar to the averages over the 100 bootstrapping runs (dots) in all the seven factors. The plot also shows the uncertainty in each mass fraction represented by the standard deviation (1σ) of these averages (indicated by whiskers about the dots). For e.g. the uncertainty in the normalized fractional proportion of CH_4 in the dairy and livestock source factor is 29 % (1σ confidence interval) of the mean CH_4 mass fraction while the uncertainty in PMF-derived N_2O fraction of agricultural and soil management factor is 70 % of the mean fraction of N_2O apportioned to that factor. The overall averaged mass fraction of compounds in all factors from the bootstrapping runs is similar to the factors from the base run (Figure 2.6) that suggests that the chemical profile of each factor is reproduced consistently in the bootstrapping runs. Within a factor, the uncertainties in individual mass fractions are lower for major constituents while minor constituents have larger uncertainties. The uncertainties of the tracers that occur in relatively minor proportions in each source factor can be high which is a known limitation as PMF is *weak* in its partitioning of the mixing ratio signals arising from collocated sources and artifacts arising due to meteorology (like strong daytime mixing), and hence suffers from the '*mixing*' and '*splitting*' phenomena (discussed above). But in spite of these high uncertainties, the 1σ confidence interval of the mass fraction of these minor CH_4 (or N_2O) fractions is significantly smaller than the confidence intervals of the major CH_4 (or N_2O) mass fractions, and as such are insignificant contributors to the overall apportionment. We conclude that the bootstrapping results show a robust 7-factor PMF solution with reasonable uncertainties for tracers that are major contributors to a source factor. The uncertainties also confirm that PMF analysis does not yield a unique solution but rather presents a range of possible combinations of mass fractions of compounds, all with low Q/Q_{exp} ratios. The uncertainties generated in the factor profile and the time series from the bootstrapping runs are propagated to determine the uncertainties in the relative apportionment of the trace gas distribution by source type (in Figure 2.11).

2.3   Results and Discussion

In Bakersfield, there are a multitude of pollutant sources, ranging from local to regional, from biogenic to anthropogenic, and from primary to secondary. We recognize that PMF analysis is not capable of precise separation of all sources. In PMF analysis, the analyst chooses the number of factor profiles to include in the solution and assigns a source category interpretation for each identified factor. The PMF factors are not unique sources but really statistical combinations of coincident sources. The chemical profile of each factor may contain some contributions from multiple sources that are co-located, or have a similar diurnal pattern. Such limitations have been observed previously by Williams et al. (2010) while applying PMF in an urban-industrial setting like Riverside, California. The user must infer the dominant source contributions to these individual factors. Our factor profile (FP) nomenclature is based on the closest explanation of the nature and distribution of emission sources in the region. The source factor names should be treated with caution bearing in mind the physical constraints of the solution and not used to over-explain our interpretation of the region's CH_4 and N_2O inventories.

A seven factor solution has been chosen to optimally explain the variability of the included trace gases. The factors have been named based on our interpretation of the emission "source" categories they represent, with corresponding colors which remain consistent in the discussion across the rest of the paper: evaporative and fugitive (black), dairy and livestock (orange), motor vehicles (red), agricultural + soil management (purple), daytime biogenics + secondary organics (light blue), non-vehicular urban (green) and nighttime anthropogenic + terpene biogenics (navy blue). Figure 2.7 presents the Factor Profile (FP) plots of each factor. The sum of the normalized contributions of the 50 species in each "source" is equal to 1 in the FP plots. Figures 2.8 (a-g) present the diurnal profiles based on mean hourly concentrations (in normalized units) of each PMF factor with standard deviations explaining the variability. The interpretation of the individual FPs is discussed below (in Section 2.3.2). Molar emission rates (ER) of tracers with respect to (w.r.t) one another can be derived for each FP (in Section 2.3.2). These ERs can then be compared to those from previous source-specific and apportionment studies (Table 2.2 through 2.5). The ratio of PMF-derived total CH_4 enhancement to the observed CH_4 enhancements ranges from 0.90 to 0.95 through the whole time series except outliers with really high values (> 500 ppb). For N_2O, the ratio is somewhat lower (0.82 - 0.92) and this is reflected in the higher PMF-derived uncertainties. The apportionment of some N_2O mass into a statistically weak and time-varying factor is discussed in Section 2.3.2.   The general assessment is that PMF analysis is able to reconstruct a majority of the measured enhancements for both CH_4 and N_2O.

2.3.1   Time trends of measured CH4, CO2, CO and N2O

The time series of CH_4, CO_2, CO, and N_2O mixing ratios have been plotted in Figures 2.9 a-d. The diurnal variations of these compounds have been plotted in Figures 2.9 e-h. The color markers in each plot indicate the median wind direction. The daily minima for the three GHGs and CO occur during the late afternoon period when daytime heating, mixing and subsequent

dilution occurs rapidly. The daily minimum values of CH_4 and N_2O were larger than that observed at National Oceanic and Atmospheric Administration's (NOAA) Mauna Loa station (Dlugokencky et al., 2014) by at least 70 ppb and 0.5 ppb, respectively, for this period. This indicates that there are large regional sources of these two GHGs that add to and keep the background mixing ratio levels high. Winds during the highest temperature period between noon and evening (12:00-20:00 hour local time) almost always arrive through the urban core in the northwest. Any PMF factor whose dominant source direction is northwest is likely to contain contributions from VOCs emitted from urban sources, regional sources further upwind or contain contributions from secondary tracers generated from photochemical processing during the day. The three GHGs show a sharp increase during the nighttime when the inversion layer builds up and traps primary emissions close to the ground. For CO, measured concentrations show two distinct peaks in the diurnal plot (Figure 2.9 g). The observed early morning peak in the concentration is a combination of decreased dilution and fresh emissions from the morning motor vehicle traffic. The late evening peak in CO concentrations is not coincident with rush hour and is a result of build-up of evening emissions in the boundary layer that is getting shallower as the night progresses. Figure 2.9 (a) indicates CH_4 enhancements of 500 ppb or more on almost every night with peak mixing ratios exceeding 3000 ppb on several occasions indicating an active methane source(s) in the region. Figure 2.9 (d) shows that peak N_2O mixing ratios rise above 330 ppb on almost every night suggesting large sources in the region. Huge enhancements of CH_4, CO_2 and N_2O (on DOY 157,164 and 165 in Figures 2.9 a, 2.9 b and 2.9 d, respectively) may appear well-correlated to each other due to regional sources emitting into the inversion layer. However, the shapes of the diurnal cycles differ indicating different emission distributions, with the early morning maximum in CH_4 occurring before the maxima for CO_2 and N_2O, and the morning maximum for CO occurring slightly later. These differences in timing allow PMF analysis to differentiate between their contributions into separate factors.

2.3.2   PMF source factors

Factor 1: Evaporative and fugitive emissions

Factor 1 has a chemical signature indicative of evaporative and fugitive losses of VOCs. The FP of this source is dominated by C_3 to C_6 straight-chain and branched alkanes and some cycloalkanes (Figure 2.7). The average diurnal cycle of Factor 1 (Figure 2.8 a) shows a broad peak during late night and early morning hours after which the concentrations begin to decrease as the day proceeds reaching a minimum at sunset before beginning to rise again. This is strong indication of a source containing primary emissions that build up in the shallow pronounced nighttime inversions of southern SJV. The subsequent dilution of primary emissions as the mixed layer expands leads to low concentrations during the daytime.

Most of the propane, n-butane and pentanes signal is apportioned to this factor, but not the typical vehicle emission tracers like isooctane or CO or any of the alkenes or aromatics. Absence of these tracers in the FP suggests this factor is not related to vehicular exhaust and is a combination of non-tailpipe emissions and fugitive losses from petroleum operations. None of the CH_4 signal at the SJV site is apportioned to this factor, but almost all of the small straight-

chain alkanes, exclusively apportion to this factor. This is in agreement with Gentner et al. (2014a) which concluded that VOC emissions from petroleum operations are due to fugitive losses of associated gas from condensate tanks following separation from CH_4. Table 2.2 compares ERs derived from this PMF study for the non-tailpipe (evaporative) and fugitive petroleum operation source factor with those from the Gentner et al. (2014a) study done on the same CalNex dataset using an independent source receptor model with chemical mass balancing and effective variance weighting method, and also to, reports of fugitive emissions from the oil and natural gas sources (Pétron et al., 2012; Gilman et al., 2013) and similar factors produced by other PMF studies (Buzcu and Fraser, 2006; Leuchner and Rappenglück, 2010; Bon et al., 2011). Good agreement of Factor 1 VOC ERs with those from the mentioned studies confirms petroleum operations in Kern County as the major source contributing to this factor. The PMF apportionment indicates that this source factor does not contribute to CH_4 enhancements observed at the SJV site (Figure 2.11 a) and thus most of the 'associated' CH_4 is likely separated from the condensate prior to emission. As mentioned before, a tiny fraction (~ 5 %) of the total input CH_4 enhancement is not resolved into source-apportioned contributions. There could be a minor contribution to CH_4 signal from this source, which is unresolved within the framework of uncertainties in the PMF analysis.

Factor 2: Motor vehicle emissions

Factor 2 has a chemical signature consistent with the tailpipe exhausts of gasoline and diesel motor vehicles. This source factor includes the combustion tracer CO, and other vehicular emissions tracers, such as isooctane (Figure 2.7). Alkenes are a product of incomplete fuel combustion in motor vehicles, and almost all of the propene and a significant portion of the isobutene signal are attributed to this source factor. The diurnal variation of Factor 2 shows two distinctive peaks (Figure 2.8 b). The first peak occurs in the morning between 06:00 and 07:00 and is influenced by morning rush hour traffic, with suppressed mixing allowing vehicle emissions to build up. As the day proceeds, accelerated mixing and dilution (and perhaps chemical processing of reactive VOCs) reduce the enhancements to a minimum by late afternoon. The evening peak mainly occurs as the dilution process slows down after sunset and emissions build up. The increased motor vehicle traffic in the evening adds more emissions to the shrinking boundary layer. This build-up reaches a peak around 22:00 in the night as winds bring in more vehicle emissions to the site from the urban core as seen in the dominant source direction rose plot (Figure 2.10). The occasional high wind events from the northwest (unstable conditions) and the reasonably lesser number of vehicles operating on the roads during the late nighttime hours contribute to the relatively lower levels of enhancements as compared to the peaks on either side of this nighttime period.

Table 2.3 compares selective PMF derived EFs from vehicle emissions factor with the measured gasoline composition collected during CalNex in Bakersfield (Gentner et al., 2012), analysis of gasoline samples from Riverside in Los Angeles basin (Gentner et al., 2009) and ambient VOC emission ratios measured during CalNex at the Pasadena supersite (Borbon et al., 2013). Although, the two Bakersfield studies employ different source apportionment techniques (and so do the studies conducted in the Los Angeles basin), we observe a broad agreement of relative emission rates of vehicular emission tracers. This agreement validates our assertion that Factor 2 represents a broad suite of vehicular tailpipe emissions.

24

The PMF derived CH_4/CO ER in Factor 2 is 0.58 (mol mol^{-1}) and is significantly higher than the range of 0.03 - 0.08 (mol mol^{-1}) calculated from results of a vehicle dynamometer study of 30 different cars and trucks (Nam et al., 2004) and an emission factor of 0.014 (mol mol^{-1}) calculated for SJV district during summer of 2010 using EMFAC, which is ARB's model for estimating emissions from on-road vehicles operating in California (EMFAC, 2011). While it is certainly a possibility that current in-use CH_4 emission factor in the inventory may be an underestimation, it seems more logical that the relatively high proportion of CH_4 signal in the vehicle source factor profile is due to contributions from coincident urban sources (e.g. natural gas leaks) mixed into the vehicle gasoline exhausts resulting in a '*mixing*' phenomena as discussed in Section 2.2.6. In spite of the non-negligible proportion of CH_4 in the Factor 2 source profile, the contribution of the factor to CH_4 enhancements (Figure 2.11 a) at Bakersfield is negligible relative to the dairy and livestock factor.

The state GHG inventory attributes about 18 % of the 2010 statewide N_2O emissions to the on-road transportation sector (CARB 2012). Our PMF analysis shows essentially a negligible enhancement of N_2O associated with the vehicle emission Factor 2 with a PMF derived N_2O/CO ER of 0.00015 (mol mol^{-1}). The EMFAC generated N_2O/CO emission factor in SJV during summer of 2010 is more than 20 times higher at 0.0034 (mol mol^{-1}). The PMF derived 'vehicle emissions' contribution to N_2O is in stark contrast to the inventory and is an important outcome suggesting a significant error in the statewide inventory for N_2O.

Factor 3: Dairy and livestock emissions

Factor 3 has a chemical signature indicative of emissions from dairy operations. This source factor is the largest contributor to CH_4 enhancements (Figure 2.11 a) and a significant portion of the N_2O signal (Figure 2.11 c). The FP also has major contributions from methanol (MeOH) and ethanol (EtOH), with minor contributions from aldehydes and ketones (Figure 2.7). A separate PMF analysis with a broader set of VOC measurements at the same site showed that most of the acetic acid (CH_3COOH) and some formaldehyde (HCHO) signal attributed to this factor as well (Goldstein et al., in prep). All the above-mentioned VOCs are emitted in significant quantities from dairy operations and cattle feedlots (Filipy et al., 2006; Shaw et al., 2007; Ngwabie et al., 2008; Chung et al., 2010)). About 70 - 90 % of the diurnal CH_4 signal is attributed to this factor (Figure 2.11 a) depending on the time of day. From propagation of errors, an uncertainty of 29 % is determined in the diurnal CH_4 enhancements in Factor 3. This source factor contributes about 60 - 70 % of the total N_2O daily enhancements as seen in Figure 2.11 (c) with a confidence interval of 33 % the PMF-derived enhancements. The dominant wind rose plot (Figure 2.10) shows dominant contributions when the winds are easterly and south-easterly which coincides with the downslope flow occurring at nighttime. This indicates that these emissions are mostly primary and their build-up in the suppressed nighttime boundary layer rather than increased emissions is responsible for the feature we observe in the dominant wind rose plot.

Comparing the Factor 3 profile to dairy source profiles from various studies is challenging. A dairy is, in essence, a collection of area sources with distinct emission pathways and chemical characteristics. Hence, a lot of dairy studies do not look at facility-wide emissions instead focusing on specific area sources within the facility. In contrast, PMF captures the covariance of

CH$_4$, N$_2$O, and VOCs emitted from the ensemble source as downwind plumes from dairies arrive at the site. Table 2.4 compares the PMF derived ERs of CH$_4$ w.r.t MeOH and EtOH with those from other studies. Previously, cow chamber experiments (Shaw et al., 2007; Sun et al., 2008) have measured emissions from ruminants and their fresh manure; emissions have also been studied in a German cowshed (Ngwabie et al., 2008) and ERs have been derived from SJV dairy plumes sampled from aircrafts (Gentner et al., 2014a; Guha et al., in prep). Since enteric fermentation and waste manure is the predominant CH$_4$ source in dairies, CH$_4$ emission rates calculated by Shaw et al. (2007) are representative of a whole facility. However, their MeOH / CH$_4$ ratios are lower than those measured by PMF and aircraft studies. Animal feed and silage are the dominant source of many VOCs including MeOH and EtOH (Alanis et al., 2010; Howard et al., 2010) and the ratios in (Shaw et al., 2007) do not reflect these emissions. In (Ngwabie et al., 2008), experiments were performed in cold winter conditions (-2°C to 8°C) when temperature dependent VOC emissions from silage and feed are at a minimum. The authors comment that MeOH emissions from California dairies is likely higher, as the alfalfa-based feed is a big source of MeOH owing to its high pectin content (Galbally and Kirstine, 2002). These observations offer explanation why MeOH / CH$_4$ ratios in these studies are lower than PMF derived ratios. The PMF range for EtOH / CH$_4$ ER for Factor 3 agrees with the slope derived from ground-site data (Gentner et al., 2014a) and is similar, but somewhat larger than the German dairy study (Ngwabie et al., 2008) . Miller and Varel (2001) and Filipy et al. (2006) did not measure CH$_4$ emission rates so a direct derivation of ER w.r.t CH$_4$ is not possible. These studies, however, reported EtOH emission rates (from dairies and feedlots in United States) which are used to derive ERs w.r.t to CH$_4$ using an averaged CH$_4$ emission rate from Shaw et al. (2007). Using this method, we get ERs that are comparable to PMF derived ER of CH$_4$ / EtOH (Table 2.4). Hence, we demonstrate within reasonable terms that the relative fractions of masses in Factor 3 are consistent with CH$_4$ and VOC emissions from dairies.

Enteric fermentation is a part of the normal digestive process of livestock such as cows, and is a large source of CH$_4$ while the storage and management of animal manure in lagoons or holding tanks is also a major source of CH$_4$. According to the state GHG inventory (CARB, 2013), ~ 58 % of the statewide CH$_4$ emissions results from a combination of these two processes. N$_2$O is also emitted during the breakdown of nitrogen in livestock manure and urine and accounts for about 10 % of the statewide N$_2$O emission inventory. Kern County has a big dairy industry with about 160,000 milk cows representing 10 % of the dairy livestock of the state in 2012 and another 330,000 heads of cattle for beef (KernAg, 2011; CASR, 2013). The dominant contributions to CH$_4$ and N$_2$O signal and the general agreement of dairy ERs with PMF ERs from Factor 3 indicate that the extensive cattle operations in the county are a big source of these emissions. We do find the proportion of regional N$_2$O enhancements attributed to this sector to be a much larger proportion of total emissions as compared to the state inventory.

Factor 4: Agricultural and soil management emissions

The chemical profile of Factor 4 is a mix of emissions from agricultural activities around the site. Factor 4 includes a major portion of the N$_2$O signal along with a number of VOCs that have crop / plant signatures like methacrolein, methyl ethyl ketone (Jordan et al., 2009; McKinney et al., 2011), methanol and acetone (Goldstein and Schade, 2000; Hu et al., 2013; Gentner et al., 2014b) (Figure 2.7). While many of these oxygenated VOCs have several prominent sources,

studies have reported substantial simultaneous emissions from natural vegetation and agricultural crops. At a rural site in the Northeast, Jordan et al. (2009) reported high concentrations of oxygenated VOCs and correlations between the diurnal concentrations of acetone, methanol, and methyl ethyl ketone. Kern County is one of the most prolific agricultural counties in California. The four main crops grown (by value as well as acreage) in 2010 were almonds, grapes, citrus and pistachios (KernAg, 2011). Table 2.5 compares the PMF derived ERs for acetone/MeOH from Factor 4 with ratios of basal emission factors (BEFs) from crop-specific greenhouse and field measurements (Fares et al., 2011, 2012; Gentner et al., 2014b). The good agreement of the ratios confirms that the FP of Factor 4 is an aggregate of biogenic VOC emissions from the agricultural sector. Nitrous oxide is emitted when nitrogen is added to soil through use of synthetic fertilizers and animal manure, while crops and plants are responsible for the VOC emissions. Hence this source factor is a combination of collocated sources (soils and crops). The PMF solution to this factor has uncertainties greater than those for other factors (Figure 2.6). This is potentially because not all crops emit the same combination of VOCs nor are all agricultural fields fertilized at the same time. The existence of this statistically weak factor is confirmed by bootstrapping runs (Section 2.2.6) and numerous PMF trials, all of which produce a distinct factor with N_2O as a dominant contributor along with certain biogenic VOCs, though often in varying proportions. CO_2 is not included in the PMF analysis reported in the paper, but PMF runs involving CO_2 indicate that most of the CO_2 is apportioned to this factor. Plant and soil respiration (especially during the night) is a major source of CO_2 and the apportionment of CO_2 to Factor 4 confirms the nature of this source. The temporal correlation between CO_2 and N_2O is also evident in their average diurnal cycles (Figures 2.9 f and h), which have a coincident early morning peak. The absence of monoterpenes from the FP of this factor can be explained by their shorter atmospheric lifetimes compared to VOCs like acetone and MeOH and the rapid daytime mixing which dilutes the terpenoid emissions arriving at the site during the day. At nights, when the atmospheric dilution has been reduced to a low, monoterpenes emissions from agriculture are more likely to get apportioned into a separate source factor dominant during nighttime, when temperature-sensitive biogenic emissions of MeOH and acetone can be expected to be a minor constituent in the FP (see Factor 7 description).

Factor 4 is a significant source of GHGs contributing about 20 - 25 % of the total N_2O enhancements in the diurnal cycle (Figure 2.11 c) with a relatively large 1σ confidence interval of 70 % of the PMF-derived enhancements. Kern County is one of the premier agricultural counties of California accounting for $4.2 billion (about 18 %) of the total agricultural revenue from fruits and nuts, vegetables and field crops (KernAg, 2011; CASR, 2013) and is also the biggest consumer of synthetic fertilizers. Agricultural soil management accounts for about 60 % of the statewide N_2O emissions inventory (CARB, 2013). Our assessment of diurnal source distribution of N_2O emissions from the agriculture source factor (Figure 2.11 c) is consistent with the inventory estimates from agricultural and soil management sector.

Factor 5: Daytime biogenics and secondary organics

The chemical composition and diurnal profile of Factor 5 points to a source whose emissions are either primary biogenic VOCs with temperature-dependent emissions (e.g. isoprene), or products of photochemical oxidation of primary VOCs (e.g. acetone) (Figure 2.7). Isoprene is a dominant component of the source FP and is mostly apportioned to Factor 5. Figure 2.8 (c)

shows a steady increase in the PMF factor mass concentration during the daytime hours that hits a peak during afternoons indicating that this source is dependent on sunlight and temperature. Figure 2.10 confirms that the contribution of this source factor peaks during the day when winds are primarily from the northwest. Potential source contributions come from oak forests on the foothills on the western edge of the SJV or scattered isoprene producing plants in the SJV (note that most crops do not emit significant amounts of isoprene). Factor 5 includes contribution from VOCs that have primary light and temperature driven (crops), as well as secondary sources in the Central Valley e.g. acetone (Goldstein and Schade, 2000), methanol (Gentner et al., 2014b) and aldehydes. A similar PMF analysis with a different objective (Goldstein et al., in prep) shows that secondary organics like glyoxal, formaldehyde and formic acid mostly apportion to Factor 5. The CO apportioned to this factor could potentially be a product of mobile and/or stationary combustion co-located or up/downwind of the biogenic VOC source. CO can also come from coincident isoprene oxidation (Hudman et al., 2008). This daytime source is not responsible for any of the observed CH_4 and N_2O enhancements.

Factor 6: Non-vehicular/miscellaneous urban emissions

The chemical signature of Factor 6 is composed of VOCs associated with an array of applications and processes, including solvents, fumigants, industrial-byproducts, etc. The diurnal profile of Factor 6 (Figure 2.8 e) is somewhat different from that of evaporative and fugitive source (Figure 2.8 a) and dairies (Figure 2.8 c) in that even during the middle of the day when vertical mixing is at its strongest, the enhancements contributing to the factor are substantial. This suggests this is a constantly emitting source(s) in close proximity to the site and hence most likely located within the urban core. This is also confirmed by the dominant wind direction plot (Figure 2.10) as the peak concentration directions are variable, all-around the site, and dominate at low wind speeds, all of which are indicators of a local but ubiquitous source. The FP has CO as an important component but relative absence of fugitive source markers (e.g. light alkanes) and vehicle emissions tracers (e.g. isooctane, cycloalkanes etc.) indicate that the origin of this source factor is potentially non-mobile combustion. Also present in a major proportion is carbon disulfide (CS_2), chlorinated alkanes like 1,2-dichloroethane and 1,2-dichlorpropane, isobutene (product of incomplete combustion), and minor contributions from aromatics and aldehydes (Figure 2.7). There is a myriad of potential sources that could be contributing to this factor, and we don't have specific tracers or other information to ascribe it to a single source or group of sources. Hence we call Factor 6 an 'urban emissions source'. There is a very minor CH_4 contribution from this factor which results in a tiny and negligible contribution to the PMF source apportionment of CH_4 (Figure 2.11 a). The source factor does not contribute to the N_2O enhancements.

Factor 7: Nighttime anthropogenic and terpene biogenic emissions

Factor 7 is primarily composed of biogenic compounds belonging to the terpene family and p-cymene (Figure 2.7). Factor 7 mostly influences the site during late night and early morning hours (Figure 2.8 g), when nighttime downslope flows usually dominate and bring winds from the east and south to the site. This is also confirmed by the dominant wind directions for this source factor in Figure 2.10. The entire flow path from the base of the foothills to the site is covered with agricultural crops emitting into a shallow nighttime boundary layer. These crops

28

include grapes, almonds, citrus and pistachios, which are the top four agricultural commodities grown in the county (KernAg, 2011; CASR, 2013), and these produce considerable monoterpenoid emissions (Fares et al., 2012; Gentner et al., 2014b). The spatial distribution of terpenoid compounds from statistical source footprint derived from FLEXPART back-trajectories is consistent with the location of croplands in southern SJV (Gentner et al., 2014b). Biogenic VOCs emitted from forests in the foothills are likely minor contributors to the downslope flows arriving at the site owing to their lifetime and distance (> 50 km) (Tanner and Zielinska, 1994).

Following the rapid rise in enhancements in the early morning hours, contributions of Factor 7 to total signal decrease rapidly when the flow moves to more typical daytime wind directions (Figure 2.8 g). A nearby source (e.g. the waste water treatment plant of Bakersfield), that is in the upwind direction of the site for only a certain part of the diurnal cycle, is expected to be more directionally constrained and emissions profile from such a source will look similar to the diurnal profile of Factor 7. Among source factors which contain non-negligible fractional contribution of both CH_4 and N_2O (i.e. dairies, agriculture and soil management, and Factor 7), the PMF derived CH_4/N_2O ER of 42 ± 20 (gC gC^{-1}) from Factor 7 is most similar to the bottom-up inventory emission factor of 56 (gC gC^{-1}) for waste water treatment in Kern County (KernGHG, 2012). Given the proximity of the waste water treatment facility and previous observations of GHGs from them, it is possible that there is a minor but noticeable contribution (~ 5 %) to CH_4 and N_2O enhancements to the nighttime source (Figures 2.11 a and c).

2.4   Summary

This study demonstrates the potential of the PMF technique to apportion atmospheric gas-phase observations of CH_4 and N_2O into source categories using a broad array of tracers. PMF is not commonly employed to perform for source attribution of these GHGs because studies generally lack simultaneous measurements of specific source-markers. Applying this statistical technique on a GHG-VOC unified data set, well-represented by a broad suite of VOC classes, allows a set of compounds acting as source markers to be partitioned into separate profiles leading to easier identification of their sources.

We provide clear analysis that dairy and livestock operations are the largest sources of emissions in the Bakersfield region accounting for a majority of the CH_4 (70 - 90 %) and N_2O (50 - 60 %) emissions. As per the CARB inventory (Figures 1.1; Chapter 1), dairy operations are the dominant source of non-CO_2 GHGs in the state. Our analysis agrees with the broad trend for CH_4 although we find higher emissions of N_2O attributed to the dairy and livestock sector than the inventory estimates. In the recent past, a number of top-down CH_4 and N_2O emission studies in the Central Valley have reported underestimation of the non-CO_2 GHG inventory (Zhao et al., 2009; Santoni et al., 2012; Jeong et al., 2012a, 2012b; Miller et al., 2013). These studies attribute a majority of this underestimation to the dairy sector. Our results emphasize the significance of this sector in the SJV although we do not derive total emission estimates to compare directly with the inventory.

The contribution of fugitive emissions from the oil and gas industry in Bakersfield to CH_4 emissions is found to be negligible especially in the presence of the much larger dairy source. The PMF analysis, though, clearly establishes an evaporative and fugitive source that contributes to emissions of lighter hydrocarbons. This supports the conclusion that the majority of the CH_4 is being separated at the point of extraction from the 'associated gas' and is not released with fugitive emissions (Gentner et al., 2014a). Kern County produces 75 % of all the oil produced in California ($\sim$ 6 % of US production) and has 81 % of the state's 60000+ active oil wells (CDC, 2013). There is, however, a surprising scarcity of measured data to quantify the estimates of fugitive CH_4 from the prolific oil fields in the County and validate the bottom-up, activity data-based inventory. Currently, fugitive emissions from fossil fuel extraction and distribution contribute $\sim$ 5 % to the County's CH_4 emissions inventory (KernGHG, 2012). Nationwide, a number of recent studies have reported significantly higher emissions of fugitive CH_4 from oil and gas operations in other regions (Pétron et al., 2012; Karion et al., 2013; Miller et al., 2013; Kort et al., 2014). The PMF apportionment in this study is consistent with the fraction of fugitive CH_4 emissions in the inventory ($<$ 5 %) but the PMF method in itself is limited in accurate partitioning of minor sources.

We find that the vehicle emissions source factor identified in this study makes no detectable contribution to observed N_2O enhancements. Our findings do not agree with the significant contribution ($\sim$ 18 %) of the transportation sector to the state's N_2O emission inventory (CAR, 2013). Vehicle dynamometer studies have indicated rapidly declining N_2O emission factors with advancement in catalyst technologies, declining sulfur content in fuel and newer technology vehicles (Huai et al., 2004). N_2O emissions from California vehicles, required to meet progressively stringent emission standards, are expected to decline and should have a minimal contribution to the CARB inventory in this decade. However, it seems the updates to the mobile N_2O emissions inventory is not keeping in pace with the improvements in vehicle catalyst technologies and corresponding decline in tailpipe N_2O emissions. Bakersfield is a fairly large population urban region ($\sim$ 500,000) and the essentially non-existent contribution of the PMF vehicle emissions source to the N_2O apportionment and large divergence of the PMF derived N_2O / CO ER from the state inventory emission factor for motor vehicles is a significant outcome pointing to overestimation of N_2O from motor vehicles in the inventory.

2.5   References

Alanis, P., Ashkan, S., Krauter, C., Campbell, S. and Hasson, A. S.: Emissions of volatile fatty acids from feed at dairy facilities, Atmos. Environ., 44(39), 5084–5092, doi:10.1016/j.atmosenv.2010.09.017, 2010.

Bao, J.-W., Michelson, S. a., Persson, P. O. G., Djalalova, I. V. and Wilczak, J. M.: Observed and WRF-Simulated Low-Level Winds in a High-Ozone Episode during the Central California Ozone Study, J. Appl. Meteorol. Climatol., 47(9), 2372–2394, doi:10.1175/2008JAMC1822.1, 2007.

Beaver, S. and Palazoglu, A.: Influence of synoptic and mesoscale meteorology on ozone pollution potential for San Joaquin Valley of California, Atmos. Environ., 43(10), 1779–1788, doi:10.1016/j.atmosenv.2008.12.034, 2009.

Bon, D. M., Ulbrich, I. M., de Gouw, J. a., Warneke, C., Kuster, W. C., Alexander, M. L., Baker, a., Beyersdorf, a. J., Blake, D., Fall, R., Jimenez, J. L., Herndon, S. C., Huey, L. G., Knighton, W. B., Ortega, J., Springston, S. and Vargas, O.: Measurements of volatile organic compounds at a suburban ground site (T1) in Mexico City during the MILAGRO 2006 campaign: measurement comparison, emission ratios, and source attribution, Atmos. Chem. Phys., 11(6), 2399–2421, doi:10.5194/acp-11-2399-2011, 2011.

Borbon, A., Gilman, J. B., Kuster, W. C., Grand, N., Chevaillier, S., Colomb, a., Dolgorouky, C., Gros, V., Lopez, M., Sarda-Esteve, R., Holloway, J., Stutz, J., Petetin, H., McKeen, S., Beekmann, M., Warneke, C., Parrish, D. D. and de Gouw, J. a.: Emission ratios of anthropogenic volatile organic compounds in northern mid-latitude megacities: Observations versus emission inventories in Los Angeles and Paris, J. Geophys. Res. Atmos., 118(4), 2041–2057, doi:10.1002/jgrd.50059, 2013.

Brown, S. G., Frankel, A. and Hafner, H. R.: Source apportionment of VOCs in the Los Angeles area using positive matrix factorization, Atmos. Environ., 41(2), 227–237, doi:10.1016/j.atmosenv.2006.08.021, 2007.

Buzcu, B., and M. P. Fraser (2006), Source identification and apportionment of volatile organic compounds in Houston, TX, Atmos. Environ., 40(13), 2385–2400, doi:10.1016/j.atmosenv.2005.12.020.

CARB (2013), California Greenhouse Gas Inventory for 2000-2012 - by IPCC Category. http://www.arb.ca.gov/cc/inventory/data/data.htm. accessesd on September 23, 2014.

CASR (2011), California Agricultural Statistics Review, 2013-14. California Department of Food and Agriculture, Sacramento, CA.

CDC (2013), 2012 Preliminary Report Of California Oil And Gas Production Statistics. California Department of Conservation, Division of Oil, Gas and Geothermal Resources. ftp://ftp.consrv.ca.gov/pub/oil/annual_reports/2012/PR03_PreAnnual_2012.pdf. accessed on September 23, 2014.

Chung, M. Y., M. Beene, S. Ashkan, C. Krauter, and A. S. Hasson (2010), Evaluation of non-enteric sources of non-methane volatile organic compound (NMVOC) emissions from dairies, Atmos. Environ., 44(6), 786–794, doi:10.1016/j.atmosenv.2009.11.033.

Comero, S., Capitani, L., and Gawlik, B. M.: Positive Matrix Factorization - An introduction to the chemometric evaluation of environmental monitoring data using PMF, JRC Scientific and Technical Reports, EUR 23946 EN-2009.

Crutzen, P. J., Mosier, a. R., Smith, K. a. and Winiwarter, W.: N$_2$O release from agro-biofuel production negates global warming reduction by replacing fossil fuels, Atmos. Chem. Phys. Discuss., 7(4), 11191–11205, doi:10.5194/acpd-7-11191-2007, 2007.

Denman, K.L., G. Brasseur, A. Chidthaisong, P. Ciais, P.M. Cox, R.E. Dickinson, D. Hauglustaine, C. Heinze, E. Holland, D. Jacob, U. Lohmann, S Ramachandran, P.L. da Silva Dias, S.C. Wofsy and X. Zhang, 2007: Couplings Between Changes in the Climate System and Biogeochemistry. In: Climate Change 2007: The Physical Science Basis. Contribution of Working Group I to the Fourth Assessment Report of the Intergovernmental Panel on Climate Change [Solomon, S., D. Qin, M. Manning, Z. Chen, M. Marquis, K.B. Averyt, M.Tignor and H.L. Miller (eds.)]. Cambridge University Press, Cambridge, United Kingdom and New York, NY, USA.

Dlugokencky, E.J., A.M. Crotwell, P.M. Lang, K.A. Masarie (2014), Atmospheric Methane Dry Air Mole Fractions from quasi-continuous measurements at Barrow, Alaska and Mauna Loa, Hawaii, 1986-2013, Version: 2014-08-12, Path: ftp://ftp.cmdl.noaa.gov/ccg/ch4/in-situ/.

EMFAC (2011). 2011 Mobile Source Emission Inventory - Current methods and data. California Air Resources Board, Sacramento, CA. http://www.arb.ca.gov/msei/modeling.htm. accessed on September 20, 2014.

Fares, S., Gentner, D. R., Park, J.-H., Ormeno, E., Karlik, J. and Goldstein, A. H.: Biogenic emissions from Citrus species in California, Atmos. Environ., 45(27), 4557–4568, doi:10.1016/j.atmosenv.2011.05.066, 2011.

Fares, S., Park, J.-H., Gentner, D. R., Weber, R., Ormeño, E., Karlik, J. and Goldstein, a. H.: Seasonal cycles of biogenic volatile organic compound fluxes and concentrations in a California citrus orchard, Atmos. Chem. Phys., 12(20), 9865–9880, doi:10.5194/acp-12-9865-2012, 2012.

Filipy, J., B. Rumburg, G. Mount, H. Westberg, and B. Lamb (2006), Identification and quantification of volatile organic compounds from a dairy, Atmos. Environ., 40(8), 1480–1494, doi:10.1016/j.atmosenv.2005.10.048.

Fischer, M.L., C. Zhao., W.J. Riley, and A.C. Andrews. 2009. Observation of CH4 and other Non-CO2 Green House Gas Emissions from California. California Energy Commission, PIER Energy-Related Environmental Research. (Report # 500-2009-096).

Forster, P. ., Ramaswamy, V. ., Artaxo, P. ., Berntsen, T. ., Betts, R. ., Fahey, D. W. ., Haywood, J. ., Lean, J. ., Lowe, D. C. ., Myhre, G. ., Nganga, J. ., Prinn, R. ., Raga, G. ., Schulz, M. . and Dorland, R. V.: 2007: Changes in Atmospheric Constituents and in Radiative Forcing, in Climate Change 2007: The Physical Science Basis. Contribution of Working Group I to the Fourth Assessment Report of the Intergovernmental Panel on Climate Change, edited by S. Solomon, D. Qin, M. Manning, Z. Chen, M. Marquis, K. B. Averyt, M.Tignor, and H. L. Miller, p. 996, Cambridge University Press. [online] Available from: http://www.ipcc.ch/publications_and_data/ar4/wg1/en/ch2.html, 2007.

Galbally, I. E., and Kirstine, W.: The Production of Methanol by Flowering Plants and the Global Cycle of Methanol, Journal of Atmospheric Chemistry, 43, 195-229, 10.1023/A:1020684815474, 2002.Galloway, J. N., Townsend, A. R., Erisman, J. W., Bekunda, M., Cai, Z., Freney, J. R., Martinelli, L. a, Seitzinger, S. P. and Sutton, M. a: Transformation of the nitrogen cycle: recent trends, questions, and potential solutions., Science, 320(5878), 889–92, doi:10.1126/science.1136674, 2008.

Galloway, J. N., A. R. Townsend, J. W. Erisman, M. Bekunda, Z. Cai, J. R. Freney, L. a Martinelli, S. P. Seitzinger, and M. a Sutton (2008), Transformation of the nitrogen cycle: recent trends, questions, and potential solutions., Science, 320(5878), 889–92, doi:10.1126/science.1136674.

Gentner, D. R., Ford, T. B., Guha, a., Boulanger, K., Brioude, J., Angevine, W. M., de Gouw, J. a., Warneke, C., Gilman, J. B., Ryerson, T. B., Peischl, J., Meinardi, S., Blake, D. R., Atlas, E., Lonneman, W. a., Kleindienst, T. E., Beaver, M. R., Clair, J. M. St., Wennberg, P. O., VandenBoer, T. C., Markovic, M. Z., Murphy, J. G., Harley, R. a. and Goldstein, a. H.: Emissions of organic carbon and methane from petroleum and dairy operations in California's San Joaquin Valley, Atmos. Chem. Phys., 14(10), 4955–4978, doi:10.5194/acp-14-4955-2014, 2014a.

Gentner, D. R., Harley, R. a, Miller, A. M. and Goldstein, A. H.: Diurnal and seasonal variability of gasoline-related volatile organic compound emissions in Riverside, California., Environ. Sci. Technol., 43(12), 4247–52 [online] Available from: http://www.ncbi.nlm.nih.gov/pubmed/19603630, 2009.

Gentner, D. R., Isaacman, G., Worton, D. R., Chan, A. W. H., Dallmann, T. R., Davis, L., Liu, S., Day, D. A., Russell, L. M., Wilson, K. R., Weber, R., Guha, A. and Harley, R. A.: Elucidating secondary organic aerosol from diesel and gasoline vehicles through detailed characterization of organic carbon emissions, , doi:10.1073/pnas.1212272109/-/DCSupplemental.www.pnas.org/cgi/doi/10.1073/pnas.1212272109, 2012.

Gentner, D. R., Ormeño, E., Fares, S., Ford, T. B., Weber, R., Park, J.-H., Brioude, J., Angevine, W. M., Karlik, J. F. and Goldstein, a. H.: Emissions of terpenoids, benzenoids, and other biogenic gas-phase organic compounds from agricultural crops and their potential implications for air quality, Atmos. Chem. Phys., 14(11), 5393–5413, doi:10.5194/acp-14-5393-2014, 2014b.

Gilman, J. B., B. M. Lerner, W. C. Kuster, and J. a de Gouw (2013), Source signature of volatile organic compounds from oil and natural gas operations in northeastern colorado., Environ. Sci. Technol., 47(3), 1297–305, doi:10.1021/es304119a.

Goldstein, A. H. and Schade, G. W.: Quantifying biogenic and anthropogenic contributions to acetone mixing ratios in a rural environment, Atmos. Environ., 34(29-30), 4997–5006, doi:10.1016/S1352-2310(00)00321-6, 2000.

Goldstein, A. H. et al.: Source apportionment of OH reactivity at Bakersfield Positive Matrix Factorization (PMF) during CalNex 2010, *in preparation*.

Guha et al.: Identifying and mapping methane (CH_4) sources over California from mixing ratio, airborne flux and VOC source tracer measurements, *in preparation*.

Hendriks, D. M. D., a. J. Dolman, M. K. van der Molen, and J. van Huissteden (2008), A compact and stable eddy covariance set-up for methane measurements using off-axis integrated cavity output spectroscopy, Atmos. Chem. Phys., 8(2), 431–443, doi:10.5194/acp-8-431-2008.

Hopke, P.: A guide to positive matrix factorization, Work. UNMIX PMF as Appl. to PM2, 1–16 [online] Available from: ftp://128.153.5.141/users/h/o/hopkepk/IAEA/PMF-Guidance.pdf (Accessed 13 March 2013), 2000.

Howard, C. J., Kumar, A., Malkina, I., Mitloehner, F., Green, P. G., Flocchini, R. G. and Kleeman, M. J.: Reactive organic gas emissions from livestock feed contribute significantly to ozone production in central California., Environ. Sci. Technol., 44(7), 2309–14, doi:10.1021/es902864u, 2010.

Hsu, Y.-K., VanCuren, T., Park, S., Jakober, C., Herner, J., FitzGibbon, M., Blake, D. R. and Parrish, D. D.: Methane emissions inventory verification in southern California, Atmos. Environ., 44(1), 1–7, doi:10.1016/j.atmosenv.2009.10.002, 2010.

Hu, L., D. B. Millet, S. Y. Kim, K. C. Wells, T. J. Griffis, E. V. Fischer, D. Helmig, J. Hueber, and a. J. Curtis (2013), North American acetone sources determined from tall tower measurements and inverse modeling, Atmos. Chem. Phys., 13(6), 3379–3392, doi:10.5194/acp-13-3379-2013.

Huai, T., Durbin, T. D., Wayne Miller, J. and Norbeck, J. M.: Estimates of the emission rates of nitrous oxide from light-duty vehicles using different chassis dynamometer test cycles, Atmos. Environ., 38(38), 6621–6629, doi:10.1016/j.atmosenv.2004.07.007, 2004.

Hudman, R. C., Murray, L. T., Jacob, D. J., Millet, D. B., Turquety, S., Wu, S., Blake, D. R., Goldstein, a. H., Holloway, J. and Sachse, G. W.: Biogenic versus anthropogenic sources of CO in the United States, Geophys. Res. Lett., 35(4), L04801, doi:10.1029/2007GL032393, 2008.

Jeong, S., C. Zhao, A. E. Andrews, L. Bianco, J. M. Wilczak, and M. L. Fischer (2012a), Seasonal variation of CH 4 emissions from central California, J. Geophys. Res., 117(D11), D11306, doi:10.1029/2011JD016896.

Jeong, S., C. Zhao, A. E. Andrews, E. J. Dlugokencky, C. Sweeney, L. Bianco, J. M. Wilczak, and M. L. Fischer (2012b), Seasonal variations in N 2 O emissions from central California, Geophys. Res. Lett., 39(16), n/a–n/a, doi:10.1029/2012GL052307.

Jordan, C., Fitz, E., Hagan, T., Sive, B., Frinak, E., Haase, K., Cottrell, L., Buckley, S. and Talbot, R.: and Physics Long-term study of VOCs measured with PTR-MS at a rural site in New Hampshire with urban influences, , (Table 1), 4677–4697, 2009.

Karion, A., Sweeney, C., Pétron, G., Frost, G., Michael Hardesty, R., Kofler, J., Miller, B. R., Newberger, T., Wolter, S., Banta, R., Brewer, A., Dlugokencky, E., Lang, P., Montzka, S. a., Schnell, R., Tans, P., Trainer, M., Zamora, R. and Conley, S.: Methane emissions estimate from airborne measurements over a western United States natural gas field, Geophys. Res. Lett., 40(16), 4393–4397, doi:10.1002/grl.50811, 2013.

KernGHG (2012), Kern County Communitywide Greenhouse Gas Emission Inventory, Methodology Documents Volume 2; Final Report - May 2012. Prepared by San Joaquin Air Pollution Control District for Kern County Planning and Community Development. http://www.kerncog.org/climate-change.

KernAg (2010). 2010 Kern County Agricultural Crop Report. Department of Agriculture and Measurement Standards. http://www.kernag.com/caap/crop-reports/crop10_19/crop2010.pdf. accessed on September 22 2014.

Kim, E., Hopke, P. K. and Edgerton, E. S.: Improving source identification of Atlanta aerosol using temperature resolved carbon fractions in positive matrix factorization, Atmos. Environ., 38(20), 3349–3362, doi:10.1016/j.atmosenv.2004.03.012, 2004.

Kort, E. A., C. Frankenberg, K. R. Costigan, R. Lindenmaier, M. K. Dubey, and D. Wunch (2014), Four corners: The largest US methane anomaly viewed from space, Geophys. Res. Lett., 41, 6898–6903, doi:10.1002/2014GL061503.

Lee, E., Chan, C. K. and Paatero, P.: Application of positive matrix factorization in source apportionment of particulate pollutants in Hong Kong, Atmos. Environ., 33(19), 3201–3212, doi:10.1016/S1352-2310(99)00113-2, 1999.

Leuchner, M., and B. Rappenglück (2010), VOC source–receptor relationships in Houston during TexAQS-II, Atmos. Environ., 44(33), 4056–4067, doi:10.1016/j.atmosenv.2009.02.029.

McKinney, K. a., Lee, B. H., Vasta, a., Pho, T. V. and Munger, J. W.: Emissions of isoprenoids and oxygenated biogenic volatile organic compounds from a New England mixed forest, Atmos. Chem. Phys., 11(10), 4807–4831, doi:10.5194/acp-11-4807-2011, 2011.

McMillan, A. M. S., Goulden, M. L. and Tyler, S. C.: Stoichiometry of CH_4 and CO_2 flux in a California rice paddy, J. Geophys. Res., 112(G1), G01008, doi:10.1029/2006JG000198, 2007.

Miller, D. N., and Varel, V. H.: In vitro study of the biochemical origin and production limits of odorous compounds in cattle feedlots, Journal of Animal Science, 79, 2949-2956, 2001.

Miller, S. M., Wofsy, S. C., Michalak, A. M., Kort, E. a, Andrews, A. E., Biraud, S. C., Dlugokencky, E. J., Eluszkiewicz, J., Fischer, M. L., Janssens-Maenhout, G., Miller, B. R., Miller, J. B., Montzka, S. a, Nehrkorn, T. and Sweeney, C.: Anthropogenic emissions of methane in the United States., Proc. Natl. Acad. Sci. U. S. A., 110(50), 20018–22, doi:10.1073/pnas.1314392110, 2013.

Montzka, S. a, Dlugokencky, E. J. and Butler, J. H.: Non-CO2 greenhouse gases and climate change., Nature, 476(7358), 43–50, doi:10.1038/nature10322, 2011.

Nam, E., Jensen, T. and Wallington, T.: Methane emissions from vehicles, Environ. Sci. …, 38(7), 2005–2010 [online] Available from: http://pubs.acs.org/doi/abs/10.1021/es034837g (Accessed 16 April 2013), 2004.

Norris, G., Vedantham, R., Wade, K., Brown, S., Prouty, J., and Foley, C.: EPA Positive Matrix Factorization (PMF) 3.0 Fundamentals and User Guide, Washington DC, USA, 2008.

Ngwabie, N. M., Schade, G. W., Custer, T. G., Linke, S. and Hinz, T.: Abundances and Flux Estimates of Volatile Organic Compounds from a Dairy Cowshed in Germany, J. Environ. Qual., 37(2), 565, doi:10.2134/jeq2006.0417, 2008.

O'Keefe, A. (1998), Integrated cavity output analysis of ultra-weak absorption, Chem. Phys. Lett. 293, 331-336 (1998).

Owen, J. J. and Silver, W. L.: Greenhouse gas emissions from dairy manure management: a review of field-based studies., Glob. Chang. Biol., doi:10.1111/gcb.12687, 2014.

Paatero, P. (1997), Least squares formulation of robust non-negative factor analysis, Chemom. Intell. Lab. Syst., 37(1), 23–35, doi:10.1016/S0169-7439(96)00044-5.

Paatero, P., Hopke, P. K., Song, X.-H. and Ramadan, Z.: Understanding and controlling rotations in factor analytic models, Chemom. Intell. Lab. Syst., 60(1-2), 253–264, doi:10.1016/S0169-7439(01)00200-3, 2002.

Paatero, P. and Tapper, U.: Analysis of different modes of factor analysis as least squares fit problems, Chemom. Intell. Lab. Syst., 18(2), 183–194, doi:10.1016/0169-7439(93)80055-M, 1993.

Paatero, P., and U. Tapper (1994), Positive matrix factorization: A non-negative factor model with optimal utilization of error estimates of data values, Environmetrics, 5(April 1993), 111–126.

Pacala, Stephen W., et al.(2010): Verifying Greenhouse Gas Emissions: Methods to Support International Climate Agreements, The National Academies Press, Washington, DC, 124 pp., 2010.

Parameswaran, K. R., D. I. Rosen, M. G. Allen, A. M. Ganz, and T. H. Risby (2009), Off-axis integrated cavity output spectroscopy with a mid-infrared interband cascade laser for real-time breath ethane measurements., Appl. Opt., 48(4), B73–9.

Paul, J. B., Scherer, J. J., O'Keefe, A., Lapson, L., Anderson, J. R., Gmachl, C. F., Capasso, F., and Cho, A. Y.: Infrared cavity ringdown and integrated cavity output spectroscopy for trace species monitoring, 2002, 1-11, Proc. SPIE 4577, Vibrational Spectroscopy-based Sensor Systems, 1 (February 13, 2002); doi:10.1117/12.455722

Peischl, J., Ryerson, T. B., Brioude, J., Aikin, K. C., Andrews, a. E., Atlas, E., Blake, D., Daube, B. C., de Gouw, J. a., Dlugokencky, E., Frost, G. J., Gentner, D. R., Gilman, J. B., Goldstein, a. H., Harley, R. a., Holloway, J. S., Kofler, J., Kuster, W. C., Lang, P. M., Novelli, P. C., Santoni, G. W., Trainer, M., Wofsy, S. C. and Parrish, D. D.: Quantifying sources of methane using light alkanes in the Los Angeles basin, California, J. Geophys. Res. Atmos., 118(10), 4974–4990, doi:10.1002/jgrd.50413, 2013.

Peischl, J., Ryerson, T. B., Holloway, J. S., Trainer, M., Andrews, a. E., Atlas, E. L., Blake, D. R., Daube, B. C., Dlugokencky, E. J., Fischer, M. L., Goldstein, a. H., Guha, a., Karl, T., Kofler, J., Kosciuch, E., Misztal, P. K., Perring, a. E., Pollack, I. B., Santoni, G. W., Schwarz, J. P., Spackman, J. R., Wofsy, S. C. and Parrish, D. D.: Airborne observations of methane emissions from rice cultivation in the Sacramento Valley of California, J. Geophys. Res., 117, D00V25, doi:10.1029/2012JD017994, 2012.

Pétron, G., Frost, G., Miller, B. R., Hirsch, A. I., Montzka, S. a., Karion, A., Trainer, M., Sweeney, C., Andrews, A. E., Miller, L., Kofler, J., Bar-Ilan, A., Dlugokencky, E. J., Patrick, L., Moore, C. T., Ryerson, T. B., Siso, C., Kolodzey, W., Lang, P. M., Conway, T., Novelli, P., Masarie, K., Hall, B., Guenther, D., Kitzis, D., Miller, J., Welsh, D., Wolfe, D., Neff, W. and Tans, P.: Hydrocarbon emissions characterization in the Colorado Front Range: A pilot study, J. Geophys. Res., 117(D4), D04304, doi:10.1029/2011JD016360, 2012.

Polissar, A. V., P. K. Hopke, P. Paatero, W. C. Malm, and J. F. Sisler (1998), Atmospheric aerosol over Alaska: 2. Elemental composition and sources, J. Geophys. Res., 103(D15), 19045–19057, doi:10.1029/98JD01212.

Ryerson, T. B., Andrews, a. E., Angevine, W. M., Bates, T. S., Brock, C. a., Cairns, B., Cohen, R. C., Cooper, O. R., de Gouw, J. a., Fehsenfeld, F. C., Ferrare, R. a., Fischer, M. L., Flagan, R. C., Goldstein, a. H., Hair, J. W., Hardesty, R. M., Hostetler, C. a., Jimenez, J. L., Langford, a. O., McCauley, E., McKeen, S. a., Molina, L. T., Nenes, a., Oltmans, S. J., Parrish, D. D., Pederson, J. R., Pierce, R. B., Prather, K., Quinn, P. K., Seinfeld, J. H., Senff, C. J., Sorooshian, a., Stutz, J., Surratt, J. D., Trainer, M., Volkamer, R., Williams, E. J. and Wofsy, S. C.: The 2010 California Research at the Nexus of Air Quality and Climate Change (CalNex) field study, J. Geophys. Res. Atmos., 118(11), 5830–5866, doi:10.1002/jgrd.50331, 2013.

Santoni, G. W.; Xiang, B.; Kort, E. A.; Daube, B.; Andrews, A. E.; Sweeney, C.; Wecht, K.; Peischl, J.; Ryerson, T. B.; Angevine, W. M.; Trainer, M.; Nehrkorn, T.; Eluszkiewicz, J.;

Wofsy, S. C. (2012) California's Methane Budget derived from CalNex P-3 Aircraft Observations and the WRF-STILT Lagrangian Transport Model. AGU Fall Meeting 2012, San Francisco, CA.

Shaw, S. L., Mitloehner, F. M., Jackson, W., Depeters, E. J., Fadel, J. G., Robinson, P. H., Holzinger, R. and Goldstein, A. H.: Volatile organic compound emissions from dairy cows and their waste as measured by proton-transfer-reaction mass spectrometry., Environ. Sci. Technol., 41(4), 1310–6 [online] Available from: http://www.ncbi.nlm.nih.gov/pubmed/17593735, 2007.

Slowik, J. G., Vlasenko, a., McGuire, M., Evans, G. J. and Abbatt, J. P. D.: Simultaneous factor analysis of organic particle and gas mass spectra: AMS and PTR-MS measurements at an urban site, Atmos. Chem. Phys., 10(4), 1969–1988, doi:10.5194/acp-10-1969-2010, 2010.

Smith, P., D. Martino, Z. Cai, D. Gwary, H. Janzen, P. Kumar, B. McCarl, S. Ogle, F. O'Mara, C. Rice, B. Scholes, O. Sirotenko, 2007: Agriculture. In Climate Change 2007: Mitigation. Contribution of Working Group III to the Fourth Assessment Report of the Intergovernmental Panel on Climate Change [B. Metz, O.R. Davidson, P.R. Bosch, R. Dave, L.A. Meyer (eds)], Cambridge University Press, Cambridge, United Kingdom and New York, NY, USA.

Sun, H., Trabue, S. L., Scoggin, K., Jackson, W. a., Pan, Y., Zhao, Y., Malkina, I. L., Koziel, J. a. and Mitloehner, F. M.: Alcohol, Volatile Fatty Acid, Phenol, and Methane Emissions from Dairy Cows and Fresh Manure, J. Environ. Qual., 37(2), 615, doi:10.2134/jeq2007.0357, 2008.

Tanner, R. L. and Zielinska, B.: Determination of the biogenic emission rates of species contributing to VOC in the San Joaquin Valley OF California, Atmos. Environ., 28(6), 1113–1120, doi:10.1016/1352-2310(94)90288-7, 1994.

Ulbrich, I. M. et al. (2009), Interpretation of organic components from Positive Matrix Factorization of aerosol mass spectrometric data, Atmos. Chem. Phys., 9(9), 2891–2918, doi:10.5194/acp-9-2891-2009.

Williams, B. J., Goldstein, a. H., Kreisberg, N. M., Hering, S. V., Worsnop, D. R., Ulbrich, I. M., Docherty, K. S. and Jimenez, J. L.: Major components of atmospheric organic aerosol in southern California as determined by hourly measurements of source marker compounds, Atmos. Chem. Phys., 10(23), 11577–11603, doi:10.5194/acp-10-11577-2010, 2010.

Wunch, D., Wennberg, P. O., Toon, G. C., Keppel-Aleks, G. and Yavin, Y. G.: Emissions of greenhouse gases from a North American megacity, Geophys. Res. Lett., 36(15), L15810, doi:10.1029/2009GL039825, 2009.

Yuan, B., Shao, M., de Gouw, J., Parrish, D. D., Lu, S., Wang, M., Zeng, L., Zhang, Q., Song, Y., Zhang, J. and Hu, M.: Volatile organic compounds (VOCs) in urban air: How chemistry affects the interpretation of positive matrix factorization (PMF) analysis, J. Geophys. Res. Atmos., 117(D24), n/a–n/a, doi:10.1029/2012JD018236, 2012.

Zhao, C., Andrews, A. E., Bianco, L., Eluszkiewicz, J., Hirsch, A., MacDonald, C., Nehrkorn, T. and Fischer, M. L.: Atmospheric inverse estimates of methane emissions from Central California, J. Geophys. Res., 114(D16), D16302, doi:10.1029/2008JD011671, 2009.

2.6 Tables and Figures

Please view next page.

Table 2. 1. PMF dataset with total samples (N) and mixing ratio range (in pptv).

Class	Compound	N	1st percentile	99th percentile	Background
GHG	CH_4[a,c]	619	1855.0	3400.8	1813.6
	CO_2[b,c]	619	390.8	468.3	390.0
	N_2O[a,d]	490	323.3	339.5	323.2
combustion tracer	CO[a,d]	653	118.9	330.6	102.1
straight chain alkanes	propane	592	580.8	30839.0	455.5
	n-butane	587	96.4	12649.0	73.6
	n-pentane	647	93.2	3805.4	64.4
	n-hexane	647	23.1	960.5	17.2
	dodecane	643	1.56	54.3	0
branched alkanes	isopentane	646	165.4	7490.5	100.4
	2,3-dimethylbutane	650	52.5	1747.7	41.1
	2,5-dimethylhexane	651	2.37	145.8	0
	isooctane	647	16.6	476.9	12.3
	4-ethylheptane	651	1.45	52.6	0
	dimethyl undecane	643	0.46	24.9	0
cyclo alkanes	methylcyclopentane	647	23.3	1329.6	20.3
	methylcyclohexane	649	8.10	813.9	0
	ethylcyclohexane	651	1.78	169.1	0
alkenes	propene	592	34.7	3299.9	28.6
	isobutene	595	16.7	422.1	10.7
aromatics	toluene	647	48.8	1749.5	33.1
	ethylbenzene	647	5.83	282.0	0
	m,p-xylene	647	21.8	1127.1	21.8
	o-xylene	647	4.31	405.0	0
	cumene	640	0.55	22.8	0
	1-ethyl-3,4-methylbenzene	651	2.22	358.6	0
	p-cymene	649	0.84	93.9	0
	indane	647	0.45	27.9	0
	1,3-dimethyl-4-ethylbenzene	635	0.46	23.9	0
	naphthalene	654	0.44	19.9	0
unsaturated aldehyde	methacrolein	573	14.2	337.0	0
alchohol	methanol	429	2636.81	88691.8	1085.2
	ethanol	598	1021.93	65759.8	1021.9
	isopropyl alcohol	583	25.7	2001.0	25.7
ketone	acetone	663	142.9	3505.8	142.9
	methyl ethyl ketone	605	8.55	1111.2	0
	methyl isobutyl ketone	629	2.03	71.9	0
aldehyde	propanal	636	3.68	140.8	0
	butanal	589	1.72	35.1	0
biogenics	isoprene	651	9.70	310.0	0
	alpha-pinene	740	1.67	525.8	0
	d-limonene	641	1.10	357.1	0
	nopinone	614	0.78	89.5	0
	alpha-thujene	591	0.52	23.8	0
	camphene	645	0.72	100.3	0
chloroalkanes	chloroform	647	34.1	209.3	31.6
	tetrachloroethylene	641	3.41	120.9	0
	1,2-dichloroethane	640	20.6	103.8	20.6
	1,2-dichloropropane	627	2.40	28.4	0
sulfides	carbon disulfide	610	7.84	133.7	0
thiol	ethanethiol	491	4.54	685.8	0

[a] parts per billion volume (ppbv)
[b] parts per million (ppmv)
[c] measured using LGR Fast Green House Gas Analyzer
[d] measured using LGR N_2O/CO analyzer

Table 2. 2. Comparison of light alkane ratios to propane (gC gC^{-1}) from PMF fugitive and evaporative factor with those from other PMF studies and oil and gas operations.

Study	Source	propane	n-butane	n-pentane	n-hexane	isopentane
Bakersfield PMF evaporative and fugitive factor[a]	This study	1	0.52 ± 0.02	0.18 ± 0.01	0.06 ± 0.01	0.33 ± 0.02
Bakersfield petroleum operations source profile[b]	Gentner et al. (2014)	1	0.53 ± 0.1	0.09 ± 0.02	0.04 ± 0.01	0.08 ± 0.02
Mexico city PMF LPG factor[c]	Bon et al. (2011)	1	0.5 (0.4 - 0.7)	0.05 (0.04 - 0.07)	0.02 (0.02 - 0.03)	0.07 (0.06 - 0.1)
Wattenberg field BAO, Colorado[d]	Gilman et al. (2013)	1	0.75 ± 1.37	0.32 ± 0.6	0.08 ± 0.13	0.28 ± 0.52
Wattenberg field BAO, Colorado[e]	Petron et al. (2012)	1	0.58 - 0.65	0.22 - 0.31	NA	0.22 - 0.31
PMF natural gas and evaporation factor, Houston Ship Channel[g]	Leuchner and Rappengluck (2010)	1	0.33	0.27	0.12	0.37
PMF natural gas factor, Houston Ship Channel[h]	Buzcu and Fraser (2006)	1	0.67 ± 0.16	0.07 ± 0.18	NA	NA

[a] Uncertainties calculated from propagation of errors (standard deviations) over FPEAK range of -1.6 to 0.4.

[b] Ratios calculated from Table 4, Gentner et al., 2014; uncertainties defined as ±20% to account for variability in oil well data.

[c] Uncertainties calculated from propagation of uncertainties over FPEAK range of -3 to 3.

[d] Emission ratios derived from multivariate regression analysis; error bars derived from propogation of uncertainty using mean and standard deviation of samples.

[e] Range over 5 regressions conducted over data collected in different seasons and from mobile lab samples.

[f] Ratios derived from mean and standard deviations, with propagation of uncertainty.

[g] Estimated from Figure 2, Leuchner and Rappengluck, 2010.

[h] Estimated from Figure 2, Buzcu and Frazer, 2006.

Table 2. 3. Comparison of hydrocarbon ratios to toluene (gC gC^{-1}) from PMF vehicle emission factor with similar ratios from other California specific studies

Study	Bakersfield PMF vehicle emissions factor[a]	Bakersfield gasoline source profile[b,c]	Riverside liquid gasoline profile[e]	CalNex Los Angeles ambient emission ratios[g]
Source	This study	Gentner et al. (2014)	Gentner et al. (2009)	Borbon et al. (2013)
CH$_4$	8.1 ± 2.1	NA	NA	NA
CO	14.0 ± 0.4	NA	NA	45
toluene	1	1	1	1
isopentane	0.69 ± 0.01	0.77 ± 0.04	0.64-0.84	1.95
isooctane	0.29 ± 0.03	0.34 ± 0.02	0.64-0.80	NA
n-dodecane	0.03 ± 0.001	(0.02 ± 0.007)[d]	NA	NA
methylcyclopentane	0.24 ± 0.01	0.32 ± 0.02	NA	NA
ethyl benzene	0.17 ± 0.01	0.14 ± 0.01	NA	0.2
m/p - xylene	0.65 ± 0.01	0.65 ± 0.03	(0.45-0.52)[f]	0.64
o - xylene	0.22 ± 0.01	0.23 ± 0.01	NA	0.24

[a] errors are standard deviation of 12 unique PMF solutions between FPEAK =-1.6 to +0.4; see section S2.
[b] derived from liquid gasoline fuel speciation profile (Table S9; Gentner et al., 2012).
[c] errors bars derived from propagation of uncertainties.
[d] derived by combining diesel fuel and gasoline speciation profile (Table S9 and S10; Gentner et al., 2012) with gasoline and diesel fuel sale data in Kern County (Table S1, Gentner et al., 2012).
[e] summer data.
[f] only m-xylene.
[g] derived from Linear Regression Fit slope of scatterplot from CalNex Pasadena supersite samples.

Table 2. 4. Comparison of PMF dairy and livestock emission rates (mmol mol^{-1}) with previous studies.

Study	Source	Cow/manure type (if applicable)	methanol / methane EF avg. (range)	ethanol / methane EF avg. (range)
PMF analysis of regional measurements	This study		15 - 47	9 - 32.2
Environmental chamber with cows and/or manure	Shaw et al. (2008)	Dry	3.2 (0.6 - 7.4)	NA
		Lactating	1.9 (0.8 - 3.6)	NA
Environmental chamber with cows and/or manure	Sun et al. (2008)	Dry	13.4 (4 - 25)	14.4 (11 - 19)
		Lactating	19.2 (15 - 25)	24.2 (18 - 32)
Cowshed with regular dairy operations (winter)	Ngwabie et al. (2008)		2.0 (1.6 - 2.4)	9.3 (4 - 16)
Cow stall area with regular dairy operations (summer)	Filipy et al. (2006)		NA	(42 - 127)[a]
Manure from cattle feedlot	Miller and Varel (2001)	Fresh (< 24 hr)	NA	14[b]
		Aged (> 24 hr)		118[b]
Measured slope of regression (CalNex 2010)	Gentner et al. (2014)		7.4 (7 - 16)[c]	18[d]
Sampling of dairy plumes from aircraft (CABERNET 2011)	Guha et al. (*in prep*)		9.6 (9 - 30)[c]	NA

[a] calculated based on CH$_4$ emission rate of 4160 µg cow^{-1} s^{-1} for mid-lactating cows (Shaw et al., 2007).
[b] calculated based on CH4 emission rate of 4160 µg cow-1 s-1 for mid-lactating cows (Shaw et al., 2007) and ethanol emission rate for fresh and aged manure of 175 and 1223 µg cow-1 s-1, respectively, derived by Filipy et al. (2006).
[c] slope of regression with range of measured slopes (in parentheses) from sampling of dairy plumes by aircraft.
[d] ground site data; lower limit of slope of non-vehicular ethanol versus methane

Table 2. 5. Comparison of PMF agricultural and soil management emission rate for acetone versus methanol (gC gC^{-1}) with ratios of basal emission factors generated for major crops grown in the Kern County. Errors denote standard deviations computed by propagation of uncertainty.

Bakersfield PMF agricultural and soil management factor	Almond greenhouse summer 2008	Table grape greenhouse summer 2008	Pistachio greenhouse summer 2008	Navel oranges greenhouse summer 2008[a]	Valencia oranges greenhouse summer 2008
This study	Gentner et al. (2014b)	Gentner et al. (2014b)	Gentner et al. (2014b)	Fares et al. (2011)	Fares et al. (2012)
0.58 ± 0.37	0.14 ± 0.2	0.04 ± 0.02	0.5 ± 0.6	0.57 ± 0.1	0.5 ± 0.3

[a] branch with flowers not removed.
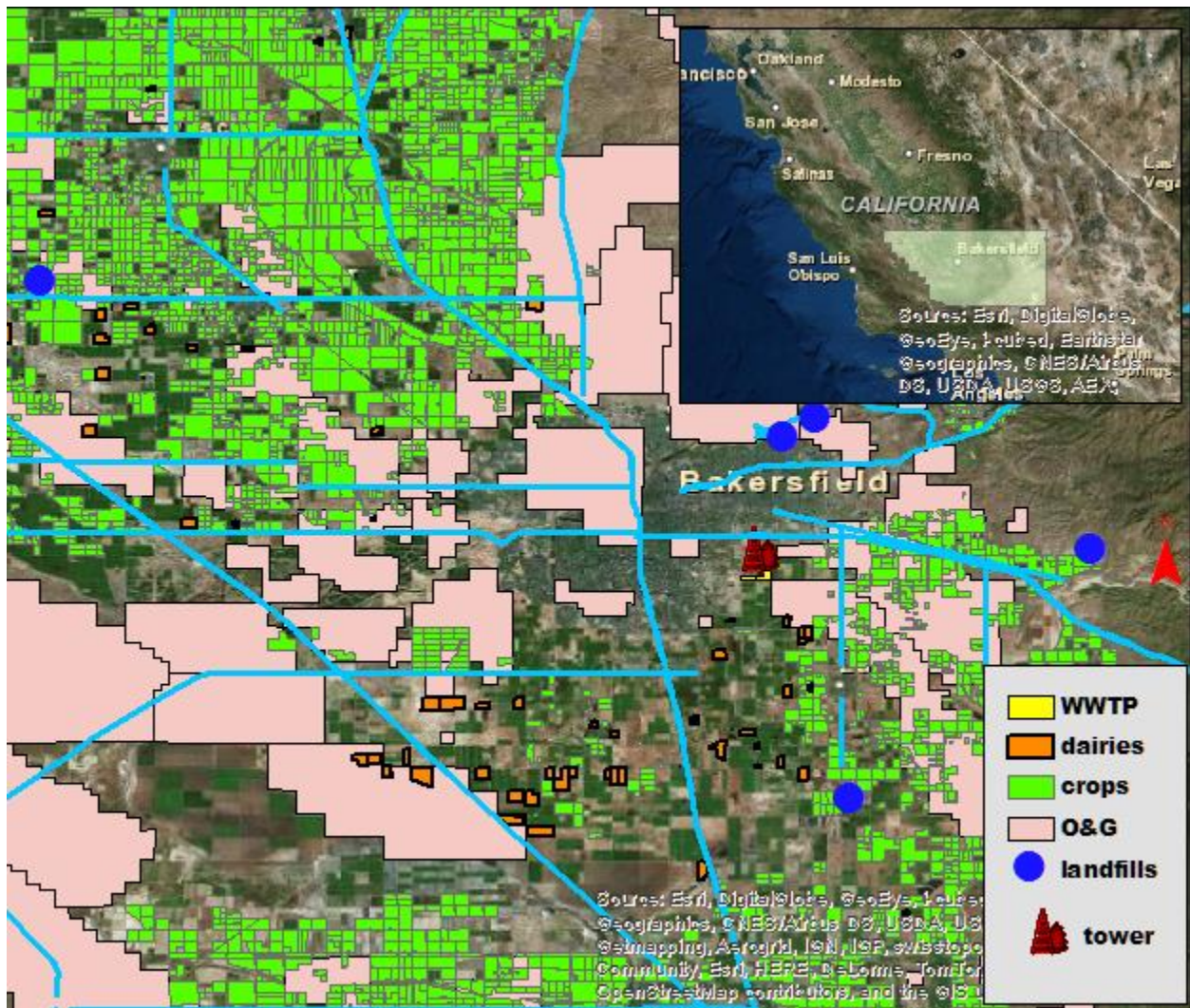
Figure 2. 1. Map of potential sources of methane and nitrous oxide in and around the city of Bakersfield and the surrounding parts of the San Joaquin Valley. The inset map is a zoomed out image of the southern part of San Joaquin Valley (SJV) with location of Kern County superimposed. The light blue lines mark the highways, WWTP stands for waste water treatment plant, and O&G stands for oil and gas fields. The location of the CalNex experiment site is marked by the 'tower' symbol.

daytime winds
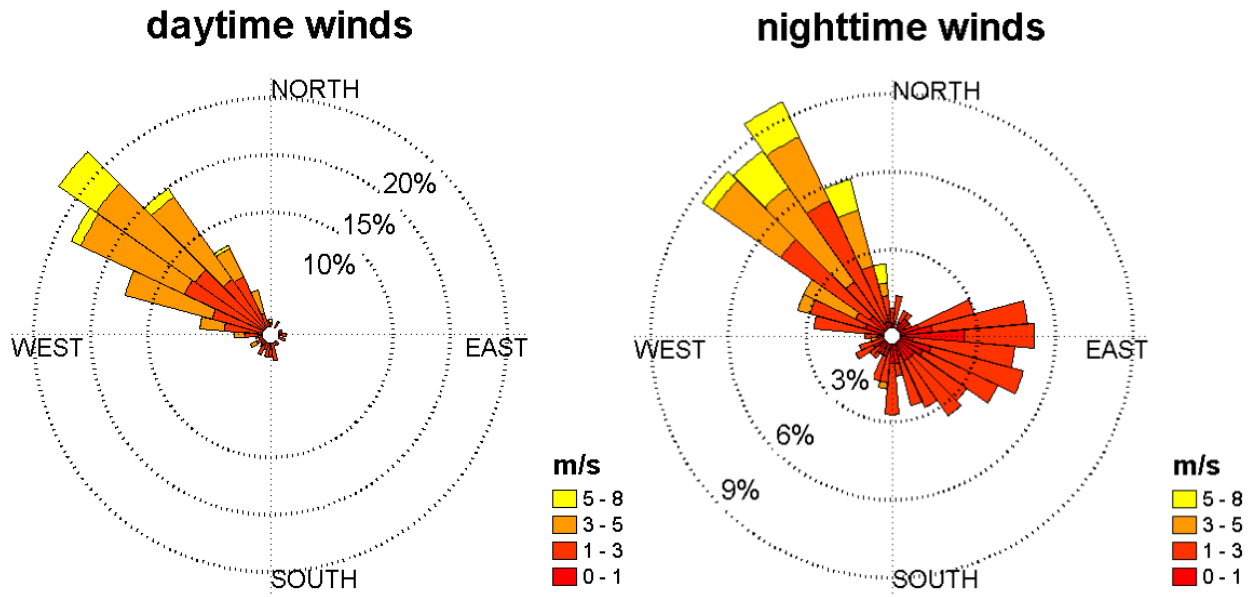
nighttime winds

Figure 2. 2. Wind rose plots showing mean wind direction measured at the site during (left) day time (07:00-16:00 hours), and (right) nighttime (17:00-06:00 hours). The concentric circles represent the percentage of total observations; each colored pie represents a range of 10° while the colors denote different wind speed ranges.

46
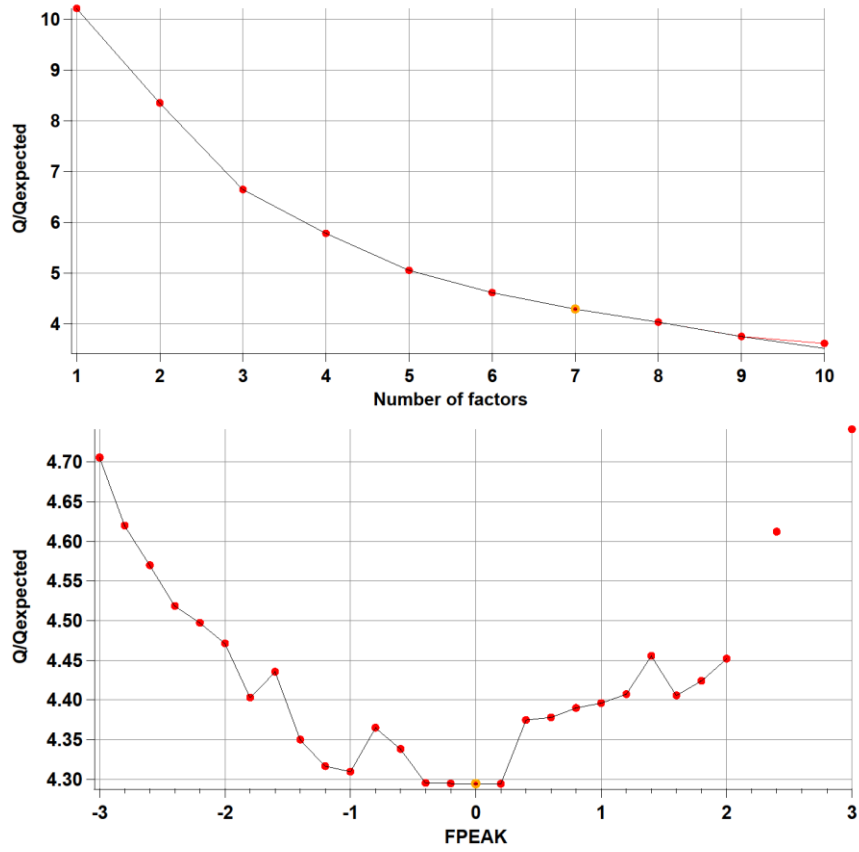
Figure 2. 3. Change in the quality of fit parameter (Q/Q_{exp}) with increasing number of factors at FPEAK = 0. The % change in the Q/Q_{exp} value is larger than 10 % at each successive step until p = 5. For p > 5, % change in Q/Q_{exp} value < 10 % for each successive step increase in p. (b) Change in the values of Q/Q_{exp} for the FPEAK range from -3 to +3. The Q/Q_{exp} values change by ~ 10 % from the minimum of 4.3 at FPEAK = 0 over this FPEAK range.

47
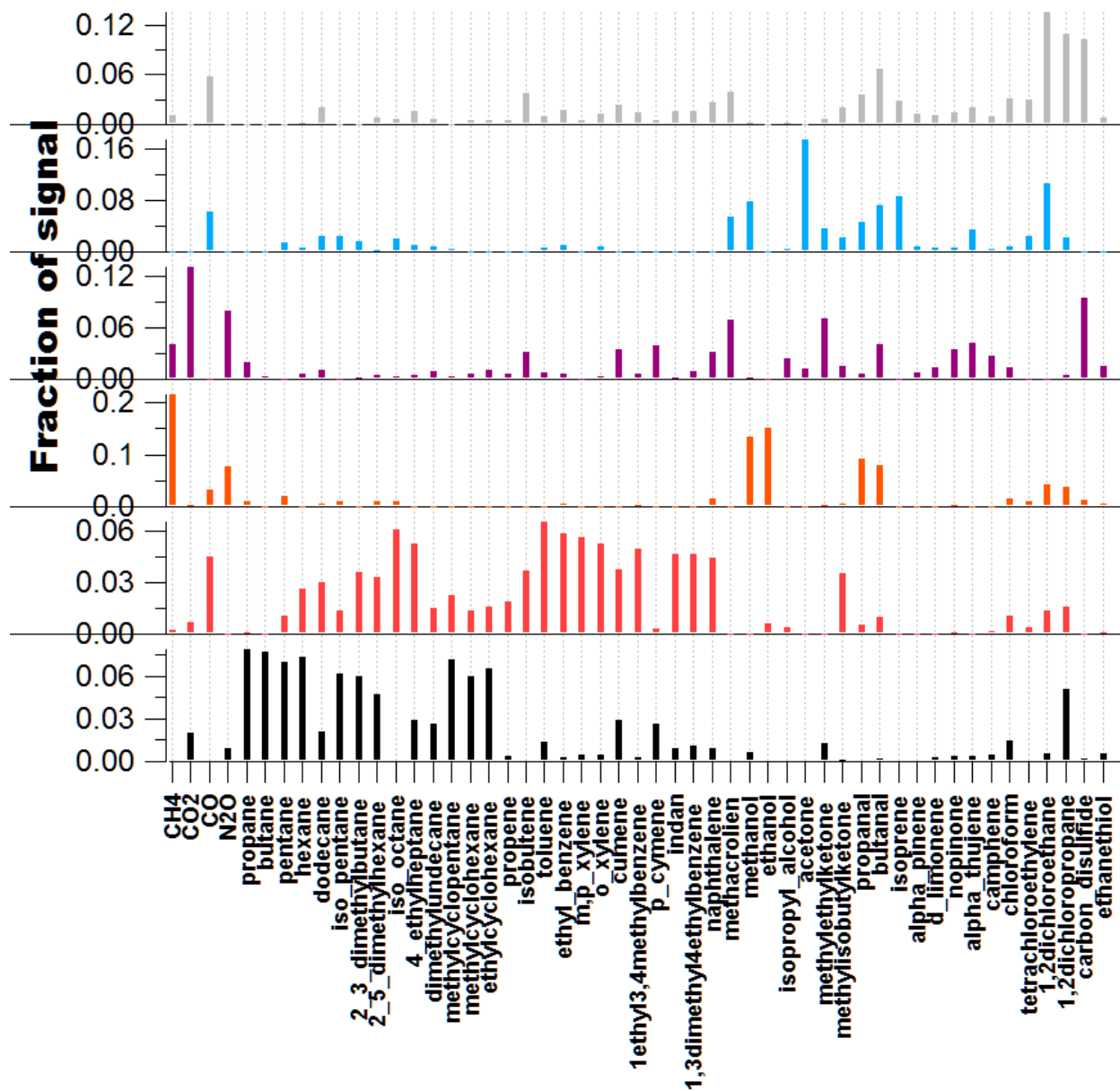
Figure 2. 4. PMF 6-factor profile (FP). The source factors are: evaporative/fugitive (in black), vehicles (in red), dairy and livestock (in orange), agricultural + soil management (in purple), daytime biogenics + secondary organics (in light blue) and a *mixed* source factor (in grey) which is not unique and has contributions from more than one source.
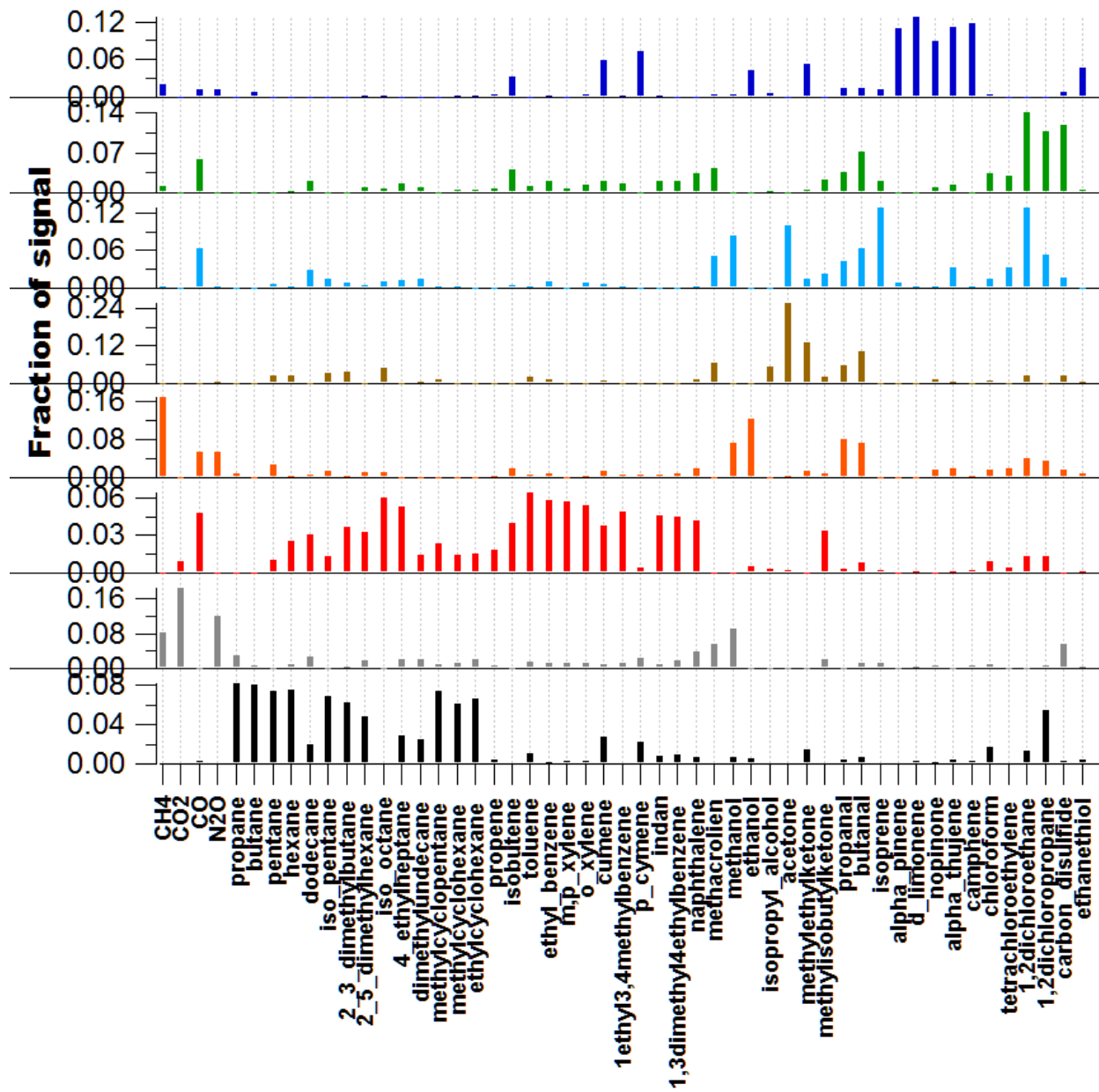
Figure 2. 5. PMF 8-factor profile (FP). The source factors are: evaporative/fugitive (in black), vehicles (in red), dairy and livestock (in orange), daytime biogenics + secondary organics (in light blue), urban (in green), nighttime anthropogenic + terpene biogenics (in navy blue) and two *split* sources (in grey and brown, respectively) which resemble a disintegration of the agricultural + soil management source (in purple) from the 7-factor solution (Figure 2.6).

49
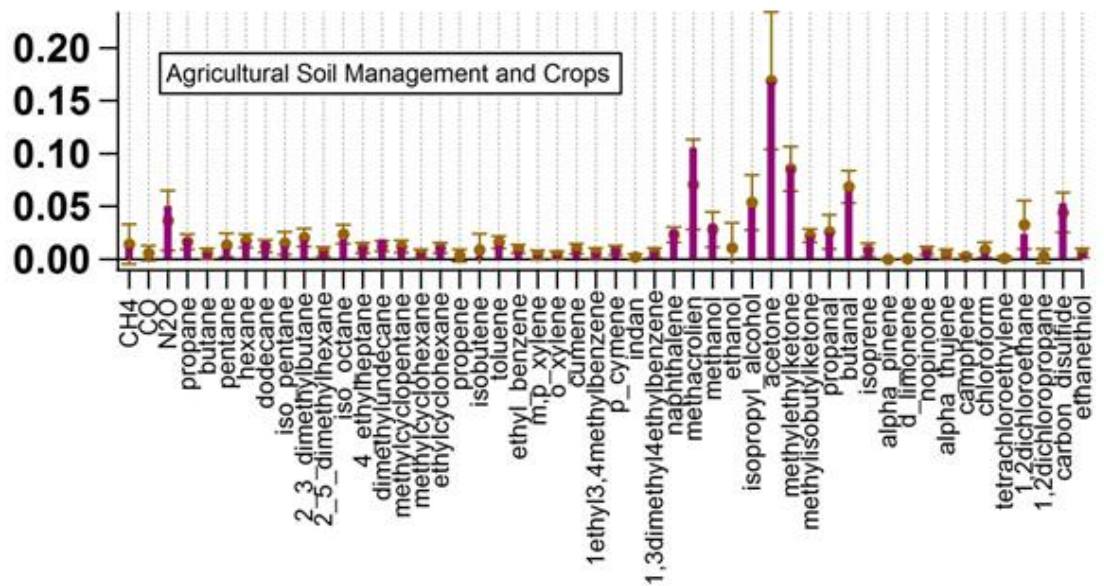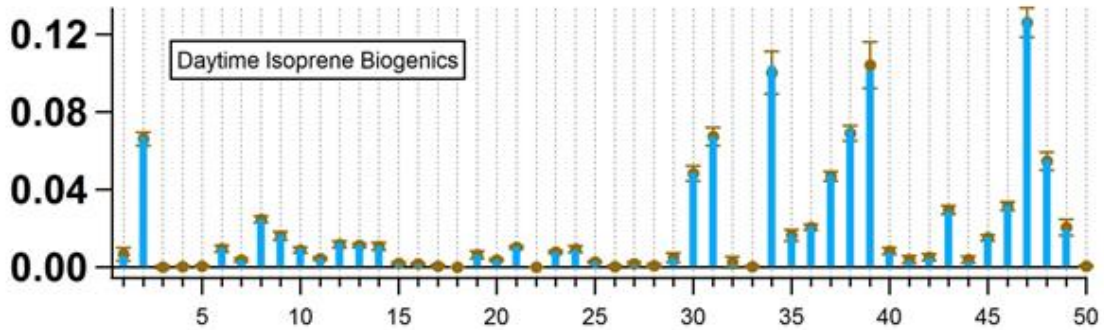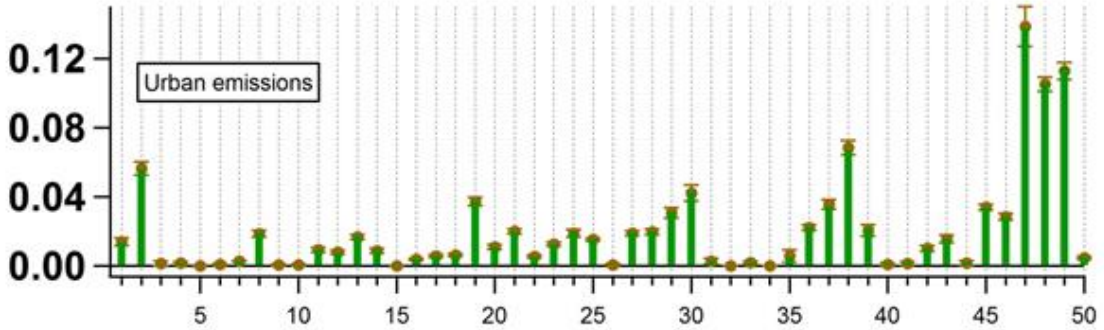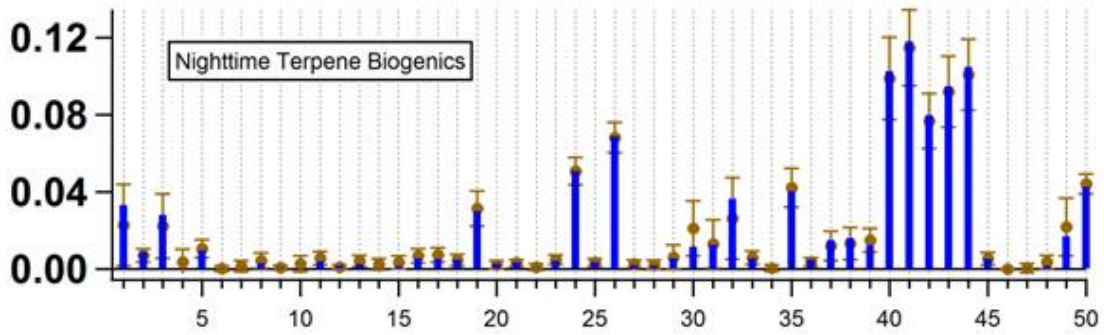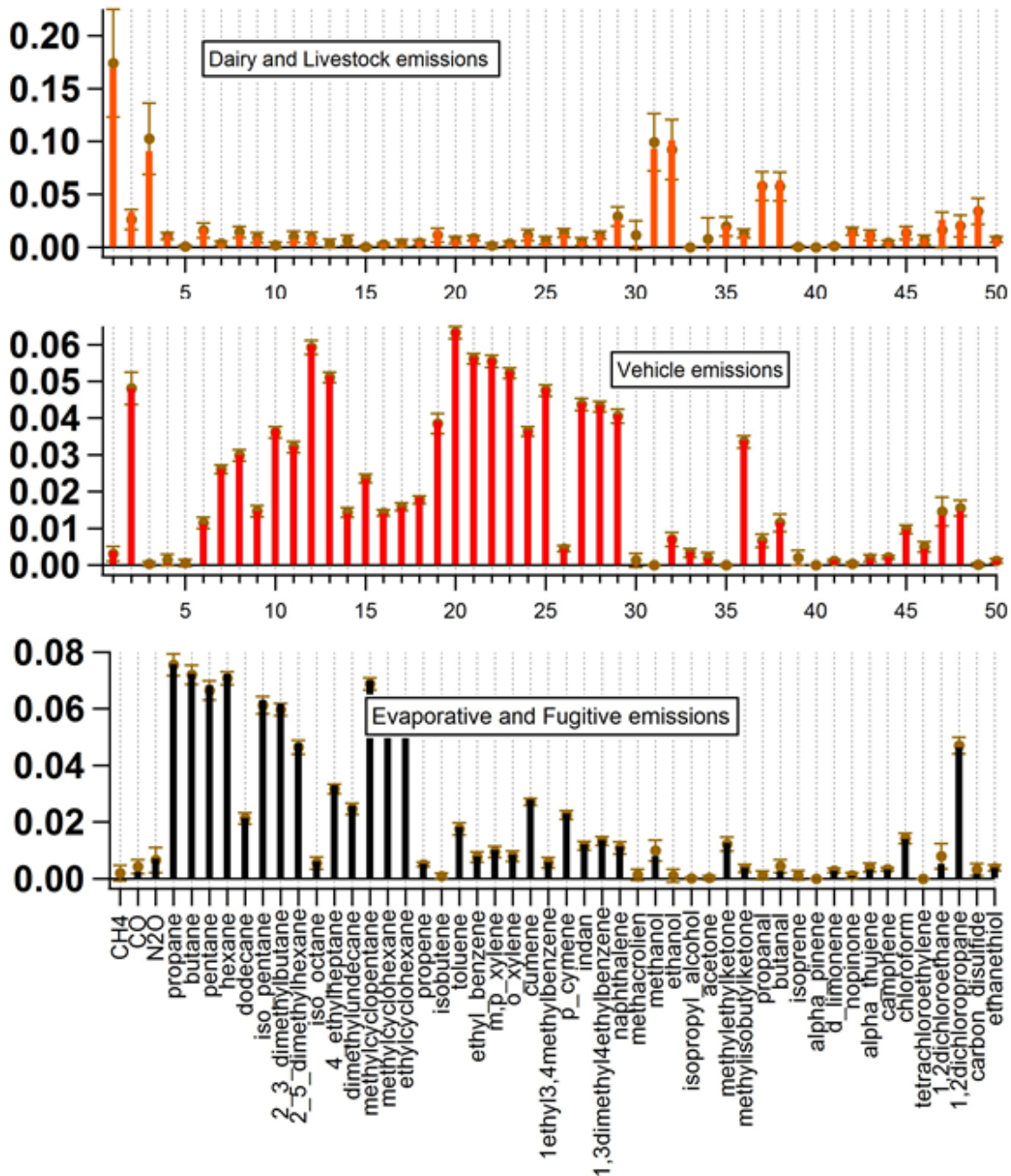
Figure 2. 6. Source profile of the seven factors (at FPEAK = +0.6) with uncertainty estimates generated from 100 bootstrapping runs. The source factors are (a) nighttime anthropogenics + terpene biogenics (b) urban (c) daytime biogenics + secondary organics (d) agricultural + soil management (e) dairy and livestock (f) vehicles and (g) evaporative and/or fugitive. The x-axis represents the normalized fraction of mass in each source factor, while the y-axis lists all the chemical species included in the PMF analysis. The numbers on the y-axis pertains to the tracer nomenclature adopted in Table 2.1. The solid brown markers denote the average of the 100 bootstrapping runs and the error bars represent the 1σ standard deviation about the average.
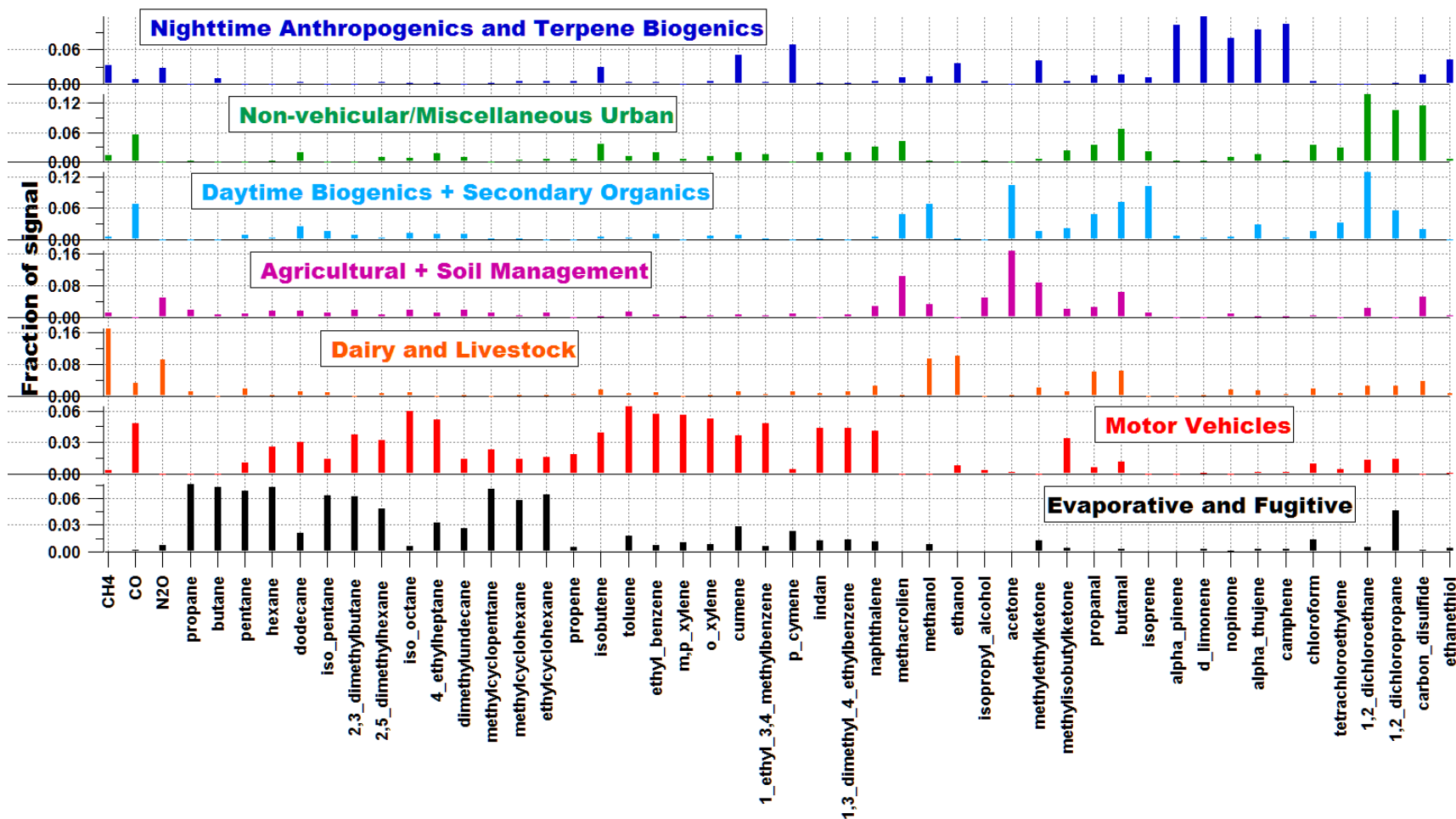
Figure 2. 7. Source profile of the seven factors derived using PMF. The source factors are evaporative and fugitive, motor vehicles, dairy and livestock, agricultural + soil management, daytime biogenics + secondary organics, urban, and nighttime anthropogenics + terpene biogenics. The x-axis represents the normalized fraction of mass in each source factor, while the y-axis lists all the chemical species included in the PMF analysis.
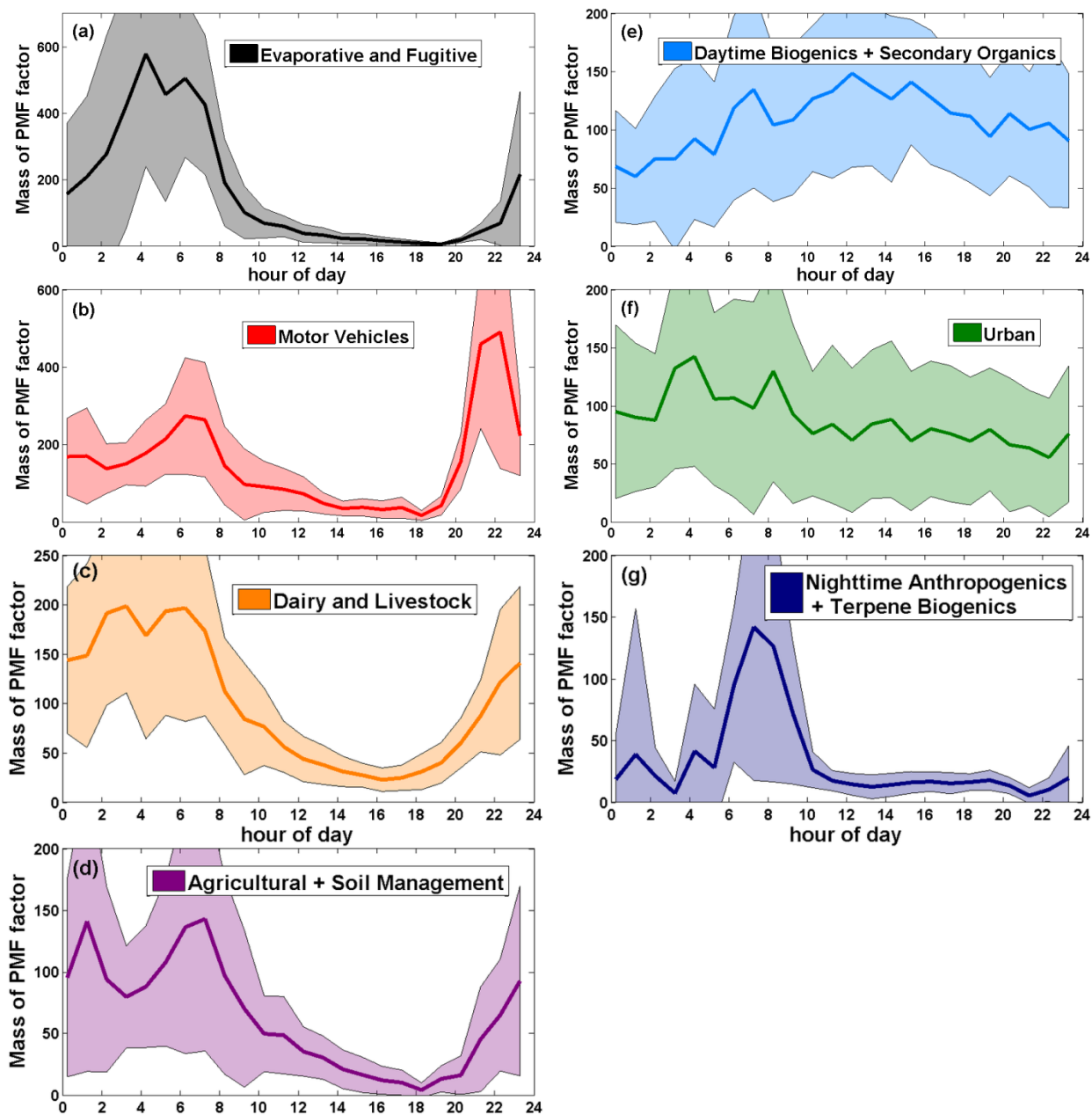
Figure 2. 8. Mean hourly diurnal plots of PMF source factor concentration enhancements for (a) evaporative and fugitive, (b) motor vehicles, (c) dairy and livestock, (d) agricultural + soil management, (e) daytime biogenics and secondary organics, (f) non-vehicular/miscellaneous urban and (g) nighttime anthropogenics + terpene biogenics. The x-axis represents sum of normalized mass concentrations from all tracers contributing to the factor. The y-axis is hour of day (local time). The solid lines represent the mean and the shaded area represents the standard deviation (variability) at each hour.
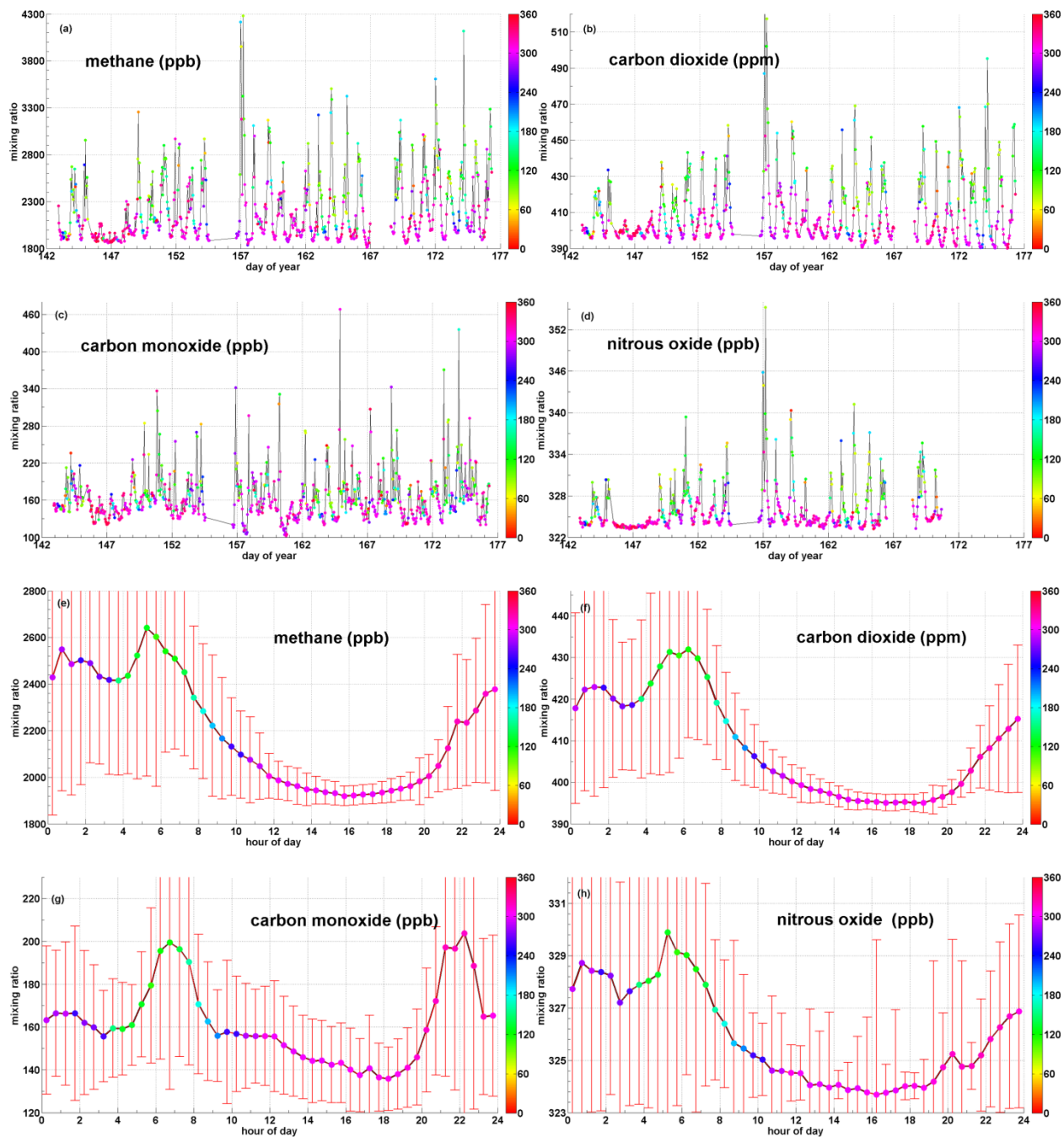
Figure 2. 9. Time series of (a) CH_4, (b) CO_2, (c) CO, and (d) N_2O obtained from 30-min averages over the entire sampling period. The color bar indicates the average wind direction during each 30-min period. Mixing ratios plotted as average diurnal cycles for (e) CH_4, (f) CO_2, (g) CO and (h) N_2O along with wind direction. The curve and the red whiskers represent the mean and the standard deviations about the mean, respectively.

54
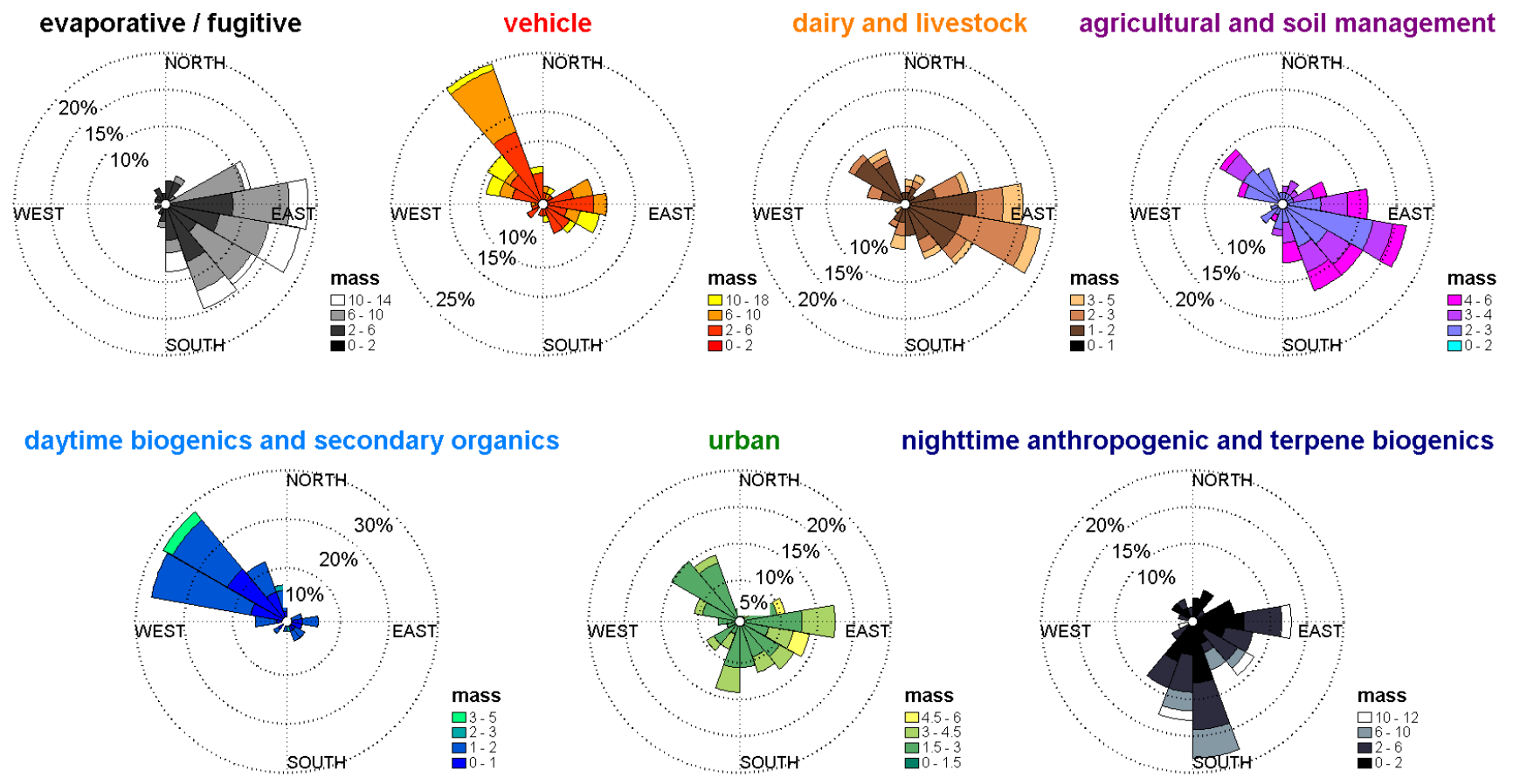
Figure 2. 10. Dominant wind direction rose plots for the seven PMF source factors. The wind rose includes those 30-min averaged wind directions for which the PMF mass concentration > mean + standard deviation of PMF mass concentration time series.
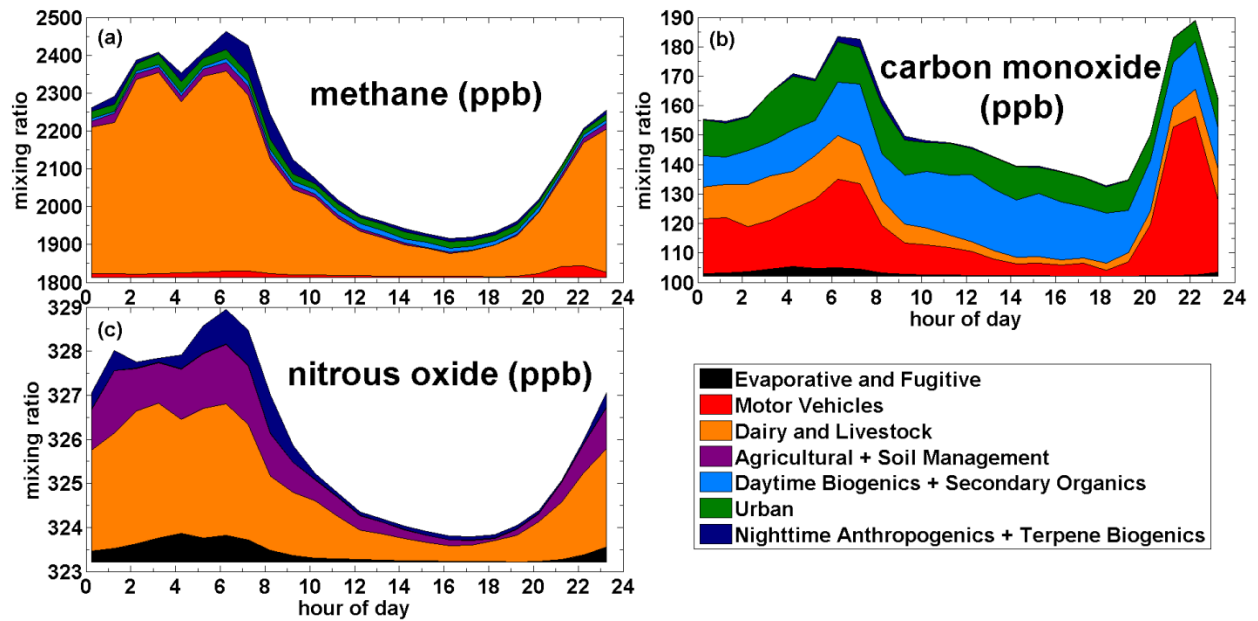
Figure 2. 11. Diurnal plot of PMF derived (a) CH_4, (b) CO, and (c) N_2O concentrations sorted by PMF source category. The legend on the bottom right shows the names of the PMF source factor which each color represents. The PMF derived enhancements from each source have been added to the background concentrations.

Chapter 3: Identifying and mapping methane (CH$_4$) sources over California from mixing ratio, airborne flux and VOC source tracer measurements

Abstract

During summer of 2011, a CH$_4$/CO$_2$ sensor (1 Hz) was deployed on-board a Twin Otter aircraft along with a customized proton transfer reaction mass spectrometer (10 Hz; PTR-MS) to measure mixing ratios of CH$_4$, CO$_2$ and certain volatile organic compounds (VOCs) like methanol, benzene, toluene and isoprene. Forty hours of flight measurements were performed over eight unique flights covering ~ 10000 km all around and across the Central Valley of California in order to identify major CH$_4$ sources in different regions that were responsible for the ambient enhancements observed at the aircraft level. For the first time, the technique of airborne eddy covariance using the Continuous Wavelet Transformation (CWT) approach was applied to determine time series of CH$_4$ fluxes over specific transects 20 to 70 km long flying "low and slow". The eddy covariance flux data were validated through spectral analysis (i.e., normalized co-spectrum and ogive) and it was demonstrated that a CH$_4$ sensor with 1 Hz temporal resolution is able to capture the bulk of the vertical eddies transporting flux at the aircraft level.

The coincident enhancements (or lack thereof) of VOC source tracers were used to identify the sources impacting the measured CH$_4$ signal. Large mixing ratios of CH$_4$ (> 2000 ppb) are observed for extended periods in all flight segments through the Central Valley of California and are usually well correlated with methanol (9 to 88 ppt methanol / ppb CH$_4$) pointing to extensive emissions from the dairy and livestock sector. The observed CH$_4$ / methanol slopes over different flight segments in the Valley were similar to those generated from ground-based dairy measurements and PMF-derived dairy and livestock source emission factor (Chapter 2). Mean ecosystem level CH$_4$ fluxes calculated from different flight segments over the dairy source regions varied from 28 to 294 nmol-CH$_4$ m^{-2} s^{-1}. Combining the flux values with an areal cowhead density factor determined for the San Joaquin Valley bioregion, CH$_4$ emission rates of 83 to 202 kg CH$_4$ cowhead^{-1} year^{-1} were determined with a segment averaged CH$_4$ flux of 873 kg CH$_4$ cowhead^{-1} year^{-1} over the most densely populated dairy and feedlot region over Kings and Tulare County. These estimates are similar but larger than emission rates obtained from previous cow-chamber experiments and the 'bottom-up' state inventory.

Elevated levels of CH$_4$ with enhancements of up to 300 ppb were observed while flying above the oil and gas industrial complex in western Kern County. These enhancements were coincident with enhancements of benzene and toluene pointing towards a source with fossil-fuel origins. CH$_4$ flux averaged over the oil and gas fields flight leg was 313 nmol-CH$_4$ m^{-2} s^{-1} and was larger than area-scaled industry-reported CH$_4$ emission rates from two large oil and gas fields in the region. A sharp fugitive/vented release of CH$_4$ (~ 200 ppb) was observed near a natural gas cogeneration facility which is potentially incorrectly identified as an insignificant point source in the current 'bottom-up' state inventory. A short flight stretch over rice paddy

fields in the western Sacramento Valley produced an anti-correlation of CH_4 and CO_2 with a slope of - 5.6 ± 0.2 ppb CH_4 ppm CO_2^{-1}. This slope was similar to flux ratios derived from ground-based studies and airborne multivariate assessments of rice cultivation. The CH_4 flux, measured early in the rice growing season, was 26 ± 16 nmol-CH_4 m^{-2} s^{-1} and is consistent with ground-based flux observations at rice paddies in California.

Large-scale advection of CH_4 emissions from valley-sources (e.g. oil and natural gas infrastructure, dairies, rice cultivation etc.) towards the eastern edges of the Central Valley led to routinely observed high concentrations along the eastern foothills, and so were enhancements of 75-125 ppb downwind of the largest landfills in Northern California. Large isolated enhancements were observed in plumes from biomass burning and wetlands alike identifying those as CH_4 sources. In regions outside the Central Valley and away from influence of major known sources (e.g. landfills etc.), observed concentrations were lowest but still higher than the expected northern mid-latitude hemispheric background levels suggesting an overall high CH_4 background over California due to vast regional emissions.

3.1   Introduction

Methane (CH_4) is an important greenhouse gas (GHG) which is responsible for about 20 % of the total anthropogenic radiative forcing increase of 2.77 Wm^{-2} since preindustrial times (year 1750) (Montzka et al., 2011). The relatively long atmospheric lifetime of ~ 10 years and large infrared absorption at unique spectral wavelengths gives CH_4 a large GWP of 25 (Forster et al., 2007; Montzka et al., 2011), thus making it a potent greenhouse gas. Greenhouse gases have been a major focus of California's environmental policy in the last decade or so. A path-breaking step in the policy formulation process took place when the Assembly Bill 32 (AB32) was passed and adopted as a law. AB32, formally known as the Global Warming Solutions Act of 2006, mandates the state to reduce its greenhouse gas emissions to 1990 levels by the year 2020. The state's main air quality regulatory agency, the California Air Resources Board (CARB), has developed an annual inventory of GHG emissions for enforcement of AB32 (CARB, 2013).

Reduction in CH_4 emissions owing to its high GWP can provide a short term fix to CARB's long term GHG emission reduction targets. Of late, the agency has turned its focus to verification and validation of their CH_4 inventory for future regulatory purposes. Currently, CH_4 accounts for a little more than 6 % or 32.5 million metric tonnes (MMT) CO_2-eq in the statewide GHG emissions inventory (Figure 1.1; CARB, 2013). CH_4 emissions occur from a suite of anthropogenic sources that include those driven by biological emissions like dairy and livestock operation, landfill, waste water treatment and rice cultivation, as well as fossil fuel based sources like oil and gas (O&G) production and distribution systems. The effectiveness of AB32 enforcement for CH_4 regulation is contingent on the accuracy of the emissions reported in the inventory. Significant uncertainties exist in what is primarily, a 'bottom-up' emissions inventory. The inventory, in most cases, is based on scaling of spatially unvarying and time-constant emission factors with activity data. Such an accounting method leads to oversimplification for large area sources with biological pathways like landfills, dairies and manure management, which also happen to be the largest sources in the CH_4 inventory accounting for ~ 80 % of total emissions. There is a lack of adequate data from source-specific 'top-down' approaches in order

to verify and validate the CH_4 inventory especially in case of emissions from the O&G sector. A range of recent 'top-down' estimates from satellite observations, tall towers and aircraft measurements point towards underestimation of the true CH_4 emissions in the 'bottom-up' inventory (Zhao et al., 2009; Wunch et al., 2009; Jeong et al., 2012; Santoni et al., 2012; Peischl et al., 2013; Kort et al., 2014). The discrepancy of the CH_4 emissions inventory with atmospheric measurements poses an impediment to the successful application of AB32 for regulation and development of comprehensive emissions control strategies. The mismatch with measurements reinforces the need to quantitatively assess the inventory source-wise in order to understand better the distribution and relative strengths of major and minor CH_4 sources across California.

A variety of 'top-down' approaches have been implemented to constrain the CH_4 inventory in California, each with its own set of potential handicaps. Satellite imagery derived emission maps (like EDGAR) have a coarse spatial resolution (~ 10 - 100 km; Miller et al., 2013; Wecht et al., 2014) which is not adequate for mapping multiple sources within the same region. Short range inverse dispersion studies using open path lasers (Flesch et al., 2004; Harper et al., 2009, 2010) can produce facility level CH_4 estimates from sources like dairies but these estimates may not be suitable for scaling up owing to the large variability in dairy practices and manure management of individual facilities that can impact CH_4 emissions greatly. Flux measurement techniques like eddy covariance (EC) from ground towers can produce reliable CH_4 flux estimates that have a good temporal coverage (Smeets et al., 2009; Baldocchi et al., 2012). The flux measurements, however, are applicable only over homogenous source areas and require certain assumptions regarding meteorology to be met that are not easily fulfilled for sources like dairies and landfills. The EC fluxes are representative only at smaller length scales of 10 - 1000 m. Atmospheric measurements from either tall towers, satellite-based remote sensing or airborne platforms (aircrafts) have been coupled with inverse dispersion techniques to infer CH_4 emissions on regional scales (10 - 100 km) (Zhao et al., 2009; Jeong et al., 2012; Santoni et al., 2012; Wecht et al., 2014). Inverse dispersion analysis conducted through aircraft measurements are limited by their temporal resolution while tall towers are not always evenly distributed across source regions to provide complete spatial coverage of the state. A recent 'top-down' study from a much broader network of tall towers indicates CH_4 emissions to be 1.3 to 1.8 times higher than the current state inventory (Jeong et al., 2013). Such regional assessments promise to overcome the issue of spatial coverage drawback and provide comprehensive estimates of CH_4 emissions throughout the state.

This study focuses on CH_4 measurements onboard an airborne platform as part of the California Airborne BVOC Emission Research in Natural Ecosystem Transects (CABERNET) campaign. The study was aimed and designed to measure biogenic volatile organic compound (BVOC) fluxes along oak woodlands surrounding California's Central Valley (CV) using an airborne virtual disjunct eddy covariance (AvDEC) approach (Misztal et al., 2014) conducted over eight unique flights in June 2011. A CH_4/CO_2 sensor was installed on the Twin Otter aircraft to take advantage of the vast spatial coverage of the flights (34°32′-39°21′N, 117°28′-123°17′W) that covered ~ 10000 km of flight paths, often flying above some of the most intensive CH_4 source regions in the Central Valley (Figures 3.1 and 3.2).

The underlying rationale behind this study is that flying at relatively low altitudes of ~ 250 - 750 m above ground level (a.g.l), and mapping large parts of California with airborne CH_4

mixing ratio measurements would provide a thorough 'top-down' view of known major, minor, and potentially under-inventoried emissions sources. With that motivation, the objective of this study is to, (a) perform ambient measurements of CH_4, CO_2 and certain VOCs serving as source tracers for comparison with bottom-up estimates from specific CH_4 sources/source regions, and (b) provide proof of concept and demonstrate the suitability of airborne eddy covariance fluxes of CH_4 with a relatively slower sensor (1 Hz effective sampling frequency). We attempt to address scientific questions like 'how can the coincident VOC measurements aid in CH_4 source identification?', and 'can the airborne eddy covariance technique be successfully applied to a slow methane sensor'. We test the hypothesis that airborne eddy covariance flux can be derived using a slow CH_4 sensor (1 Hz sampling rate) flying at reasonably low altitudes above source regions (~ 200 - 500 m) and in a slower aircraft (~ 60 m s^{-1}) without major flux losses. In the following sections, we report mixing ratio measurements from seven flight-transects and the first direct airborne CH_4 flux measurements for specific flight segments representing significant source regions where high CH_4 mixing ratio enhancements were clearly observed. We also analyze the fluxes for their spectral characteristics. Detailed explanation of flux methodology, error analysis and vertical wind speed corrections for aircraft motions have been described in recent publications emanating from this study (Karl et al., 2013; Misztal et al., 2014).

3.2   Experiment

3.2.1   Aircraft logistics and flight details

The two-engine turboprop Twin Otter aircraft was operated by the Center for Interdisciplinary Remotely-Piloted Aircraft Studies (CIRPAS), an agency affiliated to the Naval Postgraduate School located in Marina, California (36°41′N, 121°46′W). The aircraft is customized for scientific research missions and equipped with sensors for measuring a large number of micrometeorological variables (Karl et al., 2013). An isokinetic pipe-inlet above the nose of the plane (3-inch internal diameter) provides the sampling inlet for ambient air through a series of diffusers such that resulting flow speed inside the tube is about 10% of the aircraft speed (~ 60 ms^{-1}). A multi-port vertical and horizontal differential pressure based gust probe mounted on the nose of the plane measures the vertical wind speed with respect to (w.r.t) the airplane coordinate system which is later corrected to represent the vertical wind speed w.r.t the earth's surface. Corrections calculated using "Lenschow maneuvers" (Lenschow, 1986) and described in Karl et al. (2013) are applied to vertical wind speed to account for the movement of the aircraft and any distortions of flow at the nose.

The CABERNET campaign consisted of eight research flights that occurred over the month of June 2011 spanning about forty hours of total flight time. The flight tracks and their spatial coverage are shown in Figure 3.2. Each flight lasted for approximately 4-5 h and was flown during the middle of day when biogenic VOC emissions are expected to be at their peak. The airplane speed was kept relatively constant throughout the flights with an average of 58 m s^{-1}. The aircraft altitude was kept relatively constant (400 ± 50 m a.g.l) during most flight segments devoted to VOC flux measurements. The flights descended further when flying above the Central Valley (~ 200 – 300 m a.g.l). On certain flights, vertical profiling, Lenschow maneuvers and

saw-tooth sounding procedures were performed by the aircraft in order to determine parameters for flux divergence for reactive VOC species, and to perform procedures needed for vertical wind speed corrections. To perform these procedures / maneuvers, the aircraft needed to climb to high altitudes (up to 2500 m a.g.l) and fly at varied altitudes making these relatively small portions of the total track unavailable for CH_4 source assessments along with periods when target and calibration measurements were performed. We are primarily interested in understanding distribution of regional CH_4 emissions sources that are located on the surface and hence, for reporting and discussion purposes, we discard any flight stretch where the aircraft altitude a.g.l is above 750 m a.g.l.

3.2.2   Instrumentation

Instruments were installed inside the aircraft on bolted racks and air flow from the main tube was routed through community inlets into each instrument. The instruments whose measurements are reported in this study include (i) a 2 Hz CH_4/CO_2 analyzer (Picarro, USA), and (ii) a Proton Transfer Reaction Mass Spectrometer (PTR-MS) designed to measure VOC fluxes.

CH_4 and CO_2 were measured on-board by a Picarro 1301-m analyzer ($CO_2/CH_4/H_2O$ analyzer). The analyzer is based on cavity ring-down spectroscopy (Crosson, 2008) and was modified to not measure H_2O and thus effectively increase the sampling frequency of the instrument. The total uncertainty in CH_4 and CO_2 measurements combining all sources of uncertainty (primary standard, inflight standard, calibration/instrument gain and isotopic correction) was 1.2 ppbv and 0.1 ppmv, respectively. Detailed description of the operation of the instrument, application of in-flight calibration standard, sensitivity and the performance of the instrument aboard an airborne platform has been previously published (Peischl et al., 2012). The Picarro analyzer has a time resolution of 2 Hz collecting and analyzing a sample every 0.5 s for CH_4 and CO_2 separately, but since two species are sequentially analyzed, the cycle length is 1 s and hence effective sampling rate is 1 sample per second.

The customized PTR-MS used for the CABERNET campaign is capable of making high frequency measurements of VOCs (10 Hz). It operates in a virtual disjunct mode (Karl et al., 2002) allowing a number of VOCs (3 to 6) to be analyzed sequentially giving an overall effective sampling cycle of 0.5 to 0.8 s for each individual tracer measured at 10 Hz (Misztal et al., 2014). The VOCs measured during the study were generally ones with known biogenic origins keeping in line with the core objective of the CABERNET study. VOCs (represented here also by their mass-to charge ratios (*m/z*)), measured throughout or during one or more flights in this study include but are not limited to isoprene (*m/z* 69), methanol (*m/z* 33), acetaldehyde (*m/z* 45), benzene (*m/z* 79), toluene (*m/z* 93) and monoterpenes (*m/z* 81, 137). Complete description of the instrument, sampling system, zero-air and calibration standards and measured species can be found in Misztal et al. (2014) and in Karl et al. (2013).

3.2.4   Airborne eddy covariance (EC) method

Eddy covariance is an atmospheric flux measurement technique that is used to determine the net exchange of heat, momentum and trace gases in an ecosystem through continuous, rapid, in-situ measurement of vertical fluxes in the turbulent boundary layer. Air flow can be portrayed as a horizontal flow of innumerable rotating eddies of various sizes. Measurement of characteristics of the entity of interest (e.g. vertical wind speed, heat, trace gas concentration etc.) contained within these eddies past a spatial point (on a tower or aircraft) characterizes a flux (unit quantity per unit area per unit time) (Burba, 2013). The concentration flux is determined from direct measurements as the mean covariance between vertical wind velocity (w) and concentration fluctuations (c) and is represented as:

$$F = \overline{w'c'} \tag{1}$$
$$w' = w - \overline{w} \tag{2}$$
$$c' = c - \overline{c} \tag{3}$$

where w' and c' are momentary deviation from time averages, with w' being the difference between instantaneous and mean vertical wind speed and c' being the difference between instantaneous and mean trace gas concentration. The wind speed and trace gas fluctuations need to be measured very fast (usually 10 Hz) in order to capture the characteristics of the majority of eddies in the boundary layer including those that are minutely-sized. In the current set up of the eddy covariance system, the onboard flight instrumentation measures vertical wind speed at a high frequency (10 Hz). The GHG instrument has a relatively slow sampling frequency (2 Hz) but can still be effective for eddy covariance flux computation as long as most of the flux is composed of eddies with larger frequencies. This is generally true for air parcels at altitudes where the aircraft flew (~ 250-750 m a.g.l). The comparison of the cross-spectra and ogives of vertical wind speed (fast) and CH_4 concentrations (slow) with that derived for the temperature sensor (fast) indicate if the sampling system underestimates the flux due to high frequency attenuation (see section 3.2.6). More details of the disjunct eddy covariance set up for the VOC instrumentation can be found in Misztal et al. (2014). Observed CH_4 fluxes are reported in this chapter while spatial distribution of biogenic VOC fluxes can be found in the aforementioned study.

A great number of eddy covariance measurements are conducted from ground-based towers (Werner et al., 2003; Prueger et al., 2005; Teh et al., 2011). Airborne eddy covariance (EC) is an established technique and has been previously applied to measure fluxes of energy, ozone, carbon dioxide etc. from airborne moving platforms (Lenschow et al., 1981; Desjardins et al., 1992; Mauder et al., 2007; Metzger et al., 2013). In this study, CH_4 flux is computed using the Continuous Wavelet Transform (CWT) approach that was originally developed for computing isoprene fluxes during the campaign. The method along with the traditional Fast Fourier Transform (FFT) have been explained in detail and contrasted in previous publications associated with the CABERNET study (Karl et al., 2013; Misztal et al., 2014) and previous work by co-participants (Karl et al., 2009). The wavelet method does not require assumptions of homogeneity and stationarity. It enables reconstruction of fluxes on both the time (in this case, space) domain and the frequency domain. The wavelet method allows the analyst to understand

where, along the chosen flight segment, do the coherent structures occur and what are the flux contributions at given frequencies and times along a stretch, which has to be relatively long to capture sufficient number of eddies as large as planetary boundary layer (PBL) depth. The wavelet approach results in a spatially resolved flux time series instead of a single value for the entire segment (output of FFT approach). The flux time series is presented in a format appropriate for visual representation by averaging it over a larger spatial domain (e.g. several km) to denote fluxes from a homogenous source region. Sharp enhancements in the CH_4 flux time series coinciding with peaks in concentration enhancements along the chosen flight segments can be expected from specific point sources. These CH_4 fluxes, even though only a 'snapshot in time', could be evidence of potential significant emissions from such sources. The choice of flight stretch for flux calculation is such that the chosen segment should at least long enough to encompass the complete range of frequency distribution and allow sufficient spatial statistics to achieve reasonably low systematic and random errors (> 20 km is typically needed). At the same time, the flight stretch should not be so long that the turbulent characteristics of the atmosphere vary over the stretch and are affected by diurnal variations. In this chapter, we only present results from those chosen flight segments where the flight is relatively level in altitude (± 100 m a.g.l), reasonably straight, and between 20-100 km long. Airborne EC allows calculation of CH_4 fluxes over a large spatial domain instead of a relatively fixed area around a ground-based tower as is the case in conventional eddy covariance. These fluxes are not representative of larger temporal domains (like diurnal or seasonal). But the spatial coverage is useful for determining the general distribution and magnitude of CH_4 fluxes, and to inform inventories of potentially expected ranges of emissions. No prior studies in California have looked at airborne CH_4 fluxes from anthropogenic source regions like dairies or over oil and gas fields, that has a wide distribution of identical and innumerable minor point sources and that is why adding these GHG measurements next to the existing measurements of biogenic and anthropogenic VOCs was a useful exercise.

Vertical profile flights in a racetrack sequence were flown to calculate vertical flux divergence and horizontal advection parameters to relate isoprene fluxes measured at z to surface fluxes based on equation (4) and are further described in the flux theory paper for the CABERNET study in Karl et al. (2013):

$$\frac{\partial \bar{c}}{\partial t} + \overline{\boldsymbol{u}_{x,y}} \frac{\partial \bar{c}}{\partial \boldsymbol{x}_{x,y}} + \frac{\partial \overline{w'c'}}{\partial z} = S \qquad (4)$$

where $\mathbf{u}$ (: = u, v, w) represents the three dimensional wind field corresponding to positional coordinates $\mathbf{x}$ (: = x, y, z) while S is the flux loss term. In two such flights RF 6 and RF 7, five vertical profiles were conducted over a strong source of isoprene (oak woodlands) in the eastern Sierra ranges. Survey flights aimed at deriving vertical and horizontal flux scaling parameters were not flown separately over CH_4 source transects (e.g. Central Valley dairies). From the computations presented in Karl et al. (2013), the horizontal advection flux, calculated parallel and perpendicular to each race track were on the order of 3.8 to 4.9 % relative to the average turbulent flux for isoprene. Additionally, for isoprene, vertical flux divergence was found to range from 5 % to 30 % depending on the ratio of aircraft altitude to boundary layer height (z/z_i) (Misztal et al., 2014). The vertical flux divergence of isoprene is mostly attributed to its relatively short lifetime while no chemical losses of CH_4 are expected in the mixed layer owing

63

to its much longer lifetime. The flux flights are flown in the middle of the day when PBL depth is at its maximum, vertical turbulence is at its peak and intense day time mixing causes turbulent eddies with CH_4 concentration parcels to be rapidly transported aloft to altitudes at which the CH_4 flux flight segments are flown (~ 200 - 300 m a.g.l). In such conditions, we assume δc/δz to be negligible at flight altitudes of our concern, and vertical flux divergence for CH_4 to be very similar to the lower end of the range reported for isoprene or, most likely, lesser. Hence we treat the flux estimates derived and reported for CH_4 in the following sections as a lower limit but within ~ 10 % of the 'true' surface flux values of CH_4 accounting for both horizontal advection and vertical flux divergence.

3.2.5   Footprints and source attribution

The computed flux is attributed to a surface footprint that is calculated using parameterizations developed based on the approach laid out in Weil and Horst (1992). The footprint depends on the cross-wind u (horizontal wind speed), airplane altitude z_m relative to the planetary boundary layer (PBL) height h, and the convective velocity scale w*. In the mixed layer, a half-width ($dx_{0.5}$) of the footprint can be calculated as:

$$dx_{0.5} = 0.9 \times \frac{u \times z_m^{2/3} \times h^{1/3}}{w^*} \tag{5}$$

where $dx_{0.5}$ is the half-width of the horizontal footprint derived with reference to the aircraft location extending towards the upwind direction to mark the major area of flux contribution. The horizontal distance between the extreme half-width points marks the boundary where the flux falls to one-half of its peak value. The convective velocity scale is derived from the sensible heat flux. The representative source contribution area can be presented as the semi-circular projection of the half-dome calculated from the half-width parameter on the surface with $dx_{0.5}$ representing the radius of this projection. It can be deduced from equation (5) that the footprint size can vary quite a bit with varying horizontal wind speeds and convective velocity. It should be also noted that the "true" footprint can be several times larger than the half-dome footprint but areas outside the half-dome will have significantly lower contribution to the overall measured flux at the aircraft level.

The measured flux is representative of any source within the footprint area. Only a portion of the emissions from a source lying within the footprint area is observed at a given aircraft height. A part of the flux contribution contained in the emission plume crosses the vertical plane at heights above or below the aircraft altitude and is not accounted for. The aircraft, however, also receives flux contribution from areas outside of the half-dome and regions that are further upwind. If the emission source impacting the measured signals at the aircraft is a collection of countless minor area sources of CH_4 which are randomly but relatively evenly distributed in a broad regional sense, and if the areal extent of this region is much larger than the half-width of the footprint (> 10 km), then the observed flux can be treated as representative of the whole region. An ensemble average of the flux time series on a flight segment over this region can then be determined and attributed to the concerned emissions source. Dairies are a collection of

numerous small area sources randomly distributed over a vast region (e.g. the Central Valley). The areal extent of the dairy regions is more than an order of magnitude larger than the width of the half-dome footprint (~ 1 km vs ~ 100 km). The portion of CV scoped in this study is a large area source with numerous small CH_4 sources i.e. dairies which is analogous to typical ecoregions that are focus of eddy covariance studies e.g. woodland forests with oak trees. The average flux measured by the aircraft over the Central Valley dairy regions is, consequently, the CH_4 flux for the whole ecosystem containing dairies and livestock operations and not specific to any single dairy operation. We describe later in Section 3.3.2 how we can relate and compare this flux to "bottom-up" emission rates from dairy operations. In the case of large point sources e.g. refineries or natural gas cogeneration, it is reasonable to observe a sharp "instantaneous flux" coincident with mixing ratio enhancements of CH_4 as the aircraft intercepts the emission plume from such sources. Fluxes from point source should be treated with caution as they only represent a snapshot of emissions at that moment, and may vary temporally due to activity factors and production cycles. Eddy covariance derived aircraft fluxes from point source can be of significance in order to identify potential un-inventoried or underestimated CH_4 sources.

3.2.6   Error analysis

The errors in the airborne eddy covariance flux measurements are represented by flight-segment specific systematic error (SE) and random error (RE) as have been discussed by Lenschow et al. (1994) and described for the CABERNET flights in Karl et al. (2013): .

$$SE \leq \frac{2.2 \times z_i \times \left(z/z_i\right)^{1/2}}{L} \tag{6}$$

$$RE \leq 1.75 \times \left(\frac{z}{z_i}\right)^{1/4} \left(\frac{z_i}{L}\right)^{1/2} \tag{7}$$

where z_i is the PBL height, z is the aircraft altitude a.g.l, and L is the length of the flight segment chosen for flux calculation. The total uncertainty in the derived EC fluxes can be derived by propagating the above-mentioned errors along with the uncertainties in the concentration measurements (from Section 3.2.2) and reported as total uncertainty in the reported fluxes over that segment.

3.2.7   Flux computation and Spectral Analysis

For a flight leg to be deemed eligible for flux evaluation, it needs to meet stringent eddy covariance quality control requirements (Misztal et al., 2014). The selected stretch should have a relatively constant roll angle of the aircraft avoiding sharp turns. The aircraft altitude a.g.l should be relatively stable within ± 100 m, avoiding maneuvers like saw tooth soundings. The focal point of this campaign was to measure biogenic emissions fluxes, and hence flight maneuvers aimed at evaluating the height of the planetary boundary layer (PBL) were conducted before and after the aircraft flew over the forested regions. For all RFs, the soundings occurred when the

aircraft was flying above the CV. This affected our capability to obtain flight segments "ideal" for CH_4 flux estimation. As a prerequisite, the flight leg should be at least long enough such that the measured flux covers a reasonable range of frequency distribution. A shorter flight segment also increases the random and systematic errors, which are directly proportional to the length of the flight leg. Combining all the above-mentioned criteria, only a select few CV segments were chosen for flux evaluation.

An extremely important step prior to flux computation is to apply any applicable lag-time correction. A time-lag between w and c time series can result from a residence time of air, from the time it enters the sampling inlet until it is detected, whereas the data for wind speed are delivered instantaneously. Another source of lag time can be due to drift in the internal clocks of the wind sensor and the GHG instrument. The time-lag should be determined for each segment by visually observing the position of the peak in the covariance function plot (Figure 3.3a) and then applying the necessary lag-time correction to sync both the time series and produce the covariance peak at zero-lag time. The Picarro GHG sensor has a lower sampling frequency (2 Hz) than the PTR-MS (for VOC measurements; 10 Hz) and the wind sensor (10 Hz). Thus some of the small, rapid fluctuations of CH_4 concentrations in the ambient eddies are not resolved by the instrument, and the CH_4 time series is somewhat 'smoother' than the wind speed data. Hence, the covariance function for CH_4 with wind speed is not always distinct and sharp (Fig. 3.3a) as that for isoprene (Figure 3; Misztal et al., 2014). Having aligned the wind speed and CH_4 time series in this manner, we proceed to compute eddy covariance fluxes using the wavelet-analysis approach (Torrence and Compo, 1998; Misztal et al., 2014). Co-incident occurrence of vertical wind updrafts and CH_4 concentration variances (in Fig. 3.3b) will results in positive flux events as seen in Fig. 3.3d, while the time series of wavelet frequency cross spectra (Fig 3.3c) informs us which frequencies are contributing to the "instantaneous" flux from these updrafts and downdrafts. It is evident from Fig. 3.3b that the sharp features in the vertical wind speed variance are not always correlated with the somewhat smoother variance in the CH_4 time series. This may result in occasional anti-correlation and negative flux values that dampen the overall integrated flux over the whole segment. Clearly correlated or anti-correlated episodes can also be seen in most flux segments, indicating bi-directional exchange of methane fluxes. However, since background concentration of CH_4 is quite high and can be variable, the variance in CH_4 enhancements even near the sources can be small or 'smooth' and not anywhere as strong as is the case for isoprene, and may not correlate well with the 'sharp' variances of w'. Figure 3.3d plots the crossvariance time series showing 'instantaneous' flux contributions along the segment which is then averaged and reported in Table 3.2 as mean flux over each flight segment.

Spectral analysis provides a useful tool to validate the instrument's performance in both high and low frequency regimes The spectral characteristics of each stretch are analyzed by evaluating the co-spectra and ogives of vertical wind speed (w') and concentration fluctuations (c') and comparing them with the corresponding curves for the heat fluctuations (T') obtained from measurements by the fast temperature sensor as seen in plots from one example segment (Figures 3.3e-f). The spectral analysis of the CH_4 data is limited at the Nyquist frequency of 0.5 Hz (corresponding to half the sample rate) shown as the vertical black line in the plots. The normalized co-spectra shows good agreement with the heat co-spectra curve as seen in Figures 3.3 (e-f) indicating that bulk of the eddies contributing to the heat flux are also are sampled by the CH_4 sensor. The normalized co-spectra in Figure 3.5e demonstrates that the dominant

frequencies transporting flux are in the range 0.006 - 0.2 Hz, similar to the normalized co-spectrum of $w'T'$. The dominant frequency range translates to a length scale of 0.3 to 10 km on account of the typical aircraft speed (60 ms^{-1}). The range of the length of segments over which fluxes are calculated range from 20 to 65 km and hence our choice of segments is appropriate for flux computation. Normalized cumulative distributions of the sensible heat flux and CH_4 flux cospectra, commonly referred to as ogives, are contrasted and compared to check for potential high frequency attenuation losses owing to use of a slow concentration sensor. The ogives for CH_4 flux approach 1 between 0.1 and 0.5 Hz and at slightly lower frequencies than the ogives of heat flux indicating some minor flux loss in that frequency range. This is not totally unexpected given that we are dealing with a slow CH_4 sensor with a sampling rate of 1 Hz. Overall, the spectral analysis presented here and that performed for other flight stretches demonstrates that fluxes of CH_4 are well-measured by the airborne eddy covariance sampling set up.

3.3   Results and Discussion

3.3.1   Airborne methane mixing ratios

Research flights (RFs) for the CABERNET study were flown in the month of June 2011. The aircraft speed was kept relatively consistent over all flights (~ 60 m s^{-1}). The average temperature at aircraft altitude during the entire campaign was ~ 23 °C with a range of 19 – 26 °C (Misztal et al., 2014). The duration of each flight was between 4-5 h during the middle of the day. In this section, we report the spatial distribution of CH_4 concentrations from seven flights emphasizing the regions with observations of large enhancements. The onboard meteorological data recording system malfunctioned during the first part of RF 7. Consequently, we do not have a proper alignment of spatial met data with measured CH_4 mixing ratios for part of that flight that was passing over CH_4 sources. We, thereby, do not report mixing ratios from RF 7 and focus instead on RF 6 which followed the same flight path as RF 7. CH_4 and CO_2 were measured using the Picarro sensor on all flights. Isoprene was measured on each flight by the PTR-MS while methanol was measured on all reported flights except on RF 6. Aromatics were measured only on RF 1 while acetaldehyde was measured only on RF 5. A short test flight was flown on June 1 with significant parts of this flight over the Pacific Ocean along the coast. We derive a clean air marine baseline background of 1850 ppb from a part of this test flight when flying over the ocean and reasonably away from any urban influence along the coast. We use this CH_4 baseline mixing ratio to look at deviations from the baseline as the aircraft flew over different potential regions in subsequent research flights.

Table 3.1 summarizes vital meteorological, logistical and CH_4 mixing ratio information from each of the seven flights reported here.

RF 1 – 8 June

The first survey flight targeted regions around the San Joaquin Valley. The flight headed east-southeast from Marina and after crossing the coastal mountain ranges, descended into the Central Valley and flew directly above the dairy intensive regions south of Visalia (Figure 3.4). CH_4

mixing ratios observed during this segment of the flight (length ~ 70 km, average elevation ~ 350 m a.g.l) were quite high with a concentration of 2070 ± 50 ppb (mean ± standard deviation) (Figure 3.4). Simultaneous enhancements in methanol mixing ratios (7.8 ± 1.2 ppb) and significant correlation (R^2 = 0.65) of CH_4 and methanol point towards a collocated/common source. For RF 1, benzene, toluene and m/z 107 (C8-aromatics) were also measured by the PTR-MS. There was no noticeable increase in the mixing ratios of any of these fossil fuel and combustion-related tracers during this segment. This indicates that the CH_4 enhancements were occurring primarily from a biological source, namely dairy and livestock operations.

The aircraft then headed south along the foothills over the eastern edge of San Joaquin Valley where reasonably high CH_4 concentrations persisted. These enhancements are caused due to advection of CH_4 emissions from the valley floor by the up-valley north-westerly day time winds (Beaver and Palazoglu, 2009) and are a typical feature in all flights along the eastern foothills. Following this, the aircraft flew above the city of Lancaster (and a landfill) over the Mojave Desert in both the onward and return leg experiencing high CH_4 concentrations above the urban core. The aircraft, now on its return leg, traversed the southernmost part of the San Joaquin Valley, flying downwind of several dairy operations before turning northwest.

Over the next 70 km, the aircraft flew over some of the largest and most productive oil and gas fields in the state in the western part of Kern County. This region has not been surveyed before and no account of 'top-down' measurements of CH_4 exists in published literature. The aircraft maintained a low altitude ranging from 150 – 250 m a.g.l for this segment. Huge enhancements of CH_4 of up to 400 ppb above the post-segment background were observed as the aircraft flew over oil and gas operations in the city of Taft, and over Buena Vista, Midway-Sunset and Cymric oilfields, and also downwind of a natural gas cogeneration facility (Figure 3.14 a-d). These enhancements were mostly coincident with similar spikes in the time series of the aromatics pointing towards a common fossil-fuel related source. The concentrations of CH_4 stayed high throughout this period (1980 ± 45 ppb). The CH_4 concentrations fell to near-background levels as the aircraft headed away from the oil fields and out of the Central Valley. This flight was flown during the middle of the day when vertical mixing was at its strongest on a day when the boundary layer depth (from 0.9 km to 2.8 km) peaked over the entire study. The aircraft for most parts flew at least 200 m above the ground and hence the long periods of sustained enhancements of 150 ppb or more above the marine background (1850 ppb) over much of the San Joaquin Valley points to large regional CH_4 sources.

RF 2 – 9 June

The second flight headed in a north-east direction from Marina and surveyed the eastern foothills along the northern half of the Central Valley namely the Sacramento Valley (Figure 3.5 a-b). During its approach towards the foothills, the aircraft flew over small towns in the Central Valley and then above/downwind of a dairy region. The aircraft also flew downwind and in proximity (~ 20 km) to some of the largest landfills in the region when short periods of CH_4 enhancements correlated with CO_2 were observed. Along the eastern foothills, long periods of sustained high mixing ratios of CH_4 (~ 1975 - 2050 ppb) were seen even though the flight stretch was over forested regions in the eastern Sierra when the boundary layer was fairly deep (~ 1.5 km). This shows the role horizontal advection plays in moving CH_4 emissions from the valley

floor towards the eastern edge of the Central Valley by the upslope day time winds and its accumulation there. Averaged CH_4 fluxes measured during this segment (not shown) were close to zero and confirms our assessment that the high mixing ratios of CH_4 are a result of advected emissions from farther upwind sources. The enhancements during this flight stretch can be partially attributed to emissions (natural gas pipeline distribution, landfills etc.) from the broader Sacramento metropolitan region. But the majority of the enhancements observed along the eastern foothills in the Sacramento Valley are most likely due to a combination of two sources. CH_4 emissions arise from the natural gas infrastructure in the Sacramento Valley (DOGGR, 2012). Four of the five largest non-associated gas fields of California (Grimes, Willows Beehive Bend, West Grimes and Sutter Butte; DOGGR, 2012) were located 60 - 80 km east of the flight route with prevailing westerly winds during the flight. CH_4 emissions are known to occur from extensive rice cultivation occurring during the growing season in Northern California (McMillan et al., 2007). The focus of most top-down CH_4 source assessment studies in the Central Valley has been on the San Joaquin Valley region where the most extensive dairy and livestock operations of the state are located. Record of ambient CH_4 observations from the Sacramento Valley is relatively sparse. From our observations during RF 2 and RF 3, we conclude that the heart of the Sacramento Valley floor, potentially, is a significant contributor to statewide CH_4 emissions especially since two above-mentioned CH_4 sources are categories with significant disagreement between estimates in the 'bottom-up' CARB inventory and 'top-down' estimates (Peischl et al., 2012; Jeong et al., 2013; Jeong et al., 2014). After reaching the northernmost point amongst all flight paths, the return leg of this flight followed the onward path. CH_4 enhancements were observed at similar locations as recorded during the onward path with enhancements downwind of the two landfills being 75 ppb above the regional background of ~ 1900 ppb.

RF 3 – 10 June

The flight path of RF 3 was similar to that of RF 2 (Figure 3.6 a-b). RF 3 was devoted to conducting "racetrack" profile flights over the oak woodland belt to derive parameters for wavelet flux analysis and flux divergence (Karl et al., 2013). During both the onward and return leg of RF 3 in the CV, high CH_4 mixing ratio enhancements were observed immediately downwind of the same two major landfills as observed during RF 2. High concentrations were also observed when flying over the dairy regions in the CV.

RF 4 – 14 June

The initial path of survey flight RF 4 was the same as RF 2 and RF 3 until the aircraft turned north-west and flew over the Sacramento - San Joaquin delta (Figure 3.7). The aircraft then flew directly overhead the most productive non-associated gas field in the state (Rio Vista gas field; DOGGR, 2012) and recorded a sharp 120 ppb enhancement flying over the natural gas infrastructure. After crossing the Central Valley, the aircraft turned south-east and proceeded to fly straight along the eastern foothills, reached the southernmost point of this flight, and then turned back and followed north-west along the same route, the total duration of this 'foothill' segment being close to 2.5 hours and spanning ~ 500 km. Through the entire second half of this segment (> 1-h), the highest CH_4 concentrations recorded during the study were observed with a mean of 2220 ± 100 ppb, representing sustained enhancements close to 400 ppb above the

marine background, with peak concentrations touching 2500 ppb (Figure 3.7). The PBL depth during this stretch, while still increasing, ranged from 1.2 km to 1.5 km at the end of the segment. As previously mentioned, high CH_4 concentrations along the eastern foothills are a result of transportation and accumulation of emissions from the valley by prevailing up-valley and up-slope day time winds. In this case, the most densely concentrated dairy regions of the state including those in Tulare, Merced, Stanislaus, Madera and Fresno counties lied directly upwind of the flight route.

During the return leg, the aircraft turned west, south of the city of Fresno and re-entered the valley recording high CH_4 concentrations (> 2000 ppb) flying directly over dairies. It should be noted that the CH_4 concentration flying directly above dairies in all of RF 1, RF 4 or RF 6 were not as high as the levels experienced in RF 4 along the foothills. This indicates the importance of meteorology and topography in the fate of emitted gases in the valley. It shows how the bowl-like topography of the San Joaquin Valley can trap and accumulate emissions of GHGs, VOCs and other ozone precursors emitted from extensive agricultural and oil-and-gas activities in the Valley. It also underlines the importance of horizontal advection and deposition fluxes of CH_4 downwind of emitted sources (see Section 3.3.2).

RF 5 – 15 June

Research Flight 5 headed directly north and flew along just to the east of the San Francisco Bay Area (Figure 3.8). Several short-duration enhancements were observed as the aircraft flew downwind of the metropolitan region. Of particular interest was a sharp enhancement in CH_4 mixing ratio (> 100 ppb) just to the north of San Pablo Bay flying very close and immediately downwind of a large landfill in the Marin county (Figure 3.8 a) that was accompanied by a coincident peak in the CO_2 time series. A similar enhancement downwind of the same landfill was also observed in the return leg (Figure 3.8 b) though not as pronounced. After traversing over the northern coastal hills the aircraft turned south-east in its return leg and descended into the Sacramento Valley to fly directly above actively cultivated rice paddy fields. It was then that the aircraft flew through a biomass plume that was visually observed using the hi-definition camera onboard in the aircraft cockpit. Biomass burning is a known source of CH_4, CO_2 and acetaldehyde (Andreae and Merlet, 2001). Acetaldehyde was included as a tracer in RF 5. The acetaldehyde concentrations showed a huge spike of up to 25 ppb that was several folds larger than the acetaldehyde background for the majority of RF 5 (< 1 ppb). At the same time, a CH_4 spike of 150 ppb was observed along with a sharp CO_2 spike indicative of emissions from a biomass burning combustion source.

On the return leg, the aircraft recorded a sharp CH_4 enhancement just as the aircraft entered the San Pablo Bay area (discussed in Section 3.3.2). The aircraft did not directly fly above or directly downwind any of the region's five refineries and did not record any sharp CH_4 enhancements when in the refinery region. The concentrations downwind of the southern part of Bay Area during a 10 minute stretch on the return leg were high and averaged close to 2000 ppb (1990 ± 18 ppb). Along with evidence of relatively high CH_4 mixing ratios downwind of the Sacramento region in RF 2, long periods of enhancements downwind of the Bay Area indicate that CH_4 emissions from urban regions can be significant and besides landfills, leakages from the natural gas pipeline network could be a major local source of methane. Relatively constant and

low boundary layer depths along the coast of ~ 1.1 km means that the CH_4 emissions in the urban Bay Area resulting in the observed enhancements are not as large as CH_4 emissions encountered in the Central Valley resulting in similar enhancements as the boundary layer is generally deeper heading inland into the Valley.

RF 6 – 8 June

Research flight 6 was aimed at performing racetrack flights over a homogenous oak terrain in the eastern foothills as seen in Figure 3.9. To reach the targeted region, the aircraft headed out west and crossed the width of the Central Valley both during the onward as well as the return leg. During these segments, the aircraft flew over the dairies in the Madera County. The mean CH_4 concentration over the combined dairy segments (~ 110 km) was 1960 ± 22 ppb which is a significant 110 ppb more than the marine baseline during the entire stretch over the dairy and feedlot region. There were no MeOH measurements during RF 6.

RF 8 – 21 June

The last survey flight was flown on the hottest day of the campaign. The aircraft flew south from Marina over the forested regions in the hills along the Central Coast of California (Figure 3.10). The flight path, in general, had the least urban influence and there were no major landfills or dairy operations along the flight route. The coastal mountains act as a natural barrier and the daytime sea-to-land breeze prevents the agro-industrial complex in the Central Valley from influencing the mixing ratios observed during the flight path in RF 8. Consequently, RF 8 encountered relatively low CH_4 mixing ratios with the mean over the entire flight being 1890 ± 20 ppb. The boundary layer ranged from 0.7 to 1.4 km for the whole flight leg and was generally shallower than that during other flights making the observed enhancements minor . Isoprene and MeOH are two of the major VOCs emitted from vegetated regions, with large temperature dependent emissions especially during the summer (Schade and Goldstein, 2006; Guenther et al., 2012; Park et al., 2013). During certain segments of RF 8 flying above forested regions, we observed the high mixing ratios of isoprene (~ 4 - 8 ppb), that also happened to be the highest observed during any of the eight flights. This was accompanied by high levels of MeOH (~ 10 - 15 ppb). CH_4 mixing ratios, during the long flight legs over forests, were reasonably low (< 40 ppb enhancement above the marine background (Dlugokencky et al., 2014). This resulted in typical MeOH / CH_4 emission ratios of ~ 200 - 400 (mmol mol^{-1}) which is more than 20 times larger than typical ratios observed from dairy sources (see Section 3.3.2). This demonstrates that while high emissions of biogenic VOCs are expectedly observed from the forested regions, CH_4 emissions from these biogenic regions are found to be insignificant as compared to the major sources in the Central Valley. The one interesting observation was a period with some high CH_4 mixing ratios (1950-1975 ppb) very close to the coast near San Simeon on two unique runs in the region. There are no known potential CH_4 sources in this somewhat uninhabited part of the state (Figures 3.1 and 3.10) and all offshore oil/gas operations are > 200 km to the south. We have not been able to establish the cause of these enhancements.

3.3.3 Relative emission rates and Eddy Covariance fluxes

VOCs measured during the campaign act as potential source markers and are used to distinguish between biogenic and anthropogenic CH_4 emissions. Depending on the suite of VOCs measured during a particular Research Flight, it is also possible to distinguish between biological and fossil-fuel based CH_4 emissions. In this section, we narrow down our analysis on selected individual segments within different Research Flights when the aircraft is flying above (or downwind of) known and potential CH_4 source regions. We report relative emission rates (RERs) of CH_4 with respect to CO_2 and/or VOCs (e.g. in mol mol^{-1} units) and compare these RERs with literature, inventory estimates and emission rates reported in this dissertation from other studies in order to identify the major CH_4 sources contributing to the observed signals. In those segments, where criteria regarding suitable flight legs for flux derivation are met, we apply the wavelet-flux technique to compute CH_4 fluxes (Table 3.2). We then proceed to compare these flux estimates with those derived from the 'bottom-up' inventory.

Dairy and livestock operations

During various Research Flights, the aircraft flew directly above (and downwind of) dairy and livestock operations in the Central Valley (Figure 3.11 a-f). This includes flight segments during RF 1 (in Kings and Tulare County) in the San Joaquin Valley, a short segment during RF 1 over southern San Joaquin Valley (Kern County), separate segments during onward and return legs of RF 2 (in San Joaquin County), during the return leg of RF 4 (in Fresno County) and, finally, during onward and return legs of RF 6 (in Madera County). During each of these flight legs, high CH_4 concentrations were observed that were routinely accompanied by high concentrations of methanol. Methanol (MeOH) is an important dairy tracer and is emitted from animal manure, waste lagoons and from fermentation of silage (Filipy et al., 2006; Shaw et al., 2007; Ngwabie et al., 2008; Chung et al., 2010). It is coincident with CH_4 emissions which are predominantly emitted from enteric fermentation and management of manure (Shaw et al., 2007). Figure 3.12 (a) shows an example of CH_4 time series plotted along with measured VOCs during a segment over Central Valley dairies in RF 1. In Figure 3.12 (a), CH_4 and MeOH concentrations increase as the flight proceeds along the valley floor and are correlated to a certain extent. The slope of a weighted ODR fit to the MeOH / CH_4 enhancements (orange circles in Fig. 3.12 b) is 11 ($\pm$ 0.4) ppt MeOH ppb CH_4^{-1}. There are no noticeable enhancements in the benzene and toluene time series during the entire segment (Fig 3.12 a) which indicates that the CH_4 source is not related to fossil-fuel use, extraction, or combustion. The concentrations of isoprene, which is mostly emitted from oak forests in the valley foothills but not so much from crops (Karlik and Winer, 2001; Guenther et al., 2012), also remain low throughout the leg. Hence the CH_4 enhancements are attributed to the dairy and livestock operations in the region. It should be noted that agriculture in the Central Valley is another source of MeOH (Goldstein and Schade, 2000; Fares et al., 2011, 2012; Park et al., 2013). This is one reason why the linear-fit to the CH_4 and MeOH enhancements is not higher ($R^2 = 0.46$) and thus the slopes reported here are upper limits of actual dairy MeOH / CH_4 relative emission rates (RERs). The large range of measured MeOH / CH_4 slopes (9 to 88 ppt MeOH ppb CH_4^{-1}) can be explained by the variability of MeOH emissions that are strongly temperature dependent (both from dairies and crops). The MeOH / CH_4 slopes observed during return flights in RF 1 (22 ppt MeOH ppb CH_4^{-1}; late-afternoon) are higher than those during the onward flight (11 ppt MeOH ppb CH_4^{-1}; early

afternoon) when temperatures were lower. Also, slopes observed in later flights on warmer days e.g. in RF 4 (61 ppt MeOH ppb CH_4^{-1}) are higher than that observed in RF 2 (45 ppt MeOH/ppb CH_4) which, in turn, is higher than slopes observed during RF 1. Elevated levels of CH_4 were also observed in the onward and return legs of RF 6 flying over the Central Valley (Fig. 3.11e-f) although MeOH was not measured during this flight. The positive matrix factorization (PMF) derived MeOH / CH_4 RER for the dairy and livestock factor measured from the ground site at Bakersfield (Chapter 2) ranges from 15 - 47 ppt MeOH ppb CH_4^{-1} and is similar to the slopes we observe from the aircraft. The observed slopes are also similar to that measured from an aircraft during summer of 2010 over dairies in the Kern County (7 – 16 ppt MeOH ppb CH_4^{-1}; Gentner et al., 2014).

Table 3.2 reports the average flux integrated over unique flight segments flown over the dairy and livestock intensive regions in the San Joaquin Valley. Outside of the dairy segment flight in RF 1, the averaged wavelet-flux for different dairy-related segments ranged from 28 to 68 nmol-CH_4 m^{-2} s^{-1}. The largest CH_4 fluxes were observed during the flight segment over the dairy and livestock intensive regions in Kings and Tulare County (RF 1), which have the highest density of cattle population in California (Table 3.3). The average CH_4 flux over this segment was 294 nmol-CH_4 m^{-2} s^{-1}. The peak positive discrete fluxes within individual segments were up to 1390 nmol-CH_4 m^{-2} s^{-1}. We also measured significant negative flux values (down to - 260 nmol-CH_4 m^{-2} s^{-1}) during these dairy segments. It is reasonable to assume that when we fly over the dairy regions we observe CH_4 emissions, but downwind of the source the CH_4 may have a "negative flux" simply because the high concentrations aloft are advected, and then mixed back down towards the surface. This, in part, explains why we see very high CH_4 concentrations along the eastern foothills (see Section 3.3.1). Hence, horizontal advection of emissions from farther upwind dairies and subsequent deposition of emitted CH_4 fluxes are taking place in conjunction with CH_4 emission fluxes from the dairies within the region. The magnitude of the average net flux in each segment is, therefore, decreased by these occasional negative flux episodes even though strong bidirectional exchange of fluxes with large magnitudes is observed. We do not report the positive and negative fluxes separately and treat the averaged flux for the whole segment to be representative of the net flux observed above the dairy and livestock region. The length of individual segments in Table 3.2 for dairy segments conforms to the wavelet-method requirements although 'saw-tooth soundings' prevented us from getting longer segments for flux computation, thereby increasing the reported uncertainty in the eddy covariance measurements.

The bottom-up GHG inventory (CARB, 2013) reports CH_4 emissions from dairy and livestock sector in the units of mass per unit per time (e.g. kg CO_2-eq cowhead^{-1} year^{-1}). In order to evaluate airborne eddy covariance CH_4 fluxes from the dairy regions w.r.t to bottom up estimates quantitatively, we need to derive an areal distribution of cattle population at the regional level (i.e. cowhead area^{-1}). Table 3.3 reports the statistics on area and cattle population in the eight counties that comprise the San Joaquin Valley. In order to derive this information, we gathered data on the heads of cattle (including milk and beef cows, heifers, steers, calves etc.) at the county level (CASR, 2011) for the year 2011. We use spatial information on California's bio-regions (McNab et al., 2007) and geospatial data obtained from California Department of Forestry and Fire Protection (Kelly Larvie, CAL FIRE) to plot the spatial extent of these eight counties that lies within the San Joaquin Valley portion of the Central Valley (Figure 3.13). From the figure, it is evident that all dairy and livestock operations in these eight counties are

located within the relatively flat San Joaquin Valley bio-region (marked as Great Valley in the Figure). We, thus, derive a surface density of cattle in the San Joaquin Valley to be 170 cowhead km^{-2}. The ecosystem-level CH_4 fluxes from the dairy regions reported in Table 3.2 are computed on segments that fall completely within the San Joaquin Valley portion of these counties. None of our dairy flux segments were flown in the Kern County where a vast majority of oil and gas operations, which are a potential CH_4 source, are located. We still exercise caution in our approach and do not include the cattle numbers or the area of the Kern County portion of San Joaquin Valley in our calculation of the area density factor. Though landfills are a major CH_4 source in California accounting for ~ 25% of total emissions, locations of landfills (Figure 3.1) generally scale with human population. The San Joaquin Valley (not including Kern County) accounts for less than 8% of the state's population and many of the few landfills in the region are in the foothills and not in the valley. Additionally, there were no landfills within an extended footprint of 10 km upwind from the aircraft locations on any of the dairy flux segments except in the return leg of RF 4 (Fig. 3.7). During this segment, there was no observable sharp feature in the CH_4 time series as the aircraft flew ~ 8 km downwind of the landfill. We see no evidence of contamination of the CH_4 dairy region flux by any landfill source contribution. Based on the evidence from the VOC source tracers and spatial location of dairy and livestock operations, we can reasonably state that the flux measured on these segments is representative of emissions from the dairy and livestock sector. Using the above-derived area density factor, we report a range of measured average CH_4 emission rates of 83 to 873 kg CH_4 cowhead^{-1} year^{-1} from different dairy flux segments derived from airborne EC measurements with an uncertainty of ~ 23 - 29 % (Table 3.2). The large variability in the range is explained by the high mean CH_4 emission rates (873 kg CH_4 cowhead^{-1} year^{-1}) over RF 1 which also happened to be the segment through the highest cattle density region in the SJV. Excluding RF 1, the mean fluxes for other dairy segments ranged between 83 – 202 kg CH_4 cowhead^{-1} year^{-1}

Average CH_4 emission rates for the cattle population were also generated using reported emission factors from the GHG inventory (CARB, 2013). The emission factors for enteric fermentation for different cattle type is combined with activity data (cowheads) to obtain a weighted emission factor for the entire cattle population of the state. The CH_4 emission factor from enteric fermentation source category is calculated as 83 kg CH_4 cowhead^{-1} year^{-1}. A similar procedure is followed for the manure management sector and gives an average emission factor of 77 kg CH_4 cowhead^{-1} year^{-1}. It should be noted that San Joaquin Valley accounts for more than 90 % of California's cattle population and hence the population averaged-CH_4 emission factor should be a good representation of Valley's cattle population. The contributions from enteric fermentation and manure management sums to a total of ~ 160 kg CH_4 cowhead^{-1} year^{-1} emitted from the dairy and livestock sector. The top-down estimates from this study (83 – 202 kg CH_4 cowhead^{-1} year^{-1}) are in excellent agreement with the bottom-up inventory estimate for CH_4 emissions from the dairy and livestock sector. The inventory estimate is substantially low if the high CH_4 flux from the dairy segment in RF 1 (over Kings and Tulare County) is included in the comparison. Our top-down flux-based estimate is also in agreement with the range of CH_4 emission rate (92 - 132 kg CH_4 cowhead^{-1} year^{-1}) reported for enteric fermentation from a California cow-chamber study (Shaw et al., 2007). The overall conformity of our analysis results with the bottom-up inventory numbers is a validation of the airborne eddy covariance concept and its suitability for 'top-down' estimation of CH_4 from regional area sources like dairies. It is

also a useful verification of the bottom-up inventory for CH_4 emissions from dairies in this region.

Oil and gas operations

The return leg of RF 1 focused on the vast oil and gas (O&G) industrial complex located in western Kern County. This region is isolated at the south-western edge of the Central Valley and is far from major dairy and livestock operations (> 25 km). The aircraft spent about 20 minutes flying over some large O&G fields in a relatively straight flight leg ~ 70 km in length. The average aircraft altitude over this leg was reasonably low at ~ 220 m a.g.l. Figure 3.14 (a-d) shows the flight track color coded by CH_4 concentration as the aircraft flew over the Midway-Sunset oil field, Buena Vista oil field and the Cymric oil field. The entire landscape was dotted with numerous oil pumpjacks and a host of industrial operations surrounding O&G extraction as seen in images in Fig. 3.14 obtained from the onboard GPS enabled high-definition video camera (Contour Inc., USA). The mean concentration over the entire leg was high at 1980 ± 45 ppb with individual emission enhancement peaks that ranged from 100 to 300 ppb as compared to pre-and post-plume mixing ratios as seen in Figure 3.15 (a). The large CH_4 mixing ratios were accompanied by a similar trend in the CO_2 concentration time series. Benzene and toluene were measured in RF 1 and their time series showed sharp occasional peaks that were coincident with the CH_4 peaks. This points to a fossil fuel based combustion/fugitive source contributing to the CH_4 enhancements on this leg. The time series of methanol (Figure 3.15 b), whose main sources in the Central Valley are dairies and crops, did not have the structure or the peaks that were seen in the CH_4, CO_2, benzene and toluene time series. This confirms that the origin of the CH_4 enhancements was not biological and its likely source is fugitive / vented emissions from the underlying O&G complex.

Of particular interest is a snapshot in time within this O&G leg that is presented as Segment 2 in Figure 3.15 (b). The aircraft in this 7 s stretch encountered a plume with a sharp peak in CH_4 mixing ratio (~ 2150 ppb) that was 200 ppb above the immediately preceding and following background CH_4 level. Using video evidence (Figure 3.14) and GPS coordinates from the camera, the source of the plume is identified as 1124-MW La Paloma natural gas cogeneration plant near the town of McKittrick. The flight video also confirms that there were no O&G operations immediately upwind of the power plant. The direction of wind barbs and scale bar in Fig. 3.14 (b) confirms that the aircraft flew immediately downwind and within 2 km from the facility. The sharp CH_4 enhancement was coincident with simultaneous peaks in benzene, toluene and xylene (not shown) time series. Interestingly, there was no enhancement of CO_2 which would be expected if the plume is originating from the emissions stacks of the facility which strongly points towards a vented (intentional) or fugitive (unintentional) release of CH_4 from the natural gas cogeneration facility.

Outside of segment 2, portions of this flight leg (in Segment 1 and 3; Figure 3.15 b) were located above a dense distribution of O&G operations within the large spatial boundaries of the fields. The O&G source region is dotted with thousands of minor sources (pump jacks, condensate tanks etc.). We derive airborne eddy covariance fluxes for this flight leg in a similar way as we did for the dairy source regions and attribute this flux to the O&G source region (Table 3.2). The black trace in Figure 3.15 (b) represents the wavelet-method EC CH_4 flux time

series. We consider only the contributions to the flux time series from Segment 1 and 3 as being representative of the upwind O&G source regions. Eddy covariance fluxes over the O&G source region ranges from - 228 nmol-CH$_4$ m^{-2} s^{-1} over barren stretches to up to 1575 nmol-CH$_4$ m^{-2} s^{-1} over some portions of Midway-Sunset and Cymric oilfields. The average flux over the oil field segment is 313 nmol-CH$_4$ m^{-2} s^{-1} with an uncertainty of 28 %. The combined uncertainty in the measurements are estimated by propagating uncertainties arising due to instrumental and calibration error, and random and systematic errors in deriving airborne eddy covariance measurements. The airborne eddy covariance flux measured during the short Segment 2 was demonstrably due to a singular point source namely the La Paloma cogeneration plant. For the sharp flux event observed downwind of the natural gas cogeneration facility, the flux observed averaged 945 nmol-CH$_4$ m^{-2} s^{-1} with a peak value of 2468 nmol-CH$_4$ m^{-2} s^{-1}.

The majority of time in the O&G leg was spent flying above two main oil fields, Midway-Sunset and Cymric, which together account for ~ 25% of California's oil production, and are the largest and fourth largest oil fields in the state by oil production, respectively (DOGGR, 2012). We derive bottom-up areal CH$_4$ emission rates for these two oil fields. We obtain annual CH$_4$ emissions utilizing O&G industry survey data from Lee et al. (2011) taking into account emissions from combustion, venting and fugitive sources both from oil production and associated gas extraction. We combine this with activity data for oil and associated gas production for these two oil fields (DOGGR, 2012) to generate field-specific emissions for the year 2011 which we scale to the spatial extent of the two oil fields in order to generate bottom-up areal CH$_4$ emission rates. The Midway-Sunset has a CH$_4$ emission rate of 72 and 12.3 nmol-CH$_4$ m^{-2} s^{-1} from crude oil production and associated gas production, respectively while the emission rates for Cymric oil field are 70 and 81 nmol-CH$_4$ m^{-2} s^{-1}, respectively. This leads to total CH$_4$ emission rate of 85 – 151 nmol-CH$_4$ m^{-2} s^{-1} from these two oil fields which are similar but somewhat smaller than the eddy covariance fluxes observed over this stretch from the aircraft (313 nmol-CH$_4$ m^{-2} s^{-1}; Table 3.2). The total statewide CH$_4$ emissions as accounted for using the above mentioned industry reported data (~ 110,000 metric tons of CH$_4$ year^{-1}) in Lee at al. (2011) in itself is about 250 % larger than their current inventory estimate (CARB, 2013) for the O&G extraction sector which stands at ~ 3% of the total CH$_4$ inventory. Hence the CH$_4$ flux estimates we observe seem to be much larger than what is currently represented in the inventory.

The CH$_4$ emissions from the La Paloma facility in 2011 were 236 metric tons CO$_2$-eq as per Environmental Protection Agency (EPA) tool for self-reporting GHG emissions from large facilities (FLIGHT, 2014) although the 2012 and 2013 emissions are four times higher. This amounts to a total of ~ 10000 kg of CH$_4$ emitted from this facility in 2011 which is equivalent to annual CH$_4$ emissions from a 60 cowhead dairy (see Page 74 under 'Dairy and Livestock operations). California has close to 5.4 million cattle heads and thus the self-reported CH$_4$ emissions of this facility represent a surprisingly insignificant fraction. Our flights downwind of the facility clearly indicate a large CH$_4$ release (~ 200 ppb enhancement at 2 km spatial separation from source). The CH$_4$ leak we observed is a snapshot in time and a second flight downwind of this facility was not performed during the CABERNET study. Being a continuous power-generation operation, we can logically reason that the CH$_4$ leaks and the corresponding enhancements should be similar all through the year and the 'true' CH$_4$ emissions likely higher than that of a 60-cowhead facility.

The western Kern County O&G region lacks any prior published account of top-down measurements of CH_4 either from the ground or at the airborne-spatial resolution. Our mixing ratio measurements and airborne eddy covariance flux estimates are a rare account of measured data in this region. Though not exhaustive, we provide an educational account of the top-down observations in a region that accounts for well more than 50 % of the state's O&G production. The emissions in the CARB inventory for the O&G sector are lower than industry-reported CH_4 emissions (Lee et al., 2011) which are, in turn, lower than the eddy covariance areal flux estimates derived in this study. The flux observations from the O&G region are similar and somewhat larger than regional emission rates observed over the dairy source regions. Additionally, there is strong evidence of high CH_4 mixing ratios with sharp enhancements originating from this region measured during our flight. This overwhelming evidence of a data trend invites attention to further investigation of CH_4 emissions from this region.

During the first half of RF 4, the aircraft flew over the Sacramento - San Joaquin delta region east of the San Francisco Bay Area and close to the location of Walnut Grove tower (see Chapter 4). The aircraft, during this leg, flew right above and through the Rio Vista gas field at an average elevation of 375 m a.g.l (Figure 3.16 a). We observed a sharp enhancement in CH_4 time series for a 15 s period before the concentrations returned to the pre-enhancement levels (Figure 3.16 b). During this period, the CH_4 concentrations rose to ~ 2030 ppb marking an enhancement of ~ 120 ppb above the local background. The CH_4 enhancement was not accompanied by any noticeable increase in CO_2, methanol or isoprene concentrations which suggests that the origin of this sharp enhancement was not biological or combustion related but rather of fugitive nature. There were no hydrocarbon measurements on this flight to confirm our assessment. The Rio Vista gas field is the largest non-associated gas field in California accounting for 4 % of the state's total gas production (DOGGR, 2012). The observations from this leg along with the sustained period of high CH_4 mixing ratios downwind of non-associated gas fields during RF 2 (see under 'RF 2 - 9 June', Page 68 and Figure 3.5) suggest that significant sources of CH_4 emissions exist in the Sacramento Valley and these are potentially from natural gas fields. Overall, we believe that there is a definite need to verify and validate CARB's CH_4 inventory for the O&G sector through targeted source-specific or region-specific top-down measurements.

Wetlands

In both the onward and return leg of RF 5, the aircraft flew over San Pablo bay in the Bay Area and further north flying above wetlands and a tidal marsh ecosystem that are part of the San Pablo Bay National Wildlife Refuge. A large enhancement of CH_4 was observed flying above the wetland ecosystem during the return leg while a minor but noticeable increase in CH_4 concentrations were also observed during the onward leg (Figure 3.17 a-b). The time series of CH_4 is plotted against that of CO_2 in Figure 3.17 (c), and there is an anti-correlation of CH_4 and CO_2 time series. Wetland restoration habitats create anaerobic conditions and are known to release CH_4 along with simultaneous uptake of CO_2 during day time (Le Mer and Roger, 2001; Miller et al., 2011; Poffenbarger et al., 2011). This phenomenon among other factors is also temperature dependent and this is likely why we see a larger enhancement of CH_4 in the return leg when surface temperature was higher, as compared to the minor enhancements seen during the onward leg.

Biomass burning

A biomass burning plume was encountered while descending into the Sacramento valley from the Coastal Mountain ranges during RF 5 (Figures 3.8 b and 3.18 a). This event was captured by the onboard video camera which showed that the aircraft flew right through an undispersed freshly emitted plume at an altitude of 130 m a.g.l originating on the sides of an irrigation canal in the Colusa County (Figure 3.18 a). A sharp enhancement was observed with concentrations of all measured tracers showing a massive rise (Figure 3.18 b). Acetaldehyde, which was measured for this flight showed an unprecedented increase from a pre-plume background of ~ 500 ppt to more than 25000 ppt (25 ppb). CO_2 concentrations rose by more than 25 ppm while the enhancement in CH_4 was more than 120 ppb. Biomass burning is known to produce minor amounts of CH_4 as well as VOCs including methanol and acetaldehyde (Andreae and Merlet, 2001).

Rice cultivation

During the same flight stretch (RF 5), the aircraft flew over rice paddy fields as it descended into the Sacramento Valley. This region is tucked along the western edge of the Sacramento Valley and is insulated from most urban and dairy influences. The nearest major natural gas fields are about 20 km to the north. During this flight stretch (seen in Figure 3.18 c), the time series of CH_4 and CO_2 are anti-correlated indicating emissions of CH_4 with simultaneous active uptake of CO_2. Such a trend is typical of measurements from rice paddy fields where daytime photosynthetic CO_2 uptake by the maturing crop is accompanied by CH_4 emissions (McMillan et al., 2007; Baldocchi et al., 2012, Hatala et al., 2012; Knox et al., 2014). The CH_4 is produced by methanogens residing in the anaerobic regions of flooded and submerged soils primarily through the aerenchyma of rice paddy plants (Cicerone and Shetter, 1981; Le Mer and Roger, 2001). A slope generated from the CH_4 and CO_2 time series during this 'rice-paddy' leg has been previously reported in Peischl et al. (2012) and is equal to - 5.6 ± 0.2 ppb CH_4 ppm CO_2^{-1} (R^2 = 0.86). This slope is consistent with the flux ratio reported by McMillan et al. (2007) in a multiyear project during the 2000-2002 periods at a rice paddy field in the Sacramento Valley. The authors reported a flux CH_4 / CO_2 ratio of - 0.6% for rice crop in its early stages of growth while the ratio goes up to − 2.7% in the middle and later stages of vegetative growth. This slope is also consistent with the agricultural emissions slope [- 6 (± 2) ppb CH_4 ppm CO_2^{-1}] obtained from a multivariate linear regression analysis of data from flights conducted in this part of the Valley in the summer of 2010 (Peischl et al., 2012).

For this relatively short stretch (20 km), we calculated averaged airborne eddy covariance CH_4 flux to be 26 ± 16 nmol-CH_4 m^{-2} s^{-1} with a high uncertainty of 60 % in our flux measurements on account of the short length of the stretch. The prevailing wind directions (Figure 3.18 a) make it unlikely for this flight leg to be influenced by emissions from the other potential CH_4 source in the region i.e. natural gas fields in the Sacramento Valley. The rice paddy was located in the Colusa County with extensive stretches of homogenously distributed paddy fields that account for 25 % of the state's rice acreage (CASR, 2011). Thus, we attribute the measured CH_4 flux to rice cultivation. During the same time in summer of 2011, CH_4 fluxes were measured using conventional tower-based eddy covariance approach at a rice paddy field in the Sacramento − San Joaquin delta (Hatala et al., 2012; Knox et al; 2014). The mean CH_4 flux

during the daytime period (10 am – 5 pm) at this rice paddy field was 10.5 ± 16 nmol-CH_4 m^{-2} s^{-1} in the week of the airborne measurements. The two independent sets of 'top-down' measurements are in conformity with each other. The Sacramento Valley is host to ~ 95 % of the rice crop that is grown in California annually (~ 560,000 acres) and brings in close to a billion dollars in revenue (CASR, 2011). In 2011, rice cultivation accounted for about 3.3 % of the total CH_4 emissions in the state inventory (CARB, 2013) with a cumulative annual activity emission rate of 214 kg CH_4 ha^{-1}. Source-specific chamber and ground-based flux measurement studies report a higher cumulative annual emission rate of 348 to 413 kg CH_4 ha^{-1}(McMillan et al., 2007). Our CH_4 / CO_2 emission rate slopes reported in Peischl et al. (2012) are consistent with those reported in McMillan et al. (2007) where the authors conclude that the contributions of CH_4 emissions from rice cultivation are being underestimated in the CARB inventory based on year-round measurements. The airborne eddy covariance measurements were conducted when the rice crop in California is in its early stages of growth. Since CH_4 emissions from rice cultivation are temporally variable and increase deeper into the growing season, we cannot directly scale the measured CH_4 fluxes to generate an annual estimate rate which we can compare with the cumulative bottom-up inventory emission rate. We, however, find that our airborne flux measurements over the rice paddy field segment are, generally, similar to ground-level measurements conducted during the same time period.

Landfills

On different occasions on multiple flights, the aircraft flew downwind of some major landfills and encountered plumes containing large enhancements of CH_4 (Figures 3.19 a-h). These enhancements ranged from 75 – 125 ppb over four different flight segments (RF 2 and RF 3) at a distance of ~ 20 km downwind of the Vasco and Altamont landfills east of the Bay Area. The enhancements, about 20 km downwind of Kiefer landfill southeast of Sacramento on the same flights, were 75 – 100 ppb as compared to pre-plume and post-plume mixing ratios. CH_4 and CO_2 were well-correlated in all of these segments while there were no distinct enhancements in the MeOH time series. In RF 5, the aircraft flew 15 km downwind of the Redwood landfill in Marin County during both the onward and return legs and observed CH_4 enhancements ranging from 65 - 100 ppb. CH_4 emissions from landfills can theoretically be evaluated by combining the measured slope of CH_4/CO_2 in landfill plumes with activity data and waste mass to CO_2 conversion coefficients. In order to apply this approach, a downwind receptor e.g. an aircraft has to fly very close to the targeted landfill in order to sample a plume from the source that has not significantly dispersed and diluted. This is especially relevant for CO_2 emissions from the landfills that are difficult to detect above a large background if sufficiently diluted. Flight runs upwind of the landfills should also be performed to get background levels in uncontaminated air. Such a method would be best applicable over remotely located landfills with no nearby CH_4 and urban CO_2 sources. The flight stretches in Figures 3.19 (a-h) are located downwind of not just major landfills but also downwind of large urban regions. Hence the sampled plumes not only contained CH_4 emissions from the landfills but also any undiluted emissions from the upwind urban core. This prevents us from applying a correlation based approach to derive landfill-specific CH_4 / CO_2 scaling factors although most of the CH_4 is reasonably presumed to be originating from the landfills. For point sources like landfills, airborne eddy covariance cannot yield landscape–level averaged fluxes. If the aircraft flies very close to the source such that the source is completely within the footprint or very close to it, an "instantaneous" CH_4 flux peak

79

may be observed that can be scaled to the area of the landfill to generate a CH_4 emission rate for comparison with the inventory. In this study, there were no flight stretches that directly flew overhead or in close proximity to a landfill and we do not attempt to determine CH_4 flux estimates from the current segments.

3.4   Summary

We performed forty hours of flight measurements of CH_4 all across California to identify the sources of CH_4 in different regions responsible for the ambient enhancements observed at the aircraft level. We successfully apply the airborne eddy covariance (EC) technique to derive CH_4 fluxes. On all flight segments over the Central Valley of California, the mixing ratios levels of CH_4 are elevated (> 2000 ppb) for extended periods. These concentrations are well correlated with the dairy source marker methanol (9 to 88 ppt methanol ppb CH_4^{-1}). The similarity of the airborne-observed CH_4 relative emission rates over this region with respect to methanol, to that generated from ground-based dairy measurements and PMF dairy and livestock source relative emission rates (Chapter 2) points to extensive emissions from the dairy and livestock sector in the Valley. The mean ecosystem level CH_4 fluxes calculated over the dairy source regions range from 28 to 294 nmol-CH_4 m^{-2} s^{-1}. We combine the emission rates with an areal cowhead density factor determined for the San Joaquin Valley bioregion, and get CH_4 emission rates of 83 to 873 kg CH_4 cowhead^{-1} year^{-1}.

The observed mean CH_4 mixing ratios are high flying above the oil and gas (O&G) industrial complex in western Kern County (~ 1980 ppb). Individual enhancements peaks of up to 300 ppb above the local background are observed while flying above the operation-dense parts of the O&G fields. These enhancements are coincident with enhancements of benzene and toluene pointing towards a source with fossil-fuel origins. CH_4 flux averaged over the only O&G flight leg is 313 nmol-CH_4 m^{-2} s^{-1}. This flux rate is similar to the areal emission rate derived from industry-reported CH_4 emissions from the two large O&G fields covered in this stretch and scaling their CH_4 emissions to the area of the oil fields. A sharp fugitive / vented release of CH_4 (~ 200 ppb) is also observed from a natural gas cogeneration facility which is perhaps mistakenly referred to as an insignificant source in the current CARB inventory.

We observe anti-correlation of CH_4 and CO_2 with a slope of - 5.6 ± 0.2 ppb CH_4 ppm CO_2^{-1} during a short flight stretch over rice paddy fields in the western Sacramento Valley. This slope is similar to flux ratios derived from ground-based studies and airborne multivariate assessments of rice cultivation. During this early phase in the rice growing season, a flux rate of 26 ± 16 nmol-CH_4 m^{-2} s^{-1} is determined using airborne-eddy covariance over a rice paddy belt which agrees well with simultaneous ground-based eddy covariance measurements. Enhancements of 75 - 125 ppb downwind of the largest landfills in Northern California are routinely observed although no attempts are made to derive flux rates from these point sources. Forested regions along the Coastal Mountains of California to the west of the Central Valley have amongst the lowest levels of CH_4 while similar regions downwind of the valley floor (eastern foothills) have high levels of CH_4 but almost entirely from advection and transportation of valley-emitted CH_4 emissions (e.g. rice cultivation and natural gas operations in the Sacramento Valley, dairy and

livestock in the San Joaquin Valley etc.). Noticeable enhancements of CH_4 are observed in plumes from biomass burning and wetlands alike.

We have demonstrated the applicability of the airborne eddy covariance technique as a very powerful tool to investigate landscape level fluxes of CH_4. Future verification and validation of the CH_4 bottom-up inventory can be performed using targeted multiple-run airborne flux measurements. The technique is cost and labor intensive and hence its use should be reserved to investigate such sources where there is a real lack of data and where access to set up measurement sites in source regions is restricted and rare (e.g. oil and gas fields). As we have demonstrated in this study, they can be a very effective strategy to find and evaluate the contribution of CH_4 "hotspots".

3.5   References

Andreae, M. O. and Merlet, P.: Emission of trace gases and aerosols from biomass burning, Global Biogeochem. Cycles, 15(4), 955–966, doi:10.1029/2000GB001382, 2001.

Baldocchi, D., Detto, M., Sonnentag, O., Verfaillie, J., Teh, Y. A., Silver, W. and Kelly, N. M.: The challenges of measuring methane fluxes and concentrations over a peatland pasture, Agric. For. Meteorol., 153, 177–187, doi:10.1016/j.agrformet.2011.04.013, 2012.

Beaver, S. and Palazoglu, A.: Influence of synoptic and mesoscale meteorology on ozone pollution potential for San Joaquin Valley of California, Atmos. Environ., 43(10), 1779–1788, doi:10.1016/j.atmosenv.2008.12.034, 2009.

Burba, G., 2013. Eddy Covariance Method for Scientific, Industrial, Agricultural, and Regulatory Applications: A Field Book on Measuring Ecosystem Gas Exchange and Areal Emission Rates. LI-COR Biosciences, Lincoln, NE, USA, 331 pp.

CARB (2013), California Greenhouse Gas Inventory for 2000-2012 - by IPCC Category. http://www.arb.ca.gov/cc/inventory/data/data.htm. accessesd on September 23, 2014.

CASR (2011), California Agricultural Statistics Crop Report, 2011. created by California Department of Food and Agriculture, Sacramento, CA and United States Department of Agriculture.

Chung, M. Y., Beene, M., Ashkan, S., Krauter, C. and Hasson, A. S.: Evaluation of non-enteric sources of non-methane volatile organic compound (NMVOC) emissions from dairies, Atmos. Environ., 44(6), 786–794, doi:10.1016/j.atmosenv.2009.11.033, 2010.

Cicerone, R. J. and Shetter, J. D.: Sources of atmospheric methane: Measurements in rice paddies and a discussion, J. Geophys. Res., 86(C8), 7203, doi:10.1029/JC086iC08p07203, 1981.

Crosson, E. R.: A cavity ring-down analyzer for measuring atmospheric levels of methane, carbon dioxide, and water vapor, Appl. Phys. B, 92(3), 403–408, doi:10.1007/s00340-008-3135-y, 2008.

Desjardins, R. L., Hart, R. L., MacPherson, J. I., Schuepp, P. H. and Verma, S. B.: Aircraft- and tower-based fluxes of carbon dioxide, latent, and sensible heat, J. Geophys. Res., 97(D17), 18477, doi:10.1029/92JD01625, 1992.

DOGGR (2012), 2011 Preliminary report on California oil and gas production statistics, Department of Conservation's Division of Oil, Gas and Geothermal Resources; Publication No. PR03.

Dlugokencky, E.J., A.M. Crotwell, P.M. Lang, K.A. Masarie (2014), Atmospheric Methane Dry Air Mole Fractions from quasi-continuous measurements at Barrow, Alaska and Mauna Loa, Hawaii, 1986-2013, Version: 2014-08-12, Path: ftp://ftp.cmdl.noaa.gov/ccg/ch4/in-situ/.

Fares, S., Gentner, D. R., Park, J.-H., Ormeno, E., Karlik, J. and Goldstein, A. H.: Biogenic emissions from Citrus species in California, Atmos. Environ., 45(27), 4557–4568, doi:10.1016/j.atmosenv.2011.05.066, 2011.

Fares, S., Park, J.-H., Gentner, D. R., Weber, R., Ormeño, E., Karlik, J. and Goldstein, a. H.: Seasonal cycles of biogenic volatile organic compound fluxes and concentrations in a California citrus orchard, Atmos. Chem. Phys., 12(20), 9865–9880, doi:10.5194/acp-12-9865-2012, 2012.

Filipy, J., Rumburg, B., Mount, G., Westberg, H. and Lamb, B.: Identification and quantification of volatile organic compounds from a dairy, Atmos. Environ., 40(8), 1480–1494, doi:10.1016/j.atmosenv.2005.10.048, 2006.

Flesch, T. K., Wilson, J. D., Harper, L. a., Crenna, B. P. and Sharpe, R. R.: Deducing Ground-to-Air Emissions from Observed Trace Gas Concentrations: A Field Trial, J. Appl. Meteorol., 43(3), 487–502, doi:10.1175/1520-0450(2004)043<0487:DGEFOT>2.0.CO;2, 2004.

FLIGHT (2011), Facility Level Information on Greenhouse Gas Tool, Environmental Protection Agency, http://ghgdata.epa.gov/ghgp/main.do, accessed on Oct 26, 2014.

Gentner, D. R., Ford, T. B., Guha, a., Boulanger, K., Brioude, J., Angevine, W. M., de Gouw, J. a., Warneke, C., Gilman, J. B., Ryerson, T. B., Peischl, J., Meinardi, S., Blake, D. R., Atlas, E., Lonneman, W. a., Kleindienst, T. E., Beaver, M. R., Clair, J. M. St., Wennberg, P. O., VandenBoer, T. C., Markovic, M. Z., Murphy, J. G., Harley, R. a. and Goldstein, a. H.: Emissions of organic carbon and methane from petroleum and dairy operations in California's San Joaquin Valley, Atmos. Chem. Phys., 14(10), 4955–4978, doi:10.5194/acp-14-4955-2014, 2014.

Goldstein, A. H. and Schade, G. W.: Quantifying biogenic and anthropogenic contributions to acetone mixing ratios in a rural environment, Atmos. Environ., 34(29-30), 4997–5006, doi:10.1016/S1352-2310(00)00321-6, 2000.

Guenther, A. B., Jiang, X., Heald, C. L., Sakulyanontvittaya, T., Duhl, T., Emmons, L. K. and Wang, X.: The Model of Emissions of Gases and Aerosols from Nature version 2.1 (MEGAN2.1): an extended and updated framework for modeling biogenic emissions, Geosci. Model Dev., 5(6), 1471–1492, doi:10.5194/gmd-5-1471-2012, 2012.

Harper, L. A., Flesch, T. K., Powell, J. M., Coblentz, W. K., Jokela, W. E. and Martin, N. P.: Ammonia emissions from dairy production in Wisconsin., J. Dairy Sci., 92(5), 2326–37, doi:10.3168/jds.2008-1753, 2009.

Harper, L. a., Flesch, T. K., Weaver, K. H. and Wilson, J. D.: The Effect of Biofuel Production on Swine Farm Methane and Ammonia Emissions, J. Environ. Qual., 39(6), 1984, doi:10.2134/jeq2010.0172, 2010.

Hatala, J. a., Detto, M., Sonnentag, O., Deverel, S. J., Verfaillie, J. and Baldocchi, D. D.: Greenhouse gas (CO2, CH4, H2O) fluxes from drained and flooded agricultural peatlands in the Sacramento-San Joaquin Delta, Agric. Ecosyst. Environ., 150, 1–18, doi:10.1016/j.agee.2012.01.009, 2012.

Jeong, S., Hsu, Y.-K., Andrews, A. E., Bianco, L., Vaca, P., Wilczak, J. M. and Fischer, M. L.: A multitower measurement network estimate of California's methane emissions, J. Geophys. Res. Atmos., 118(19), 11,339–11,351, doi:10.1002/jgrd.50854, 2013.

Jeong, S., Zhao, C., Andrews, A. E., Bianco, L., Wilczak, J. M. and Fischer, M. L.: Seasonal variation of CH 4 emissions from central California, J. Geophys. Res., 117(D11), D11306, doi:10.1029/2011JD016896, 2012.

Karl, T., Apel, E., Hodzic, a., Riemer, D. D., Blake, D. R. and Wiedinmyer, C.: Emissions of volatile organic compounds inferred from airborne flux measurements over a megacity, Atmos. Chem. Phys., 9(1), 271–285, doi:10.5194/acp-9-271-2009, 2009.

Karl, T. G., Spirig, C., Rinne, J., Stroud, C., Prevost, P., Greenberg, J., Fall, R. and Guenther, A.: Virtual disjunct eddy covariance measurements of organic compound fluxes from a subalpine forest using proton transfer reaction mass spectrometry, Atmos. Chem. Phys., 2(4), 279–291, doi:10.5194/acp-2-279-2002, 2002.

Karl, T., Misztal, P. K., Jonsson, H. H., Shertz, S., Goldstein, a. H. and Guenther, a. B.: Airborne Flux Measurements of BVOCs above Californian Oak Forests: Experimental Investigation of Surface and Entrainment Fluxes, OH Densities, and Damköhler Numbers, J. Atmos. Sci., 70(10), 3277–3287, doi:10.1175/JAS-D-13-054.1, 2013.

Karlik, J. F. and M. Winer, A.: Measured isoprene emission rates of plants in California landscapes: comparison to estimates from taxonomic relationships, Atmos. Environ., 35(6), 1123–1131, doi:10.1016/S1352-2310(00)00258-2, 2001.

Knox, S. H., Sturtevant, C., Matthes, J. H., Koteen, L., Verfaillie, J. and Baldocchi, D.: Agricultural peatland restoration: effects of land-use change on greenhouse gas (CO2 and CH4)

fluxes in the Sacramento-San Joaquin Delta., Glob. Chang. Biol., 1–16, doi:10.1111/gcb.12745, 2014.

Kort, E. A., C. Frankenberg, K. R. Costigan, R. Lindenmaier, M. K. Dubey, and D. Wunch (2014), Four corners: The largest US methane anomaly viewed from space, Geophys. Res. Lett., 41, 6898–6903, doi:10.1002/2014GL061503.

Lee, S., Nyarady, J. F., Vergara, F., and Corey, R.: 2007 Oil and Gas Industry Survey Results, Final Report, California Air Resources Board, 2011.

le Mer, J. and Roger, P.: Production, oxidation, emission and consumption of methane by soils : A review, Eur. J. Soil Biol., 37(1), 25–50 [online] Available from: http://cat.inist.fr/?aModele=afficheN&cpsidt=978757 (Accessed 28 October 2014), 2001.

Lenschow, D. H., Pearson, R. and Stankov, B. B.: Estimating the Ozone Budget in the Boundary Layer by Use of Aircraft Measurements of Ozone Eddy Flux and Mean Con : entration, , 86, 7291–7297, 1981.

Mauder, M., Desjardins, R. L. and MacPherson, I.: Scale analysis of airborne flux measurements over heterogeneous terrain in a boreal ecosystem, J. Geophys. Res., 112(D13), D13112, doi:10.1029/2006JD008133, 2007.

McMillan, A. M. S., Goulden, M. L. and Tyler, S. C.: Stoichiometry of CH 4 and CO 2 flux in a California rice paddy, J. Geophys. Res., 112(G1), G01008, doi:10.1029/2006JG000198, 2007.

Metzger, S., Junkermann, W., Mauder, M., Butterbach-Bahl, K., Trancón y Widemann, B., Neidl, F., Schäfer, K., Wieneke, S., Zheng, X. H., Schmid, H. P. and Foken, T.: Spatially explicit regionalization of airborne flux measurements using environmental response functions, Biogeosciences, 10(4), 2193–2217, doi:10.5194/bg-10-2193-2013, 2013.

Miller, R. L.: Carbon Gas Fluxes in Re-Established Wetlands on Organic Soils Differ Relative to Plant Community and Hydrology, Wetlands, 31(6), 1055–1066, doi:10.1007/s13157-011-0215-2, 2011.

Montzka, S. A., Dlugokencky, E. J. and Butler, J. H.: Non-CO2 greenhouse gases and climate change., Nature, 476(7358), 43–50, doi:10.1038/nature10322, 2011.

Miller, S. M., Wofsy, S. C., Michalak, A. M., Kort, E. a, Andrews, A. E., Biraud, S. C., Dlugokencky, E. J., Eluszkiewicz, J., Fischer, M. L., Janssens-Maenhout, G., Miller, B. R., Miller, J. B., Montzka, S. a, Nehrkorn, T. and Sweeney, C.: Anthropogenic emissions of methane in the United States., Proc. Natl. Acad. Sci. U. S. A., 110(50), 20018–22, doi:10.1073/pnas.1314392110, 2013.

Misztal, P. K., Karl, T., Weber, R., Jonsson, H. H., Guenther, a. B. and Goldstein, a. H.: Airborne flux measurements of biogenic volatile organic compounds over California, Atmos. Chem. Phys. Discuss., 14(6), 7965–8013, doi:10.5194/acpd-14-7965-2014, 2014.

Ngwabie, N. M., Schade, G. W., Custer, T. G., Linke, S. and Hinz, T.: Abundances and Flux Estimates of Volatile Organic Compounds from a Dairy Cowshed in Germany, J. Environ. Qual., 37(2), 565, doi:10.2134/jeq2006.0417, 2008.

Park, J.-H., Goldstein, a H., Timkovsky, J., Fares, S., Weber, R., Karlik, J. and Holzinger, R.: Active atmosphere-ecosystem exchange of the vast majority of detected volatile organic compounds., Science, 341(6146), 643–7, doi:10.1126/science.1235053, 2013.

Peischl, J., Ryerson, T. B., Brioude, J., Aikin, K. C., Andrews, a. E., Atlas, E., Blake, D., Daube, B. C., de Gouw, J. a., Dlugokencky, E., Frost, G. J., Gentner, D. R., Gilman, J. B., Goldstein, a. H., Harley, R. a., Holloway, J. S., Kofler, J., Kuster, W. C., Lang, P. M., Novelli, P. C., Santoni, G. W., Trainer, M., Wofsy, S. C. and Parrish, D. D.: Quantifying sources of methane using light alkanes in the Los Angeles basin, California, J. Geophys. Res. Atmos., 118(10), 4974–4990, doi:10.1002/jgrd.50413, 2013.

Peischl, J., Ryerson, T. B., Holloway, J. S., Trainer, M., Andrews, a. E., Atlas, E. L., Blake, D. R., Daube, B. C., Dlugokencky, E. J., Fischer, M. L., Goldstein, a. H., Guha, a., Karl, T., Kofler, J., Kosciuch, E., Misztal, P. K., Perring, a. E., Pollack, I. B., Santoni, G. W., Schwarz, J. P., Spackman, J. R., Wofsy, S. C. and Parrish, D. D.: Airborne observations of methane emissions from rice cultivation in the Sacramento Valley of California, J. Geophys. Res., 117, D00V25, doi:10.1029/2012JD017994, 2012.

Poffenbarger, H. J., B. A. Needelman, and J. P. Megonigal. 2011. Salinity Influence on Methane Emissions from Tidal Marshes. Wetlands 31:831-842.

Prueger, J. H., Hatfield, J. L., Parkin, T. B., Kustas, W. P., Hipps, L. E., Neale, C. M. U., MacPherson, J. I., Eichinger, W. E. and Cooper, D. I.: Tower and Aircraft Eddy Covariance Measurements of Water Vapor, Energy, and Carbon Dioxide Fluxes during SMACEX, J. Hydrometeorol., 6(6), 954–960, doi:10.1175/JHM457.1, 2005.

Schade, G. W. and Goldstein, A. H.: Seasonal measurements of acetone and methanol: Abundances and implications for atmospheric budgets, Global Biogeochem. Cycles, 20(1), n/a–n/a, doi:10.1029/2005GB002566, 2006.

Shaw, S. L., Mitloehner, F. M., Jackson, W., Depeters, E. J., Fadel, J. G., Robinson, P. H., Holzinger, R. and Goldstein, A. H.: Volatile organic compound emissions from dairy cows and their waste as measured by proton-transfer-reaction mass spectrometry., Environ. Sci. Technol., 41(4), 1310–6 [online] Available from: http://www.ncbi.nlm.nih.gov/pubmed/17593735, 2007.

Smeets, C. J. P. P., Holzinger, R., Vigano, I., Goldstein, a. H. and Röckmann, T.: Eddy covariance methane measurements at a Ponderosa pine plantation in California, Atmos. Chem. Phys., 9(21), 8365–8375, doi:10.5194/acp-9-8365-2009, 2009.

Teh, Y. A., Silver, W. L., Sonnentag, O., Detto, M., Kelly, M. and Baldocchi, D. D.: Large Greenhouse Gas Emissions from a Temperate Peatland Pasture, Ecosystems, 14(2), 311–325, doi:10.1007/s10021-011-9411-4, 2011.

Torrence, C. and Compo, G. P.: A Practical Guide to Wavelet Analysis, Bull. Am. Meteorol. Soc., 79(1), 61–78, doi:10.1175/1520-0477(1998)079<0061:APGTWA>2.0.CO;2, 1998.

Wecht, K. J., Jacob, D. J., Sulprizio, M. P., Santoni, G. W., Wofsy, S. C., Parker, R., Bösch, H. and Worden, J.: Spatially resolving methane emissions in California: constraints from the CalNex aircraft campaign and from present (GOSAT, TES) and future (TROPOMI, geostationary) satellite observations, Atmos. Chem. Phys., 14(15), 8173–8184, doi:10.5194/acp-14-8173-2014, 2014.

Weil, J. C. and Horst, T. W.: Footprint Estimates for Atmospheric Flux Measurements in the Convective Boundary-Layer, Precipitation Scavenging and Atmosphere-Surface Exchange, 1–3, 717–728, 1992.

Werner, C., Davis, K., Bakwin, P., Yi, C., Hurst, D. and Lock, L.: Regional-scale measurements of CH4 exchange from a tall tower over a mixed temperate/boreal lowland and wetland forest, Glob. Chang. Biol., 9(9), 1251–1261, doi:10.1046/j.1365-2486.2003.00670.x, 2003.

Wunch, D., Wennberg, P. O., Toon, G. C., Keppel-Aleks, G. and Yavin, Y. G.: Emissions of greenhouse gases from a North American megacity, Geophys. Res. Lett., 36(15), L15810, doi:10.1029/2009GL039825, 2009.

Zhao, C., Andrews, A. E., Bianco, L., Eluszkiewicz, J., Hirsch, A., MacDonald, C., Nehrkorn, T. and Fischer, M. L.: Atmospheric inverse estimates of methane emissions from Central California, J. Geophys. Res., 114(D16), D16302, doi:10.1029/2008JD011671, 2009.

3.6 Tables and figures

Table 3. 1. Summary of logistical information from the seven CABERNET flights discussed in this chapter along with an overview of CH_4 concentrations observed over each flight.

Research Flight (RF)	region of focus	temperature (° C)[a]	VOCs measured	mean CH_4 (ppbv)	inter-quartile range[b] (ppbv)
RF 1 8 Jun	San Joaquin valley (SJV) dairies, Kern County oil and gas fields	20.6	methanol, isoprene, benzene, toluene, C8 aromatics	1916	1855 - 2008
RF 2 9 Jun	SJV dairies and eastern foothills along Sacramento valley (SV)	23.1	methanol, isoprene, methyl vinyl ketone/methacrolein (MVK +MACR), monoterpenes (MT), methyl butenol (MBO)	1908	1857 - 1972
RF 3 10 Jun	SJV dairies and eastern foothills along SV	24.4	methanol, isoprene, MVK +MACR, hydroxyacetone	1890	1855- 1929
RF 4 14 Jun	delta, eastern foothills along SJV, SJV dairies	27.8	methanol, isoprene, MVK + MACR, MT, MBO	1992	1863 - 2256
RF 5 15 Jun	San Francisco Bay Area, rice fields, coastal mountains	28.5	methanol, isoprene, acetaldehyde, MVK + MACR, MT	1880	1852 - 1918
RF 6 16 Jun	eastern foothills, SJV dairies	24.8	isoprene, MVK + MACR, MBO	1896	1859 - 1940
RF 8 21 Jun	central coastal ranges	32.5	methanol, isoprene, MVK + MACR, MT, MBO	1893	1873 - 1921

[a] as reported in Misztal et al. (2014).
[b] range represents 10th and 90th percentile.

Table 3. 2. Landscape level airborne eddy covariance (EC) CH_4 fluxes from flight segments flown over dairy and livestock intensive regions in the San Joaquin valley (SJV).

Research Flight (RF)	mean EC flux (nmol-CH_4 m^{-2} s^{-1})	inter-quartile range[c] (nmol-CH_4 m^{-2} s^{-1})	length of segment (km)	uncertainty[d] (%)
RF 1	294	32 - 455	56	23
RF 1[a]	313	110 - 448	40	28
RF 2 onward	44	23 - 61	38	29
RF 2 return	58	14 - 91	50	25
RF 3 onward	56	-3.5 - 84	47	26
RF 4 onward	65	11 - 114	51	24
RF 4 return	28	-12 - 56	53	25
RF 5[b]	26	18 - 32	20	60
RF 6 onward	32	-16 - 53	43	29
RF 6 return	68	25 - 86	66	22

[a] over oil and gas fields in western Kern County
[b] over rice paddy fields in Colusa County
[c] interquartile range represents values between the 25th and 75th percentile.
[d] uncertainty = total instrumental uncertainty + random error + systematic error.

Table 3. 3. San Joaquin Valley (SJV)-specific spatial and cattle inventory data.

County	area within SJV[a,b] (10^6 m^2)	dairy cows[c] (10^3 cowheads)	beef and other cattle[c,d] (10^3 cowheads)
Tulare	4093	490	982
Merced	4006	262	526
Kings	2692	188	378
Stanislaus	2815	180	362
Kern	8191	169	507
Fresno	6674	118	353
San Joaquin	3466	106	213
Madera	2107	77	155
SJV TOTAL	34044	1590	3476

[a] calculated using geoprocessing tool in ESRI's ArcMap 10.2.
[b] geospatial data provided by Kelly Larvie, California Department of Foresty and Fire Protection (CAL FIRE) and based on 2007 USDA report on Description of "Ecological Subregions: Sections of the Conterminous United States".
[c] data accumulated from California Agricultural Statistics 2011 Crop Report (USDA ,2012).
[d] other cattle includes replacement beef and milk heifers, calves, bulls and steers
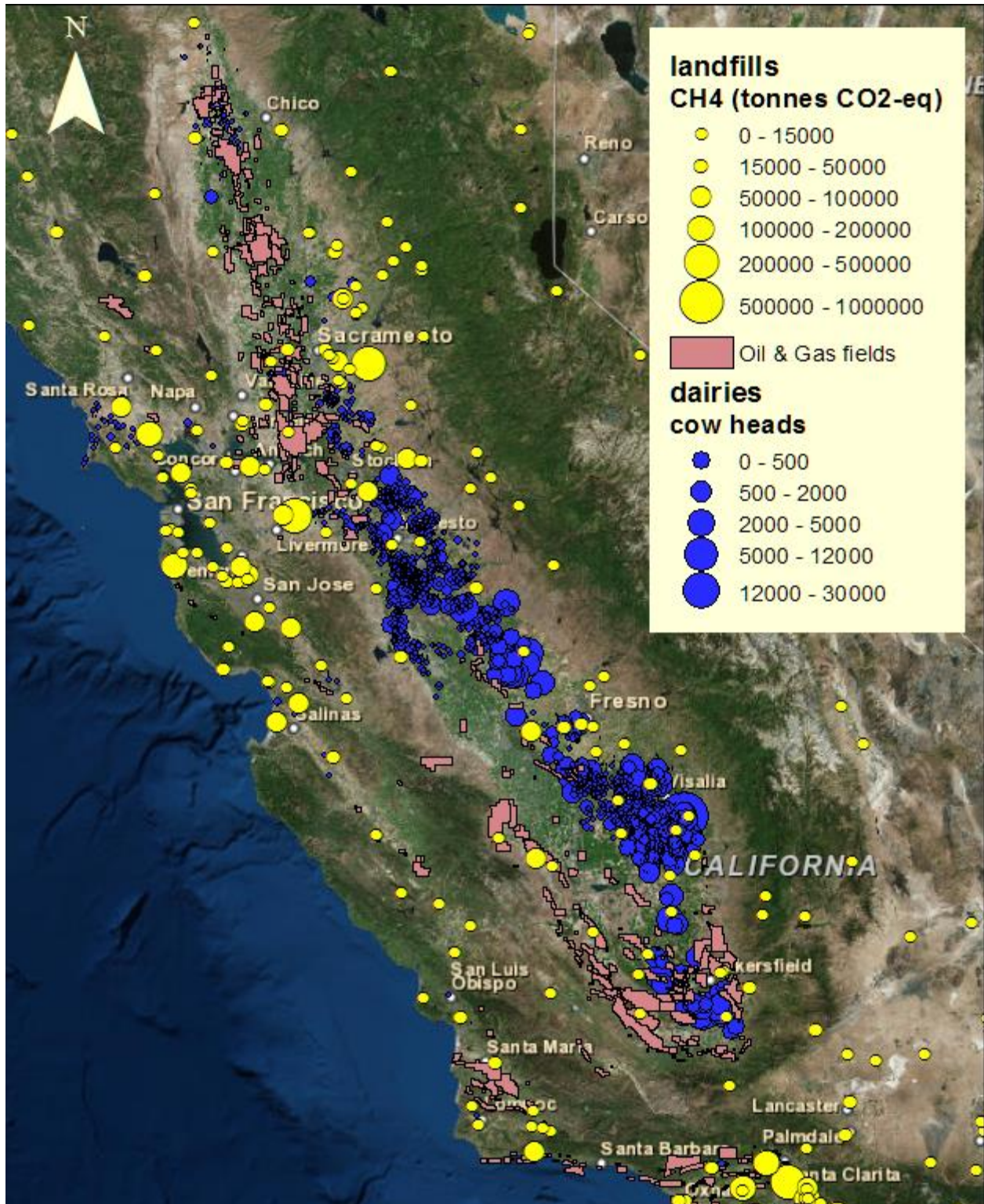
Figure 3. 1. Map of prominent CH₄ sources (dairies and landfills) in the Central Valley of California along with locations of oil and gas (O&G) fields in the region. The scales and symbols represented in the legend for dairy, landfill and O&G sources apply to all subsequent figures.
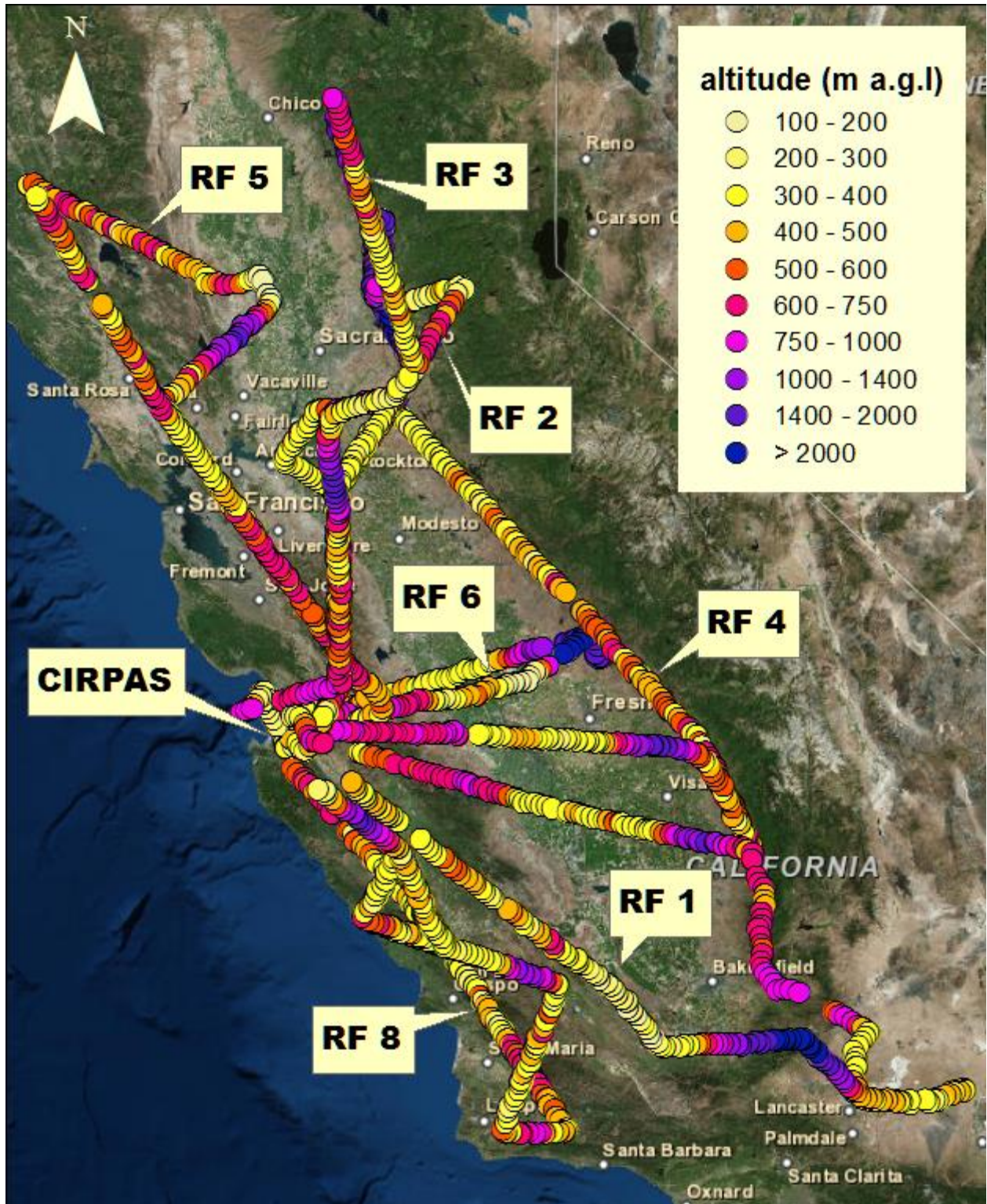
Figure 3. 2. Research flights (RFs) flown during CABERNET study color-coded by flight altitude above ground level (m). There is overlap between the onward and return leg of RF 2, RF 3 and RF 5. CIRPAS is the origin and end point of all flights.
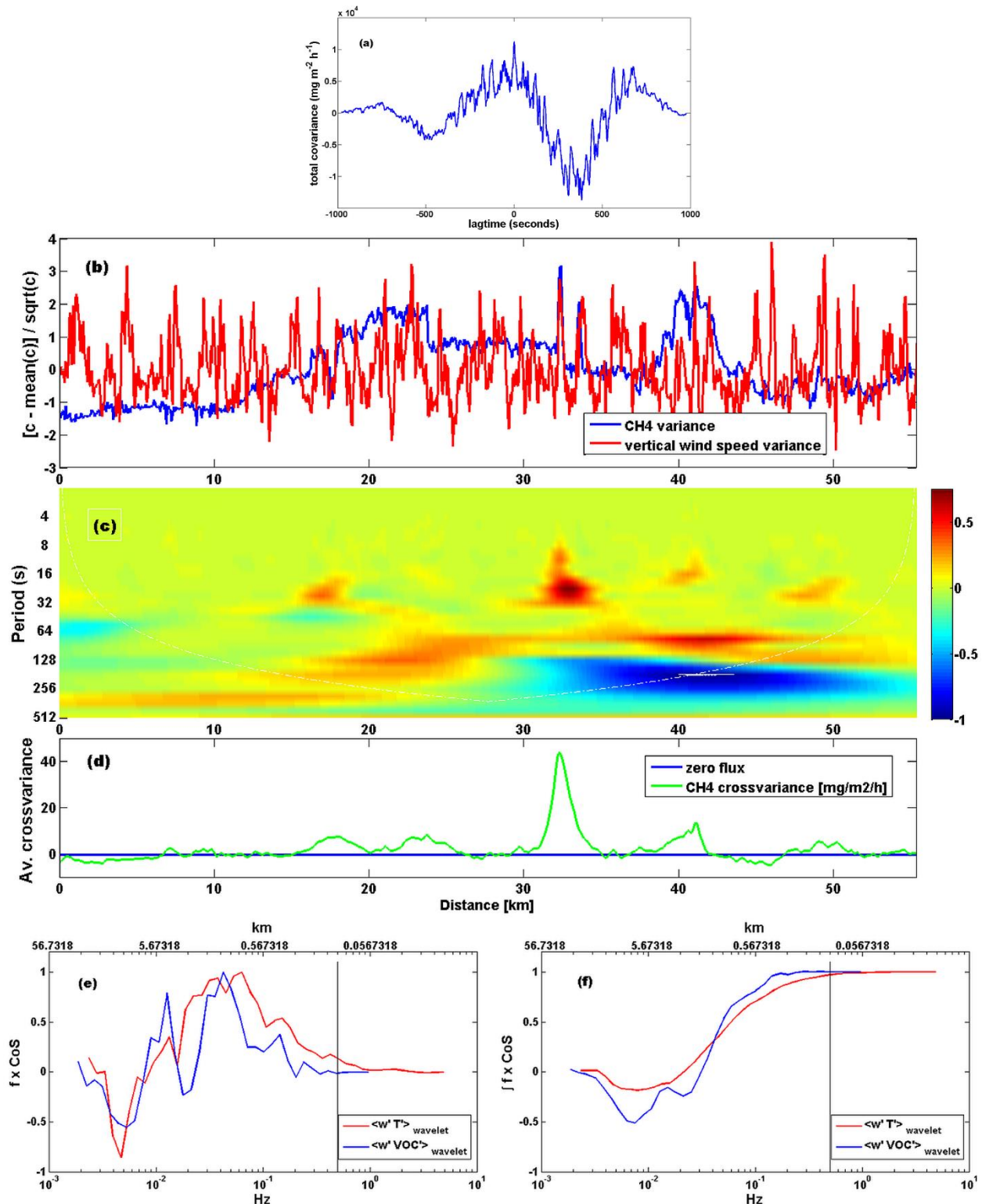
Figure 3. 3. (a) A lag-time corrected covariance plot of vertical wind speed (w) and CH_4 (c) concentrations showing a peak at zero-lag time; (b) variance of w and c along the length of a chosen flight segment; (c) wavelet cross spectra showing flux contributions at different frequencies along the segment; (d) crossvariance time series showing "instantaneous" fluxes ; (e) normalized co-spectra for CH_4 flux and heat flux obtained by wavelet method with length scale on top axis; and (f) cumulative co-spectra (ogive) for CH_4 flux and heat flux.

Figure 3. 4. Methane mixing ratios (1-sec resolution) mapped along the path of Research Flight 1. Location of methane emissions sources are also shown and represented as blue circles (dairies), yellow circles (landfills) and light red polygons (oil and gas fields). The legend shown here for methane is used in all subsequent figures.
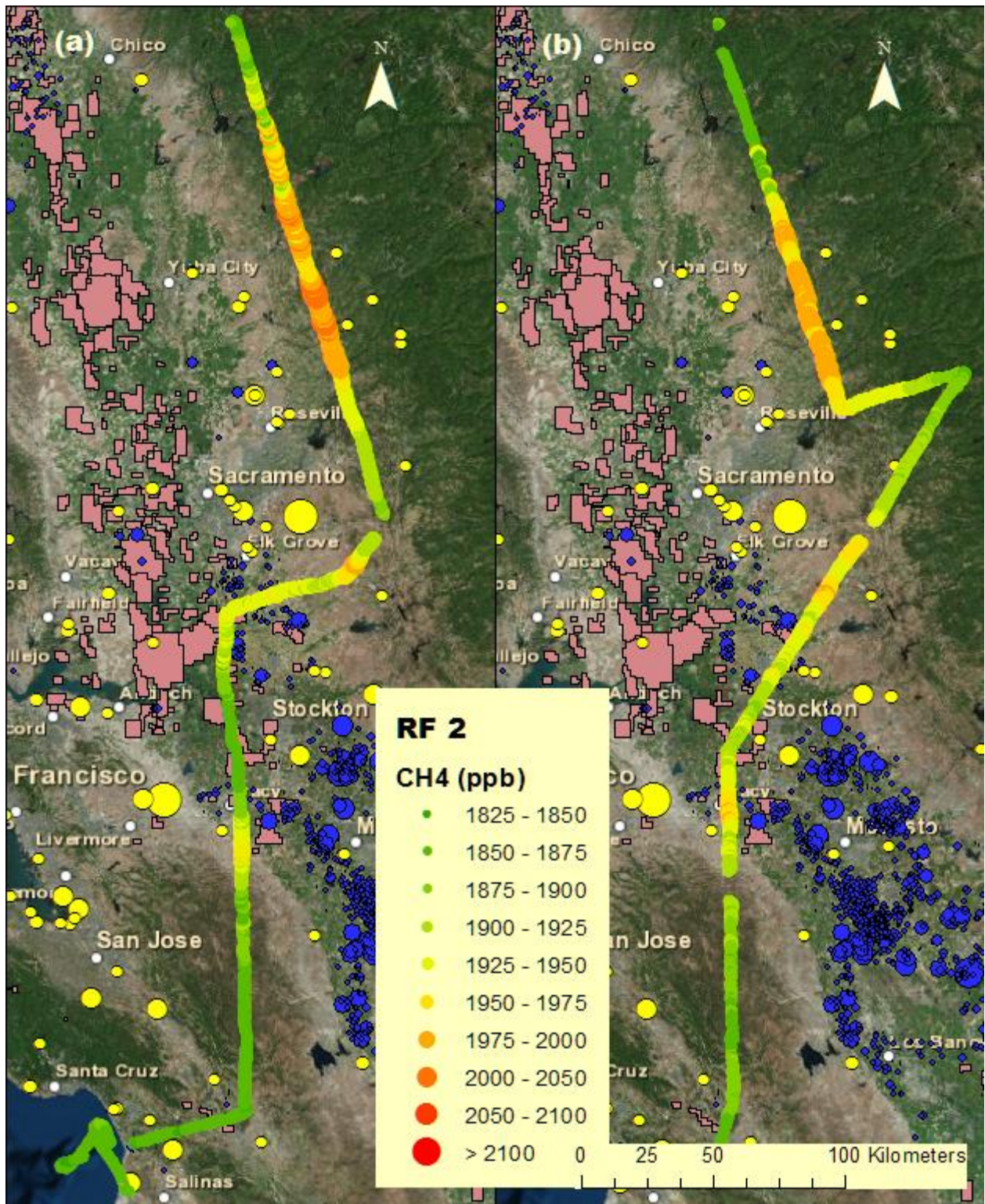
Figure 3. 5. Methane mixing ratios (1-sec resolution) mapped along the path of (a) onward leg of RF 2, and (b) return leg of RF 2. Location of methane emissions sources are also shown and represented as blue circles (dairies), yellow circles (landfills) and light red polygons (oil and gas fields). Legend for the methane sources is presented in Figure 3.1.

94
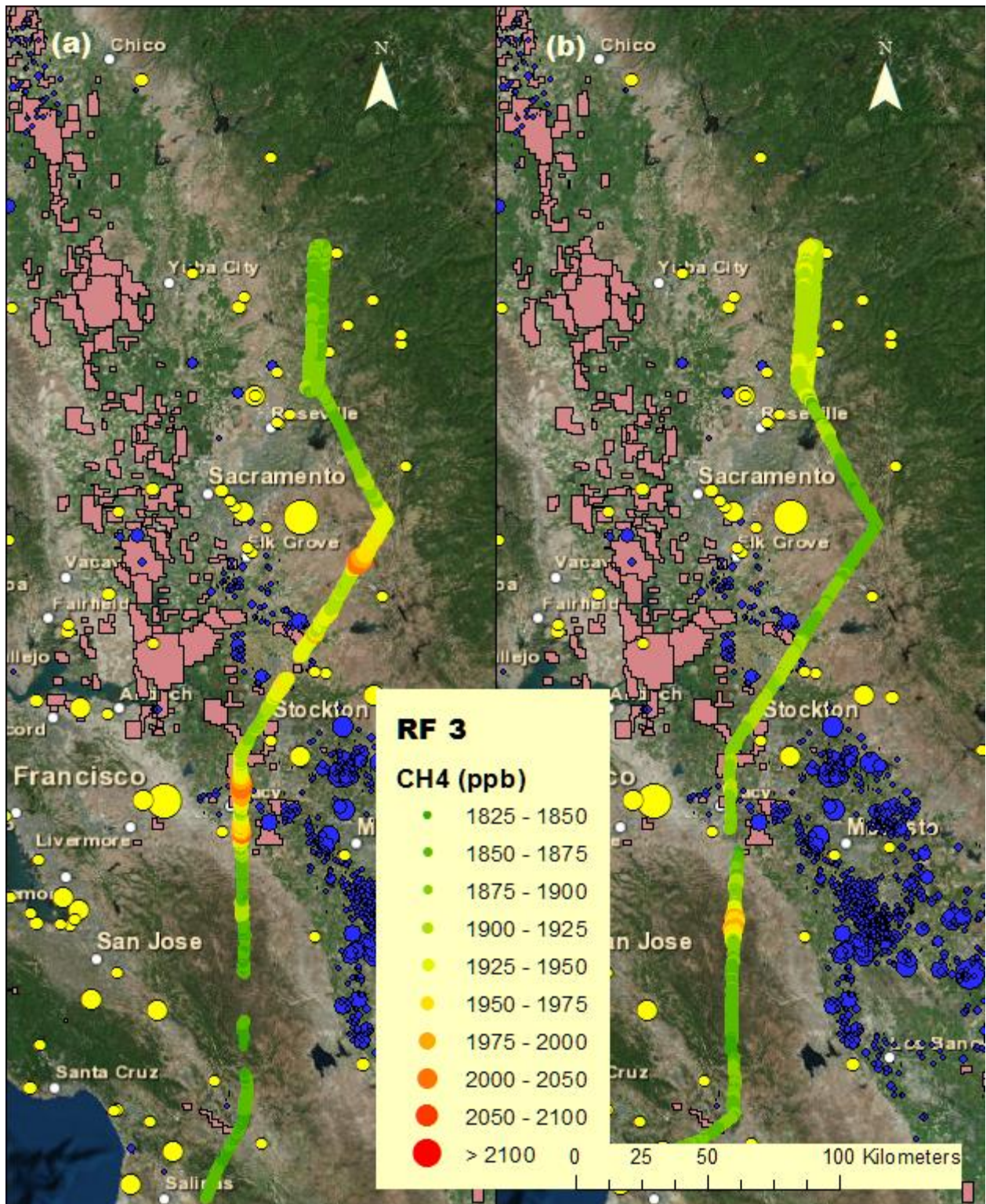
Figure 3. 6. Methane mixing ratios (1-sec resolution) mapped along the path of (a) onward leg of RF 3, and (b) return leg of RF 3. Location of methane emissions sources are also shown and represented as blue circles (dairies), yellow circles (landfills) and light red polygons (oil and gas fields). Legend for the methane sources is presented in Figure 3.1.
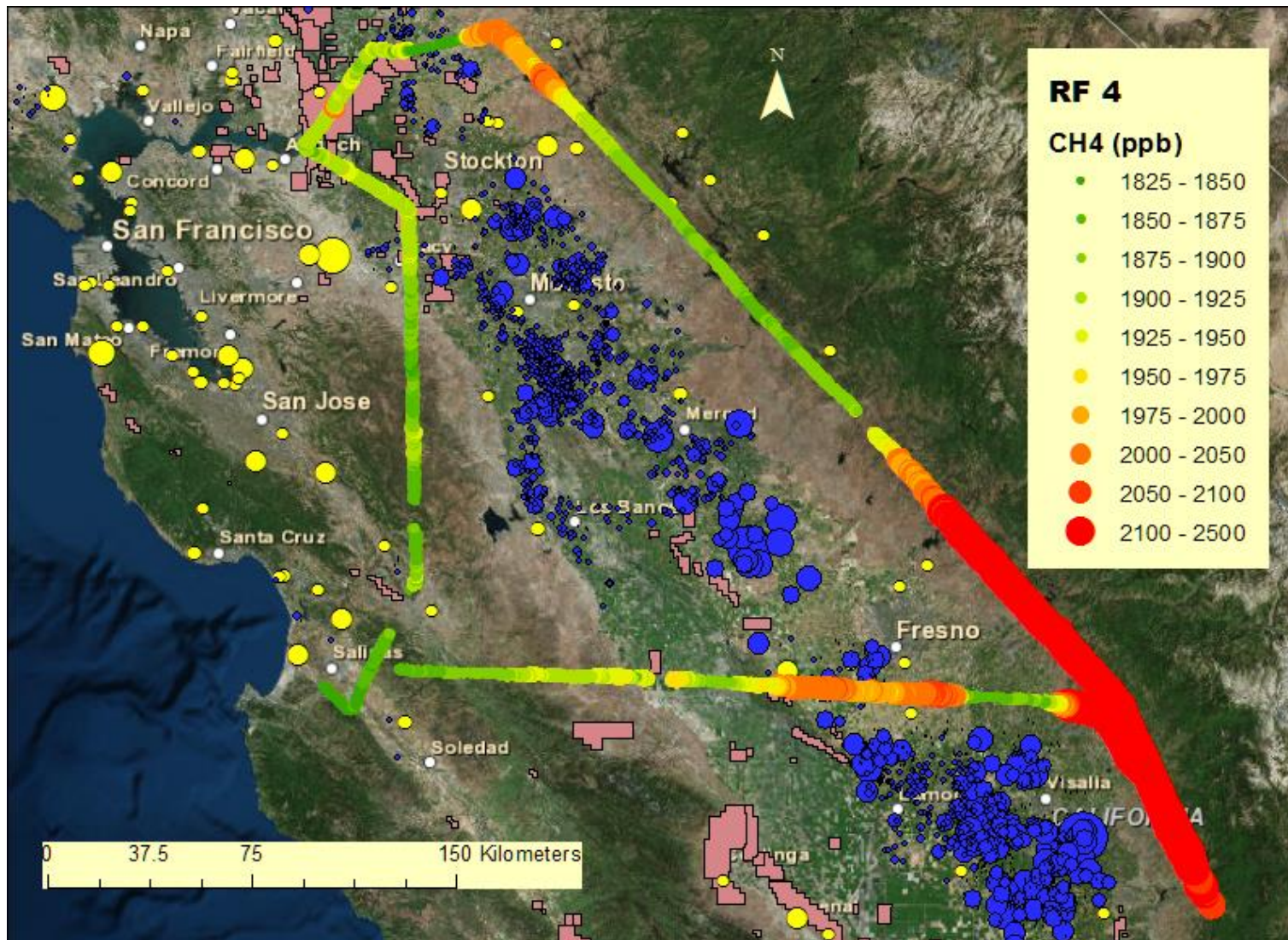
Figure 3. 7. Methane mixing ratios (1-sec resolution) mapped along the path of RF 4. Location of methane emissions sources are also shown and represented as blue circles (dairies), yellow circles (landfills) and light red polygons (oil and gas fields). Legend for the methane sources is presented in Figure 3.1.
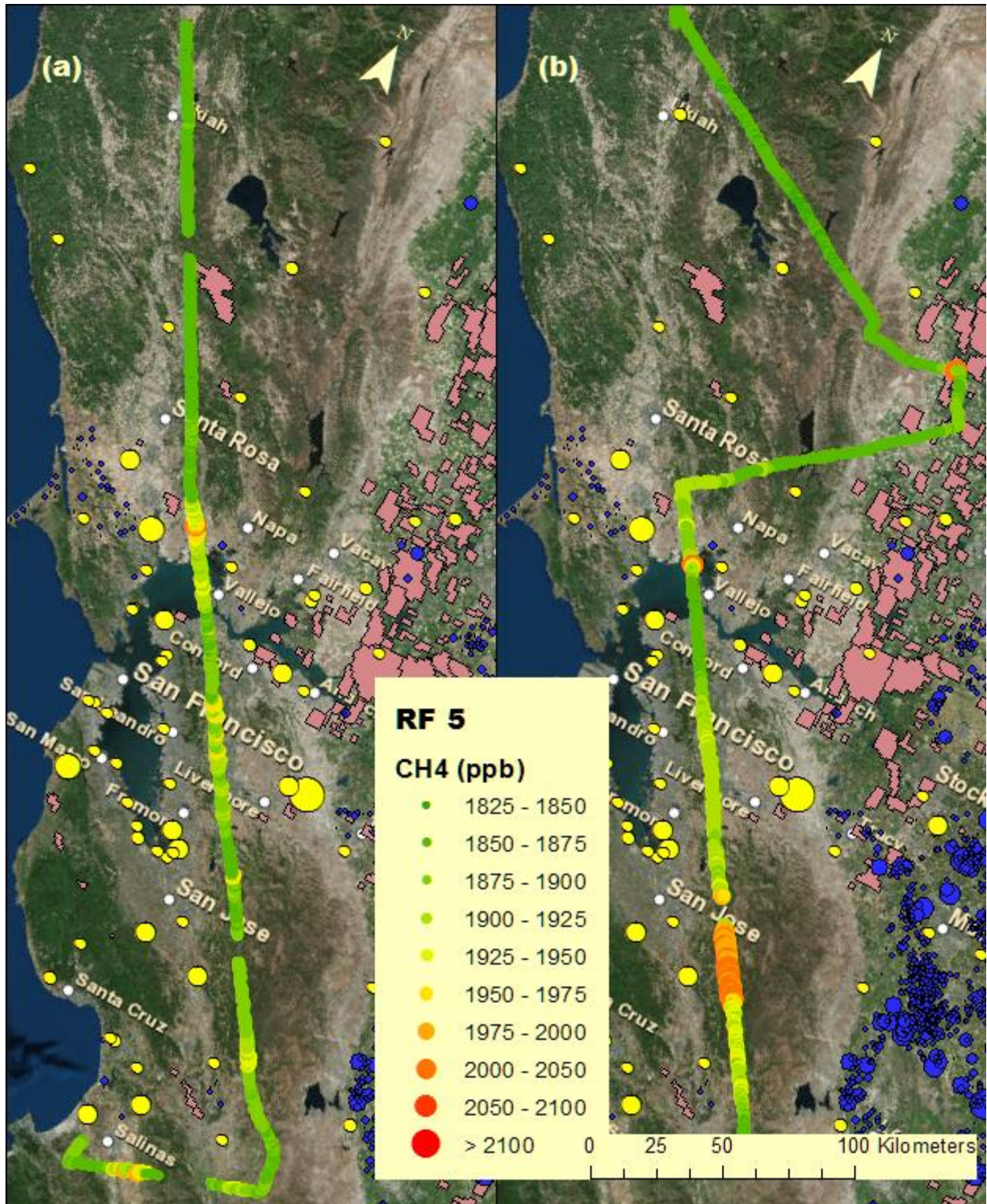
Figure 3. 8. Methane mixing ratios (1-sec resolution) mapped along the path of (a) onward leg of RF 5, and (b) return leg of RF 5. Location of methane emissions sources are also shown and represented as blue circles (dairies), yellow circles (landfills) and light red polygons (oil and gas fields). Legend for the methane sources is presented in Figure 3.1. Note that the orientation of the plot is not 'north-up'.
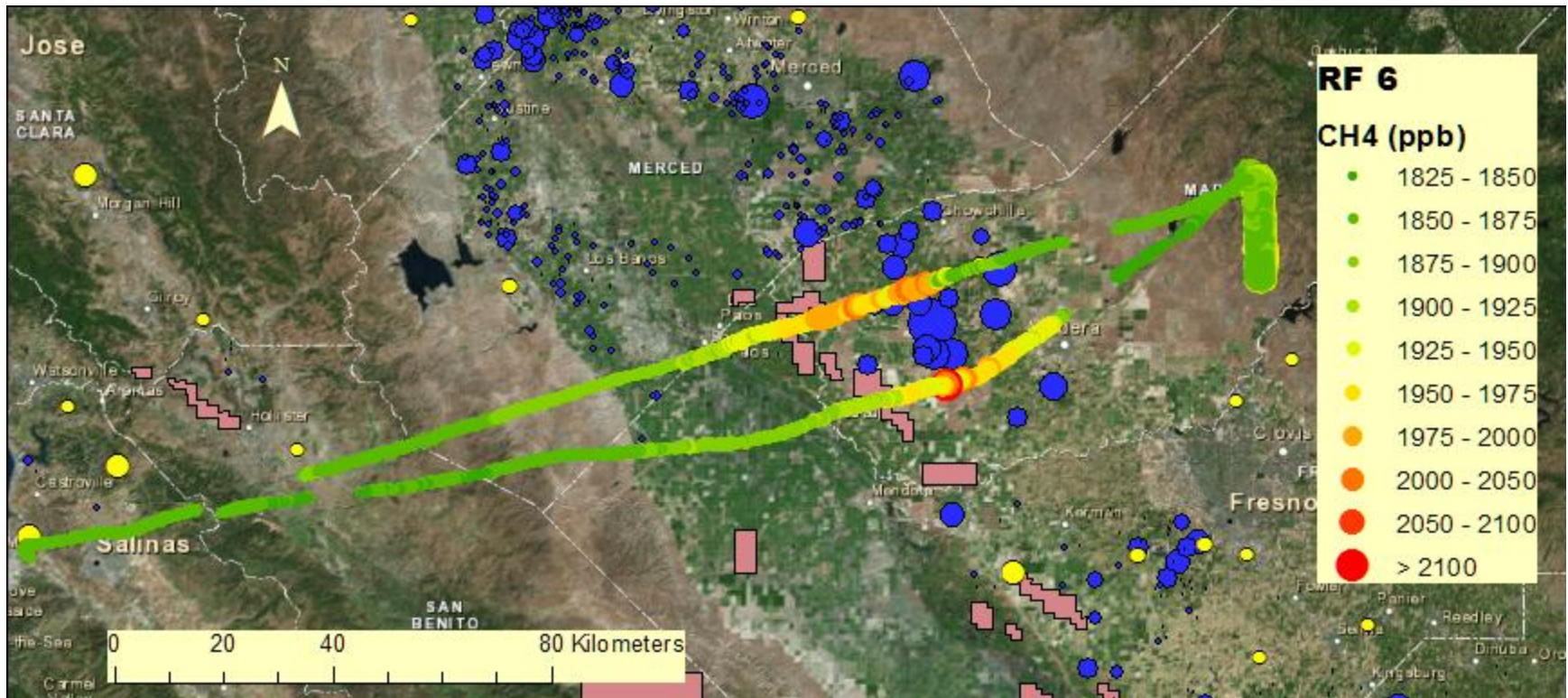
Figure 3. 9. Methane mixing ratios (1-sec resolution) mapped along the path of RF 6. Location of methane emissions sources are also shown and represented as blue circles (dairies), yellow circles (landfills) and light red polygons (oil and gas fields). Legend for the methane sources is presented in Figure 3.1.
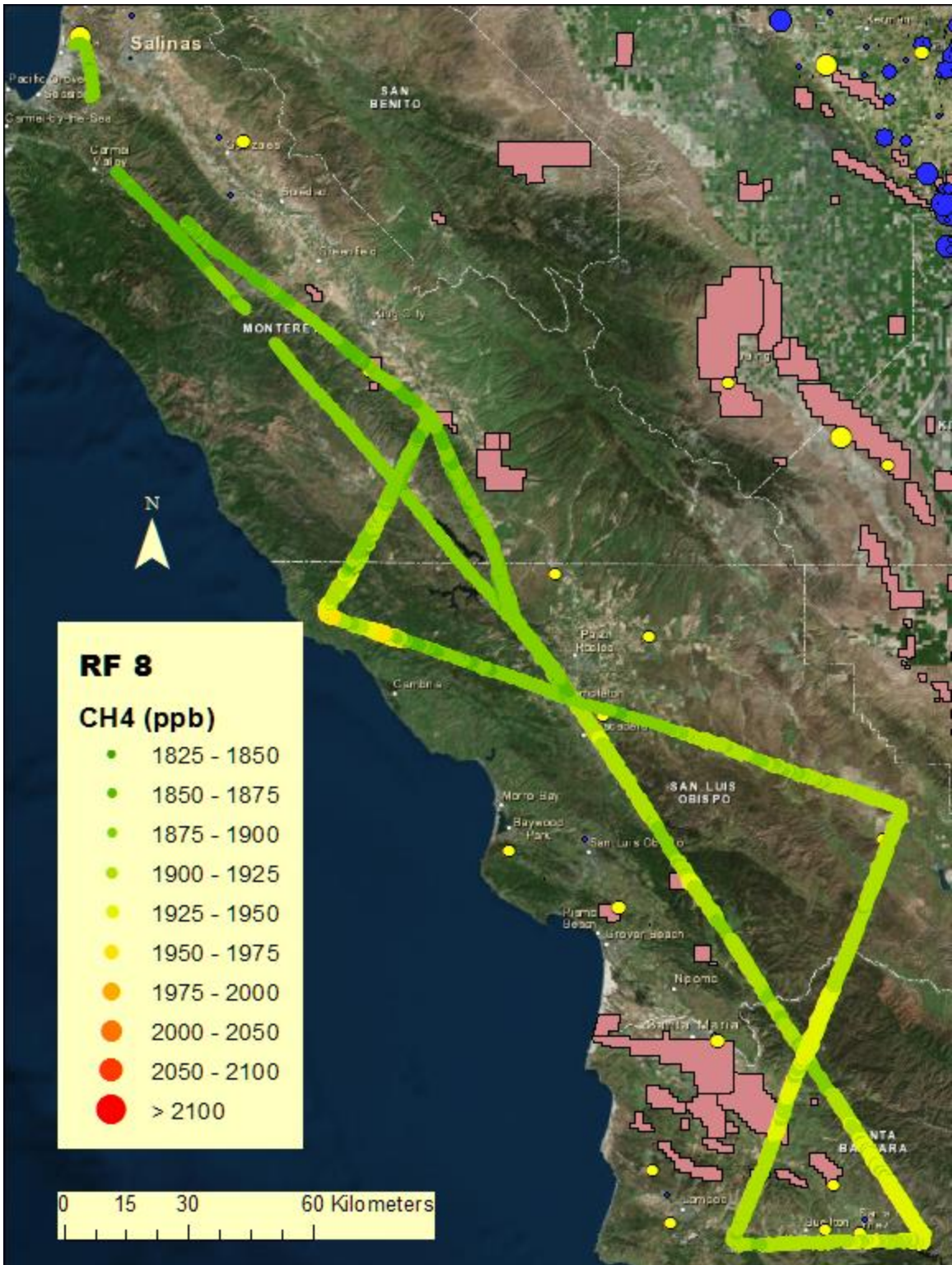
Figure 3. 10. Methane mixing ratios (1-sec resolution) mapped along the path of RF 8. Location of methane emissions sources are also shown and represented as blue circles (dairies), yellow circles (landfills) and light red polygons (oil and gas fields). Legend for the methane sources is presented in Figure 3.1.

99
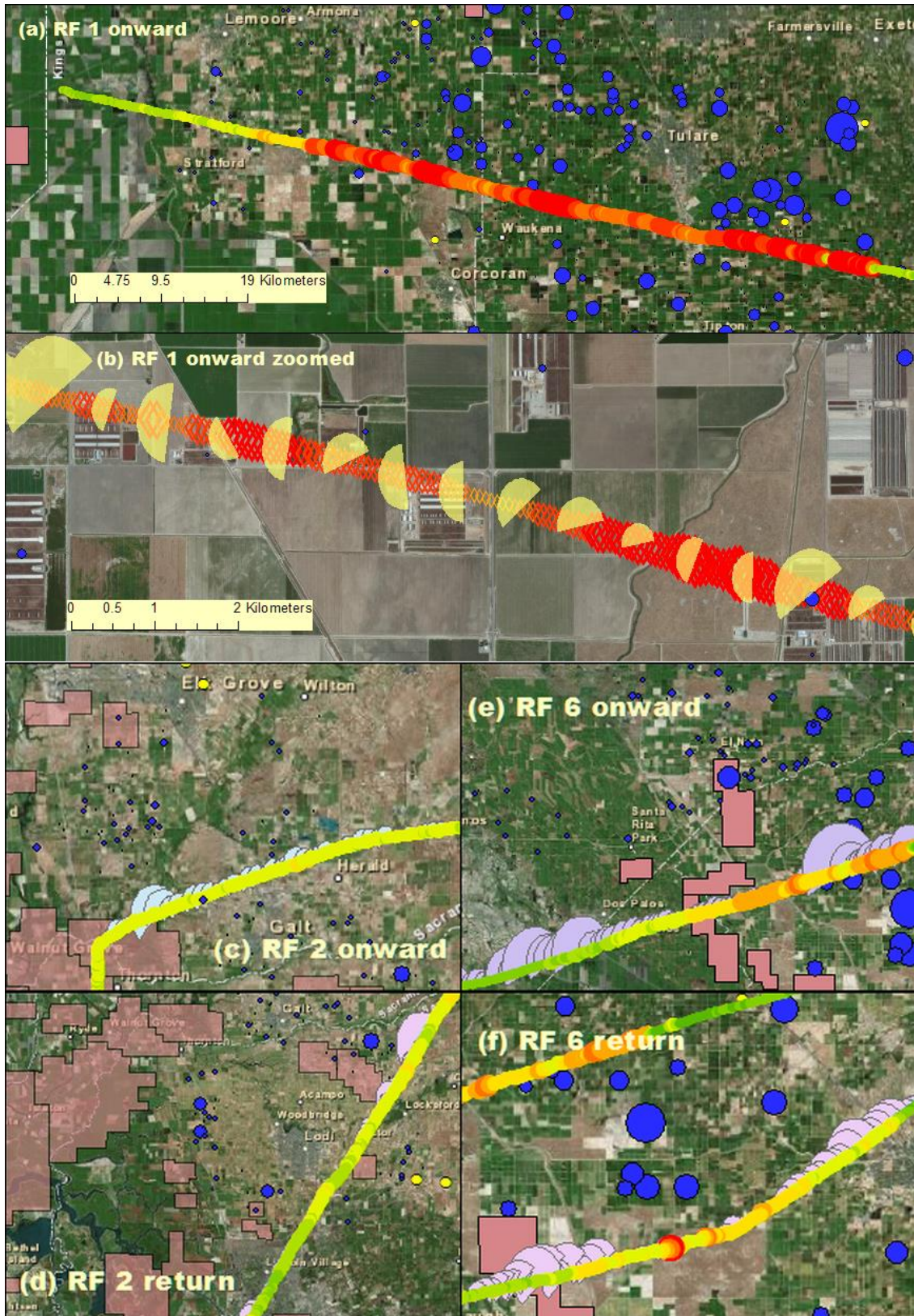
Figure 3. 11. Central Valley flight segments through dairy intensive regions (RF 4 dairy leg not shown). Dairies indicated by blue circles.
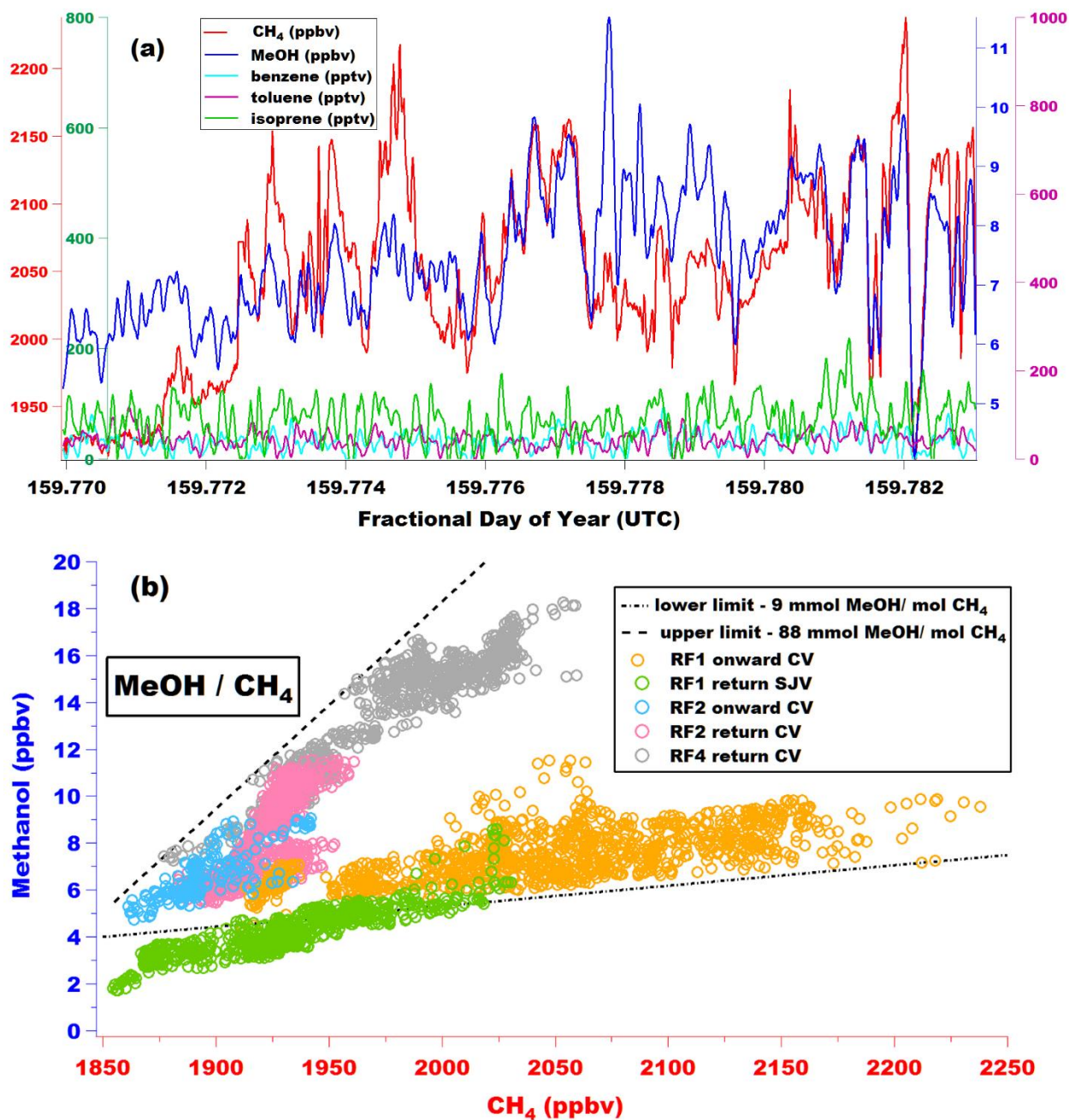
Figure 3. 12. (a) Mixing ratio time series of CH_4 and selected VOCs measured by the PTR-MS during the flight segment over Central Valley dairies in RF 1. The segment is ~ 19 minutes in duration and ~ 65 km in length. The color of the scale on the y-axis corresponds to the color of the trace as listed in the legend. Benzene (light blue) has the same y-axis scale as toluene (pink). (b) Scatter plot of methanol vs methane mixing ratios from flight segments in the Central Valley over dairy and livestock regions. The dashed and dotted lines represent the upper and lower bounds, respectively of MeOH / CH_4 slopes observed over the different segments.
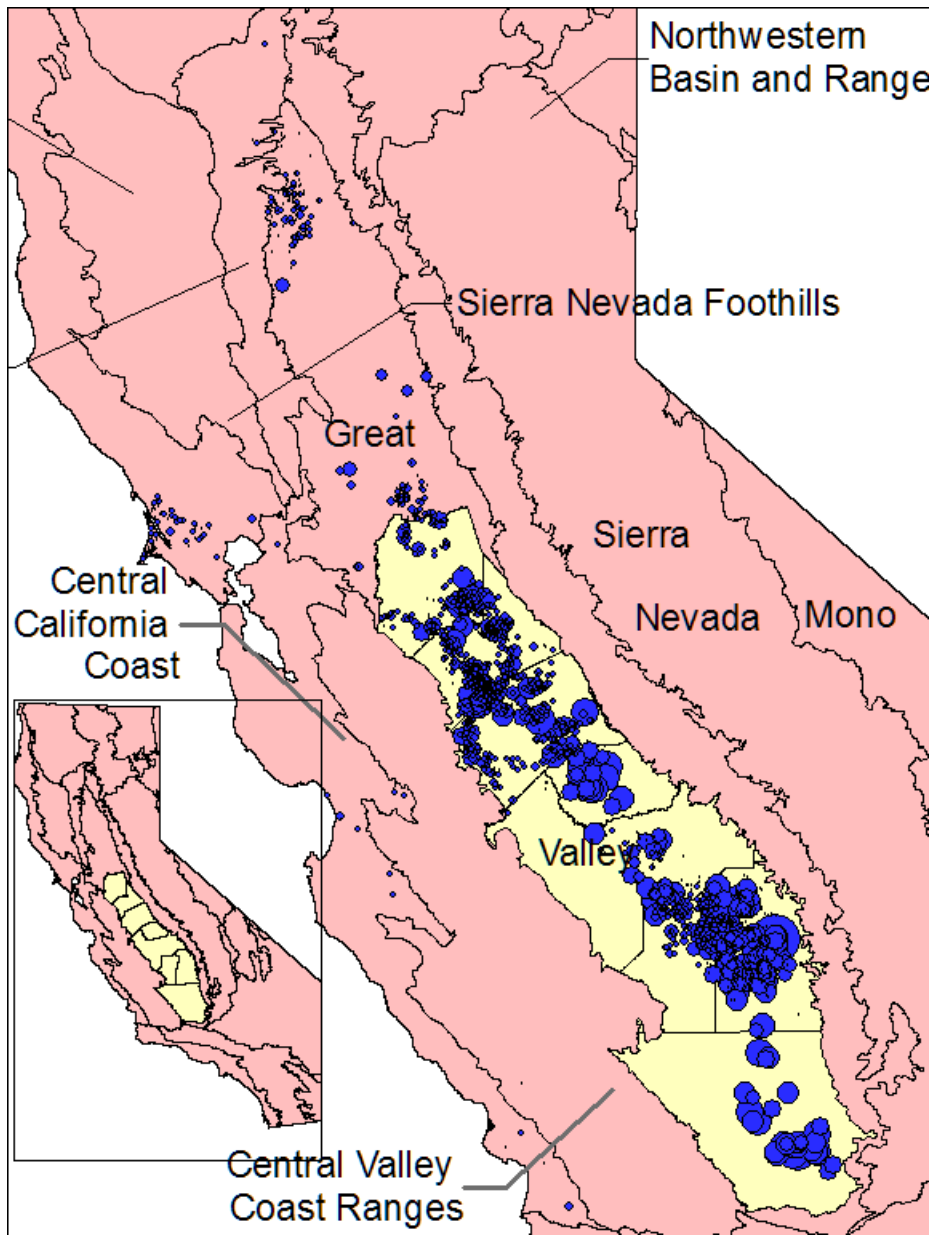
Figure 3. 13. California ecoregion map showing the extent of San Joaquin Valley (SJV) within the Central Valley (marked as Great Valley here). The portion of eight counties in the region that falls within the boundaries of SJV have been highlighted in yellow.

Figure 3. 14. Flight segment over oil and gas fields in western Kern County color coded by CH$_4$ concentrations. The spatial extent of the oil fields are shown as a semi-transparent over lay with the black arrows and half-dome footprints indicating incoming wind direction and representative fetch, respectively. The plots depict flight stretch over (a) Midway-Sunset and Buena Vista oil field; (b) La Paloma natural gas cogeneration plant; (c) and (d) Cymric oil field. The bottom four images are taken from the on-board GPS enabled high-definition video camera and shows the real time image capture of oil and gas operations and the natural gas co-generation facility.

103
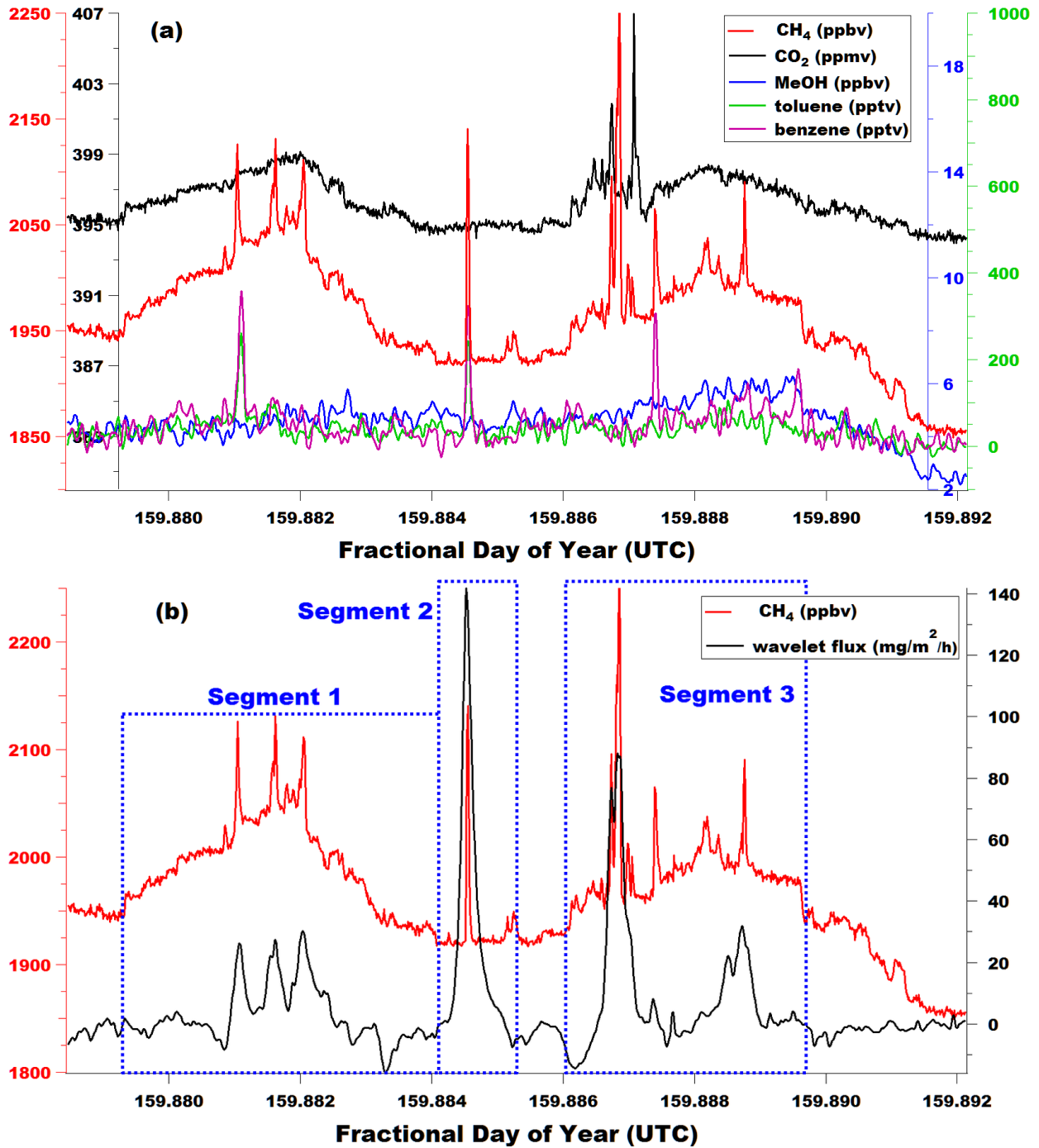
Figure 3. 15. Time series plots over the duration of flight over oil and gas fields in western Kern County during RF 1 showing (a) mixing ratios of CH_4, CO_2 and VOCs, and (b) mixing ratios of CH_4 with eddy covariance-derived CH_4 wavelet-flux time series. In figure (b), the time series is further split into three shorter segments denoting (1) flight duration over Midway-Sunset oil field around the city of Taft; (2) La Paloma natural gas cogeneration plant, McKittrick; and (3) Cymric oil field.
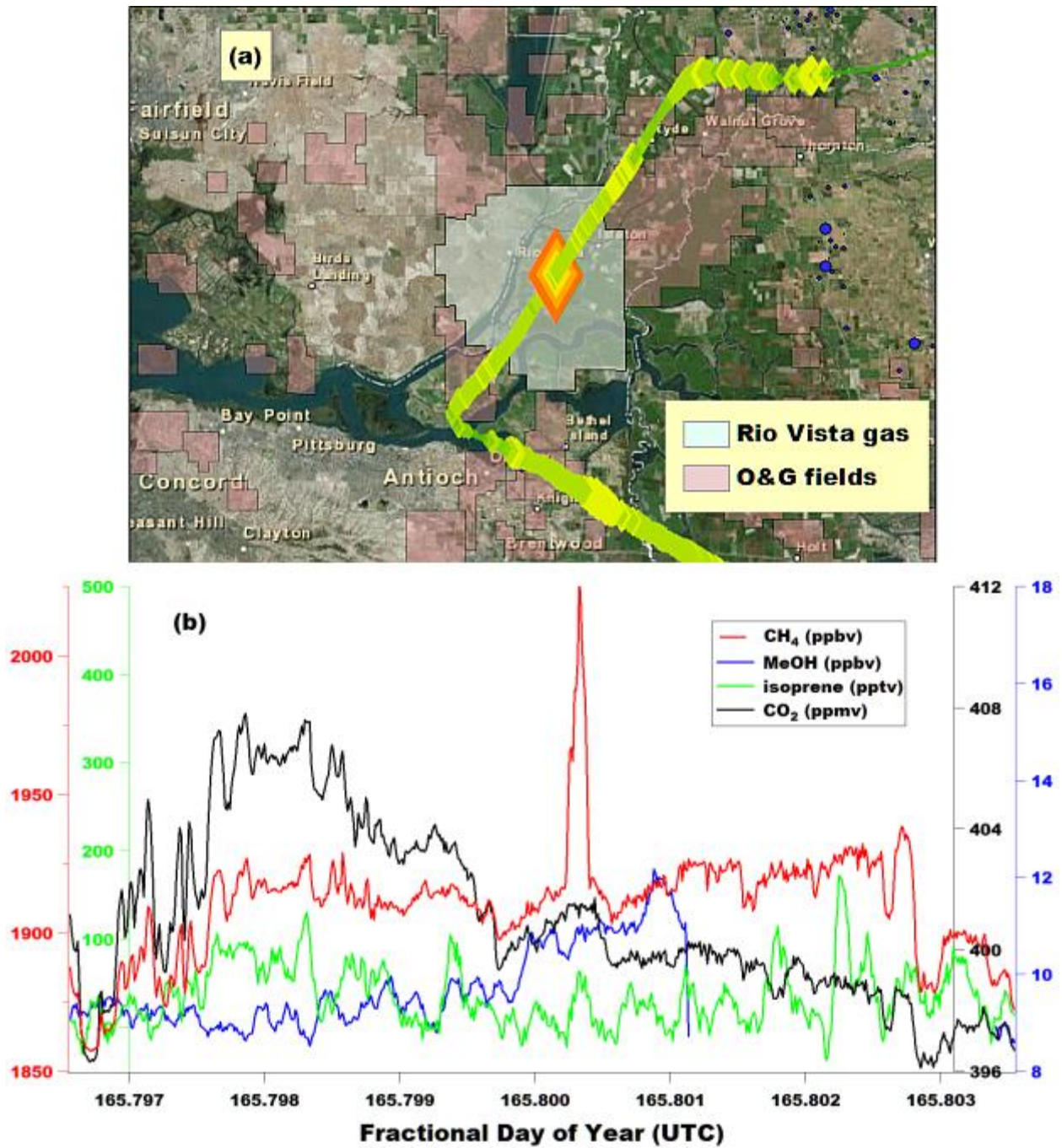
Figure 3. 16. (a) Flight leg over the Sacramento - San Joaquin delta during RF 4 color coded and sized by CH_4 concentration. The spatial extent of the Rio Vista gas field is highlighted in the semi-transparent blue polygon; (b) Time series of CH_4, CO_2 and VOC mixing ratios with a sharp CH_4 enhancement above Rio Vista gas field.
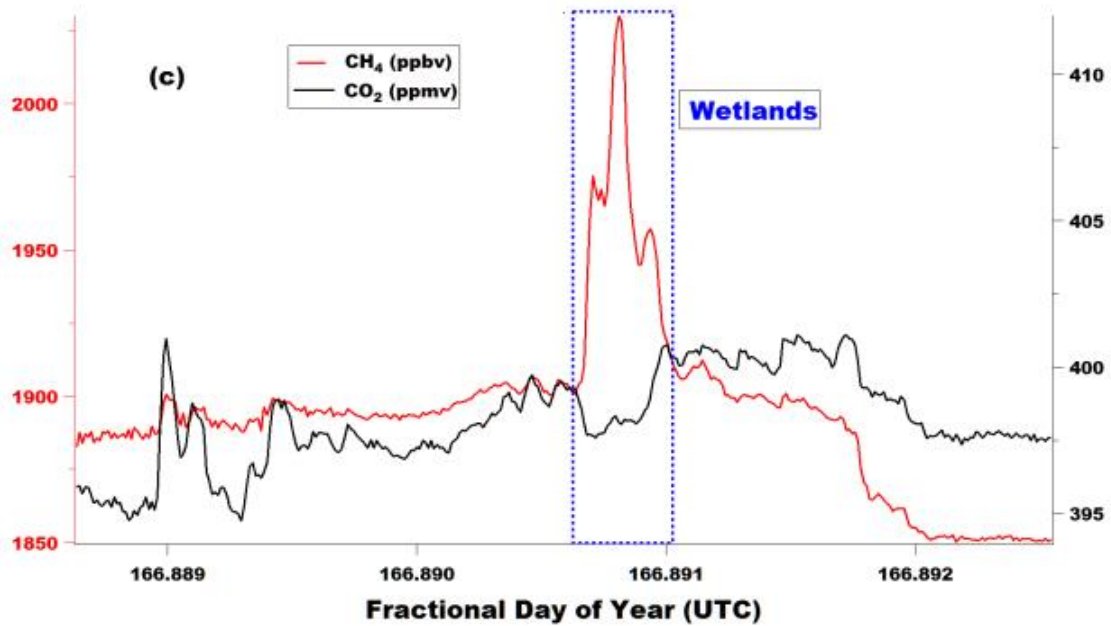
Figure 3. 17. (a) Onward and (b) return flight leg over wetlands north of San Pablo Bay during RF 5 color coded and sized by CH_4 enhancements. The prevailing wind direction is shown in black arrows. (c) Time series of CH_4 and CO_2 during return stretch north of San Pablo Bay with the duration over wetland regions highlighted in blue.
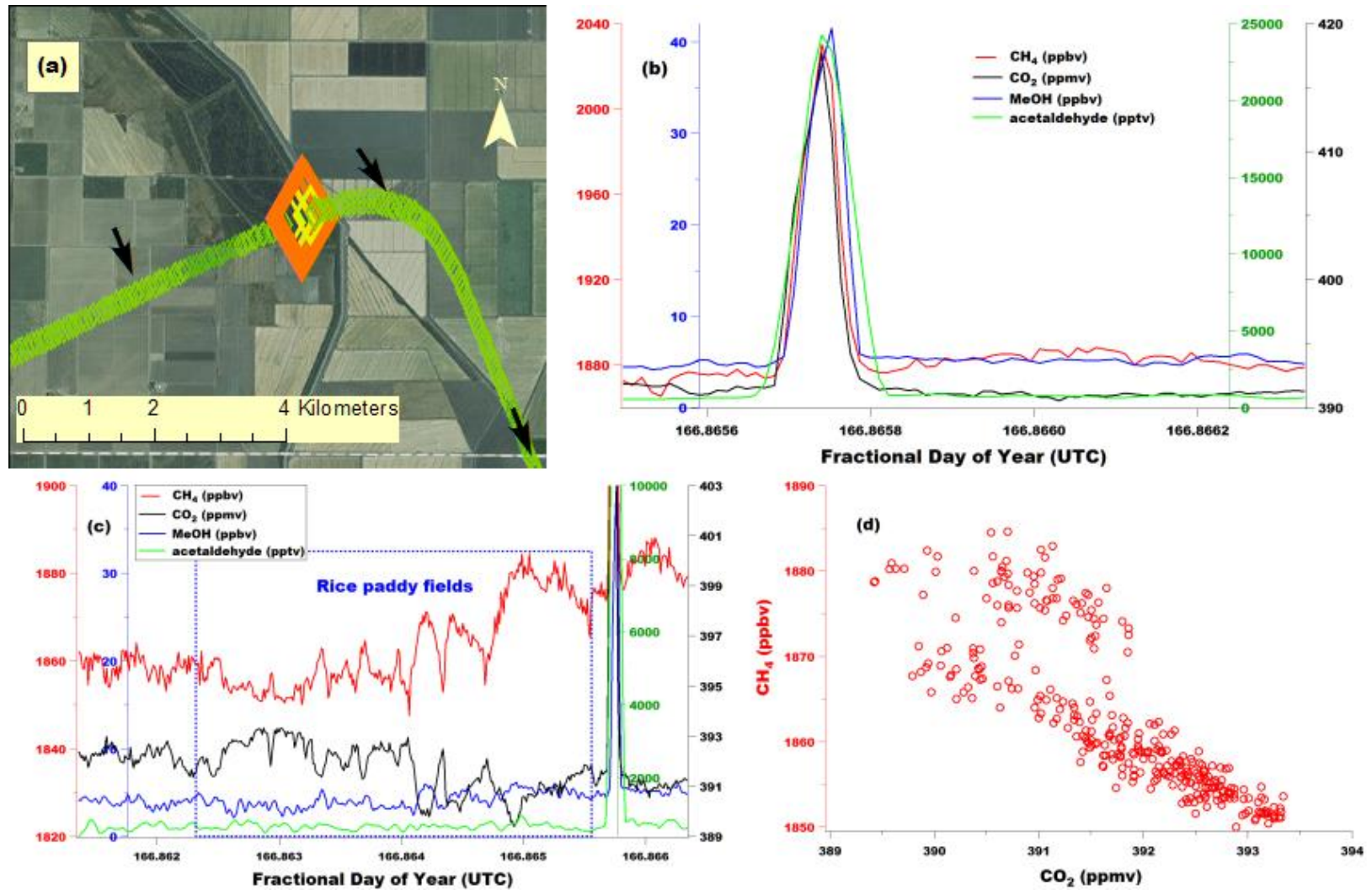
Figure 3. 18. (a) A biomass burning plume event encountered while flying into the Sacramento valley during RF 5. The flight track is color coded by CH_4 enhancements; (b) time series depicting the sudden and large rise in mixing ratios of CH_4, CO_2 and other VOCs in the biomass plume; (c) time series of CH_4, CO_2 and other VOCs flying over the rice paddy fields immediately preceding the biomass plume (highlighted in blue box); and (d) scatter plot of CH_4 and CO_2 enhancements over the rice paddy flight stretch (blue box in figure c) showing anti-correlation between the two species.
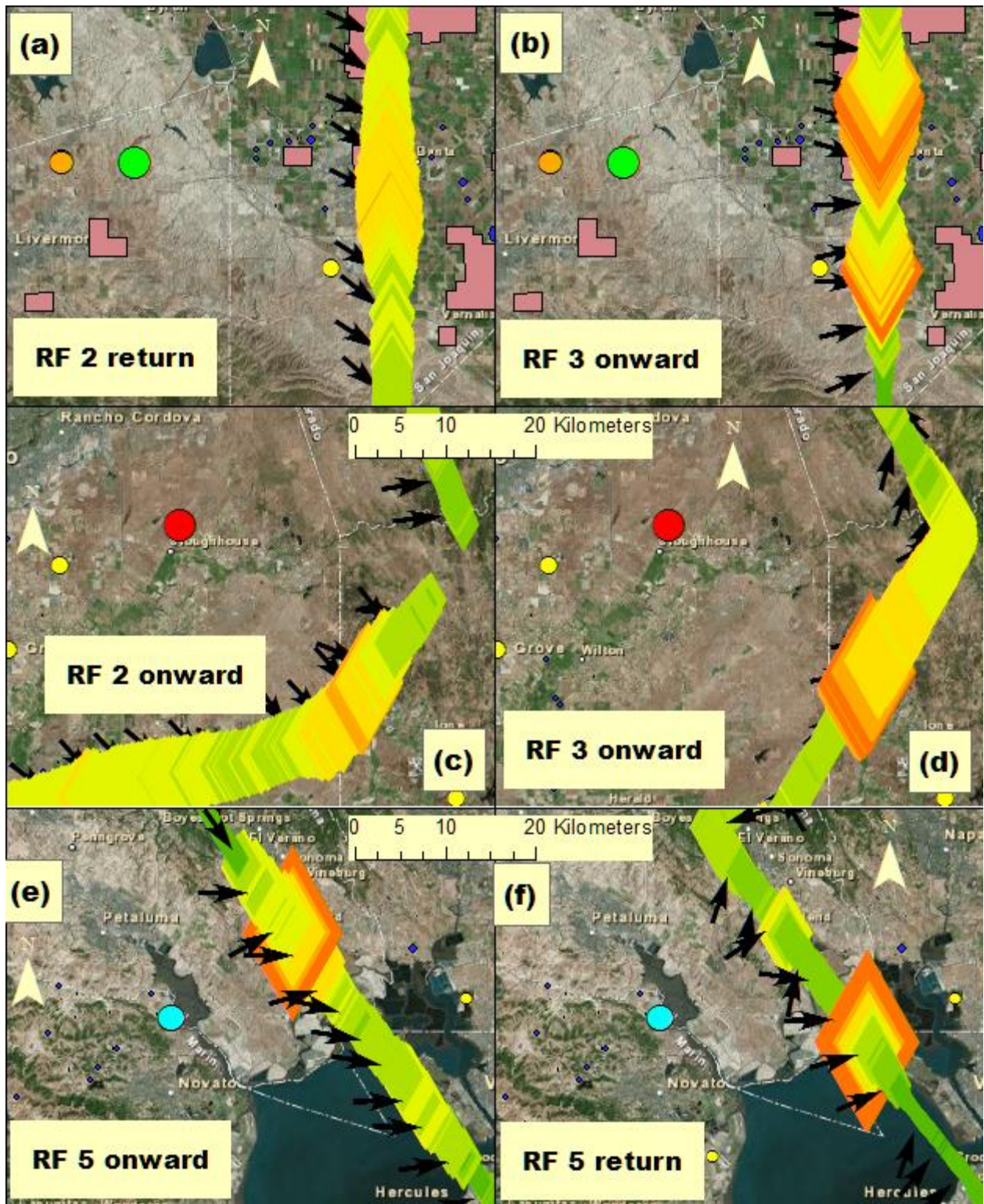
Figure 3. 19. (a - f) Flight tracks colored coded by CH_4 mixing ratios showing the impact of plumes from major landfills in the region. The landfills shown in these figures include Vasco (orange circle) and Altamont (green circle) serving the East Bay Area region, Kiefer (red circle) landfill serving the Sacramento metropolitan region, and Redwood (blue circle) landfill serving the North Bay region.

Chapter 4: Seasonal variability in methane and nitrous oxide source apportionment in California's Central Valley

Abstract

We conducted continuous measurements of greenhouse gases CH_4 and N_2O, CO and a suite of VOCs at Walnut Grove tower near the Sacramento San Joaquin River Delta in California's Central Valley over the 2012-13 annual cycle. Measured compounds represented a broad array of source tracers including CO (combustion), acetonitrile (biomass burning), benzene and toluene (fossil fuel), oxygenated VOCs methanol (livestock, vegetation, secondary), acetaldehyde (vegetation, photooxidation, livestock), acetone (vegetation, photooxidation, livestock, biomass burning), methyl ethyl ketone (photooxidation, livestock), biogenic hydrocarbons isoprene and monoterpenes, and biogenic oxidation products methyl vinyl ketone + methacrolein. We perform a source apportionment on the combined GHG - VOC data set using the statistical technique of positive matrix factorization (PMF) in order to evaluate the major sources influencing the diurnally resolved observations of CH_4 and N_2O at the site. The year-long measurements are parsed into seven separate periods representative of the broad seasonal patterns observed in the region and unique PMF analysis is performed for each of these individual periods to investigate the seasonal variability of CH_4 and N_2O source apportionment. Vertical profiles were measured continuously from 10 to 525 m for the VOCs, and from 30 to 483 m for the greenhouse gases, and these data along with wind direction were used as confirmation of the patterns observed from specific source categories.

Dairies and livestock are the largest regional sources contributing to the enhancements of CH_4 accounting for 55 – 90 % of total emissions over different seasons. The variability is caused by the seasonally changing proportion of CH_4 from the 'agriculture + soil management + delta' source. The CH_4 emissions from this microbially-mediated temperature-dependent source are principally occurring due to land / soil management practices and natural wetland ecosystems in the surrounding Delta. During summers, this source can account for up to 30 - 40 % of the diurnal CH_4 enhancements, ~ 20 % during early spring and early fall periods, and the source is practically absent during the winter season. A third CH_4 source, the 'urban and oil / gas source', contains a bulk of the apportioned CO and aromatics and is theorized to be emitted from an aggregation of upwind sources that include the urban core of San Francisco Bay Area and the nearby Rio Vista natural gas fields. This source, which generally accounts for 10 - 20 % of the observed CH_4 enhancements, does not show any clear seasonal dependence although prevailing meteorology combined with absence of the Delta-related CH_4 source in late fall season can increase its relative share to ~ 30% of the observed diurnal enhancements.

Only two significant source categories of N_2O influencing the observed signals at Walnut Grove tower could be discerned from the PMF analysis. The first is the microbe-driven soil emissions of N_2O that results from fertilizer use in the vast agricultural operations around Walnut Grove that gets apportioned to the 'agriculture + soil management + delta' source. The second is

manure-management related N_2O emissions attributed to dairy and other livestock. The emissions from the agriculture-related source is largest during the growing season, accounting for about 80 – 90 % of the observed enhancements during peak fertilizer use in the spring and summer season, reducing to about 20 % of the observed enhancements in late fall season when fertilizer use reaches a minimum at the end of the growing season and as cultivated crops are harvested. In contrast, N_2O apportioned to the dairy and livestock source, is relatively constant across seasons, accounting for > 80 % of the total enhancements in fall and winter and correspondingly less when agricultural emissions are larger. Consistent with expectation, no CH_4 and N_2O enhancements are identified in the 'biogenics' factor associated with direct plant emissions.

CH_4 emissions from the managed wetland / peatland ecosystems in the Delta are currently not included in the statewide greenhouse gas inventories. Evidence of significant CH_4 emissions from this source are seen which should be quantified in the inventory. The lack of N_2O in the 'urban and oil / gas' source raises questions about its significant attribution to the transportation sector in the state greenhouse gas inventory. We observe a strong seasonal dependence for certain source categories of CH_4 and N_2O emissions. These findings highlight the importance of long-term measurements to validate the inventory of non-CO_2 greenhouse gas sources and places a caveat on annual estimates derived from measurements suffering from limited temporal resolution.

4.1   Introduction

Methane (CH_4) and Nitrous Oxide (N_2O) are two greenhouse gases that together contribute two-thirds of the total non-carbon dioxide (CO_2) greenhouse gas radiative forcing (~ 1 W m^{-2}) (Forster et al., 2007). Owing to its high global warming potential (GWP) of ~ 25 (Montzka et al., 2011) resulting from efficient trapping of heat, but a relatively short life time of about 10 years as compared to CO_2, reduction of anthropogenic emissions of CH_4 can be an important strategy to delay the most immediate effects of climate change as long term solutions and remedies are implemented through international agreements. The longer persistence of N_2O in the atmosphere (~ 120 years) results in a GWP of ~ 300 (Montzka et al., 2011) and makes it a likely candidate for a long term global strategy to reduce greenhouse gas emissions and its associated radiative forcing. California has adopted an ambitious climate change strategy of reducing its 2050 carbon emissions to 80% below 1990 emissions levels through the California Global Warming Solutions Act of 2006 (popularly known as AB32). AB32 requires the state to first meet a shorter-term target of reduction of greenhouse gas emissions to 1990 levels by the year 2020 representing a 25 % decrease from business-as-usual scenario. The state's main air quality regulatory agency, the California Air Resources Board (ARB), is entrusted with the responsibility of enforcing AB32. As part of their AB32 implementation process, the ARB initially focused its regulatory efforts on those major point sources of CO_2 that are fairly well-quantified and can bring about large scale greenhouse gas reductions e.g. power plant and vehicle emissions (CARB, 2013). Following stricter regulation of these sectors, ARB's attention now turns towards regulating CH_4 emissions in pursuit of achieving the near-term year 2020 greenhouse gas reduction goal. The agency is

also working towards constraining the bottom-up inventory of N_2O through 'top-down' assessments.

The success of ARB's efforts is contingent on accurate accounting of CH_4 emissions. A majority of CH_4 emissions are produced by agricultural sources namely enteric fermentation from cattle and management of animal waste (> 60 %) and if decomposition of waste from landfills and waste water treatment is included, a vast majority of the emissions originate from microbially-mediated biological pathways (~ 90 %; CARB, 2013). Such emissions sources are more likely to be area sources that are spatially and temporally variable, and thus difficult to quantify. The greenhouse gas inventory compiled by ARB for emission accounting is based on a 'bottom-up' emission factor (EF) approach that may not be suitable for estimating emissions from source categories like dairies and livestock, landfills, rice cultivation etc. that have a large annual range of emissions that depend on a number of factors. For instance, differences in manure management practices in dairies from that in feedlots have been reported to result in drastically different CH_4 emissions (Owen and Silver, 2014). Emission factors derived from ground-based and airborne measurements from rice agriculture in California suggest an underestimation of this source category in the ARB greenhouse gas inventory (McMillan et al., 2007; Peischl et al., 2012) which is based on a single emission factor for the whole year. Previous literature, mostly evolving from studies conducted in California, has demonstrated the spatiotemporal nature and seasonal dependence of CH_4 emissions from dairy and livestock (Owen and Silver, 2014), natural and restored peatlands / wetlands (Cicerone et al., 1983; Teh et al., 2011; Hatala et al., 2012; Knox et al., 2014), and from agriculture (including rice) (Salas et al., 2006; Knox et al., 2014; McMillan et al., 2007). Currently, the oil and natural gas (O&G) production / extraction sector accounts for just ~ 3 % of the state's total CH_4 emissions. A comprehensive spatially resolved state CH_4 emissions inventory for the oil production and natural gas system sector, generated from an assortment of public information and US-EPA (Environmental Protection Agency) emission factors, estimates emissions that are 3-7 times larger than the state inventory (Jeong et al., 2014) pointing to significant uncertainties in the latter.

A series of 'top-down' measurement campaigns conducted in Southern California report a range of CH_4 emissions from oil and natural gas activities, all of which are larger than that is currently attributed to this region in the ARB greenhouse gas inventory (Wunch et al., 2009; Peischl et al., 2013). Inverse modeling of airborne CalNex 2010 observations over California suggest underestimation of the CH_4 emissions from landfills and wastewater and the oil and gas sector in the greenhouse gas inventory (Wecht et al., 2014). Airborne eddy covariance CH_4 flux estimates for the dairy and livestock sector determined in Chapter 3 point towards potential underestimation of these emissions in the 'bottom-up' inventory. Most or all of these studies suffer from some or the other caveat. Inverse modeling from aircraft observations or direct airborne flux computation can estimate surface CH_4 emissions but are unable to capture temporal variations in the absence of long term monitoring. Ground based flux towers (Baldocchi et al., 2012; Hatala et al., 2012; Knox et al., 2014) are very suitable and representative measurement methods over homogenous area source configurations (e.g. wetlands, rice etc.) but not so much over O&G production areas and dairy / livestock regions. Inverse dispersion of either tower or remote sensing observations can provide continuous long term monitoring but are constrained by potential inaccuracies in the transport model and *a priori* emission maps. It is difficult to

evaluate the inventory at regional scales accurately in the absence of continuous measurements over long periods of time covering large areas. Year-long WRF-STILT inversion of atmospheric CH_4 observations have been performed at the Walnut Grove tower (WGC) in the Central Valley of California to estimate seasonally averaged CH_4 emissions that show clear patterns of seasonal variations along with 55 – 84 % higher emissions than California-specific *a priori* models (Jeong et al., 2012a). These measurements, when executed over a network of tall towers, allow for constraining emissions from individual sub-regions over a larger regional scale with lower uncertainties (Jeong et al., 2013).

Global atmospheric concentrations of N_2O have been steadily increasing at a rate of 0.2 - 0.3 % per year (Denman et al., 2007) with current global background levels in excess of 325 ppb. Significant portions of this atmospheric increase have been attributed to extensive use of nitrogen-based fertilizers (Park et al., 2012). The Central Valley of California is a major agricultural region with a per capita output that surpasses any other region in the world (CASR, 2011). The Valley has a multitude of agricultural and biological sources of N_2O including synthetic and organic fertilizer application, manure management, wetlands, wastewater treatment, and crop residue management (Xiang et al., 2013). Emissions of N_2O from agricultural soils are estimated in the ARB inventory using an emission factor approach (Guo et al., 2011). N_2O emissions from the soil are microbially-driven and are affected by numerous environmental factors like N fertilizer application rate, soil organic matter content, moisture, management practices, meteorological conditions etc., which make these emissions spatially and temporally variable, and thus challenging to characterize (van Groenigen et al., 2010; Guo et al., 2011; Hoben et al., 2011; Linquist et al., 2012). Large uncertainties exist in the bottom-up regional estimation of N_2O emissions (NRC, 2010). Very few regional 'top-down' assessments of the N_2O inventory in the US exist, and even fewer over the Central Valley of California. A top down inverse approach based on STILT LPDM back trajectory analysis of aircraft observations across the US reported under-prediction of N_2O emissions in the EDGAR and GEIA inventory by a factor of ~ 2.6 to 3.0, respectively (Kort et al., 2008). There were, however, no airborne flask samples collected over the Central Valley in this study and the estimates were limited to the early summer period. Atmospheric column-based abundance studies in the Los Angeles region have reported significant underestimation of N_2O by EDGAR and ARB GHG inventories but with high uncertainties. Jeong et al. (2012b) reported the first top-down inverse estimates of N_2O emissions measured at a tall tower based on the WRF-STILT framework that captured the complete annual cycle of N_2O emissions in the Central Valley of California. Spatially averaged N_2O emissions from regions within ~ 150 km of the tower with a large agriculture and dairy / livestock influence were higher than EDGAR inventories by a factor of about 1.6 - 2.5 over different seasons. A comprehensive account of N_2O emissions from field-scale measurements conducted in dairies worldwide show a great discrepancy with modeled emissions derived using inventory emission factors (Owen and Silver, 2014).   The PMF results in Chapter 2 indicate that statistically no N_2O is apportioned to the vehicle emissions source factor even though it is included as a significant source in the ARB inventory.

In this study, we measured mixing ratios of CH_4, N_2O, combustion tracer CO, along with a suite of VOCs, over a complete annual cycle at the Walnut Grove site (WGC; Andrews et al., 2013) in California's Central Valley in order to assess the greenhouse gas (GHG) source apportionment in this region. Measurements included vertical profiles from the ground to near

the top of the WGC tower (525 m) for most species. We parse the year-round measurements into smaller data sets representative of the prevailing season and applied the statistical source apportionment tool of Positive Matrix Factorization (PMF) on individual temporal periods of the combined GHG - VOC data subsets. The first goal of this study was to determine the major categories of emissions sources contributing to the apportionment of CH_4 and N_2O in this region. For this purpose, we used the simultaneous apportionment of VOCs as potential source markers, wind rose plots, and diurnal and vertical profiles to identify and categorize the PMF-generated statistical combinations (factors) as sources or combinations of collocated sources. We hypothesized that the regional dairy and cattle industry will have a significant imprint on the apportionment of both CH_4 and N_2O while the vast expanse of agriculture around the site is likely to impact N_2O signals. The second objective was to investigate the seasonal variation of the CH_4 and N_2O emissions distribution over seven different time periods from mid-2012 until mid-2013. This has implications for short term GHG measurement studies in multi-source regions that only provide a snapshot in time like airborne flux measurements, or back-trajectory analysis on aircraft observations and atmospheric column abundances retrieved by satellite observations. We hypothesized the N_2O emissions from agriculture will show a seasonal trend that coincides with the primary agricultural growing season in the Central Valley while no major seasonal dependence will be observed for CH_4 originating from dairies and cattle feedlots.

4.2   Experiment

4.2.1   Site, Greenhouse Gas sources and Meteorology

The greenhouse gas and VOC measurements were made at Walnut Grove tower (WGC; Andrews et al., 2013) near Walnut Grove, California (121.49°W, 38.27°N, and 0 m above sea level). WGC is a tall TV signal transmission tower extending 525 m above ground level (a.g.l). WGC is located about 50 km south of the Sacramento metropolitan area and about 50 - 100 km west-southwest from various urban cores within the extended San Francisco Bay Area as seen in the land cover and potential source map of the region in Figure 4.1. WGC is located at the eastern edge of the ~ 3800 km^2 Sacramento - San Joaquin River Delta (referred to as the Delta from here on), an expansive inland river delta and estuary. Much of the land in the Delta, through the past century, has been reclaimed through construction of levee barriers and subsequently drained and used for agriculture. Currently, the Delta serves as an agricultural hotspot of California producing $ 500 million worth of crops that include corn, walnuts, pears, tomatoes, nursery stock, hay and importantly, dairy and livestock (CCCR 2013; SacCR 2013; SCR 2013). As seen in Figure 4.1 created using the National Land Cover Database (Homer et al., 2007), cultivated crop land is ubiquitous around WGC especially to the west and south west of the site, which is the predominant wind direction during a major part of the annual cycle as evidenced in the seasonal day time and night time wind rose plots in Figures 4.2 and 4.3, respectively. Thus we can expect strong influence of biogenic VOC tracers on signals measured at WGC during the growing season. Fertilizer use on farm lands is a major source of N_2O, and thus the intensive agriculture around WGC is expected to be a significant contributor to N_2O signals measured at WGC. WGC is in close proximity to many dairy and livestock operations, providing an

additional major CH_4 and N_2O source. Immediately to the south of WGC lies the San Joaquin County which is home to more than 300,000 dairy and livestock cattle (Table 3.3, Chapter 3). Some portions of the Delta exist as natural wetlands (Figure 4.1), while some of the low lying islands are being converted and restored as wetlands by permanent flooding (Miller et al., 2008) to reverse land subsidence due to peat oxidation. Alongside the relatively newer practice of flooded agricultural systems (like rice) in the Delta (Hatala et al., 2012; Knox et al., 2014), these wetland / peatland ecosystems are a CH_4 source (Le Mer and Roger, 2001; Miller, 2011; Teh et al., 2011) and such signals if large enough may be detected at WGC due to its proximity. The intensive rice agriculture in the Sacramento Valley, much of which lies around 100 km north-northwest of WGC, is a known CH_4 source that can be a significant contributor to the local CH_4 budget during the growing season (McMillan et al., 2007; Peischl et al., 2012). One of the major natural gas fields in California, the Rio Vista gas field, is located 15 - 25 km immediately upwind from WGC in the Delta. Though a number of smaller landfills exist in and around the urban regions, there are no landfills in the Delta.

WGC experiences a Mediterranean climate characterized by hot and dry summers and mild and rainy winters. In summers (Jun - Aug), the seasonal mean daytime temperatures (at 10 m a.g.l) reach a high of ~ 30°C with early morning lows of about ~ 14°C (Table 4.1). In winters (Dec - Feb), the seasonal daytime highs are ~ 14°C and nighttime lows are about 4°C. From annual precipitation records of the nearby town of Lodi located ~ 25 km southeast of WGC (CIMIS, 2013), the bulk of precipitation in the reported measurement period (Jun 2012 - Aug 2013; 14 inches) occurred during Dec 2012 – Jan 2013 with minor rain events during Feb - Mar 2013. A low-level day time marine inflow moves air inland from the San Francisco Bay Area into the Central Valley through the Carquinez Straits and along the Delta (Bao et al., 2007). This synoptic onshore wind provides the prevalent wind direction at WGC (91 m a.g.l) during the spring, summer and early fall season (Apr – Sep) that is driven by intense daytime heating in the Central Valley that creates a low pressure over WGC as compared to the coast (Figure 4.2). The day time air flow is strongest in the late afternoon hours and weakest during the morning. This flow can transport pollution from the San Francisco Bay Area into the Central Valley past WGC (Zhong et al., 2004). These dominant flows are likely to bring greenhouse gas and VOC emissions from the upwind sources in the greater San Francisco Bay Area and the Delta to WGC. The intensity of this flow is reduced in the night due to nocturnal cooling such that down-valley flows and down-slope flows are observed over the plains and the eastern edges of the Central Valley, respectively. At WGC, however, at least during the warmer months (Apr - Sep), the coast - inland temperature gradient is still significant enough that the westerly upslope flows are maintained even during the nighttime (Figure 4.3). Higher up in the PBL, where the top air inlet was at 525 m a.g.l (Figure 4.4), downslope drainage flows brings air down the Sierra Nevada mountains from the east, thereby biogenic emissions from oak and coniferous forests and their oxidation products (not shown) accumulate in the residual layer at night and mix down during the morning when vertical mixing begins (Misztal et al., 2014). In the absence (or rather, weakening) of diurnal surface radiative heating/cooling cycle in the late fall, winter and early spring months (Figures 4.2 c-e and 4.2 c-e), the mean flows at WGC are more variable and diffused, with confluence of down-valley winds from both the Sacramento Valley in the north and the San Joaquin Valley to the south at WGC. The site, thus, experiences mean flows from a directionally broader but more local (hence smaller) zone of influence during the cooler / wetter

114

months (Oct-Mar). The fall / winter south-easterly flows make the dairy and livestock intensive regions of San Joaquin County directly upwind of WGC.

4.2.2   Instrumentation and measured VOCs

The greenhouse gas measurements were made using a long-term set up and suite of instruments that are being used for inverse emissions estimates of CH_4 (and later N_2O) at WGC since 2007. More details about the instrumentation set-up can be found in literature emanating from previous studies at WGC (Zhao et al., 2009; Jeong et al., 2012a, 2012b). Briefly, the GHG measurements are made using a sampling and analysis system that combines pumps, air driers, and gas analyzers. Air samples are drawn from three heights (30, 91 and 483 m a.g.l) as seen in Figure 4.4 on the tower sequentially, then dried first to a water vapor dew point of 5°C using a condensing system and then on a temperature stabilized membrane drier to - 33°C dew point before being supplied to the gas analyzers. When switching between the three heights, the first 4.5 minutes of each sampling period is allowed for equilibration of the gas concentrations and instrument response, and thereafter the last 30 seconds is used as the actual measurement. CH_4 is measured using a cavity ring-down spectrometer (Picarro EnviroSense 1301) with an accuracy and precision of 0.3 ppb over a 30 second averaging period. The offset and gain are measured periodically and corrected for every six hours using NOAA primary gas standards. In addition to this, ambient air is drawn from a separate line at 91 m a.g.l into flask samples that are collected every other day at 1400 PST and later analyzed at NOAA-ESRL to provide further quality check on the in-situ measurements. For CH_4, the measurement accuracy determined using the synchronized flask and in-situ measurements is ~ 1 ppb (Jeong et al., 2012a) which is significantly less than the daily range of atmospheric variations seen at WGC.

N_2O was measured using an off-axis Integrated Cavity Output Spectroscopy (ICOS) analyzer (LGR Model 907-0015; Los Gatos Research Inc.). The offset and gain of the LGR instrument were measured every 3 hours using secondary standards tied to the NOAA calibration scale. Following periodic calibration, the N_2O instrument has precision of near 0.05 ppb on 2 minute averages and an absolute accuracy near 0.1 ppb, which is limited by the uncertainties in propagating the NOAA scale from the primary calibration gases to the individual tower measurements.

CO was measured using a gas filter correlation analyzer (TEC, 48C Trace Level, Thermo Electron Corporation) as part of the NOAA Earth System Research Laboratory's (ESRL) Tall Tower Greenhouse Gas Observing Network (Andrews et al., 2013). Typical long term analytical uncertainty for the CO measurements is ~ 6 ppb which is reasonably precise to resolve variability on timescales used in this analysis (1 h). In addition, the LGR ICOS instrument also measures CO with precision of near 1 ppb. The CO data from the coincident measurements (TEC and LGR) were compared over the campaign and showed a high correlation ($R^2 > 0.99$). We are, thereby, confident about the accuracy of the TES CO measurements. We fill gaps in the CO time series using measurements from the LGR analyzer. The CH_4, CO and N_2O data are finally averaged to hourly intervals in order to create a series with similar time resolution as the VOC measurements.

Automated in-situ measurement of VOCs was performed using a Proton Transfer Reaction Mass Spectrometer (PTR-MS) (IONICON Analytik, Innsbruck, Austria). The instrument is based on soft chemical ionization of gas phase compounds by hydronium ions (H_3O^+) in which a wide variety of VOCs with proton affinity higher than that of water can be measured simultaneously at high time resolutions (e.g. seconds) (de Gouw and Warneke, 2007; Blake et al., 2009). Details on the detection limits and calibration approach of the PTR-MS instrument used at WGC can be found in previous literature (Holzinger et al., 2005; Fares et al., 2012; Park et al., 2013). At WGC, a 400 ml/min air sample stream was drawn from five separate Teflon sample intakes at different heights (10, 131, 262, 394, and 525 m a.g.l) as seen in Figure 4.4. Air was drawn continuously through all the five tubes and sub-samples were sequentially drawn from these tubes into the PTR-MS instrument for VOC analyses. A set of Teflon solenoid valves performed this switch of sample flow every two minutes thus requiring a 10 minute total cycle for one vertical profile measurement consisting of each of the five heights (10 m, 131 m, 262 m, 394 m, and 525 m a.g.l). After switching to a new inlet height, the first 30 s of a two minute period were discarded leaving 90 s of sample flow that was analyzed for ambient tracers. There were 6 of such two-minute periods in each hour of measurement and so effectively 540 s of data per hour was averaged from each inlet level in order to achieve detection limits in the lower pptv range. The instrumental background was evaluated two times each day by sampling zero air created by automated drawing of ambient air through a heated Pt/Al_2O_3 (to 350°C) catalyst to remove VOCs. Regular automated calibrations with certified gas standards were performed twice daily for all the measured ions (*m/z*). The standards contained the compounds at 1 ppm each which were diluted using the catalyst zero air. The PTR-MS was configured to measure approximately 20 masses. After intensive quality checks and post-processing of data, the following masses, represented here by their mass-to-charge ratios (*m/z*), were deemed high quality and included in the subsequent PMF analysis: methanol (*m/z* 33), acetonitrile (*m/z* 42), acetaldehyde (*m/z* 45), acetone + propanal (*m/z* 59), isoprene (*m/z* 69), methyl vinyl ketone (MVK) + methacrolein (MAC) (*m/z* 71), methyl ethyl ketone (MEK) (*m/z* 73), benzene (*m/z* 79), toluene (*m/z* 93), and monoterpenes (*m/z* 137). Acetonitrile (*m/z* 42) is a tropospheric tracer of biomass burning (Lobert et al., 1990; Holzinger et al., 1999; Bange and Williams, 2000) but a minor contribution from alkanes during pollution episodes to *m/z* 42 is possible. Similarly, *m/z* 93 (toluene) can see some contribution from biogenic monoterpene fragments if the concentration of the latter is high. Two more masses, green leaf volatiles (*m/z* 83) and C-9 aromatics (*m/z* 121), were deemed medium to medium-high quality. They have not been included in the PMF analysis but have been utilized for independent comparison with and verification of PMF source factors (Chapter 4.3).

4.2.3   Choice of sampling periods

In this study, we began with the assumption that we would perform PMF-based source apportionment over four separate periods consistent with local seasonal distinctions, as opposed to one composite PMF analysis through the entire measurement period (June 2012 – August 2013). There were two principal reasons behind this choice. Firstly, the factor profiles produced in a PMF analysis represent constant linear source configurations that do not change over the

whole analysis cycle. Some VOCs included in this study have principally light and temperature driven sources (e.g. isoprene) and have non-linear dependence on such parameters. Similarly, for some compounds, emissions from their majorly biological sources would depend and vary with the stage of vegetative growth or microbial activity (e.g. methanol, acetone, N_2O). Hence, we anticipate that the fractional composition of certain source categories can vary significantly during different times in the annual cycle and as such, a single factor profile representing a source category for the entire year may result in an inaccurate PMF fitting with a higher residual error. This constraint can be overcome to a reasonable extent by performing unique PMF analyses over shorter time periods when the meteorological variables (like light, temperature and rainfall) impacting the site are more homogenous. Hence, the optimal choice of total number of separate PMF analyses to be performed on the larger dataset seemed to be four. These study periods were summer (Jun-Aug), fall (Sep-Nov), winter (Dec-Feb), and spring (Mar-May). Secondly, this choice of sampling period made more sense as it was consistent with those used in previous evaluation of CH_4 and N_2O emissions from inverse dispersion analysis of atmospheric observations at WGC (Jeong et al., 2012a, 2012b). The choice of four seasonal study periods would, hence, allow for a potential comparison of PMF results with WRF-STILT derived CH_4 emissions (being evaluated currently).

We, however, did not have complete data coverage of all tracers through the course of the entire campaign as seen in Table 4.1. Two key tracers in the PMF analysis are N_2O and MeOH. It is vital to perform PMF analyses over entirely non-missing periods of N_2O measurements in order to achieve the objective of the study i.e. PMF-based apportionment of N_2O sources in the region. We had the first N_2O measurements at WGC begin from mid-October 2012 until end of January 2013 and then after a significant period of missing data, measurements continued from start of April until mid-August 2013. Additionally, having continuity in MeOH measurements was important as it served as a primary indicator of CH_4 from dairy and livestock sources as opposed to fugitive and/or urban sources. In order to comply with the assumptions of seasonality and similar meteorological conditions over a sampling period, and at the same time ensure minimal missing data of CH_4, CO (combustion / industrial tracer), N_2O and methanol, we decided to perform PMF analyses over seven distinct periods based on continuous times of consistent sets of tracers being available, and seasons. Table 4.1 lists the meteorological characteristics at WGC and a summary of the tracers included in the PMF analysis during each of these periods.

4.2.4   Positive Matrix Factorization (PMF)

The PMF technique is applied to the combined data set of greenhouse gases, CO and VOCs to apportion their contributions to major source categories influencing the WGC site. The fundamentals of the PMF technique have been explained in Chapter 2 (see Section 2.2.4), and are based on the principles laid out in relevant literature (Paatero and Tapper, 1994; Paatero, 1997; Comero et al., 2009; Ulbrich et al., 2009). PMF is a multivariate factor analysis tool that breaks down a dataset of speciated trace gas measurements into two matrices. The first matrix represents the factor profiles (**F**) or the mass fraction of each species in each factor while the second matrix contains the factor contributions (**G**) or the total mass contributed by each factor

at each time step in the data series. The PMF technique does not require assumption of any a priori information regarding the composition of source factors and does require the constraint of non-negativity of the factor solutions. In the recent past, PMF has been utilized to perform ambient source apportionment of organic aerosols (Ulbrich et al., 2009; Slowik et al., 2010; Williams et al., 2010) as well as VOCs (Brown et al., 2007; Bon et al., 2011; Yuan et al., 2012).

A customized software tool (PMF Evaluation Tool v2.06, PET) developed by Ulbrich et al. (2009) was used to perform the multivariate analysis. Time series of 13 tracers (two GHGs CH_4 and N_2O, CO and 10 VOCs) were initially combined into a unified data set. An account of the statistics on the year-long measurements of each of these tracers is listed in Table 4.1. A number of data preparation steps are involved prior to decomposing the unified data matrix into smaller periods based on our choice of PMF sampling periods. These steps have been explained in detail in Section 2.2.5 in the dissertation. The uncertainties (s_{ij}) were calculated and attributed to measurements of each tracer based on the guidelines set forth and discussed in Section 2.2.5 (Hopke, 2000; Comero et al., 2009; Williams et al., 2010). The data matrix (**X**) and the uncertainty matrix (**S**) are the main inputs into the PET model.

Backgrounds of GHG, CO and VOC tracers

Background concentrations were determined based on interpolated running 10 day 0.05 quantile curves for each tracer and subtracted from the mixing ratio time series to generate enhancements of individual VOCs at each hourly time stamp. For three tracers that had a relatively short life-time of the order of few hours or less, e.g. isoprene, methyl vinyl ketone plus methacrolein (MVK / MAC), and, monoterpenes, no background was assumed (0 ppt). All the other VOC tracers in the PMF study had variable season-dependent atmospheric lifetimes that range from a few days (e.g. toluene in summer) or longer and their backgrounds can be a significant percentage of the absolute mixing ratios (e.g. benzene in winter). CH_4, N_2O and CO, have longer lifetimes than the VOCs in this study and have background curves which either have a seasonality (like CH_4 and CO) and / or are steadily increasing with time (e.g. N_2O). The sources of CH_4, N_2O and CO are predominantly primary (not secondary production) and surface-based hence for these three tracers, the running 10 day 0.05 quantile curve at the upper measurement height (483 m a.g.l) was assumed as the background. The background-adjusted mixing ratio enhancements are used as the input data (x_{ij}) in the PMF data matrix allowing attribution of the variability of different tracers into mutually co-varying groups that provide unique source factors (factor profiles).

N_2O data was available at two inlet heights (91 m and 483 m a.g.l) with no measurements at the bottom-most level (30 m a.g.l). The variability in the hourly diurnal patterns, during different seasons, in CH_4, N_2O and CO enhancements at the middle (91 m a.g.l) and top (483 m a.g.l) inlet heights were found to be consistent and similar (Figures 4.5 a-d, 4.7 i-l and 4.5 e-h, respectively). We, thus, conclude that the variability of greenhouse gases and CO signals measured at the middle inlet height and its covariance with VOCs measured at 131 m a.g.l would be the same as that between interpolated fictitious greenhouse gas and CO concentration curves and VOCs measured at the 131 m a.g.l inlet height. The 91 m a.g.l inlet height was, thus, chosen as the optimum inlet for regional-scale PMF analysis. GHG and CO measurements from that height were paired with PTRMS-derived VOC measurements from the nearest inlet height (131 m a.g.l)

to create the unified GHG-VOC data matrix. This logical assumption is not expected to alter results from the PMF analysis. Past inverse dispersion studies at the Walnut Grove tower have utilized CH_4 and N_2O observations from the 91 m a.g.l inlet (Jeong et al., 2012 a,b). Coincident inverse analysis by the same research group is also underway. Our choice of 91 m.a.g.l inlet for PMF analysis will allow future comparison of results from concurrent inverse dispersion studies.

PMF factor number, rotations and error analysis

A detailed account of how to arrive at a user-defined optimal PMF solution, rotations of factors to generate factor profiles with higher degree of plausibility albeit at a higher "quality of fit" parameter Q value, and bootstrapping analysis to determine quantitative uncertainties of the chosen PMF solution is presented in Sections 2.2.6. We will avoid repeating those details here but instead summarize the overall procedures performed for each of the seven different PMF analyses. Specific results of these operations, if relevant, are reported in the description of the PMF results in Section 4.3.

PMF factor numbers (p) were explored from 1-8 for each PMF analysis to determine the optimal or "best explained" combination of factor profiles. Care was taken to avoid considering a p-factor solution where a clear splitting of an existing factor from a (p-1)-factor solution into two resulting factors was observed, such that the two factors in the p-factor solution had similar diurnal profiles and time series but with different constituents. At each p, different random starting points (SEEDs) were tested (from 1-10) to find the local minimum of a particular p-factor PMF solution (Paatero, 1997). This gave a better idea of the existence of additional "real" factors in the ultimate solution. The rotational ambiguity was explored using the FPEAK parameter that was varied from -1.0 to +1.0 at 0.2 unit increments without changing p to explore solutions which may present more physically realistic combinations of factor profiles (Paatero et al., 2002) as opposed to that in the base solution (at FPEAK = 0). It should be noted that there were a maximum of 13 tracers in certain PMF runs but when N_2O and/or MeOH were missing completely, these tracers were not included in the PMF analysis for that seasonal period, hence decreasing the actual number of included tracers (Table 4.1). This directly impacts the degrees of freedom in each successive higher p-factor solution. Such high p-factor solutions may have a significantly lower Q but may represent apportionment of individual tracers completely and exclusively to separate factors that does not make physical sense and defeats the purpose of performing PMF analysis. Hence, we are cautious in considering and accepting solutions at higher numbers of factors unless they make clear physical sense to the analyst and can be attributed to a source category.

Finally, bootstrapping analysis of the chosen p-factor solution was performed (Norris et al., 2008; Ulbrich et al., 2009) with 100 runs, in order to determine the standard deviations (1σ uncertainty) of the averaged mass fraction of each tracer in each factor profile.

4.4   Results and Discussion

4.4.1   Description of PMF source factors

In this sub-section, we present the composition of the different factors that result from the PMF analysis on seven individual sampling periods from June 2012 to Aug 2013 at WGC. The PMF source factors are statistical combinations of co-varying signal contributions and as such, covariance due to diurnal changes in vertical mixing and shifts in wind direction may result in contributions of coincidentally located sources being apportioned to the same source factor. This is also known as factor 'splitting' and 'mixing' and has been discussed in Section 2.2.6 in Chapter 2. Our choice of source factor nomenclature reflects our interpretation of the dominant source contributions to the composition of each factor resulting from VOC source marker evaluation, comparison of relative emission rates and diurnal trends. The factors reveal a break-down of the major CH_4 and N_2O source categories that can be deconstructed from the input data matrix on the basis of the input uncertainties ascribed to each data value in the time series.

For each sampling period related to a particular season, we identify the number of factors in the 'best case' PMF solution based on the guidelines in Section 2.2.6. In the following paragraphs, we list and describe all the source factors that make up the factor profiles resulting from one or multiple PMF analyses. The specific factor profiles resulting from the apportionment of each unique seasonal PMF run are shown in Figures 4.8, 4.10, 4.12, 4.14, 4.16, 4.18, and 4.20.

Dairy and Livestock emissions

This source factor is represented in all plots and figures in orange color. The major contributors to this factor are CH_4 and N_2O (whenever included in the PMF analysis). This factor contains some contributions from oxygenated VOCs like methanol, acetaldehyde, acetone + propanal and MEK in seasonally varying proportions over the seven PMF periods. These VOCs have been reported to be emitted from various processes within dairy and feedlot operations in significant quantities (Filipy et al., 2006; Shaw et al., 2007; Ngwabie et al., 2008; Chung et al., 2010). The presence of methanol in this factor points to the essentially biological origin of emissions from this source as opposed to a combustion / fugitive source. This source factor is a minor contributor to the enhancements of the included aromatics (benzene and toluene) and combustion tracer CO. The minor contributions of aromatics to this source have been detected in all the above-mentioned studies. The m/z 93 can also potentially be a fragment from monoterpenes as opposed to toluene. The CO can also result from the large-scale industrialized nature of dairy agriculture in the Central Valley where a lot of commercial motor-driven equipment is used. The MeOH / CH_4 (mmol mol^{-1}) relative emission rates (ER) derived from different seasonal 'dairy and livestock' factor profiles in this study range from 3.4 to 9.3. This is in general agreement with emission rates reported from dairy and feedlot studies in Table 2.4 in Chapter 2. Particularly, our range of observed emission rates show conformity with cow chamber studies (Shaw et al., 2007), regression slopes from dairy plumes measured by aircraft (Gentner et al., 2014) and the lower end of slopes observed in flights over the Central Valley in Figure 3.12b in Chapter 3. The N_2O / CH_4 emission rate range of 2.8 – 12.8 (mmol mol^{-1}) over four different

seasonal PMF periods in this study is similar to that of the dairy and livestock factor in the PMF analysis at Bakersfield of 5.5 mmol mol^{-1} (Chapter 2). Hence, we demonstrate that the principal contributor to the orange factor is emissions from intensive dairy and livestock operations surrounding WGC and CH_4 and N_2O are the principal constituents of this source factor.

Urban and Oil & Gas emissions

This source factor is represented in black color in all factor profiles and diurnal distribution plots. This source factor is by far the dominant source of CO and aromatics like benzene and toluene. This suggests that the sources contributing to this factor have an imprint of combustion-related emissions. The rural location of WGC and absence of any major highways immediately upwind of the site suggests that these emissions are not dominated by a local vehicle combustion source. This can also be deduced from the toluene to benzene molar ratios reported in Table 4.2 which is used as an indicator of traffic emissions. A range of 1.5 to 4.3 (mol mol^{-1}) has been suggested as typical emission ratios of toluene to benzene from fresh plumes in various urban environments (Warneke et al., 2007; Baker et al., 2008; Liu et al., 2009; Bon et al., 2011; Borbon et al., 2013; Lan and Minh, 2013). Photochemical aging of a fresh plume depletes emitted toluene faster than benzene owing to the difference in their OH radical rate constants, the OH removal process being the principal atmospheric loss mechanism for these aromatics (Gelencsér et al., 1997; Warneke et al., 2007). Hence, toluene / benzene ratios are expected to decrease with time (distance) from the source and consequently, be lower in rural environments than in urban environments as seen in a study conducted at multiple urban and rural sites located unique traffic-equivalent distances (hours) apart (Gelencsér et al., 1997). The range of toluene / benzene ratios we observe in this PMF factor is $0.4 - 1.1$ (with lower end of the ratios during winters) which is significantly less than typical urban emission ratios and gasoline-speciation profiles observed in Table 4.2. This indicates that a significant contribution to aromatics and CO attributed to this factor may be emitted from sources in the upwind urban regions in the outer San Francisco Bay Area that get photochemically depleted (more toluene depletion versus benzene depletion) as they arrive at WGC and hence the difference in the observed emission rates. The factor profile has some mass apportioned to CH_4 and this could originate from a multitude of sources including the O&G refineries in the North Bay area (< 60 km from WGC), a couple of landfills, fugitive emissions from urban natural gas pipeline distribution network etc..

The largest natural gas producing field in California, Rio Vista, is located about 15 - 25 km south-west of WGC. It is possible that the emissions contributing to this factor are predominantly from industrial operations in this field and the associated CH_4 is due to fugitive losses. A large enhancement of CH_4 (up to 120 ppb) was observed while flying over this field during the CABERNET campaign (Section 3.2.2 in Chapter 3) pointing to fugitive emissions that could very well be responsible for the CH_4 apportioned to this factor. Additionally, no N_2O is present in the chemical profile in even minor fractions which adds weight to the possibility of the 'black' factor being dominantly an Oil and Gas fugitive + combustion source. In a measurement study of VOCs and CH_4 in 43 Chinese cities, significantly higher CH_4 mixing ratios were observed in 15 cities where toluene / benzene ratios were < 1 (mol mol^{-1}) and not typical of the 10 "traffic-related cities" where the ER was ~ 1.7 or higher (Barletta et al., 2005). Additionally, the abundance of light alkane fraction of ethane (associated with natural gas leakage), relative to other hydrocarbons, was significantly higher in these 15 cities. This suggests that fugitive CH_4

emissions along with VOC emissions from related natural gas extraction process at the Rio Vista field is likely to have lower toluene / benzene ratios in line with our observations in this factor. In the absence of measurements of light alkanes, it is difficult to verify and validate the exact source / origin of the emissions contributing to this factor. Lower toluene / benzene ratios (< 1) have also been reported from biofuel / wood burning (~ 0.58), forest fires and agricultural residue burning (~ 0.82) (Andreae and Merlet, 2001; Jordan et al., 2009). Since upwind emissions plumes from the Bay Area will always flow over the gas field and croplands before arriving at WGC, we conclude it is best to define this source factor as a combination of fugitive / combustion emissions from the urban core and the O&G sector.

Secondary production of acetaldehyde from photo-oxidation of light alkanes is the largest global source of acetaldehyde (Millet et al., 2009) and a minor source of acetone (Goldstein and Schade, 2000; Schade and Goldstein, 2006; Hu et al., 2013). Urban / O&G plumes are likely to contain light alkanes emissions and hence, expectedly, we see acetaldehyde and some acetone apportioning on to this factor. This source factor also contains some contributions of m/z 42 which are potentially alkanes emitted into the polluted plumes arriving at WGC. In winters, this factor sees some anthropogenic contributions on masses that have traditionally dominant biogenic contributions in summers. Some m/z 69, which is predominantly isoprene in summers, apportions on to this factor. These are mostly contributions from pentadienes and cyclopentenes which are by-products in petroleum industry plumes. Similarly, m/z 137 contribution during winters is from known anthropogenic monoterpenes while m/z 71 potentially sees contributions from refinery by-products like pentenes and 2-methyl-2-butene. No methanol is apportioned to this factor in any seasonal PMF analysis.

Primary Biogenics and Secondary Organics

This source factor is one of the three that is produced in all of the seven PMF evaluations and is shown in green color in all plots. This source factor is the dominant contributor of oxygenated VOCs all of which have major primary biogenic and secondary photochemical sources surrounding WGC. This includes methanol (Baker et al., 2001; Schade and Goldstein, 2001, 2006; Harley et al., 2007; Hu et al., 2011), acetaldehyde (Kesselmeier and Staudt, 1999; Karl et al., 2002), acetone (Kirstine et al., 1998; Goldstein and Schade, 2000; Hu et al., 2013) and methyl ethyl ketone (Kirstine et al., 1998; de Gouw et al., 1999). A number of studies have reported significant fluxes of these compounds from Central Valley agriculture (Fares et al., 2011, 2012; Park et al., 2013). The diurnal profiles of these oxygenated VOCs (Figure 4.6) are generally consistent with that from year-round measurements at a largely rural site in New Hampshire (Jordan et al., 2009). The vertical profiles in Figure 4.6 and diurnal cycle in Figure 4.15c indicates that these compounds are predominantly produced from local ground-based sources with maximum emissions during daytime. As mentioned in Section 4.2.1, the region surrounding WGC is predominantly farm land with a variety of cultivated crops. Primary biogenic VOC emissions from nearby agriculture reach a maximum during the day. Secondary VOCs produced from surrounding biogenic precursor sources are primarily photochemically-driven so would also peak during daytime. Prevailing daytime winds arriving at WGC contain a combination of these two above-mentioned categories of emissions (Figure 4.6). There is no noticeable apportionment of CO, aromatics and acetonitrile to the factor profile and this confirms the majorly biogenic nature of the sources influencing this factor. There is no CH_4 and N_2O

(except in summer 2013 PMF; Section 4.3.2 and explained later) apportioned to this factor. This is an expected outcome, based on our knowledge of CH_4 and N_2O emissions sources.

The rise and decline of the peak enhancements at the measurement height (131 m a.g.l) occur at slightly different times for different oxygenated VOCs e.g. the peak of methanol during summers (Figure 4.6 a) occurs at 1100 PST, which is one hour after the peak occurs for acetaldehyde (Figure 4.6 e) but a couple of hours before peak concentrations are achieved for acetone (Figure 4.6 i). Different emission mechanisms and biological triggers within the plant system have been previously proposed. For instance, large methanol emissions result from leaves controlled by opening and closing of the stomata (Harley et al., 2007; Hüve et al., 2007), higher methanol emissions occur due to pectin-hardening during stages of rapid plant growth (Galbally and Kirstine, 2002; Hüve et al., 2007) in late spring/early summer, acetaldehyde is released throughout the day in forest canopies under varying light conditions (Karl et al., 2002), while MEK is the largest VOC released from grass and clover pastures (Kirstine et al., 1998) located farther from the site compared to crop lands (Figure 4.1) followed by methanol and acetone. Acetone can be emitted from primary biogenic emissions that are light and temperature dependent and simultaneously occur from photochemical production thus peaking in mid to late summer time (Hu et al., 2013; Jacob et al., 2002; Schade and Goldstein, 2006). The apportionment through PMF analysis is based on simultaneous linear covariance of enhancements. At WGC, differences in release mechanisms of the oxygenated VOCs from their biogenic sources and photochemical reaction rates lead to staggering of diurnal timelines. In spite of this, the collective similarity in the non-linear enhancement features in the diurnal profiles result in major portions of oxygenated VOC signals being apportioned to a common source factor which we describe as 'Primary Biogenics and Secondary Organics'.

Even during winters, agricultural residues in the post-harvested fields, and potential double cropping may result in some biogenic emissions that lead to this factor appearing in the PMF analysis even as other biogenic / agriculture related factors are not identified (Figure 4.12).

Agriculture + Soil Management + Delta emissions

This source factor is represented in purple color in all factor profile and PMF diurnal distribution plots. This factor is a major contributor to N_2O enhancements in all seasonal PMF runs where N_2O is measured and included. In addition, most of the monoterpene emissions (*m/z* 137) are attributed to this factor along with minor contributions of oxygenated VOCs (OVOCs), isoprene and MVK / MAC, all of which have mostly biogenic sources around WGC. A similar factor was observed in the PMF analysis at Bakersfield (Section 2.3.2 and Figure 2.7 in Chapter 2). In this source factor, we principally see microbially-mediated soil emissions of N_2O arising from preceding use of synthetic and organic fertilizers on nearby agricultural farmlands that include corn, a variety of fruits and vegetables and large swaths of rice agriculture (~ 100 km from WGC), all of which require N fertilizer input (van Groenigen et al., 2010; Hoben et al., 2011; Linquist et al., 2012; Rosenstock et al., 2013). As discussed later in Section 4.3.2, N_2O signal apportioned to this factor varies seasonally and depends on the annual cycle of agriculture and corresponding use of fertilizers. Collocated with the N_2O emissions are minor contributions from agricultural crops. The emissions of N_2O are primary in nature and result in minor enhancements above a large tropospheric background. The diurnal profile is mostly governed by

day time dilution in an increasing volume of the expanding boundary layer followed by accumulation of emissions in the shrinking boundary layer and night time inversion (Figure 4.7 i-l). The emissions of OVOCs from crops, on the other hand, are dependent on various factors with a major exponential dependence on temperature (and in some cases light) and vary non-linearly. Hence the majority of crop OVOC emissions get apportioned to the 'green' factor profile (**F**) with exponentially varying factor contributions (**G**) in the time series. In addition to this, minor contributions of primary OVOCs co-vary with collocated emissions due to boundary layer dynamics rather than temperature and light dependence. These contributions, mostly minor, also help explain the reconstructed PMF time series and get apportioned to the 'purple' factor. This 'purple' factor would contain other similarly varying tracers in the air parcels that arrive at WGC simultaneously e.g. coincident emissions of N_2O and monoterpenes. Biogenics like monoterpenes (*m/z* 137) are emitted from crops and have a diurnal profile, which is different from other oxygenated VOCs (explained in the next section). Its diurnal profile is, however, similar to that of N_2O and a major proportion of the monoterpene enhancements are apportioned to this source category.

This source factor also contains some contributions from *m/z* 93 which is calibrated to toluene in this experiment. The *m/z* 93 diurnal profile (named toluene in Figure 4.5 m) is similar to that of N_2O (Figure 4.7 i) and monoterpenes (Figure 4.7 m) during the summer season. The diurnal profile of benzene (Figures 4.5 i-l) and CO (Figures 4.5 e-h) are similar to each other in all seasons. But a comparison with seasonal diurnal profiles of toluene (Figure 4.5 m-p) reveals that in the summer season, the diurnal profile of toluene is quite different. This points to an additional summertime source of toluene (or another VOC detected on *m/z* 93) that masks the general expected profile of toluene similar to that of benzene and CO if they had completely similar emissions sources. This additional enhancement is coming from the 'purple' source factor. Similar observations at a rural site in New Hampshire have been observed for summertime toluene and local vegetative emissions have been estimated to have a significant contribution to the enhancements (White et al., 2008). Some methanol also gets apportioned to this factor. Methanol, monoterpenes and toluene emissions from corn and corn harvesting has been reported to be significant (Graus et al., 2013) with some minor emissions of benzene. Methanol and monoterpenes are also emitted in significant quantities during harvesting of managed grasslands (Ruuskanen et al., 2011). The region around WGC has a lot of corn plantations and large areas at the edge of the Delta are managed grasslands and pastures (Figure 4.1). The literature on the emissions of the above-mentioned VOCs conforms well to our observed chemical apportionment of this factor. Monoterpenes are stored by plants in storage pools and are released in large amounts during damage and stress (like during harvesting and early growth). We find that mass fraction of monoterpenes attributed to this factor is significantly larger in the PMF apportionments during early fall and late fall seasons (Figures 4.8 and 4.10), which coincide with the harvesting season and also during early spring (Figure 4.14), which coincides with the planting season. This reaffirms the agricultural origin of this source factor.

A small mass fraction of CH_4 is apportioned to this factor. Most of the upwind regions around WGC are part of the Sacramento – San Joaquin Delta and as such, contain large tracts of lands that are periodically flooded and drained like peatland pastures, natural and restored wetlands, and some rice agriculture (Figure 4.1). This land cover is ubiquitous and coterminous

with agricultural farm lands and as such, any greenhouse gas and VOC emissions from the two above mentioned land-types is coincident in the plumes arriving at WGC. If the diurnal profile of these emissions is essentially controlled by boundary layer dynamics and meteorology, these emissions will be attributed to a common factor even though they may represent separate source categories. CH_4 (as well as N_2O) fluxes have been reported from a variety of flooded / drained ecosystems in the Delta like restored wetlands, peatland pastures and rice cultivation (Teh et al., 2011; Hatala et al., 2012; Knox et al., 2014). Hence, we explain the origin of the methane attributed to this factor as that coming from anaerobic mechanisms (both man-made and natural) in the Delta region around WGC. We understand that this factor is influenced by an aggregation of these collocated sources and best represented by a statistical combination of their contributions as a unique factor in the PMF analysis and we therefore define this source factor as 'Agriculture + Soil management + Delta'.

Fresh Isoprene emissions

This factor is highly seasonal, and is observed as an output of PMF analysis in the late spring, summer and early fall. This factor is represented in 'light blue' color in the plots. This factor mostly contains fresh isoprene emissions with minor contributions from oxygenated VOCs. The diurnal profile of isoprene has a peak during the day and the concentrations reach a low during the evenings and stay close to being negligible before beginning to rise in the morning again as seen in the diurnal profile plots for isoprene (Figures 4.7 a-d). Isoprene comprises a third of annual global VOC emissions from all natural and anthropogenic sources with > 90% of the emissions coming from terrestrial plant foliage (Guenther et al., 2006). Isoprene is mostly emitted by chloroplasts as a function of light and temperature (Steeghs et al., 2004). Hence its emissions occur during the day and stop at night. Isoprene has a short lifetime (~ 1 h), as compared to some of the other coincident OVOCs, the reaction with OH radicals being its principal sink. Due to differences in emission sources and loss processes such as chemical reactions, advection, and vertical dilution, isoprene almost exclusively gets apportioned to its own PMF factor. Emissions of isoprene are much higher in the summer time as compared to winter and early spring and hence this factor is not produced in those respective PMF runs. There is no CH_4 and N_2O attributed to this factor.

Monoterpenes (Figure 4.7 m-p) have a different diurnal profile than isoprene with peak concentrations occurring in the night time / early morning and daytime minima. This is also observed in forest environments and rural agricultural locations alike (Bouvier-Brown et al., 2009; Jordan et al., 2009; McKinney et al., 2011). Monoterpene emissions from surrounding tree crops (and nearby deciduous forests) and grasses are primarily a function of temperature (from stored pools within resin ducts) and not light. During the summer and fall, monoterpene emissions during the night time are enhanced due to warmer night time temperatures resulting in continued emissions that are now able to build up in a shallow boundary layer and under suppressed removal by OH, O_3 and NO_3 mechanisms.

Isoprene oxidation products

This source factor is represented in 'navy blue' color in the PMF-related plots. This factor principally contains methyl vinyl ketone (MVK) and methacrolein (MAC) (measured as a sum

by PTR-MS), which are atmospheric oxidation products of isoprene. Hence, this factor is closely associated with the 'fresh isoprene' factor and shows up in the PMF apportionment only when isoprene emissions are significant, which occurs in the summer season only. The diurnal profile of MVK and MAC follows and lags behind the isoprene diurnal profile reaching peak concentrations around 1800 PST. A visual analysis of the observed diurnal concentration plots (Figures 4.7 e-h) reveal that a part of the MVK / MAC signal directly results from oxidation of locally emitted isoprene at the ground level while another part of the signal measured at 131 m a.g.l at WGC is a result of entrainment of advected MVK / MAC from upper levels at WGC (see Figure 4.7 e). This MVK / MAC prevalent at the upper levels of WGC is contained in biogenic plumes in the easterly downslope winds blowing from the oak forests along the foothills in the Sierra Nevada mountain range to the east of the site (Misztal et al., 2014). No observable CH_4 or N_2O is apportioned to this source factor or observed at the upper levels in the diurnal profiles of CH_4 (Figures 4.5 a-d) or N_2O (Figures 4.7 i-l). Hence it is clear that the biogenic plumes from the forested regions in the foothills do not have any CH_4 or N_2O imprint.

4.4.2   Seasonal PMF results

We herein present the relative strength of CH_4 and N_2O sources in the region as determined using PMF. One of the objectives of this analysis is to investigate the seasonal distribution of the relative contributions of major greenhouse gas sources over a complete annual cycle. We present the diurnal profiles of CH_4 and N_2O enhancements apportioned by source strength for each seasonal PMF analysis and discuss the reasons behind the variability in the relative source strengths between seasons, if observed. As will be seen in the seasonal absolute concentration diurnal plots, both CH_4 and N_2O mixing ratios have a diurnal pattern resulting from primary sources that emit into an expanding boundary layer during the day time as atmospheric mixing increases, followed by a shallow boundary layer in stable atmospheric conditions during the nighttime. Observed absolute concentrations are lower in the summertime as boundary layers are deeper and while wintertime concentrations are higher due to a shallower boundary layer. From the visual analysis of the source-apportioned relative diurnal distribution plots accompanying the absolute diurnal plots for each season, we do not observe a rectifier effect forcing of boundary layer dynamics on the PMF apportionment of CH_4 and N_2O enhancements as is typically observed in the correlation between diurnal / seasonal boundary layer dynamics and ecosystems CO_2 fluxes. The relative contributions of a source to CH_4 and N_2O enhancements is driven majorly by relative strengths of emissions sources in different seasons and meteorology (e.g. high westerly winds in summers versus low along-valley winds in winters).

The GHG and VOC measurements were conducted over a complete annual cycle from mid-2012 to mid-2013 with data from the summers of 2012 and 2013 analyzed separately. Since, we do not have N_2O measurements during summer 2012 (measurements of N_2O only begin in mid-Oct), we consider the PMF apportionment during summer of 2013 to complete the annual cycle that begins in early Fall 2012. We do include the PMF analysis results from summer of 2012 in order to compare CH_4 apportionment results from two consecutive summers and to evaluate any anomalies, if present.

Early Fall 2012 (Sep 1 – Oct 15)

A 6-factor solution is able to optimally describe the apportionment of GHGs and VOCs during the first half of fall 2012 as shown in Figure 4.8. N_2O was not measured during this period. Most of the CH_4 (~ 55 - 80 %) is apportioned to the 'dairy and livestock' source depending on the time of day as seen in the PMF diurnal distribution plots in Figures 4.9 a and c. The diurnal profile of reconstructed CH_4 resembles that of emissions with primary sources whose concentrations vary with boundary layer depth and vertical mixing. The 'urban and oil/gas' source is responsible for about 15 to 30 % of the daily enhancements. It should be noted that both daytime and nighttime winds (Figures 4.2 b and 4.3 b) are predominantly arriving from the west-southwest. This is expected to increase the influence of sources upwind of WGC, namely the urban core of San Francisco Bay Area and Rio Vista gas fields. The proportion of CH_4 apportioned to the 'urban and oil/gas' source is less in the later seasons when winds are more multi-directional (Figure 4.13 c). A minor contribution to the CH_4 enhancements (5 - 15 %) is also observed from the 'ag soil and delta' source factor. Temperatures during this season are fairly warm and the emissions of CH_4 from wetlands / peatlands (and possibly rice agriculture) can certainly contribute to the CH_4 observed in this factor. As is seen later in the PMF plots for seasons where N_2O is included in the analysis (e.g. 4.10 d), this source is a significant contributor to N_2O enhancements. Most of the monoterpenes, which are essentially biogenic in nature (Bouvier-Brown et al., 2009) are attributed to this factor. Monoterpenes have been reported to be emitted in significant quantities during the harvesting season (Ruuskanen et al., 2011; Graus et al., 2013) and this confirms the agriculture origin of this source. We distinguish this factor from the 'primary biogenics and secondary organics' source by including the PMF-based source wise diurnal distribution of methanol (in Figure 4.9 b). This figure shows that the majority of emissions for methanol and oxygenated VOCs, which mostly apportion on to this source, peak during day time. This is in contrast with the 'ag + soil + delta' diurnal profile (also shown in Figures 4.15 c-d) even though these sources are probably collocated. The multi-source apportionment of methanol in Figure 4.9 b shows that PMF can distinguish between different sources having varied influence on the measured signal depending on factors like timing of active source mechanisms, advection, meteorology etc.

In summary, three sources of CH_4 are identified in the fall 2012 PMF sampling period with 'dairies and livestock' as the dominant source, followed by the 'urban and oil / gas' source and a minor contribution from the 'ag + soil management + delta' source.

Late Fall 2012 (Oct 16 – Nov 30)

The apportionment of the latter half of the fall 2012 season can be best explained by a 4-factor solution (Figure 4.10). As compared to the period preceding it (early fall 2012), temperatures drop significantly (Table 4.1) and hence the isoprene emissions decrease substantially to the extent that a separate source factor containing fresh isoprene emissions is not reproduced in the PMF analysis for this period. Consequently, there is no 'isoprene oxidation products' factor either in the solution. During this period, N_2O was also measured at WGC. CH_4 is apportioned to two factors: the 'dairy and livestock' source which accounts for ~ 65 - 80% of the daily variation and the 'urban and oil/gas' source which accounts for ~ 20 - 35 % of the

observed enhancements (Figures 4.11 a and c). As opposed to early fall, there is no contribution to CH_4 enhancements from the 'ag soil and delta' source factor. This is most likely due to cooler temperatures during this period (Table 4.1) as average highs drop by about 8°C as compared to early fall season thus reducing production of CH_4 from wetland and drained agricultural systems in the Delta (Baldocchi et al., 2012; Hatala et al., 2012; Knox et al., 2014). Dairy and livestock operations, on the other hand, are a year round activity and even though CH_4 emissions from manure management may be reduced during this relatively cooler period, the overall CH_4 enhancements resulting from this sector remain high and the dominant contributor to the CH_4 apportionment in the absence of other competing sources. Winds are more variable in this period (Figures 4.2 c and 4.3 c) and the contributions from local sources may be more important. This suggests that the 'urban and oil / gas' factor may contain significant contributions from the nearby Rio Vista gas field.

For N_2O, we observe that the 'dairy and livestock' sector are the largest contributor to N_2O emissions accounting for ~ 80 % of the total daily enhancements (Figures 4.11 b and d). The remaining N_2O (~ 20 %) is mostly attributed to the 'agriculture' source factor, which is also the main source for monoterpene emissions, possibly resulting from the vast harvesting activity during this season. It is important to recognize that the relative amounts of these two sources will differ regionally, and may not be the same in the northern and southern ends of the Central Valley due to the relative distributions of dairy / livestock / fertilizer use. The N_2O apportionment to the 'dairy and livestock' sector is somewhat higher than the proportion of N_2O attributed to the dairy source in Bakersfield in Chapter 2 (Figure 2.11). In this case, this is likely due to less fertilizer input as the agricultural season winds down (Oct - Nov) which would significantly decrease the N_2O emissions resulting from and attributed to the agricultural sector, as compared to the relatively unchanging N_2O emissions from manure management in the dairy sector. By that logic, we expect the proportion of N_2O to be higher during the growing season and we visit this hypothesis in the later sections.

Winter / Wet season (Dec 1, 2012 – Jan 29, 2013)

During the winter season, a 3-factor PMF solution (Figure 4.12) is most suitable to describe the apportionment of CH_4 and N_2O (Figures 4.13 a-d). In the winters, there is substantially less active agriculture in the region as most of the crops have been harvested in the fall. This means that fertilizer use and subsequent N_2O emissions from crop agriculture should be negligible. Additionally, low temperatures in the inland Central Valley (Table 4.1) means that microbially mediated CH_4 emissions from wetlands and peatland pastures should be low too and possibly below the level of detection within the framework of input uncertainties. These assumptions are validated in the PMF solution as it does not reproduce the 'agriculture + soil management + delta' source factor from the previous period. The CH_4 enhancements (Figures 4.13 a and c) are predominantly attributed to the 'dairy and livestock' source which accounts for ~ 90 % of the enhancements with about 10 % of the emissions coming from the 'urban and oil / gas' source. This is a reasonable outcome as the dominant wind direction during the winters is along the floor of the Central Valley (northwest and southeast) as seen in Figures 4.2 d and 4.3 d. The prevailing winds causes the densely concentrated dairy and feedlot complex in the San Joaquin County (to the southeast of the site) to become directly upwind of the site for majority of this period. The above-mentioned reason coupled with reduced or almost absent contributions from agriculture

related N_2O emissions causes the observed N_2O enhancements to be almost exclusively attributed to the dairy and livestock sector (Figures 4.13 b and d). A very tiny (< 5 %) of the emissions are attributed to the 'biogenics' factor and this may be related to precipitation-driven N_2O release from left-over soil N on fallow crop lands in the post-harvesting period or a small amount of ongoing regional agricultural activity, although this contribution is well-within the bounds of uncertainties ascribed to the N_2O data.

Late Winter / early Spring season 2013 (Feb 15 – Apr 5)

The source apportionment during late winter and early spring period is best described by a 4-factor PMF solution for this period (Figure 4.14) which resembles a similar factor solution observed during the late fall period (Figure 4.10) with the exception that N_2O was missing from the input data set during this period. The diurnal plots of the scaled factor mass distribution (Figures 4.15 a-d) give a glimpse into the differences in the diurnal patterns which PMF analysis is able to suitably resolve. We observe that even though the 'dairy and livestock', 'urban and oil / gas' and the 'agriculture and delta-related' sources have early morning peaks in concentrations followed by day time lows (Figure 4.15 a, b and d, respectively), there are finer differences in their diurnal profiles (like timing of peaks and lows), which allow the PMF tool to analyze and resolve these non-covarying features in the time series, and apportion combinations of tracers with similar features into distinct factors. Also, the 'primary biogenics and secondary organics' source has peak concentrations during the early afternoon period coincident with periods of highest temperature and sunlight received (Figure 4.15 c) and this reaffirms our understanding of the biogenic origin of this source factor.

The bulk of the CH_4 (~ 60 - 70 %) enhancements are attributed to the 'dairy and livestock' source while smaller contributions are observed from the 'urban and oil / gas' source (~ 20 %) and the 'ag soil management + delta' source (15 - 25 %) in Figures 4.15 e-f. Higher daily temperatures during this period compared to the immediately preceding winter period (Table 4.1) results in an increase in anaerobic activity of microbes in the Delta wetlands (Miller, 2011). It should be noted that the % contribution from the 'ag + delta' source to the CH_4 apportionment (Figure 4.15 e) is somewhat larger than that observed from the same source in early fall 2012 (4.9 c). This cannot be reasonably explained on the basis of average ambient temperatures as temperatures in this period are cooler than that observed in early fall 2012 (Table 4.1). Drainage of agricultural fields (including rice paddy) in preparation for new plantings has been reported to be responsible for large releases of CH_4 (Hatala et al., 2012; Knox et al., 2014). In this season, the dominant day time wind direction is from the northwest (Figure 4.2 e) where 90% of California's rice crop is grown in the upwind Sacramento Valley This is the season when large amounts of flooded rice paddy fields with huge amounts of plant residue are drained before seeds of the new crop are sown, and this could be responsible for the CH_4 seen in this 'ag + delta' source factor. Drainage of water-logged fields (from the rainy season) containing agricultural residues in the Delta, in preparation for the growing season can also lead to CH_4 emissions that apportion to this source.

Spring 2013 (Apr 6 – May 31)

The PMF analysis during the spring season results in a 5-factor solution with an additional factor related to 'isoprene and oxidation products' being produced in this seasonal period (Figure 4.16) as compared to the winter / spring 2013 period (Figure 4.14). This is primarily due to significantly warmer temperatures in this period along with greater sunlight input which increases isoprene emissions from vegetation surrounding WGC. Isoprene and its oxidation products, apportion into their own factor owing to a sharp diurnal cycle resulting from their different source distribution as compared to other oxygenated VOCs.

The majority of the CH_4 signals, ~ 70 %, are apportioned to the 'dairy and livestock' factor (Figure 4.17 c), with about 10 to 15 % of the enhancements apportioned to the 'urban and oil / gas' source factor. Contributions from the 'ag + soil management + delta' source factor to the CH_4 enhancements remain relatively high at 20 – 25 % and this conforms with increasing CH_4 emissions from wetland ecosystems in Delta (Figure 6; Knox et al., 2014). The CH_4 fluxes observed from these wetland ecosystems during the spring and summer season (Knox et al., 2014) are on the same scale as that reported from the airborne flux measurements over the dairy intensive regions in the Central Valley in the CABERNET study (Table 3.2; Chapter 3). This indicates there are significant natural and anthropogenic (managed lands) sources of CH_4 in the Delta with predominantly microbially-mediated emission pathways that are more active in warmer temperature regimes with saturated soil conditions. As also indicated by the wind rose plots (Figure 4.2 f and 4.3 f), there is a marked change in mesoscale meteorology in this season as the up and down valley flow pattern gives way to land-sea breezes and the prevailing wind direction is more westerly (Zhong et al., 2004; Bao et al., 2007). This should increase the influence of the 'urban and oil / gas' factor on the CH_4 signals given their upwind location. We do not, however, observe any increase in the CH_4 apportionment to this factor, possibly due to simultaneous and larger input from CH_4 emissions occurring in the Delta ecosystem which masks the influence of the 'urban + oil/gas' source on CH_4 apportionment.

There is a significant difference in N_2O source apportionment in the spring season (Figures. 4.17 b and d) as compared to the late fall (Figures. 4.11 b and d) and winter season (Figures 4.13 b and d). In this season, the 'agriculture + soil management + Delta' source factor is the overwhelming contributor to the N_2O enhancements (~ 80 %) with the 'dairy and livestock' sector accounting for the rest. This is in sharp contrast with the apportionment in the above-mentioned seasons when the 'dairy and livestock' sector was the dominant source of N_2O emissions. By reasonable logic, manure management practices that are the principal source of N_2O from dairies are not expected to widely vary over the annual cycle. Additionally, CH_4 emissions from dairies are relatively unchanged over the course of the year and this indicates that dairies and feedlots generally operate in the same manner through the annual cycle. Hence, the higher proportion of N_2O enhancements from the 'ag + soil management' factor can be attributed to a tremendous increase in emissions from this sector. Most of the inorganic / organic fertilizer and animal manure application to the farms take place early in the growing season that can range from Mar -Apr (for rice) to May-Jun (for corn and other crops). Hence major N_2O emissions can be expected in these months as the fields are flooded and irrigated which acts as a trigger for subsequent denitrification and N_2O emissions (Rosenstock et al., 2013). Thus, we note that N_2O emissions from the 'ag + soil management' sector show a strong pattern of seasonality with

much higher contribution to the apportionment of the measured signals during the spring (and as we see later, in the summer season) as opposed to the end of the growing season (in late fall) or winter when application of N fertilizer for agriculture is at its minimum in California.

Figure 4.17 e indicates that most of the methanol emissions in the spring season arise from 'biogenic and secondary' sources far outweighing the contribution from the 'dairy and livestock' sector. This is consistent with literature on biogenic methanol emissions which point to springtime pectin biosynthesis during plant and leaf growth as a principal methanol source (Galbally and Kirstine, 2002; Karl, 2003; Schade and Goldstein, 2006). The exponential variance of methanol emissions with temperature (Harley et al., 2007) during the spring and summer months seen in this work agree well with the trends observed in a similar year-round tall-tower measurement at a semi-rural site (Hu et al., 2011) and previous studies in California (Schade and Goldstein, 2006). The lack of CH_4, in this source factor, though not surprising, is a confirmation that there are major plant biogenic sources of methanol that do not contribute any methane.

Summer 2013 (Jun 1 – Aug 4)

The factor profiles in the 6-factor PMF solution for the summer 2013 season are represented in Figure 4.18. The 'dairy and livestock', 'urban and oil / gas', and 'agriculture + soil management + delta' source factors look similar in composition to the same factors from the preceding spring analysis (Figure 4.16). In terms of source wise apportionment, a majority of CH_4 emissions are still apportioned to the 'dairy' factor ($\sim 55 - 70$ %) even though its relative share is reduced, while the delta-related CH_4 emissions are responsible for about 20 - 40 % of the observed enhancements (Figure 4.19 c) which is the maximum amongst all the PMF sampling periods for this source. This can be partly due to wind directions as winds are primarily westerly and south-westerly during the summer season (Figures 4.2 g and 4.3 g) and this makes WGC directly downwind of the Delta region. The major reason is most probably increased CH_4 emissions from wetlands, peatlands and rice cultivation in the upwind Delta. The contributions from wetland and flooded agricultural systems scale with temperature and hence peak during the summers (Hatala et al., 2012; Knox et al., 2014). We observe that the source contribution of the 'ag + soil + delta' factor to the apportionment of CH_4 signals peaks during this season and then decreases in the early fall season as ambient temperatures drop (Figure 4.9 c) before reducing to undetectable proportions in the late fall (Figure 4.11 c) and winter season (Figure 4.13 c). Contributions from urban and oil / gas sources remain about 10 %.

The bulk of the N_2O signal is apportioned to the 'agriculture-related' source factor (Figures 4.19 b and d). In this analysis, we observe the 'splitting of factors' phenomena explained in Section 2.2.6 in Chapter 2. A portion of the N_2O enhancements gets apportioned to the 'biogenics' and the 'isoprene' factors. A 'splitting' phenomena is likely to be observed in high-factor solutions with less degrees of freedom (total included species in the data set) when contributions from collocated sources may get apportioned between each other. It should be noted that both the 'biogenics' and the 'isoprene' factor are originating from natural plants and non-woody and woody crops being grown on agricultural farmlands in the Delta in the vicinity of WGC. These farm lands are the major source of soil emissions of N_2O being apportioned to the 'ag soil management + delta' factor. Hence the total contribution of the agriculture-related N_2O emissions to the observed enhancements should be looked upon as the sum of the

contributions of the three above-mentioned factors which amounts to 80 - 90% with the rest being attributed to the 'dairy and livestock' factor. The current N_2O source apportionment, along with a similar apportionment in the spring season, underlines the importance of fertilizer-related emissions of N_2O from the agricultural sector during the growing season (Apr – Oct). We do not have N_2O measurements during early Fall but in late fall of 2012, we observe that the proportion of agriculture-related N_2O in the total enhancements reduces to 20 % coinciding with decreasing inputs of fertilizers to farm lands as the growing season draws to a close and crops are harvested. As is observed during spring, methanol emissions are dominated by the 'biogenic' factors with a minor contribution from the 'dairy' source (Figure 4.19 e).

Summer 2012 (Jun 15 – Aug 31)

The profiles in the 6-factor PMF solution in summer 2012 (Figure 4.20) are similar to those from summer 2013 (Figure 4.18), with the exception that N_2O was not present in the 2012 analysis. N_2O is the dominant constituent of the 'ag + soil + delta' profile, and in its absence, the mass fractions of other tracers in this factor are reasonably larger. The CH_4 source apportionment result (Figures 4.21 a and c) from summer 2012 has three contributing sources: the 'dairy and livestock' source, 'ag + soil + delta' source, and the 'urban and oil / gas source' in nearly the same proportions as seen in the summer 2013 analysis.

The chemical composition of the 'urban and oil /gas' source factor, at first glance, does not look similar for the two summer periods as acetonitrile and acetone + propanal fractions in the summer 2012 solution look significantly larger. A deeper investigation leads to an interesting finding. A 7-factor solution (not shown here explicitly) produces an additional factor which is mostly dominated by acetonitrile and acetone (Figure 4.22 a) that was formerly present in the 'urban and oil / gas' factor in the 6-factor solution. This new factor also has minor mass fractions attributed to combustion tracers CO, benzene and a minor amount of CH_4. Acetonitrile is a well-known biomass burning tracer (Bange and Williams, 2000; de Gouw, 2003). On analyzing the average vertical diurnal profile of measured acetonitrile in summer 2012, we find that huge concentrations of acetonitrile were present in the upper levels of WGC at all times of the day (Figure 4.22 b), and they were transported down during the day time when vertical mixing is rapid. Significant amounts of acetone were also present in the upper parts of the mixed layer (Figure 4.6 i) and vertical mixing during the day caused this signal to be detected at the 131 m a.g.l level. The source of this acetonitrile and acetone was the large forest fire in northeastern California that occurred in August 2012 known as the Rush Fire. This wildfire was the second largest in the state's recorded history (since 1932). Since forest fires are associated with intensely hot plumes, the VOCs in the fire emissions plumes are carried aloft above the boundary layer quickly by the rising hot air. These emissions arrive at the 131 m a.g.l measurement level on WGC during the middle of the day when peak vertical mixing occurs. This is also the time of day when emissions contained in 'urban and oil /gas plumes' arrive at the site with the day time westerly sea breeze. This is the reason that the 6-factor solution 'mixes' both these unique source contributions (from two vertically divergent directions) into a single factor. With a total of only 12 apportioned tracers in the whole time series, we observe 'splitting' of other source factors (not shown and as described above and in Chapter 2), if we try to use the 7-factor solution as the 'best case' solution. Hence we do not choose the 7-factor solution as our final solution but instead present the 'urban and oil/gas' factor profile and the 'forest fires' factor profile from the 7-factor

solution separately (in Figure 4.22 a) to explain the observed chemical profile of the 'urban and oil / gas factor' in the 6-factor solution (Figure 4.20). It should be noted that in summer 2013, acetonitrile concentrations in the upper elevations of the mixed layer were significantly lower in the absence of a large fire like the one in August 2012. The 'infamous' Rim Fire in Yosemite National Park occurred in August 2013 following the conclusion of our summer 2013 PMF analysis and is hence not captured in our analysis. The contribution of CH_4 from the forest fires source factor was found to be insignificant compared to other regional sources and well-within the range of ascribed uncertainties.

4.4.3   Comparison with inventory source distribution

We herein present a direct comparison of PMF-derived CH_4 and N_2O source apportionment with the statewide inventory (CARB, 2013) (Figures 4.23 a and 4.24 a, respectively) and other 'bottom-up' sources (Figures 4.23 b and 4.24 b, respectively). Spatially resolved sector-wise 0.1° × 0.1° a priori CH_4 emissions maps with seasonal components, developed and scaled to match the 2008 statewide inventory (CALGEM, 2013; Jeong et al., 2013), have been included in the comparison (Figure 4.23 b). The PMF analysis that we perform is reflective of regional sources and source contributions. Hence, in the derivation of the annual CALGEM CH_4 source distribution pie chart, we only include source contributions from the three zones that surround the WGC site and are expected to have maximum contribution to the observed CH_4 enhancements (Regions 6,7, and 8; Figure 1; Jeong et al., 2013).

We find that the contribution of CH_4 emissions from the dairy and livestock sector remain dominant in both the statewide ARB inventory (60 %) as well as the regional CALGEM inventory (58 %). This trend is consistent with PMF-based apportionment across all seasons (61-90 %; Figure 4.23 c-h) though the relative share of CH_4 from the dairy and livestock sector is higher during the fall and winter season as compared to summers, when other local sources of CH_4 are more active. The waste management source (landfills and waste water treatment combined) is the next largest contributor to the 'bottom-up' inventories (21 - 26 %). This source is not separately detected in the season-wise PMF results at WGC as contributions from this primarily urban source is likely to be included in the 'urban and oil / gas' source sector (in black color in Figures 4.23 c-h). In the early fall season, the wind directions are predominantly westerly (Figure 4.3 b) which causes the San Francisco Bay Area and its constituent landfills, waste water treatment plants and natural gas distribution CH_4 sources to lie upwind of WGC thus increasing the influence of the mostly urban Region 7 defined in Jeong et al. (2013) on WGC signals. We see that during this season, the relative share of CH_4 emissions arising from the 'urban and oil / gas source' (26 %) is similar to that observed from summing of 'waste management' and 'oil and gas' CH_4 emissions in the regional CALGEM inventory (31 %) and also in the ARB inventory (35 %). In winters, when prevailing wind directions are generally along the valley floor (Figures 4.2 d and 4.3 d), the 'urban and oil / gas' source has a lesser influence on CH_4 emissions distribution (Figure 4.23 e) while influence of the dairies present in the Central Valley is much more prominent.

The differences we observe in the annual accounting are mostly due to CH_4 emissions from wetlands (natural or anthropogenic) which are not accounted for in the ARB inventory. These emissions are accounted for in the CALGEM inventory. Together with the CH_4 emissions from rice cultivation, the flooded agriculture/wetland ecosystems in the region account for about 11 % of CH_4 emissions annually in the CALGEM inventory (purple portions in Figure 4.23 b). We find seasonality to CH_4 emissions from the equivalent 'ag + soil + delta' source sector with an almost non-existent contribution to the CH_4 apportionment during winter, and up to 28 % of the local CH_4 emissions during the summer. In general, the 'bottom-up' inventories for CH_4 are reasonable with the PMF-derived seasonal distribution of CH_4 emissions at WGC with respect to the major sources. The variations in the distributions that we encounter principally result from and can be accounted for based on the seasonal nature of certain CH_4 sources (e.g. rice cultivation and wetlands), missing sources (e.g. wetlands in the ARB inventory), and prevailing seasonal meteorology (e.g. for urban sources). CH_4 emissions from anthropogenic wetland / soil management processes in the Delta are significant contributors to the observed ambient CH_4 enhancements at WGC and should be accounted for in the 'bottom-up' state inventory.

We include the source distribution pie chart from the 2012 N_2O CARB inventory in Figure 4.24 a (CARB, 2013) for comparison with seasonally resolved PMF-derived N_2O source distribution pie charts (Figures 4.24 c-f). Additionally, we also include comparison with high-resolution (0.1° × 0.1°) US-totaled N_2O emission model maps EDGAR42 (European Commission Joint Research Centre and Netherlands Environmental Assessment Agency, Emission Database for Global Atmospheric Research (EDGAR), release version 4.2, 2010, http://edgar.jrc.ec.europa.eu) in Figure 4.24 b. The statewide N_2O emissions distribution in the ARB inventory is, in general, consistent with that calculated for the entire country in the EDGAR inventory with respect to major sources with the exception being that N_2O emissions from industrial sources (primarily by-product of industry production of nitric acid and adipic acid) are primarily located outside of California and hence do not feature in the ARB inventory. But there are certain contrasting features that stand out when these 'bottom-up' inventories are compared with the PMF-derived source distributions at WGC. Firstly, manure management in dairy and livestock sector is a significantly larger source of N_2O at WGC than the EDGAR inventory although the observed distributions are more in-line with the ARB inventory. Secondly, N_2O emissions from 'agricultural soil management' at WGC display a strong seasonal nature with the emission trend coinciding with that of N fertilizer use during the agricultural growing season. Negligible N_2O emissions are observed during the winter fallow season. This seasonal variability is not captured in the ARB inventory using a single emission factor approach. This could potentially result in a different annual emission estimate than that computed using an approach which takes environmental factors causing the seasonality of N_2O emissions into account and this variability should be incorporated by ARB in their inventory verification and validation process for N_2O. Finally, but perhaps most importantly, we do not see evidence of N_2O emissions originating from the transportation sector (primarily from urban regions) influencing the WGC site. The PMF analysis consistently produces an 'urban and oil / gas source' (black factor in Figures 4.23 c-h) that likely contains CH_4 contributions from urban sources but no N_2O is apportioned to this source in any season. This finding is consistent with the absence of N_2O in the 'vehicle emission' source profile observed at Bakersfield (Section 2.3.2; Chapter 2). Both the statewide ARB inventory (Figure 4.24 a) and the national EDGAR inventory (Figure 4.24 b) have a substantial fraction of N_2O emissions attributed to the

transportation sector indicating a major error and corresponding need for revisions to the bottom-up statewide accounting of N_2O emissions.

4.5   Summary

We performed PMF-based source apportionment on a combined GHG - VOC data set measured at the 131 m a.g.l inlet height on the Walnut Grove tower (WGC) near the Sacramento-San Joaquin River Delta region in California's Central Valley, in order to investigate the sources of CH_4 and N_2O influencing the measured signals at this site. The year-long measurements were divided up into seven unique periods representative of broad temperature / precipitation regimes encountered in this region, and also to match the data continuity of measured tracers in each individual period. We find that dairies and livestock operations in the region surrounding WGC are the largest contributor to the observed CH_4 enhancements accounting for $55 - 90$ % of the emissions depending on time of the year. The variation in proportion of CH_4 enhancements ascribed to this source is mainly caused by the varying contribution from the 'agriculture + soil management + delta' source, which was the second most important contributor to methane enhancements and varied substantially over the course of the year.   This source contains anaerobically mediated emissions from a combination of wetlands, peatland pastures and flooded / drained agricultural systems in the surrounding Delta. The CH_4 contribution from this sector is temperature driven with peak contributions in the summer season (20 - 40 % of enhancements) as opposed to late fall and winter season when contributions to CH_4 signals from this source are negligible and hence undetectable by PMF. CH_4 contributions from a third source, the 'urban and oil / gas' source, were observed in all seasonal periods. This source contains emissions from the upwind urban core and natural gas operations in the Delta and accounts for 10 - 20 % of the total CH_4 enhancements. This sources' relative contribution was highest during the early fall period (up to 30 %) when the temperature-dependent CH_4 emissions from the Delta emissions are decreasing, and in the late fall period (up to 35 %) when CH_4 emissions from the Delta are absent and observed wind speeds and directions are more variable increasing the influence of the nearby Rio Vista gas fields on the apportioned signals at WGC.

N_2O is measured in four periods (late fall, winter, mid-spring and summer) in this study. There are two apportioned sources contributing to the N_2O enhancements. One of the sources is the 'agricultural + soil management' source arising from the N fertilizer application for intensive crop cultivation in the Delta. This N_2O source is very seasonal with peak contributions occurring in the spring and summer season ($\sim 80 - 90$ %) coinciding with the cycle of fertilizer use in the first half of the growing season. In the late part of the fall season, as agricultural activities around WGC are winding down and so is the added synthetic N input to farmlands, this source only accounts for about 20 % of the observed N_2O enhancements with the dominant share (~ 80 %) being attributed to N_2O emissions from the dairy and livestock sector. In the winters, there is much less agricultural activity taking place around WGC, and the 'ag +soil management' source factor is not observed in the PMF of the wintertime data. Subsequently almost all of the N_2O in winters is attributed to the dairy and livestock sector. We also observe that a source consisting of contributions from primary biogenics and secondary organics is consistently produced in PMF

analysis for all seasonal periods. No detectable contributions of CH_4 and N_2O signals come from this source, which reinforces that plants and crops do not emit these GHGs as direct emissions.

We conclude that, for CH_4, the seasonally resolved apportionment of major sources at WGC is consistent with the distribution in the state inventory. The relative contribution of CH_4 emissions from wetlands / land management practices in the Delta to the overall apportionment at WGC is substantial in warm temperature regimes (e.g. summers) and the bottom-up inventory needs to account for these emissions in the inventory. The consistent lack of N_2O in the 'urban' source factor in all seasonal PMF analyses highlights the insignificant contribution of vehicle emissions to ambient N_2O observations. Thus, the significant attribution of N_2O to the transportation sector seen in the statewide ARB inventory is questionable and calls for a reevaluation of the inventory for that sector. The seasonal variations we observe in emissions of CH_4 and N_2O from certain sources has implications for how data from short-term studies should be used for inventory development. Data from ground-based studies, 'snapshot' airborne measurements and back-trajectory analysis on temporally-limited data may not be able to capture the complete cycle of emissions produced from these sources leading to bias in estimates resulting from such studies. The use of singular emission factors in the 'bottom-up' inventories to derive annual estimates for seasonally varying sources is not adequate. In light of our findings, we propose long-term source-specific ground-measurements as a more representative method to account for CH_4 and N_2O emissions from sources that can be expected to have a seasonal pattern of variability.

4.6   References

Andreae, M. O. and Merlet, P.: Emission of trace gases and aerosols from biomass burning, Global Biogeochem. Cycles, 15(4), 955–966, doi:10.1029/2000GB001382, 2001.

Andrews, A. E., Kofler, J. D., Trudeau, M. E., Williams, J. C., Neff, D. H., Masarie, K. A., Chao, D. Y., Kitzis, D. R., Novelli, P. C., Zhao, C. L., Dlugokencky, E. J., Lang, P. M., Crotwell, M. J., Fischer, M. L., Parker, M. J., Lee, J. T., Baumann, D. D., Desai, A. R., Stanier, C. O. and de Wekker, S. F. J.: CO2, CO and CH4 measurements from the NOAA Earth System Research Laboratory's Tall Tower Greenhouse Gas Observing Network: instrumentation, uncertainty analysis and recommendations for future high-accuracy greenhouse gas, Atmos. Meas. Tech. Discuss., 6(1), 1461–1553 [online] Available from: https://ezp.lib.unimelb.edu.au/login?url=https://search.ebscohost.com/login.aspx?direct=true&db=a9h&AN=85935592&scope=site\nhttp://www.atmos-meas-tech-discuss.net/6/1461/2013/amtd-6-1461-2013.pdf, 2013.

Baker, A. K., Beyersdorf, A. J., Doezema, L. a., Katzenstein, A., Meinardi, S., Simpson, I. J., Blake, D. R. and Sherwood Rowland, F.: Measurements of nonmethane hydrocarbons in 28 United States cities, Atmos. Environ., 42(1), 170–182, doi:10.1016/j.atmosenv.2007.09.007, 2008.

Baker, B., Guenther, A., Greenberg, J. and Fall, R.: Canopy level fluxes of 2-methyl-3-buten-2-ol, acetone, and methanol by a portable relaxed eddy accumulation system, Environ. Sci. Technol., 35(9), 1701–1708, 2001.

Baldocchi, D., Detto, M., Sonnentag, O., Verfaillie, J., Teh, Y. A., Silver, W. and Kelly, N. M.: The challenges of measuring methane fluxes and concentrations over a peatland pasture, Agric. For. Meteorol., 153, 177–187, doi:10.1016/j.agrformet.2011.04.013, 2012.

Bange, H. W. and Williams, J.: New Directions: Acetonitrile in atmospheric and biogeochemical cycles, Atmos. Environ., 34(28), 4959–4960, doi:10.1016/S1352-2310(00)00364-2, 2000.

Bao, J.-W., Michelson, S. a., Persson, P. O. G., Djalalova, I. V. and Wilczak, J. M.: Observed and WRF-Simulated Low-Level Winds in a High-Ozone Episode during the Central California Ozone Study, J. Appl. Meteorol. Climatol., 47(9), 2372–2394, doi:10.1175/2008JAMC1822.1, 2007.

Barletta, B., Meinardi, S., Sherwood Rowland, F., Chan, C.-Y., Wang, X., Zou, S., Yin Chan, L. and Blake, D. R.: Volatile organic compounds in 43 Chinese cities, Atmos. Environ., 39(32), 5979–5990, doi:10.1016/j.atmosenv.2005.06.029, 2005.

Blake, R. S., Monks, P. S. and Ellis, A. M.: Proton-transfer reaction mass spectrometry, Chem. Rev., 109(3), 861–896, 2009.

Bon, D. M., Ulbrich, I. M., de Gouw, J. a., Warneke, C., Kuster, W. C., Alexander, M. L., Baker, a., Beyersdorf, a. J., Blake, D., Fall, R., Jimenez, J. L., Herndon, S. C., Huey, L. G., Knighton, W. B., Ortega, J., Springston, S. and Vargas, O.: Measurements of volatile organic compounds at a suburban ground site (T1) in Mexico City during the MILAGRO 2006 campaign: measurement comparison, emission ratios, and source attribution, Atmos. Chem. Phys., 11(6), 2399–2421, doi:10.5194/acp-11-2399-2011, 2011.

Borbon, A., Gilman, J. B., Kuster, W. C., Grand, N., Chevaillier, S., Colomb, a., Dolgorouky, C., Gros, V., Lopez, M., Sarda-Esteve, R., Holloway, J., Stutz, J., Petetin, H., McKeen, S., Beekmann, M., Warneke, C., Parrish, D. D. and de Gouw, J. a.: Emission ratios of anthropogenic volatile organic compounds in northern mid-latitude megacities: Observations versus emission inventories in Los Angeles and Paris, J. Geophys. Res. Atmos., 118(4), 2041–2057, doi:10.1002/jgrd.50059, 2013.

Bouvier-Brown, N. C., Goldstein, A. H., Gilman, J. B., Kuster, W. C. and de Gouw, J. A.: In-situ ambient quantification of monoterpenes, sesquiterpenes, and related oxygenated compounds during BEARPEX 2007 – implications for gas- and particle-phase chemistry, Atmos. Chem. Phys. Discuss., 9(2), 10235–10269, doi:10.5194/acpd-9-10235-2009, 2009.

Brown, S. G., Frankel, A. and Hafner, H. R.: Source apportionment of VOCs in the Los Angeles area using positive matrix factorization, Atmos. Environ., 41(2), 227–237, doi:10.1016/j.atmosenv.2006.08.021, 2007.

Burba, G., 2013. Eddy Covariance Method for Scientific, Industrial, Agricultural, and Regulatory Applications: A Field Book on Measuring Ecosystem Gas Exchange and Areal Emission Rates. LI-COR Biosciences, Lincoln, NE, USA, 331 pp.

CALGEM (2013), California greenhouse gas emissions measurement project emissions maps (http://calgem.lbl.gov/prior_emission.html, document:CA-CH4-CALGEM-v2.1-20121221.zip).

CARB (2013), California Greenhouse Gas Inventory for 2000-2012 - by IPCC Category. http://www.arb.ca.gov/cc/inventory/data/data.htm. accessesd on September 23, 2014.

CASR (2011), California Agricultural Statistics Crop Report, 2011. created by California Department of Food and Agriculture, Sacramento, CA and United States Department of Agriculture.

CCCR (2013), Contra Costa County Annual Crop Report, 2013. Created by California Department of Food and Agriculture, Concord, CA. http://www.co.contra-costa.ca.us/DocumentCenter/View/34207. Accessed on November 23, 2014.

Chung, M. Y., Beene, M., Ashkan, S., Krauter, C. and Hasson, A. S.: Evaluation of non-enteric sources of non-methane volatile organic compound (NMVOC) emissions from dairies, Atmos. Environ., 44(6), 786–794, doi:10.1016/j.atmosenv.2009.11.033, 2010..

Cicerone, R. J., Shetter, J. D. and Delwiche, C. C.: Seasonal variation of methane flux from a California rice paddy, J. Geophys. Res., 88(C15), 11022, doi:10.1029/JC088iC15p11022, 1983.

CIMIS (2013), California Irrigation Management Information System daily station report, Station 166, Lodi West. http://wwwcimis.water.ca.gov/WSNReportCriteria.aspx. Accessed on August 27, 2014

Comero, S., Capitani, L. and Gawlik, B. M.: Positive Matrix Factorisation (PMF) environmental monitoring data using PMF., 2009.

de Gouw, J. a.: Emission sources and ocean uptake of acetonitrile (CH 3 CN) in the atmosphere, J. Geophys. Res., 108(D11), 4329, doi:10.1029/2002JD002897, 2003.

de Gouw, J. A., Howard, C. J., Custer, T. G. and Fall, R.: Emissions of volatile organic compounds from cut grass and clover are enhanced during the drying process, Geophys. Res. Lett., 26(7), 811–814, 1999.

de Gouw, J. and Warneke, C.: Measurements of Volatile Organic Compounds in the Earth ' S Atmosphere Using Proton-Transfer-Reaction Mass Spectrometry, Mass Spectrom. Rev., 26, 223– 257, doi:10.1002/mas, 2007.

Denman, K.L., G. Brasseur, A. Chidthaisong, P. Ciais, P.M. Cox, R.E. Dickinson, D. Hauglustaine, C. Heinze, E. Holland, D. Jacob, U. Lohmann, S Ramachandran, P.L. da Silva

Dias, S.C. Wofsy and X. Zhang, 2007: Couplings Between Changes in the Climate System and Biogeochemistry. In: Climate Change 2007: The Physical Science Basis. Contribution of Working Group I to the Fourth Assessment Report of the Intergovernmental Panel on Climate Change [Solomon, S., D. Qin, M. Manning, Z. Chen, M. Marquis, K.B. Averyt, M.Tignor and H.L. Miller (eds.)]. Cambridge University Press, Cambridge, United Kingdom and New York, NY, USA.

DOGGR (2012), 2011 Preliminary report on California oil and gas production statistics, Department of Conservation's Division of Oil, Gas and Geothermal Resources; Publication No. PR03.

Dlugokencky, E.J., A.M. Crotwell, P.M. Lang, K.A. Masarie (2014), Atmospheric Methane Dry Air Mole Fractions from quasi-continuous measurements at Barrow, Alaska and Mauna Loa, Hawaii, 1986-2013, Version: 2014-08-12, Path: ftp://ftp.cmdl.noaa.gov/ccg/ch4/in-situ/.

Fares, S., Gentner, D. R., Park, J.-H., Ormeno, E., Karlik, J. and Goldstein, A. H.: Biogenic emissions from Citrus species in California, Atmos. Environ., 45(27), 4557–4568, doi:10.1016/j.atmosenv.2011.05.066, 2011.

Fares, S., Park, J.-H., Gentner, D. R., Weber, R., Ormeño, E., Karlik, J. and Goldstein, a. H.: Seasonal cycles of biogenic volatile organic compound fluxes and concentrations in a California citrus orchard, Atmos. Chem. Phys., 12(20), 9865–9880, doi:10.5194/acp-12-9865-2012, 2012.

Filipy, J., Rumburg, B., Mount, G., Westberg, H. and Lamb, B.: Identification and quantification of volatile organic compounds from a dairy, Atmos. Environ., 40(8), 1480–1494, doi:10.1016/j.atmosenv.2005.10.048, 2006.

FLIGHT (2011), Facility Level Information on Greenhouse Gas Tool, Environmental Protection Agency, http://ghgdata.epa.gov/ghgp/main.do, accessed on Oct 26, 2014.

Forster, P. ., Ramaswamy, V. ., Artaxo, P. ., Berntsen, T. ., Betts, R. ., Fahey, D. W. ., Haywood, J. ., Lean, J. ., Lowe, D. C. ., Myhre, G. ., Nganga, J. ., Prinn, R. ., Raga, G. ., Schulz, M. . and Dorland, R. V.: 2007: Changes in Atmospheric Constituents and in Radiative Forcing, in Climate Change 2007: The Physical Science Basis. Contribution of Working Group I to the Fourth Assessment Report of the Intergovernmental Panel on Climate Change, edited by S. Solomon, D. Qin, M. Manning, Z. Chen, M. Marquis, K. B. Averyt, M.Tignor, and H. L. Miller, p. 996, Cambridge University Press. [online] Available from: http://www.ipcc.ch/publications_and_data/ar4/wg1/en/ch2.html, 2007.

Galbally, I. E. and Kirstine, W.: The Production of Methanol by Flowering Plants and the Global Cycle of Methanol, , 195–229, 2002.

Gelencsér, A., Siszler, K. and Hlavay, J.: Toluene-benzene concentration ratio as a tool for characterizing the distance from vehicular emission sources, Environ. Sci. …, 31(10), 2869–

2872 [online] Available from: http://pubs.acs.org/doi/abs/10.1021/es970004c (Accessed 30 November 2014), 1997.

Gentner, D. R., Ford, T. B., Guha, a., Boulanger, K., Brioude, J., Angevine, W. M., de Gouw, J. a., Warneke, C., Gilman, J. B., Ryerson, T. B., Peischl, J., Meinardi, S., Blake, D. R., Atlas, E., Lonneman, W. a., Kleindienst, T. E., Beaver, M. R., Clair, J. M. St., Wennberg, P. O., VandenBoer, T. C., Markovic, M. Z., Murphy, J. G., Harley, R. a. and Goldstein, a. H.: Emissions of organic carbon and methane from petroleum and dairy operations in California's San Joaquin Valley, Atmos. Chem. Phys., 14(10), 4955–4978, doi:10.5194/acp-14-4955-2014, 2014.

Goldstein, A. H. and Schade, G. W.: Quantifying biogenic and anthropogenic contributions to acetone mixing ratios in a rural environment, Atmos. Environ., 34(29-30), 4997–5006, doi:10.1016/S1352-2310(00)00321-6, 2000.

Graus, M., Eller, A. S. D., Fall, R., Yuan, B., Qian, Y., Westra, P., de Gouw, J. and Warneke, C.: Biosphere-atmosphere exchange of volatile organic compounds over C4 biofuel crops, Atmos. Environ., 66, 161–168, doi:10.1016/j.atmosenv.2011.12.042, 2013.

Guenther, A., Karl, T., Harley, P., Wiedinmyer, C., Palmer, P. I. and Geron, C.: Estimates of global terrestrial isoprene emissions using MEGAN (Model of Emissions of Gases and Aerosols from Nature), Atmos. Chem. Phys. Discuss., 6(1), 107–173, doi:10.5194/acpd-6-107-2006, 2006.

Guo, L., Luo, D., Li, C. and Fitzgibbon, M.: Development of Spatial Inventory of Nitrous Oxide Emissions from Agricultural Land Uses in California Using Biogeochemical Modeling, 2011.

Harley, P., Greenberg, J., Niinemets, Ü. and Guenther, A.: Environmental controls over methanol emission from leaves, Biogeosciences Discuss., 4(4), 2593–2640, 2007.

Hatala, J. a., Detto, M., Sonnentag, O., Deverel, S. J., Verfaillie, J. and Baldocchi, D. D.: Greenhouse gas (CO2, CH4, H2O) fluxes from drained and flooded agricultural peatlands in the Sacramento-San Joaquin Delta, Agric. Ecosyst. Environ., 150, 1–18, doi:10.1016/j.agee.2012.01.009, 2012.

Hoben, J. P., Gehl, R. J., Millar, N., Grace, P. R. and Robertson, G. P.: Nonlinear nitrous oxide (N2O) response to nitrogen fertilizer in on-farm corn crops of the US Midwest, Glob. Chang. Biol., 17(2), 1140–1152, 2011.

Holzinger, R., Lee, A., Paw, K. T. and Goldstein, U. A. H.: Observations of oxidation products above a forest imply biogenic emissions of very reactive compounds, Atmos. Chem. Phys., 5(1), 67–75, doi:10.5194/acp-5-67-2005, 2005.

Holzinger, R., Warneke, C., Hansel, A., Jordan, A., Lindinger, W., Scharffe, D. H., Schade, G. and Crutzen, P. J.: Biomass burning as a source of formaldehyde, acetaldehyde, methanol, acetone, acetonitrile, and hydrogen cyanide, Geophys. Res. Lett., 26(8), 1161, 1999.

Homer, C., Dewitz, J., Fry, J., Coan, M., Hossain, N., Larson, C., Herold, N., McKerrow, A., VanDriel, J. N. and Wickham, J.: Completion of the 2001 National Land Cover Database for the Counterminous United States, Photogramm. Eng. Remote Sensing, 73(4), 337–341 [online] Available from: http://www.ncbi.nlm.nih.gov/pmc/articles/PMC3339477/pdf/ehp.120-a152.pdf, 2007.

Hopke, P.: A guide to positive matrix factorization, Work. UNMIX PMF as Appl. to PM2, 1–16 [online] Available from: ftp://128.153.5.141/users/h/o/hopkepk/IAEA/PMF-Guidance.pdf (Accessed 13 March 2013), 2000.

Hu, L., Millet, D. B., Kim, S. Y., Wells, K. C., Griffis, T. J., Fischer, E. V., Helmig, D., Hueber, J. and Curtis, a. J.: North American acetone sources determined from tall tower measurements and inverse modeling, Atmos. Chem. Phys., 13(6), 3379–3392, doi:10.5194/acp-13-3379-2013, 2013.

Hu, L., Mohr, M. J., Wells, K. C., Griffis, T. J., Helmig, D. and Millet, D. B.: Sources and seasonality of atmospheric methanol based on tall tower measurements in the US Upper Midwest, Atmos. Chem. Phys. Discuss., 11(6), 17473–17505, doi:10.5194/acpd-11-17473-2011, 2011.

Hüve, K., Christ, M. M., Kleist, E., Uerlings, R., Niinemets, Ü., Walter, A. and Wildt, J.: Simultaneous growth and emission measurements demonstrate an interactive control of methanol release by leaf expansion and stomata, J. Exp. Bot., 58(7), 1783–1793, 2007.

Jacob, D. J., Field, B. D., Jin, E. M., Bey, I., Li, Q., Logan, J. A., Yantosca, R. M. and Singh, H. B.: Atmospheric budget of acetone, J. Geophys. Res. Atmos., 107(D10), ACH 5–1–ACH 5–17, doi:10.1029/2001JD000694, 2002.

Jeong, S., Hsu, Y.-K., Andrews, A. E., Bianco, L., Vaca, P., Wilczak, J. M. and Fischer, M. L.: A multitower measurement network estimate of California's methane emissions, J. Geophys. Res. Atmos., 118(19), 11,339–11,351, doi:10.1002/jgrd.50854, 2013.

Jeong, S., Millstein, D. and Fischer, M. L.: Spatially Explicit Methane Emissions from Petroleum Production and the Natural Gas System in California, 2014.

Jeong, S., Zhao, C., Andrews, A. E., Bianco, L., Wilczak, J. M. and Fischer, M. L.: Seasonal variation of CH 4 emissions from central California, J. Geophys. Res., 117(D11), D11306, doi:10.1029/2011JD016896, 2012a.

Jeong, S., Zhao, C., Andrews, A. E., Dlugokencky, E. J., Sweeney, C., Bianco, L., Wilczak, J. M. and Fischer, M. L.: Seasonal variations in N 2 O emissions from central California, Geophys. Res. Lett., 39(16), n/a–n/a, doi:10.1029/2012GL052307, 2012b.

Jordan, C., Fitz, E., Hagan, T., Sive, B., Frinak, E., Haase, K., Cottrell, L., Buckley, S. and Talbot, R.: and Physics Long-term study of VOCs measured with PTR-MS at a rural site in New Hampshire with urban influences, , (Table 1), 4677–4697, 2009.

Karl, T.: Seasonal variation of biogenic VOC emissions above a mixed hardwood forest in northern Michigan, Geophys. Res. Lett., 30(23), 2186, doi:10.1029/2003GL018432, 2003.

Karl, T., Curtis, A. J., Rosenstiel, T. N., Monson, R. K. and Fall, R.: Transient releases of acetaldehyde from tree leaves-products of a pyruvate overflow mechanism?, Plant, Cell Environ., 25(9), 1121–1131, 2002.

Kesselmeier, J. and Staudt, M.: Biogenic volatile organic compounds (VOC): An overview on emission, physiology and ecology, J. Atmos. Chem., 33(1), 23–88, 1999.

Kirstine, W., Galbally, I., Ye, Y. and Hooper, M.: Emissions of volatile organic compounds (primarily oxygenated species) from pasture, J. Geophys. Res., 103(D9), 10605, 1998.

Knox, S. H., Sturtevant, C., Matthes, J. H., Koteen, L., Verfaillie, J. and Baldocchi, D.: Agricultural peatland restoration: effects of land-use change on greenhouse gas (CO_2 and CH_4) fluxes in the Sacramento-San Joaquin Delta., Glob. Chang. Biol., 1–16, doi:10.1111/gcb.12745, 2014.

Kort, E. a., Eluszkiewicz, J., Stephens, B. B., Miller, J. B., Gerbig, C., Nehrkorn, T., Daube, B. C., Kaplan, J. O., Houweling, S. and Wofsy, S. C.: Emissions of CH_4 and N_2O over the United States and Canada based on a receptor-oriented modeling framework and COBRA-NA atmospheric observations, Geophys. Res. Lett., 35(18), L18808, doi:10.1029/2008GL034031, 2008.

Lan, T. T. N. and Minh, P. A.: BTEX pollution caused by motorcycles in the megacity of HoChiMinh, J. Environ. Sci. (China), 25(2), 348–356, 2013.

Lee, S., Nyarady, J. F., Vergara, F., and Corey, R.: 2007 Oil and Gas Industry Survey Results, Final Report, California Air Resources Board, 2011.

Linquist, B., Van Groenigen, K. J., Adviento-Borbe, M. A., Pittelkow, C. and Van Kessel, C.: An agronomic assessment of greenhouse gas emissions from major cereal crops, Glob. Chang. Biol., 18(1), 194–209, 2012.

Liu, J., Mu, Y., Zhang, Y., Zhang, Z., Wang, X., Liu, Y. and Sun, Z.: Atmospheric levels of BTEX compounds during the 2008 Olympic Games in the urban area of Beijing, Sci. Total Environ., 408(1), 109–116, 2009.

Lobert, J. M., Scharffe, D. H., Hao, W. M. and Crutzen, P. J.: Importance of biomass burning in the atmospheric budgets of nitrogen-containing gases, Nature, 346(6284), 552–554, 1990.

McKinney, K. a., Lee, B. H., Vasta, a., Pho, T. V. and Munger, J. W.: Emissions of isoprenoids and oxygenated biogenic volatile organic compounds from a New England mixed forest, Atmos. Chem. Phys., 11(10), 4807–4831, doi:10.5194/acp-11-4807-2011, 2011.

McMillan, A. M. S., Goulden, M. L. and Tyler, S. C.: Stoichiometry of CH 4 and CO 2 flux in a California rice paddy, J. Geophys. Res., 112(G1), G01008, doi:10.1029/2006JG000198, 2007.

LE MER, J. and ROGER, P.: Production, oxidation, emission and consumption of methane by soils : A review, Eur. J. Soil Biol., 37(1), 25–50 [online] Available from: http://cat.inist.fr/?aModele=afficheN&cpsidt=978757 (Accessed 28 October 2014), 2001.

Miller, R. L.: Carbon Gas Fluxes in Re-Established Wetlands on Organic Soils Differ Relative to Plant Community and Hydrology, Wetlands, 31(6), 1055–1066, doi:10.1007/s13157-011-0215-2, 2011.

Miller, R. L., Fram, M., Fujii, R. and Wheeler, G.: Subsidence reversal in a re-established wetland in the Sacramento-San Joaquin Delta, California, USA, San Fr. Estuary Watershed Sci., 6(3), 1 [online] Available from: file:///C:/DOCUME~1/John/LOCALS~1/Temp/eScholarship UC item 5j76502x.pdf\nfile:///C:/Users/John/AppData/Local/Temp/eScholarship UC item 5j76502x.pdf, 2008.

Millet, D. B., Guenther, A., Siegel, D. A., Nelson, N. B., Singh, H. B., de Gouw, J. A., Warneke, C., Williams, J., Eerdekens, G., Sinha, V., Karl, T., Flocke, F., Apel, E., Riemer, D. D., Palmer, P. I. and Barkley, M.: Global atmospheric budget of acetaldehyde: 3-D model analysis and constraints from in-situ and satellite observations, Atmos. Chem. Phys. Discuss., 9(6), 24225–24279, doi:10.5194/acpd-9-24225-2009, 2009.

Montzka, S. A., Dlugokencky, E. J. and Butler, J. H.: Non-CO2 greenhouse gases and climate change., Nature, 476(7358), 43–50, doi:10.1038/nature10322, 2011.

Ngwabie, N. M., Schade, G. W., Custer, T. G., Linke, S. and Hinz, T.: Abundances and Flux Estimates of Volatile Organic Compounds from a Dairy Cowshed in Germany, J. Environ. Qual., 37(2), 565, doi:10.2134/jeq2006.0417, 2008.

Norris, G., Vedantham, R., Wade, K. and Brown, S.: EPA positive matrix factorization (PMF) 3.0 fundamentals & user guide, Prep. US … [online] Available from: http://scholar.google.com/scholar?hl=en&btnG=Search&q=intitle:EPA+Positive+Matrix+Factorization+(PMF)+3.0+Fundamentals+&+User+Guide#0 (Accessed 9 April 2013), 2008.

NRC (2010), National Research Council, Verifying Greenhouse Gas Emissions: Methods to Support International Climate Agreements, National Academies Press, Washington, D. C.

Owen, J. J. and Silver, W. L.: Greenhouse gas emissions from dairy manure management: a review of field-based studies., Glob. Chang. Biol., doi:10.1111/gcb.12687, 2014.

Paatero, P.: Least squares formulation of robust non-negative factor analysis, Chemom. Intell. Lab. Syst., 37(1), 23–35, doi:10.1016/S0169-7439(96)00044-5, 1997.

Paatero, P., Hopke, P. K., Song, X.-H. and Ramadan, Z.: Understanding and controlling rotations in factor analytic models, Chemom. Intell. Lab. Syst., 60(1-2), 253–264, doi:10.1016/S0169-7439(01)00200-3, 2002.

Paatero, P. and Tapper, U.: Positive matrix factorization: A non–negative factor model with optimal utilization of error estimates of data values, Environmetrics, 5(April 1993), 111–126 [online] Available from: http://onlinelibrary.wiley.com/doi/10.1002/env.3170050203/abstract (Accessed 13 March 2013), 1994.

Park, J.-H., Goldstein, a H., Timkovsky, J., Fares, S., Weber, R., Karlik, J. and Holzinger, R.: Active atmosphere-ecosystem exchange of the vast majority of detected volatile organic compounds., Science, 341(6146), 643–7, doi:10.1126/science.1235053, 2013.

Park, S., Croteau, P., Boering, K. a., Etheridge, D. M., Ferretti, D., Fraser, P. J., Kim, K.-R., Krummel, P. B., Langenfelds, R. L., van Ommen, T. D., Steele, L. P. and Trudinger, C. M.: Trends and seasonal cycles in the isotopic composition of nitrous oxide since 1940, Nat. Geosci., 5(4), 261–265, doi:10.1038/ngeo1421, 2012.

Peischl, J., Ryerson, T. B., Brioude, J., Aikin, K. C., Andrews, a. E., Atlas, E., Blake, D., Daube, B. C., de Gouw, J. a., Dlugokencky, E., Frost, G. J., Gentner, D. R., Gilman, J. B., Goldstein, a. H., Harley, R. a., Holloway, J. S., Kofler, J., Kuster, W. C., Lang, P. M., Novelli, P. C., Santoni, G. W., Trainer, M., Wofsy, S. C. and Parrish, D. D.: Quantifying sources of methane using light alkanes in the Los Angeles basin, California, J. Geophys. Res. Atmos., 118(10), 4974–4990, doi:10.1002/jgrd.50413, 2013.

Peischl, J., Ryerson, T. B., Holloway, J. S., Trainer, M., Andrews, a. E., Atlas, E. L., Blake, D. R., Daube, B. C., Dlugokencky, E. J., Fischer, M. L., Goldstein, a. H., Guha, a., Karl, T., Kofler, J., Kosciuch, E., Misztal, P. K., Perring, a. E., Pollack, I. B., Santoni, G. W., Schwarz, J. P., Spackman, J. R., Wofsy, S. C. and Parrish, D. D.: Airborne observations of methane emissions from rice cultivation in the Sacramento Valley of California, J. Geophys. Res., 117, D00V25, doi:10.1029/2012JD017994, 2012.

Rosenstock T, Liptzin D, Six J, Tomich T. 2013. Nitrogen fertilizer use in California: Assessing the data, trends and a way forward. Calif Agr 67(1):68-79. DOI: 10.3733/ca.E.v067n01p68. http://californiaagriculture.ucanr.edu/landingpage.cfm?article=ca.E.v067n01p68&fulltext=yes

Ruuskanen, T. M., Müller, M., Schnitzhofer, R., Karl, T., Graus, M., Bamberger, I., Hörtnagl, L., Brilli, F., Wohlfahrt, G. and Hansel, A.: Eddy covariance VOC emission and deposition fluxes above grassland using PTR-TOF., Atmos. Chem. Phys., 11(2), 611–625, doi:10.5194/acp-11-611-2011, 2011.

SacCR (2013), Sacramento County Crop and Livestock Report, 2013. created by California Department of Food and Agriculture, Sacramento, CA. http://www.agcomm.saccounty.net/Documents/CropandLivestockReports/2013Report.pdf. Accessed on November 23, 2014.

Salas, W., P. Green, S. Frolking, C. Li, and S. Boles (2006), Estimating irrigation water use for California agriculture: 1950s to present, Rep. CEC-500-2006-057, Public Interest Energy Res. Program, California Energy Commission, Sacramento, California.

Schade, G. W. and Goldstein, A. H.: Fluxes of oxygenated volatile organic compounds from a ponderosa pine plantation, J. Geophys. Res., 106(D3), 3111, doi:10.1029/2000JD900592, 2001.

Schade, G. W. and Goldstein, A. H.: Seasonal measurements of acetone and methanol: Abundances and implications for atmospheric budgets, Global Biogeochem. Cycles, 20(1), n/a–n/a, doi:10.1029/2005GB002566, 2006.

SCR (2013), Solano County Crop and Livestock Report, 2013. created by California Department of Food and Agriculture, Fairfield, CA. http://www.solanocounty.com/civicax/filebank/blobdload.aspx?BlobID=18405. Accessed on November 23, 2014.

Shaw, S. L., Mitloehner, F. M., Jackson, W., Depeters, E. J., Fadel, J. G., Robinson, P. H., Holzinger, R. and Goldstein, A. H.: Volatile organic compound emissions from dairy cows and their waste as measured by proton-transfer-reaction mass spectrometry., Environ. Sci. Technol., 41(4), 1310–6 [online] Available from: http://www.ncbi.nlm.nih.gov/pubmed/17593735, 2007.

Slowik, J. G., Vlasenko, a., McGuire, M., Evans, G. J. and Abbatt, J. P. D.: Simultaneous factor analysis of organic particle and gas mass spectra: AMS and PTR-MS measurements at an urban site, Atmos. Chem. Phys., 10(4), 1969–1988, doi:10.5194/acp-10-1969-2010, 2010.

Steeghs, M., Bais, H. P., de Gouw, J., Goldan, P., Kuster, W., Northway, M., Fall, R. and Vivanco, J. M.: Proton-transfer-reaction mass spectrometry as a new tool for real time analysis of root-secreted volatile organic compounds in Arabidopsis., Plant Physiol., 135(1), 47–58, 2004.

Teh, Y. A., Silver, W. L., Sonnentag, O., Detto, M., Kelly, M. and Baldocchi, D. D.: Large Greenhouse Gas Emissions from a Temperate Peatland Pasture, Ecosystems, 14(2), 311–325, doi:10.1007/s10021-011-9411-4, 2011.

Ulbrich, I. M., Canagaratna, M. R., Zhang, Q., Worsnop, D. R. and Jimenez, J. L.: Interpretation of organic components from Positive Matrix Factorization of aerosol mass spectrometric data, Atmos. Chem. Phys., 9(9), 2891–2918, doi:10.5194/acp-9-2891-2009, 2009.

van Groenigen, J. W., Velthof, G. L., Oenema, O., Van Groenigen, K. J. and Van Kessel, C.: Towards an agronomic assessment of N2O emissions: A case study for arable crops, Eur. J. Soil Sci., 61(6), 903–913, 2010.

Warneke, C., McKeen, S. a., de Gouw, J. a., Goldan, P. D., Kuster, W. C., Holloway, J. S., Williams, E. J., Lerner, B. M., Parrish, D. D., Trainer, M., Fehsenfeld, F. C., Kato, S., Atlas, E. L., Baker, a. and Blake, D. R.: Determination of urban volatile organic compound emission ratios and comparison with an emissions database, J. Geophys. Res., 112(D10), D10S47, doi:10.1029/2006JD007930, 2007.

Wecht, K. J., Jacob, D. J., Sulprizio, M. P., Santoni, G. W., Wofsy, S. C., Parker, R., Bösch, H. and Worden, J.: Spatially resolving methane emissions in California: constraints from the CalNex aircraft campaign and from present (GOSAT, TES) and future (TROPOMI, geostationary) satellite observations, Atmos. Chem. Phys., 14(15), 8173–8184, doi:10.5194/acp-14-8173-2014, 2014.

Weil, J. C. and Horst, T. W.: Footprint Estimates for Atmospheric Flux Measurements in the Convective Boundary-Layer, Precipitation Scavenging and Atmosphere-Surface Exchange, 1–3, 717–728, 1992.

White, M. L., Russo, R. S., Zhou, Y., Ambrose, J. L., Haase, K., Frinak, E. K., Varner, R. K., Wingenter, O. W., Mao, H., Talbot, R. and Sive, B. C.: Are biogenic emissions a significant source of summertime atmospheric toluene in rural Northeastern United States?, Atmos. Chem. Phys. Discuss., 8(3), 12283–12311, doi:10.5194/acpd-8-12283-2008, 2008.

Williams, B. J., Goldstein, a. H., Kreisberg, N. M., Hering, S. V., Worsnop, D. R., Ulbrich, I. M., Docherty, K. S. and Jimenez, J. L.: Major components of atmospheric organic aerosol in southern California as determined by hourly measurements of source marker compounds, Atmos. Chem. Phys., 10(23), 11577–11603, doi:10.5194/acp-10-11577-2010, 2010.

Wunch, D., Wennberg, P. O., Toon, G. C., Keppel-Aleks, G. and Yavin, Y. G.: Emissions of greenhouse gases from a North American megacity, Geophys. Res. Lett., 36(15), L15810, doi:10.1029/2009GL039825, 2009.

Xiang, B., Miller, S. M., Kort, E. a., Santoni, G. W., Daube, B. C., Commane, R., Angevine, W. M., Ryerson, T. B., Trainer, M. K., Andrews, A. E., Nehrkorn, T., Tian, H. and Wofsy, S. C.: Nitrous oxide (N 2 O) emissions from California based on 2010 CalNex airborne measurements, J. Geophys. Res. Atmos., 118(7), 2809–2820, doi:10.1002/jgrd.50189, 2013.

Yuan, B., Shao, M., de Gouw, J., Parrish, D. D., Lu, S., Wang, M., Zeng, L., Zhang, Q., Song, Y., Zhang, J. and Hu, M.: Volatile organic compounds (VOCs) in urban air: How chemistry affects the interpretation of positive matrix factorization (PMF) analysis, J. Geophys. Res. Atmos., 117(D24), n/a–n/a, doi:10.1029/2012JD018236, 2012.

Zhao, C., Andrews, A. E., Bianco, L., Eluszkiewicz, J., Hirsch, A., MacDonald, C., Nehrkorn, T. and Fischer, M. L.: Atmospheric inverse estimates of methane emissions from Central California, J. Geophys. Res., 114(D16), D16302, doi:10.1029/2008JD011671, 2009.

Zhong, S., Whiteman, C. and Bian, X.: Diurnal evolution of three-dimensional wind and temperature structure in California's Central Valley, J. Appl. …, (1962), 1679–1699 [online] Available from: http://journals.ametsoc.org/doi/abs/10.1175/JAM2154.1 (Accessed 6 March 2013), 2004.

4.7 Tables and Figures

Table 4. 1. Summary of information for seven seasonal sampling periods chosen for PMF analysis along with average temperatures during this period, data coverage and list of measured tracers.

Season	Start/End date	Hourly average temperature range[a] (° C)	Species not measured[b]	Number of hourly samples[c]
Summer 2012	Jun 16 / Aug 31	14 - 30	N_2O	1583
Early Fall 2012	Sep 1 / Oct 16	13 - 28	N_2O	1061
Late Fall 2012	Oct 17 / Nov 30	9 - 20	N.A.	774
Winter / Wet season	Dec 1 / Jan 29	4 - 13	MeOH	744
Winter/ Spring 2013	Feb 16 / Apr 4	4 - 17	N_2O , MeOH	1072
Spring 2013	Apr 6 / May 31	12 - 25	N.A.	1151
Summer 2013	Jun 1 / Aug 4	15 - 30	N.A.	1056

[a] range reflects average daily low and average daily high over the sampling period measured at 10 m a.g.l.
[b] N.A. - not applicable; all 13 tracers measured and included in PMF analysis; measured tracers include CH_4, N_2O, CO, benzene, toluene, acetonitrile, methanol, acetaldehdye, acetone, methyl ethyl ketone, methyl vinyl ketone + methacrolein, isoprene and monoterpenes.
[c] rows of data containing extended periods of missing VOCs removed all together.

Table 4. 2. Comparison of PMF urban and oil / gas source factor benzene and toluene emission ratios relative to carbon monoxide with those derived from urban measurements and gasoline speciation profiles. Relative emission ratios of toluene to benzene are also included as an indicator of aging of emission plumes arriving at WGC.

Study	Source	benzene / CO (pptv ppbv^{-1})	toluene / CO (pptv ppbv-1)	toluene / benzene (pptv pptv-1)
WGC PMF urban and oil/gas factor[a]	This study	1.1 - 1.8	0.4 - 1.5	0.4 - 1.1
Mexico city 2006	Bon et al. (2011)	4.2 ± 0.4	1.21 ± 0.06	3.5 ± 0.4
CalNex Los Angeles ambient emission ratios[b]	Borbon et al. (2013)	1.30	3.18	2.40
New England 2004	Warneke et al. (2007)	0.62	2.62	4.2
28 US cities (1999-2005)[c]	Baker et al. (2008)	0.7	2.7	3.9
Berkeley liquid gasoline speciation 2010[d]	Gentner et al. (2012)	NA	NA	9.708 ± 1.375
Berkeley evaporative gasoline speciation 2010[e]	Gentner et al. (2012)	NA	NA	2.906 ± 0.246

[a] Range of mean ratios over seven unique PMF experiments for different seasonal periods.
[b] Derived from Linear Regression Fit slope of scatterplot from CalNex Pasadena supersite samples.
[c] Ratios represent average of emission ratios from 28 cities.
[d] Ratios calculated from Table S9, Gentner et al., 2012; uncertainties are ± standard deviation.
[e] Ratios calculated from Table S11, Gentner et al., 2012; uncertainties are ± standard deviation.
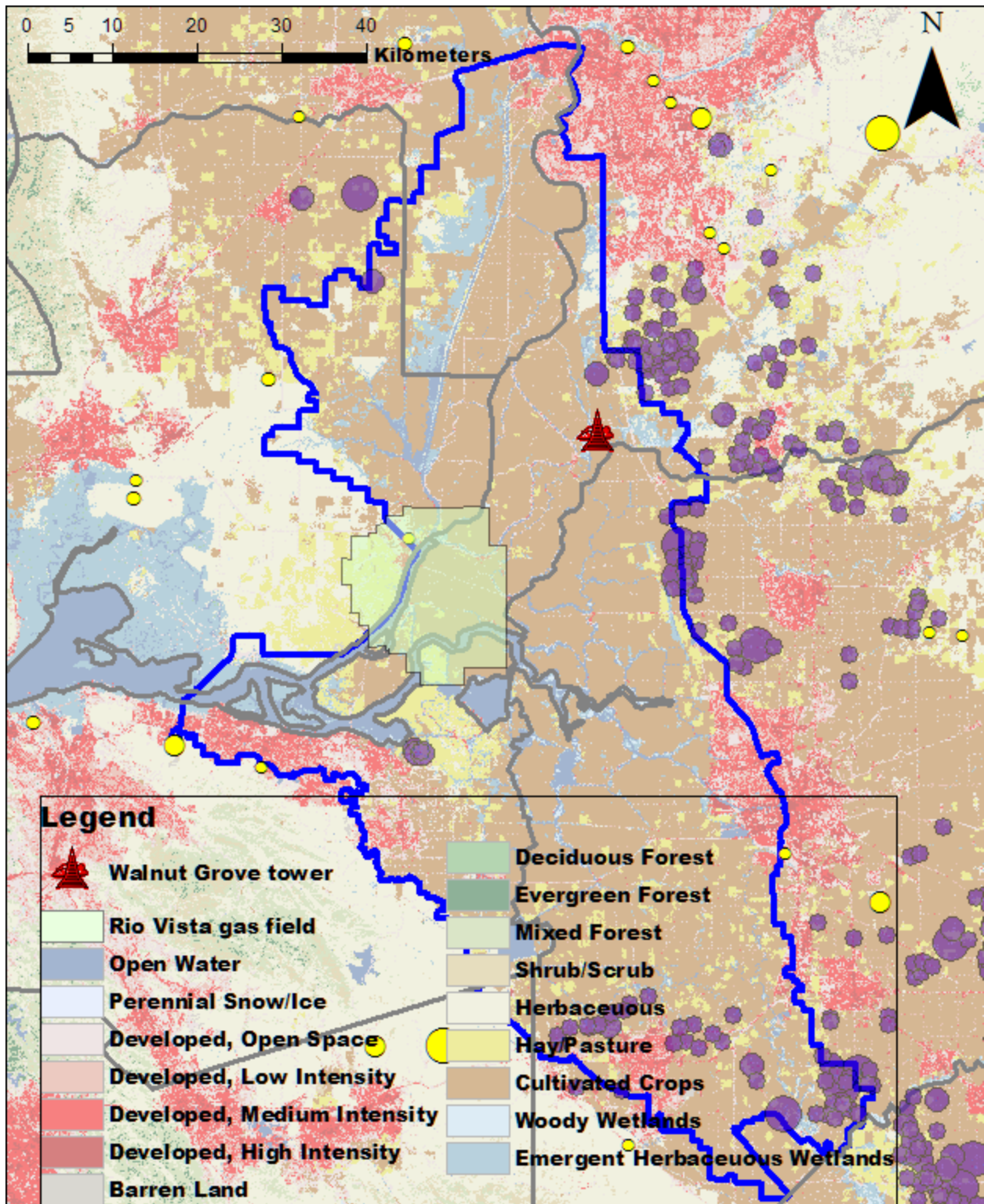
Figure 4. 1. Walnut Grove tower (WGC) site map showing land cover (Homer et al., 2007) and location of local CH$_4$ and N$_2$O sources, including dairies (solid purple circles) and landfills (solid yellow circles). The scale of the dairy and landfill symbols can be found in Figure 3.1 in Chapter 3. The solid blue boundary line represents the extent of the Sacramento-San Joaquin River Delta.
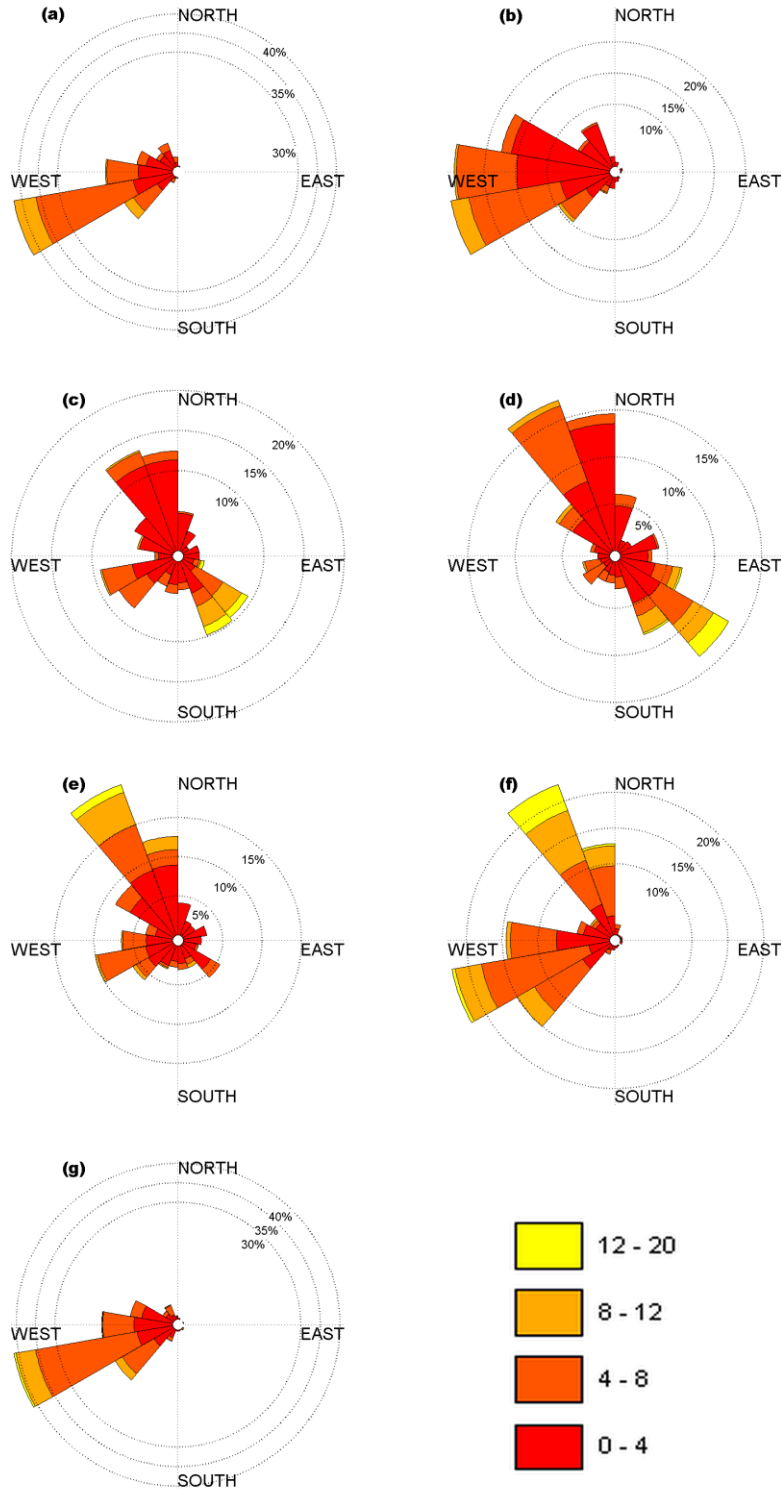
Figure 4. 2. Daytime distribution of wind speed and direction at WGC during (a) Summer 2012; (b) early Fall 2012 (Sep 1 – Oct 15); (c) late Fall 2012 (Oct 16- Nov 30); (d) Winter (Dec-Jan); (e) Winter/Spring 2013 (Feb- Mar); (f) Spring 2013 (Apr- May); and (g) Summer 2013 (Jun- Aug). The values are measured at 91 m a.g.l, the color scale denotes wind speeds (in m/s) and the concentric circles represent the intensity subdivisions (in percent).

151
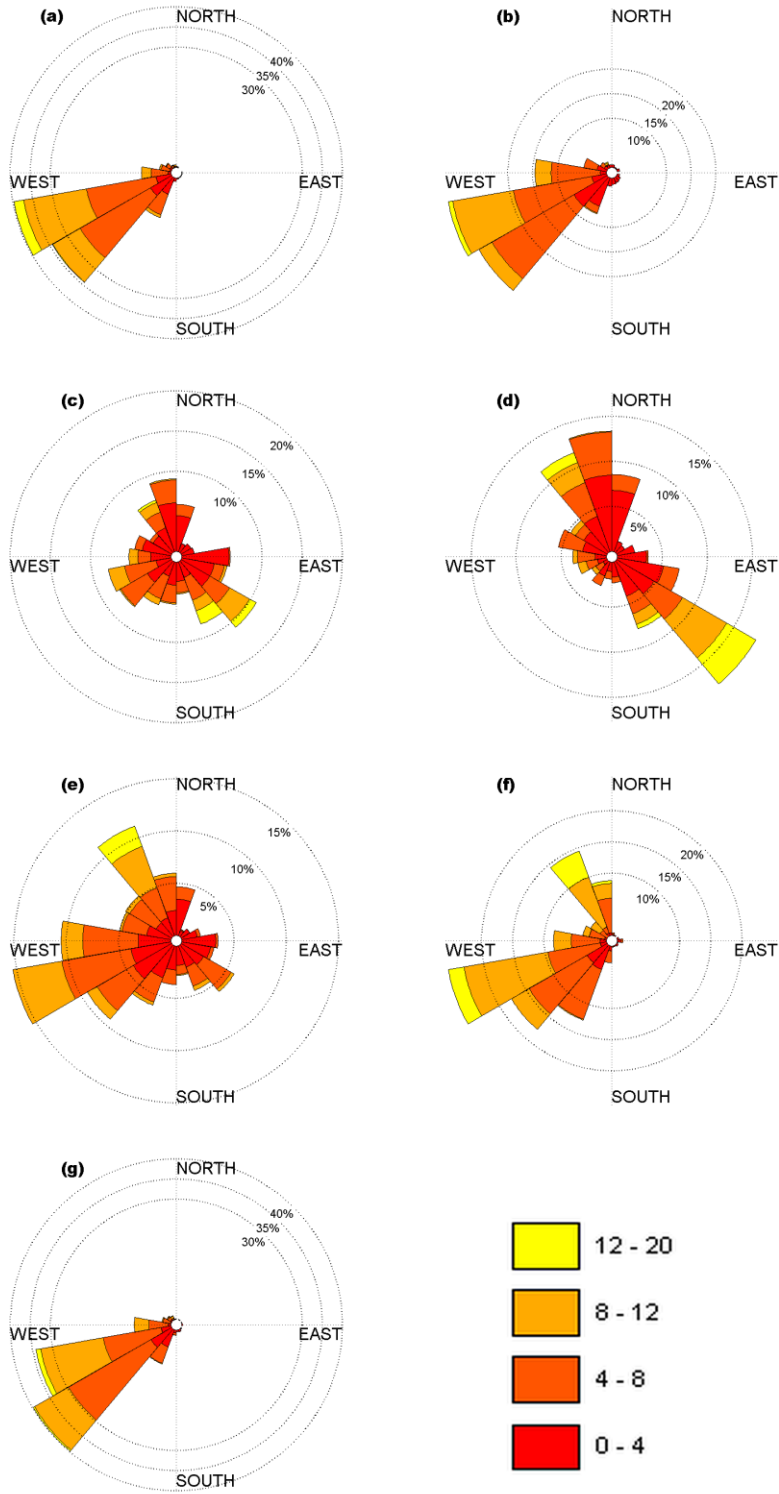
Figure 4. 3. Nighttime distribution of wind speed and direction at WGC during (a) Summer 2012; (b) early Fall 2012 (Sep 1 – Oct 15); (c) late Fall 2012 (Oct 16- Nov 30); (d) Winter (Dec-Jan); (e) Winter/Spring 2013 (Feb-Mar); (f) Spring 2013 (Apr- May); and (g) Summer 2013 (Jun- Aug). The values are measured at 91 m a.g.l, the color scale denotes wind speeds (in m/s) and the concentric circles represent the intensity subdivisions (in percent).

152
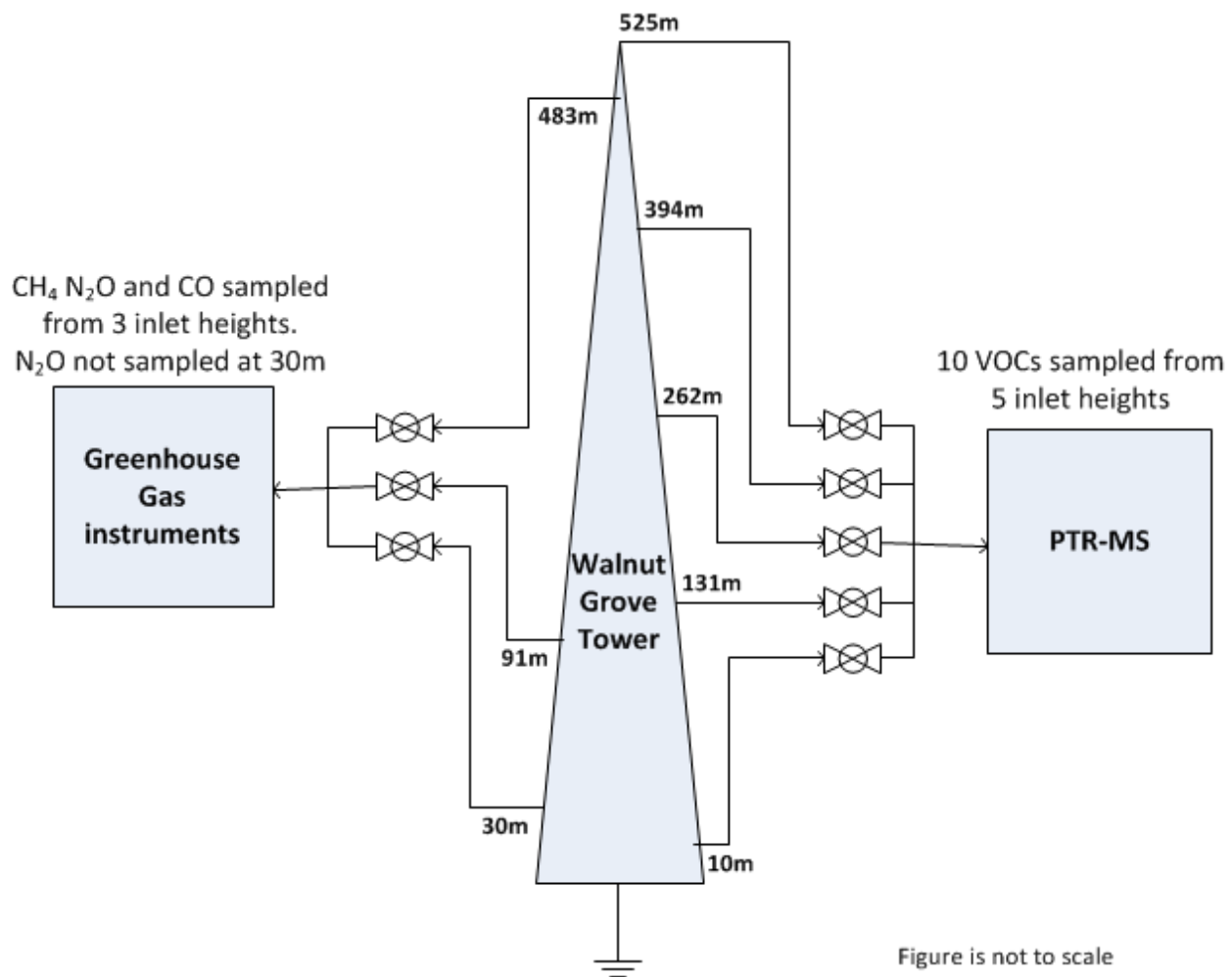
Figure 4. 4. Simplified schematic at Walnut Grove tower showing location of sampling inlets for the GHG and PTR-MS instruments.
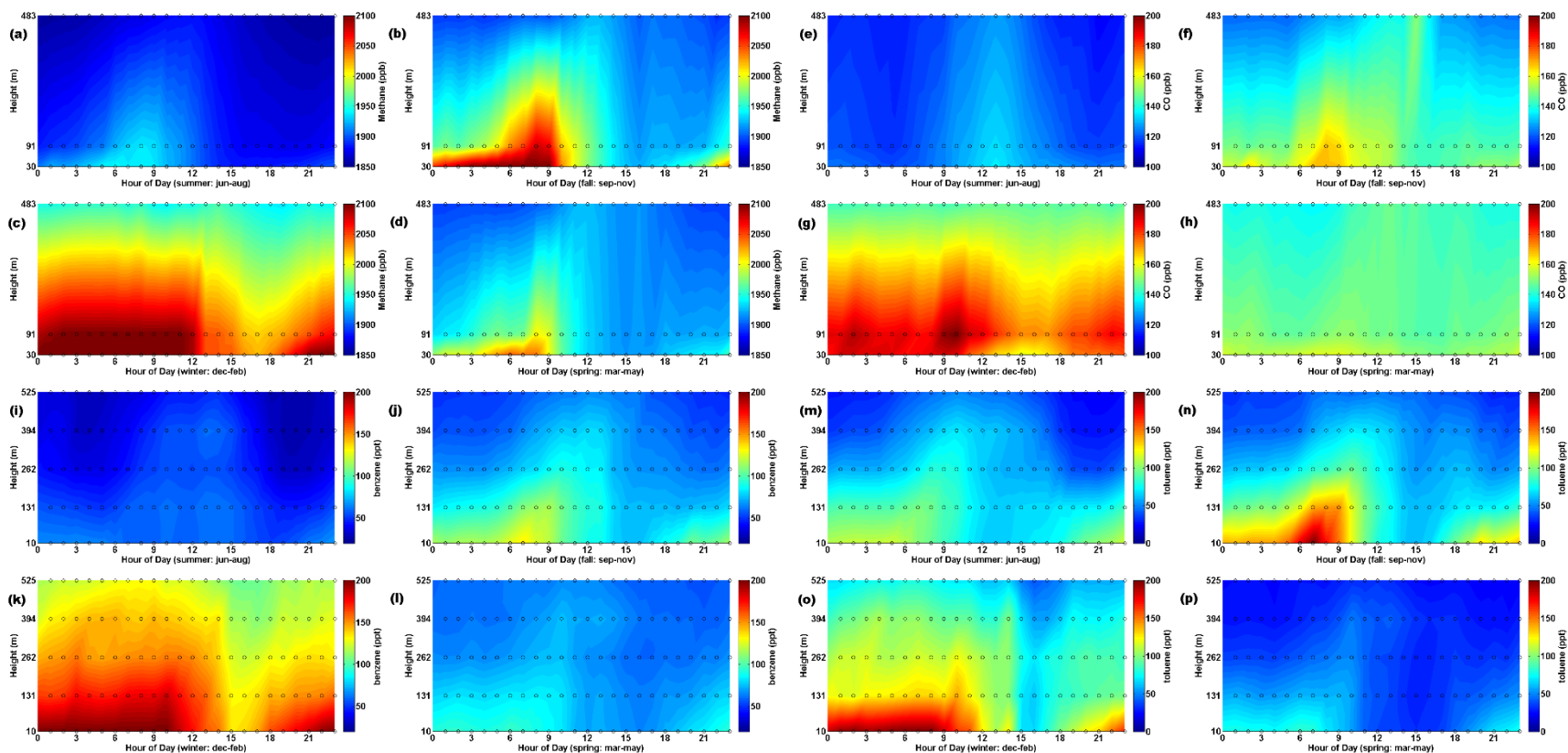
Figure 4. 5. Mean diurnal distribution (x-axis) of CH₄, combustion tracer CO and aromatic VOCs showing interpolated vertical profiles across all measured heights (y-axis) during different seasons at WGC. The color axis represents the mixing ratio of each compound. Species shown include (a-d) CH₄, (e-h) CO, (i-l) benzene, and (m-p) toluene. The x-axis of each figure lists the season for which the concentrations have been plotted. The horizontal dotted lines in each plot represent the height (m a.g.l) on WGC at which the measurements are made.
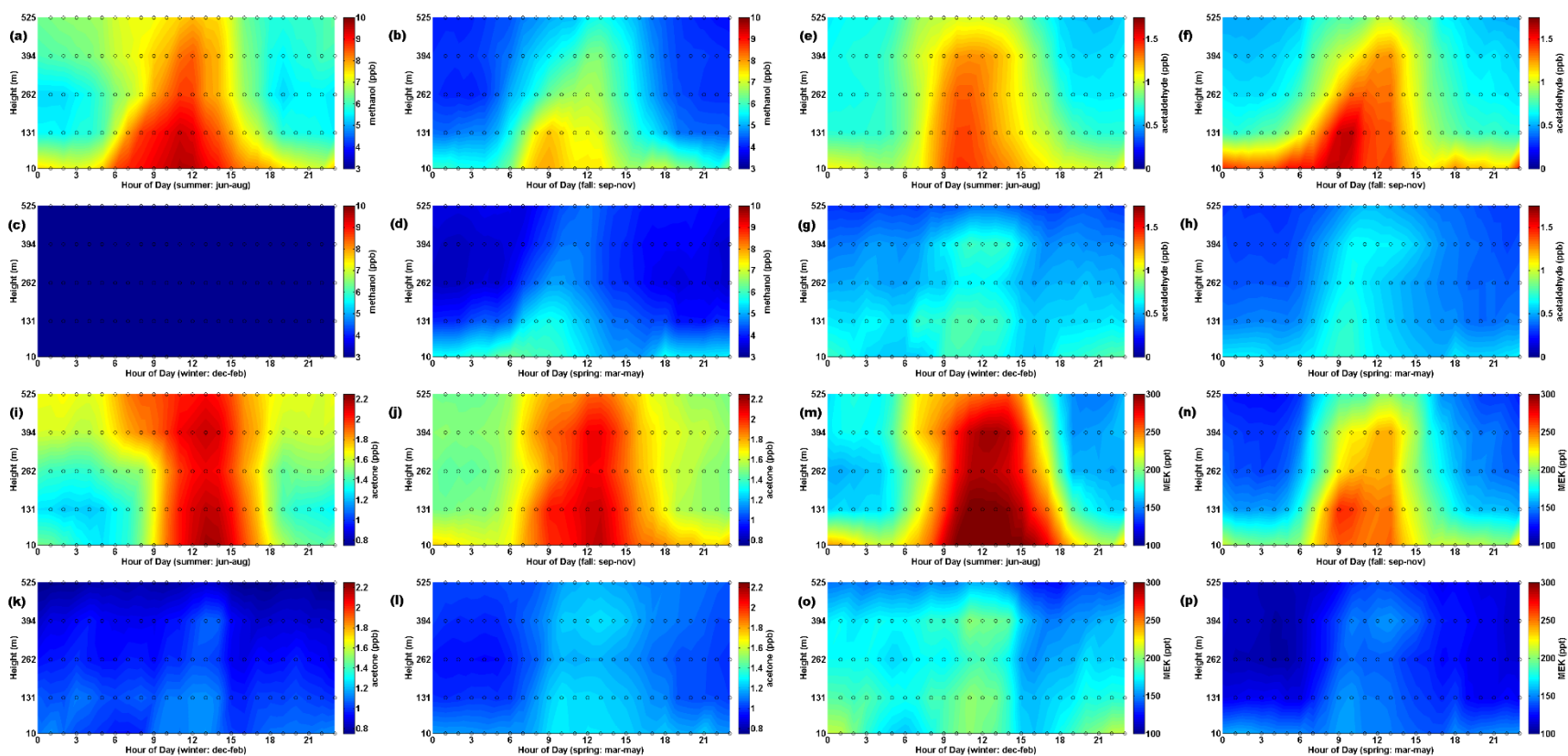
Figure 4. 6. Mean diurnal distribution (x-axis) of oxygenated VOCs showing interpolated vertical profiles across all measured heights (y-axis) during different seasons at WGC. The color axis represents the mixing ratios of each VOC. Species shown include (a-d) methanol, (e-h) acetaldehyde, (i-l) acetone, and (m-p) methyl ethyl ketone (MEK). The x-axis of each figure lists the season for which the concentrations have been plotted. The horizontal dotted lines in each plot represent the height (m a.g.l) on WGC at which the measurements are made. There were no methanol measurements in the winter season at any height (Figure c).
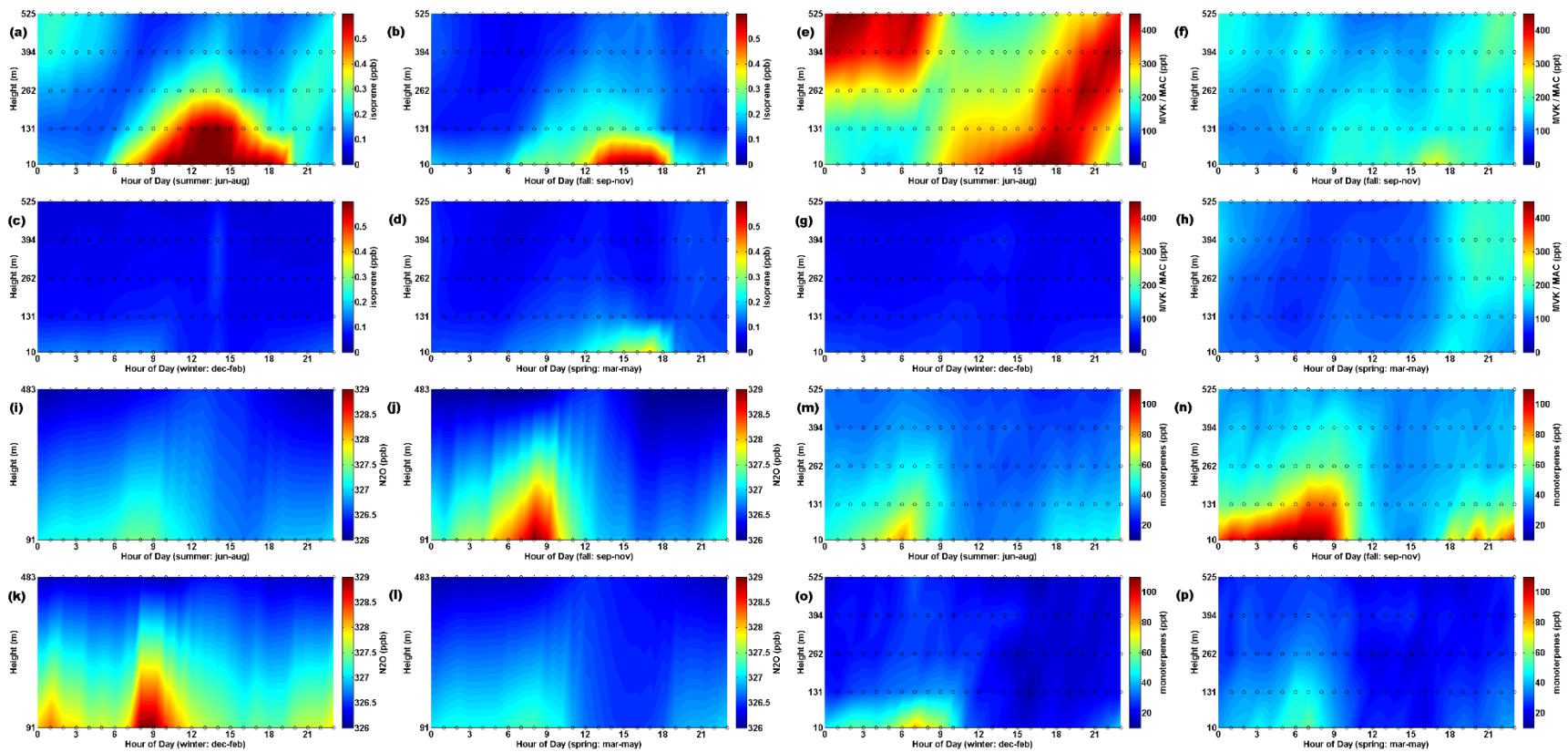
Figure 4. 7. Mean diurnal distribution (x-axis) of primary and secondary biogenic VOCs along with N_2O showing interpolated vertical profiles across all measured heights (y-axis) during different seasons at WGC. The color axis represents the mixing ratios of each VOC. Species shown include (a-d) isoprene, (e-h) methyl vinyl ketone (MVK) + methacrolein (MAC), (i-l) N_2O, and (m-p) monoterpenes (*m/z* 137). The x-axis of each figure lists the season for which the concentrations have been plotted. The horizontal dotted lines in each plot represent the elevation (m a.g.l) on WGC at which the measurements are made. N_2O was not measured at 30 m a.g.l, hence measurements begin at 91 m a.g.l.
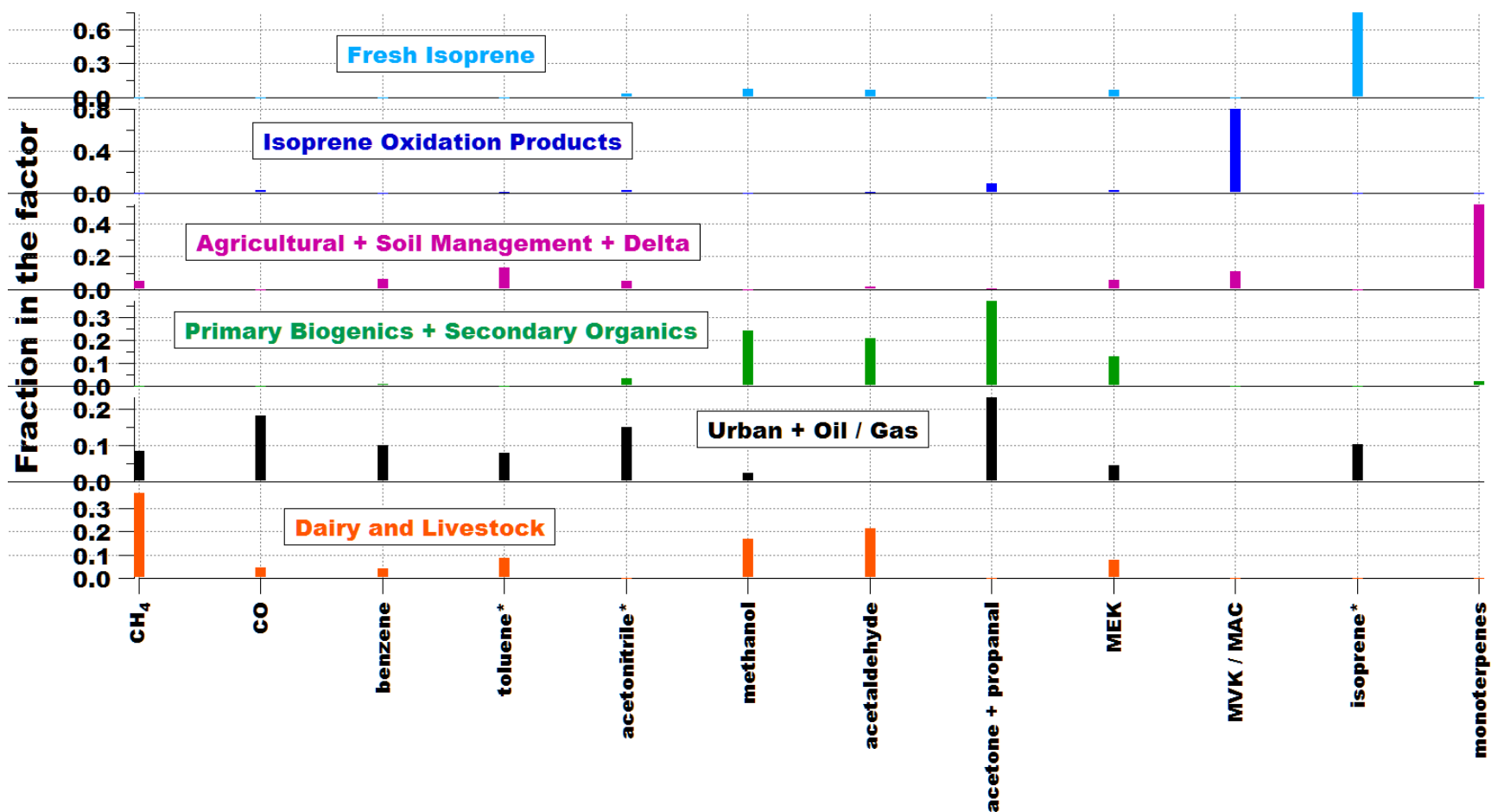
Figure 4. 8. Factor profiles of resolved PMF source factors denoting major source categories influencing the chemical composition of each profile during early fall of 2012 (Sep 1 – Oct 16). The sum of the scaled mass fractions of all species adds up to unity for each profile. The VOCs with an asterisk sign may have minor contributions from other VOCs detected at the same *m/z* depending on the season (see text).
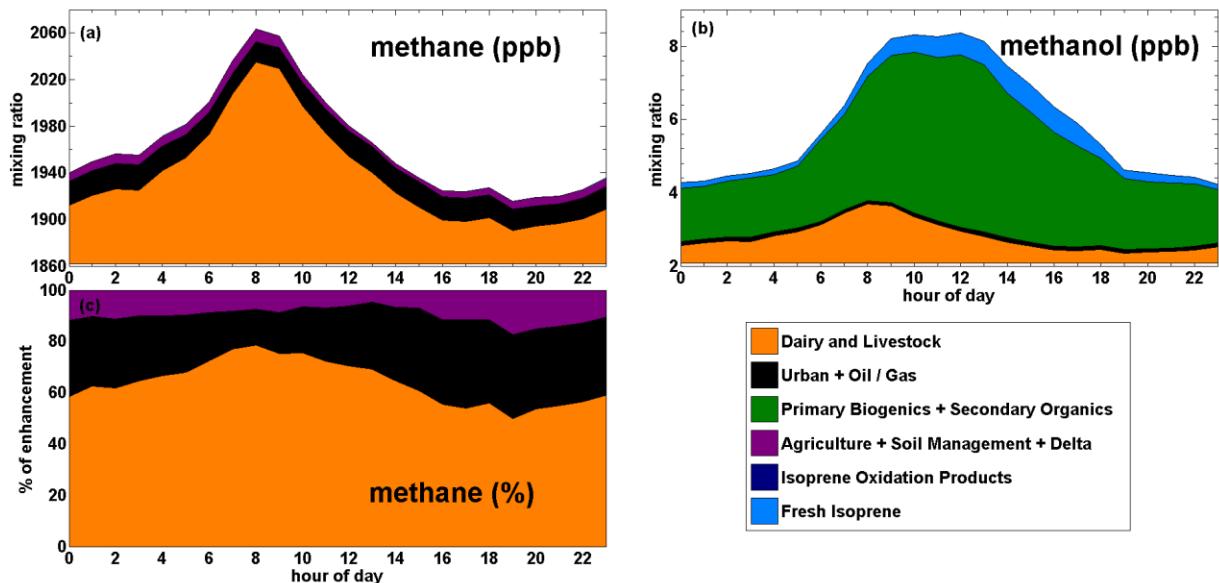
Figure 4. 9. Mean diurnal distribution plots apportioned by PMF generated source factors for early Fall 2012 period (Sep 1 – Oct 16). The plots include (a) source-wise distribution of methane enhancements above seasonal minimum, (b) source-wise distribution of methanol enhancements, and (c) source-wise distribution of methane enhancements by percentage. The legend represents the factor source categories of the 6-factor PMF solution for early Fall 2012.
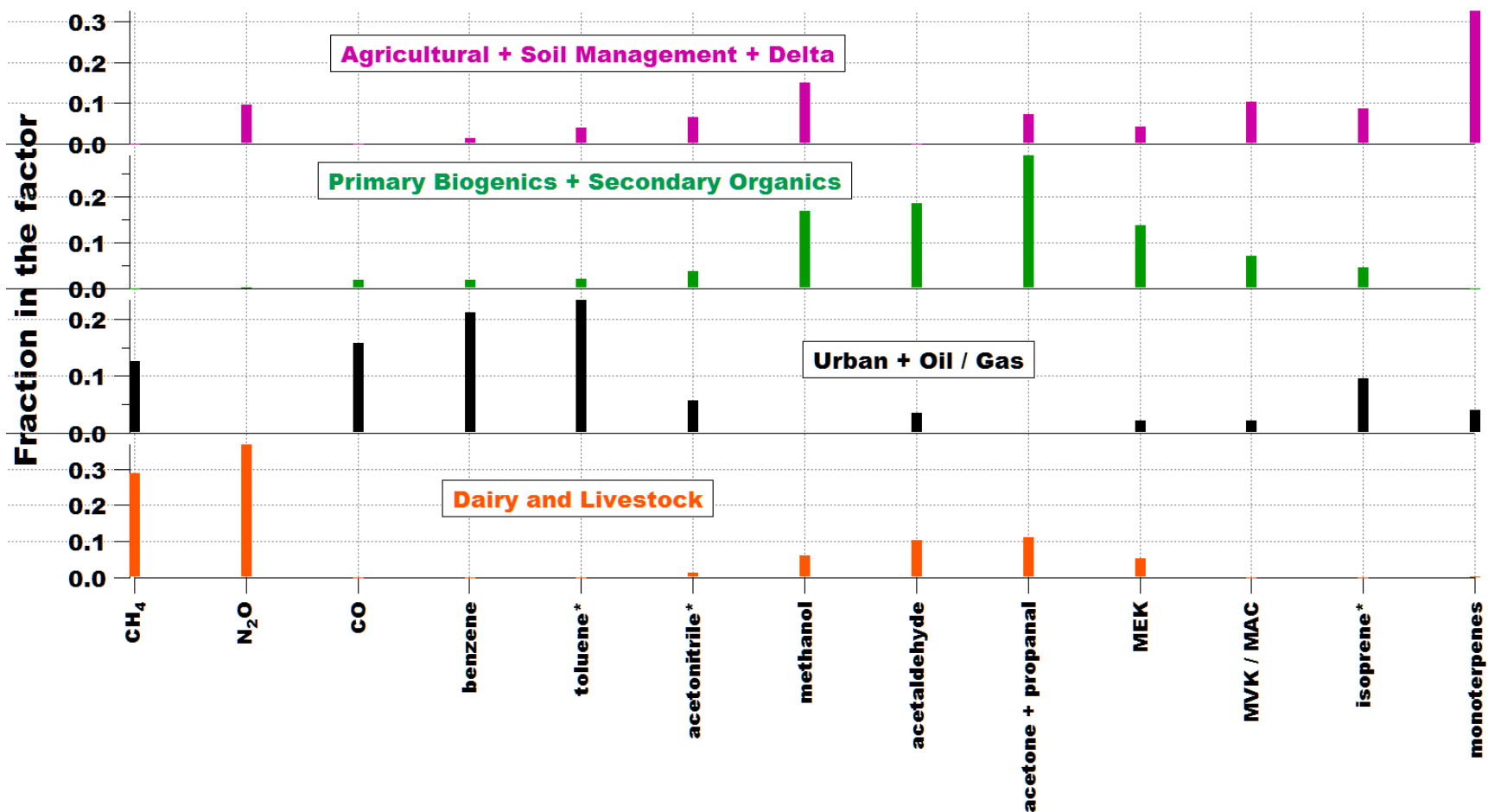
Figure 4. 10. Factor profiles of resolved PMF source factors denoting major source categories influencing the chemical composition of each profile during late fall of 2012 (Oct 17 – Nov 30). The sum of the scaled mass fractions of all species adds up to unity for each profile. The VOCs with an asterisk sign may have minor contributions from other VOCs detected at the same *m/z* depending on the season (see text).
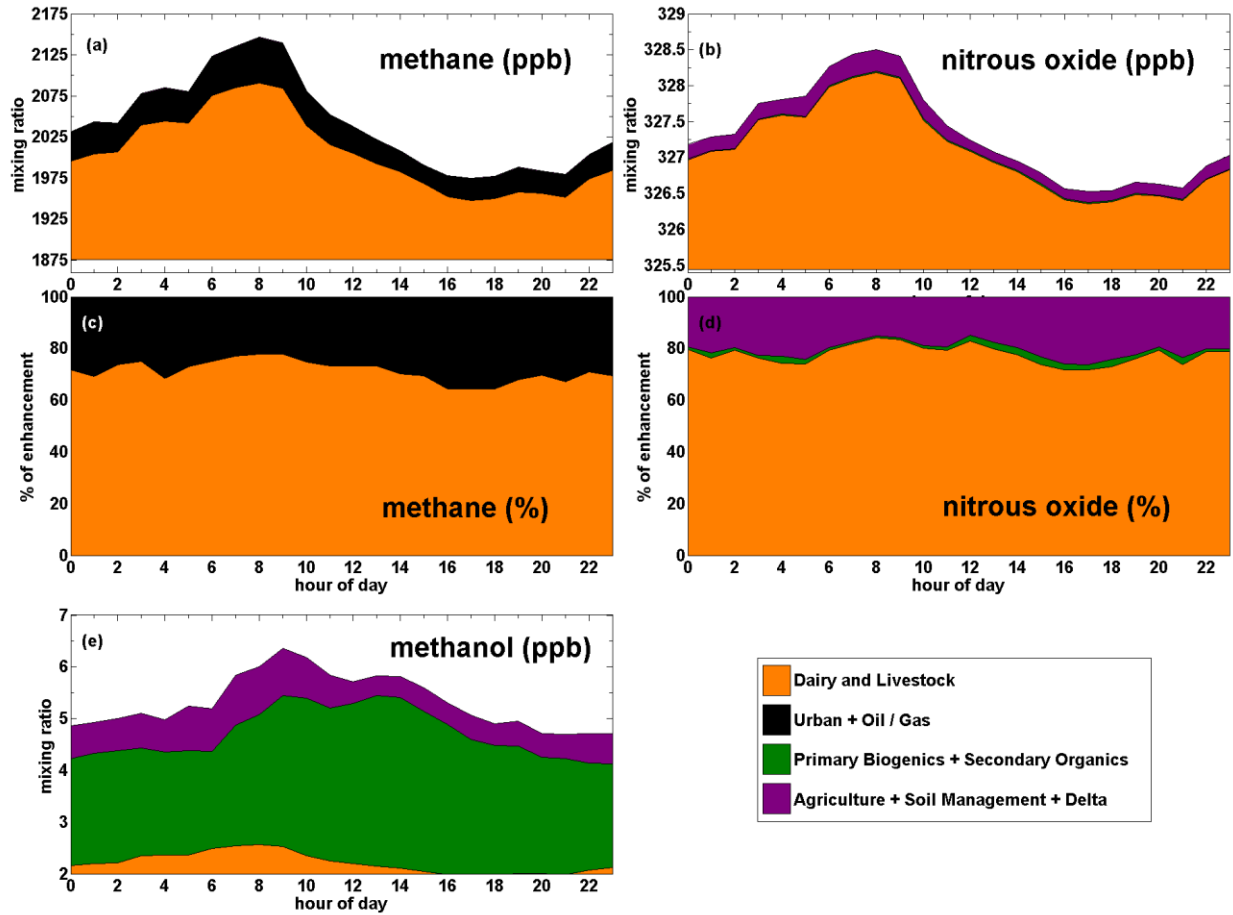
Figure 4. 11. Mean diurnal distribution plots apportioned by PMF generated source factors for late Fall 2012 period (Oct 17 – Nov 30). The plots include source-wise distribution of methane enhancements (a) in ppb above seasonal minimum and (c) by percentage; source-wise distribution of nitrous oxide enhancements (b) in ppb above seasonal minimum and (d) by percentage, and (e) source-wise distribution of methanol enhancements above seasonal minima. The legend represents the factor source categories of the 4-factor PMF solution for late Fall 2012.
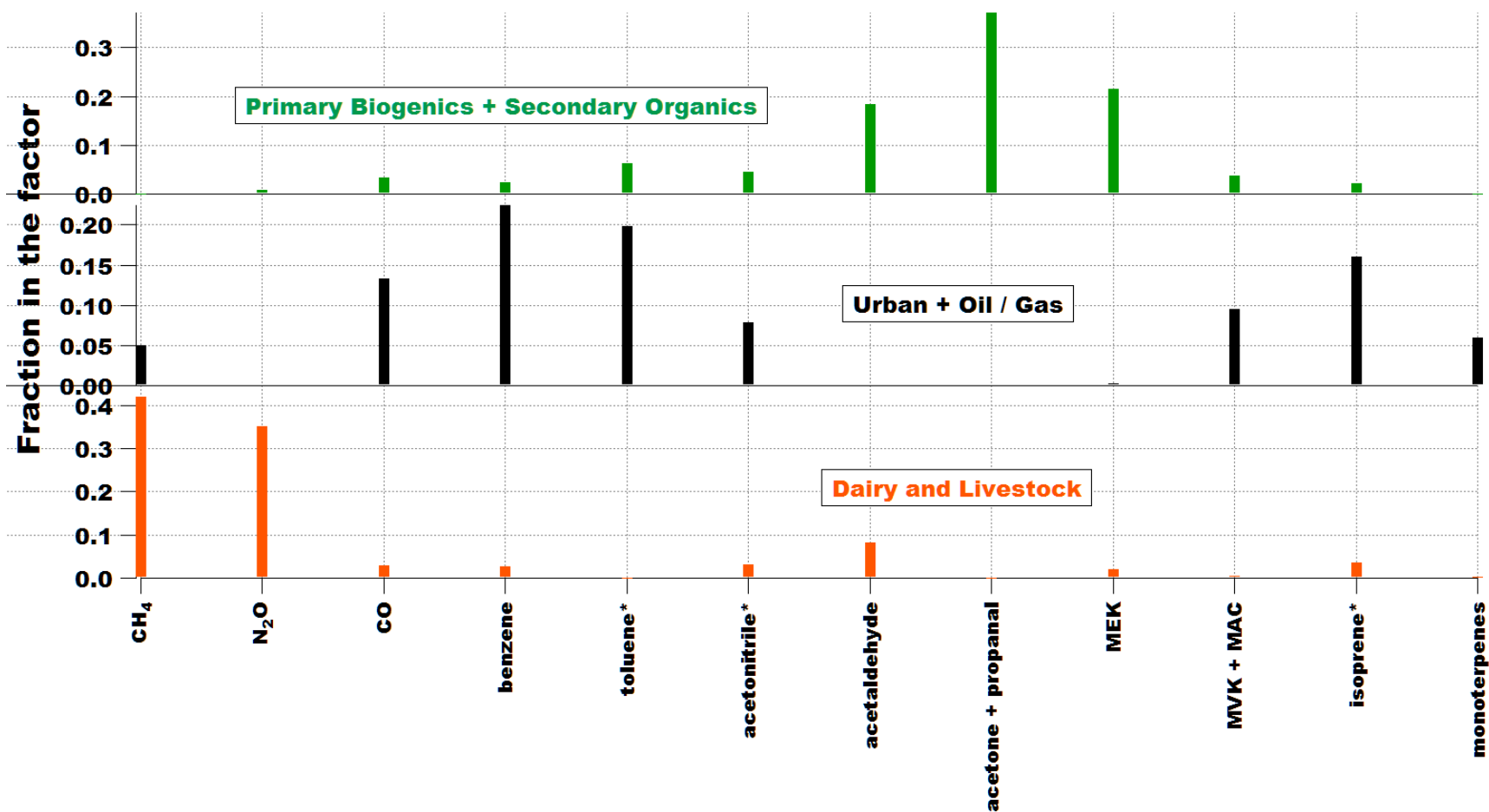
Figure 4. 12. Factor profiles of resolved PMF source factors denoting major source categories influencing the chemical composition of each profile during winter / wet season (Dec 1 – Jan 29). The sum of the scaled mass fractions of all species adds up to unity for each profile. The VOCs with an asterisk sign may have minor contributions from other VOCs detected at the same *m/z* depending on the season (see text).
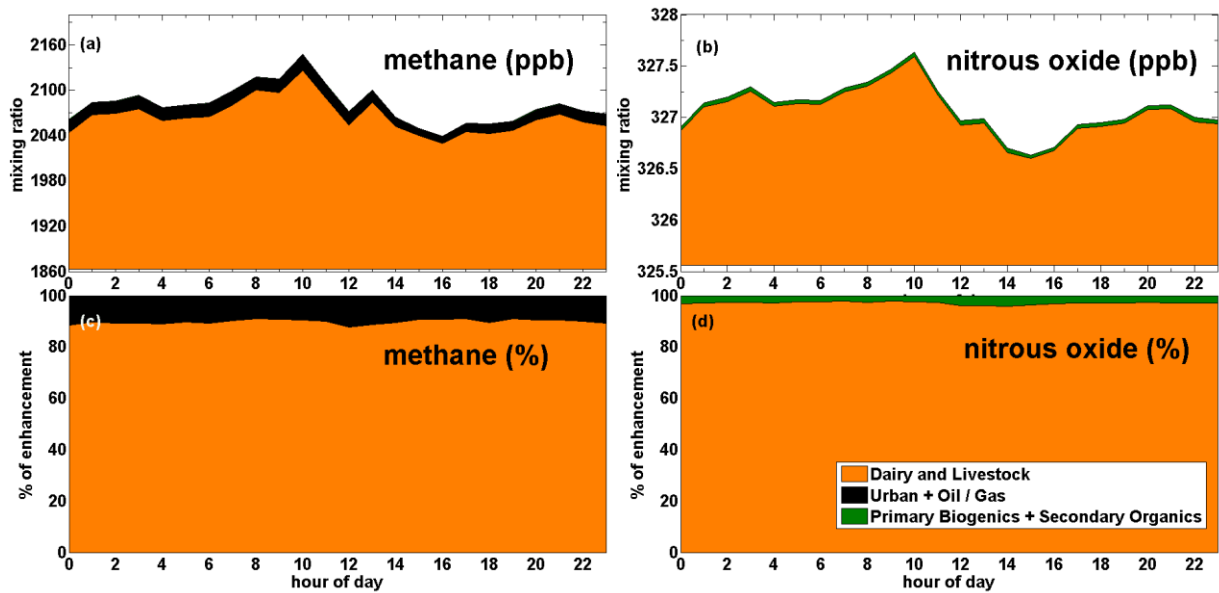
Figure 4. 13. Mean diurnal distribution plots apportioned by PMF generated source factors for winter (wet season) period (Dec 1 – Jan 29). The plots include source-wise distribution of methane enhancements (a) in ppb above seasonal minimum and (c) by percentage; source-wise distribution of nitrous oxide enhancements (b) in ppb above seasonal minimum and (d) by percentage. The legend represents the factor source categories of the 3-factor PMF solution for this season.

162

Figure 4. 14. Factor profiles of resolved PMF source factors denoting major source categories influencing the chemical composition of each profile during winter / early spring of 2013 (Feb 16 – Apr 4). The sum of the scaled mass fractions of all species adds up to unity for each profile. The VOCs with an asterisk sign may have minor contributions from other VOCs detected at the same *m/z* depending on the season (see text).

Figure 4. 15. Mean diurnal distribution plots apportioned by PMF generated source factors for the late winter / early spring season (Feb 16 – Apr 4). The plots include mass distribution of (a) scaled 'dairy and livestock' factor concentrations, (b) scaled 'urban + oil / gas' factor concentrations, (c) scaled 'primary biogenics and secondary organics' factor concentrations, and (d) scaled 'agriculture + soil management + delta' factor concentrations. The solid colored line represents the average concentration for that hour of day while the semi-transparent shaded region represents the 1σ standard deviation. The remaining plots show source-wise distribution of methane enhancements (e) in ppb above seasonal minimum and (c) by percentage of enhancement. The legend represents the source categories of the 4-factor PMF solution.
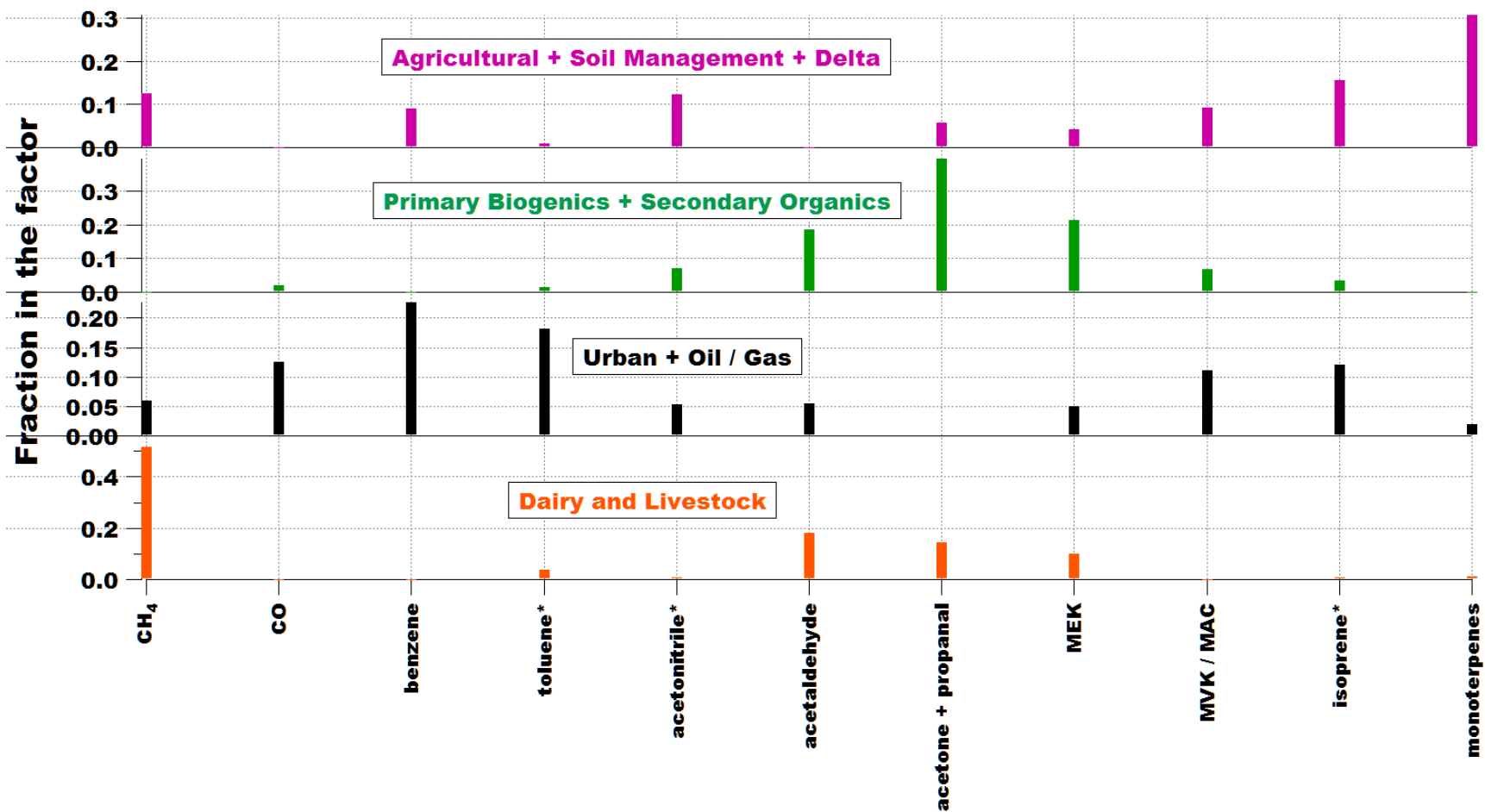
Figure 4. 16. Factor profiles of resolved PMF source factors denoting major source categories influencing the chemical composition of each profile during spring of 2013 (Apr 6 – May 31). The sum of the scaled mass fractions of all species adds up to unity for each profile. The VOCs with an asterisk sign may have minor contributions from other VOCs detected at the same *m/z* depending on the season (see text).
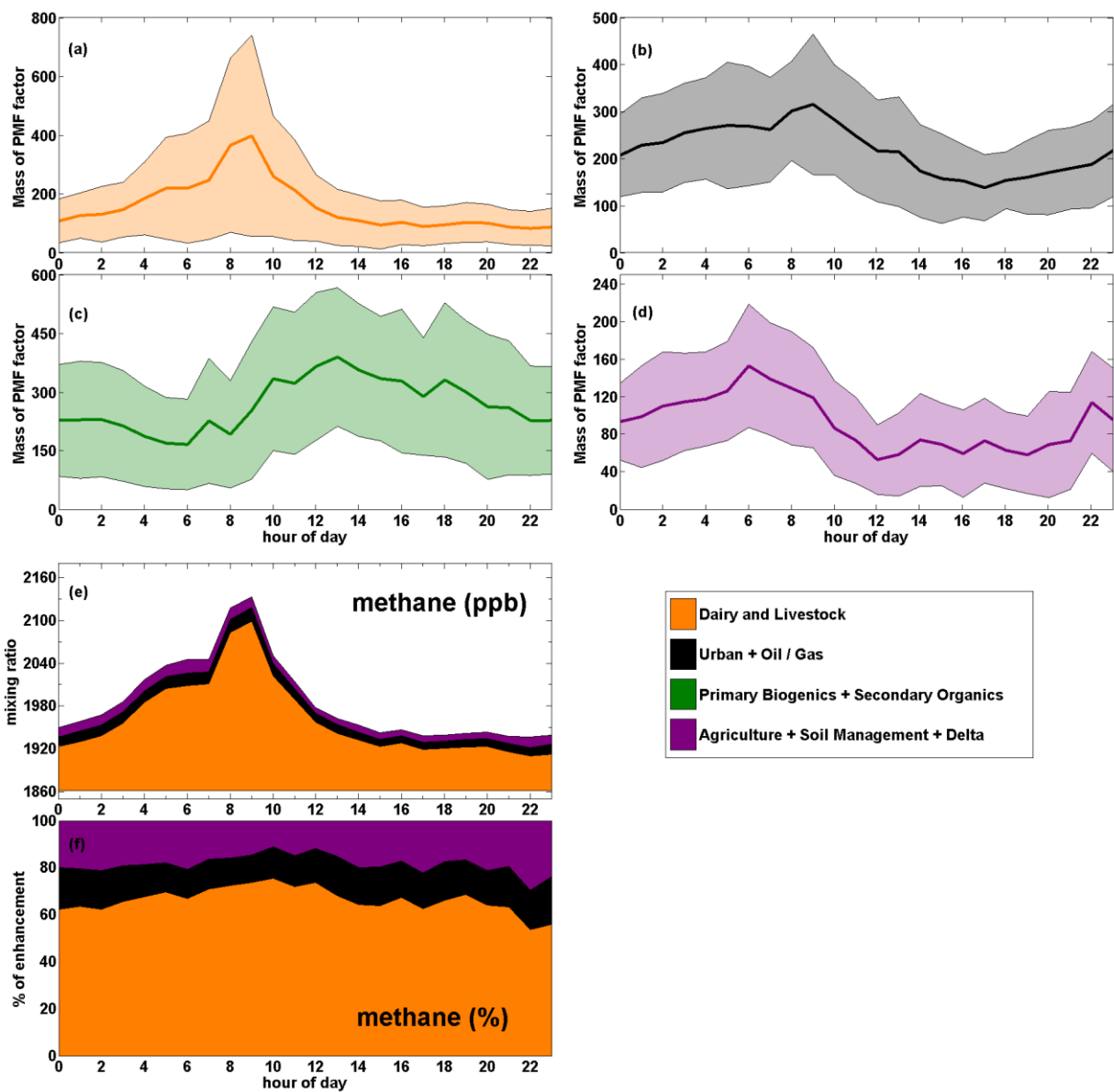
Figure 4. 17. Mean diurnal distribution plots apportioned by PMF generated source factors for spring 2013 period (Apr 6 - May 31). The plots include source-wise distribution of methane enhancements (a) in ppb above seasonal minimum and (c) by percentage; source-wise distribution of nitrous oxide enhancements (b) in ppb above seasonal minimum and (d) by percentage, and (e) source-wise distribution of methanol enhancements above seasonal minima. The legend represents the factor source categories of the 5-factor PMF solution for spring 2013 season.
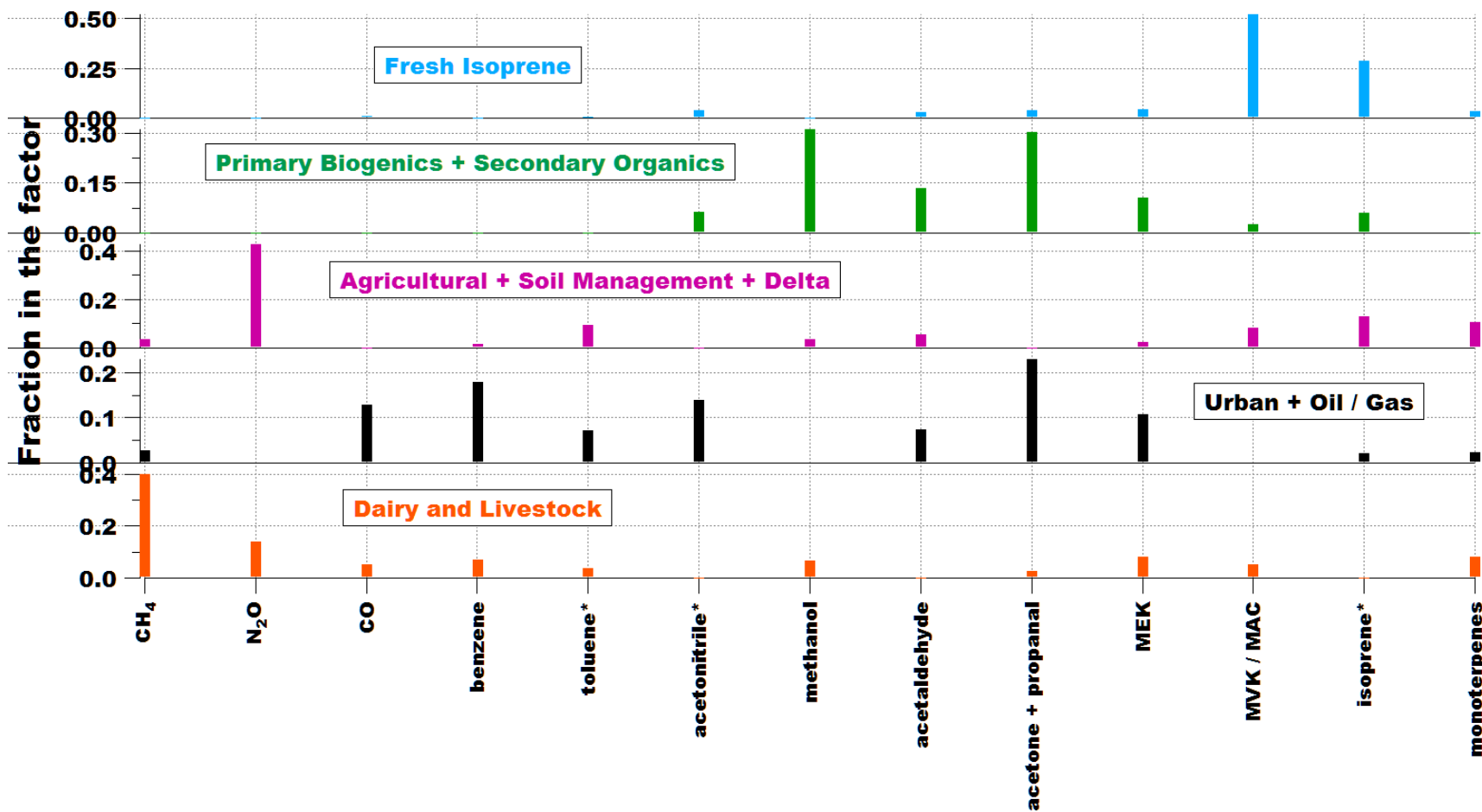
Figure 4. 18. Factor profiles of resolved PMF source factors denoting major source categories influencing the chemical composition of each profile during summer of 2013 (Jun 1 – Aug 4). The sum of the scaled mass fractions of all species adds up to unity for each profile. The VOCs with an asterisk sign may have minor contributions from other VOCs detected at the same *m/z* depending on the season (see text).
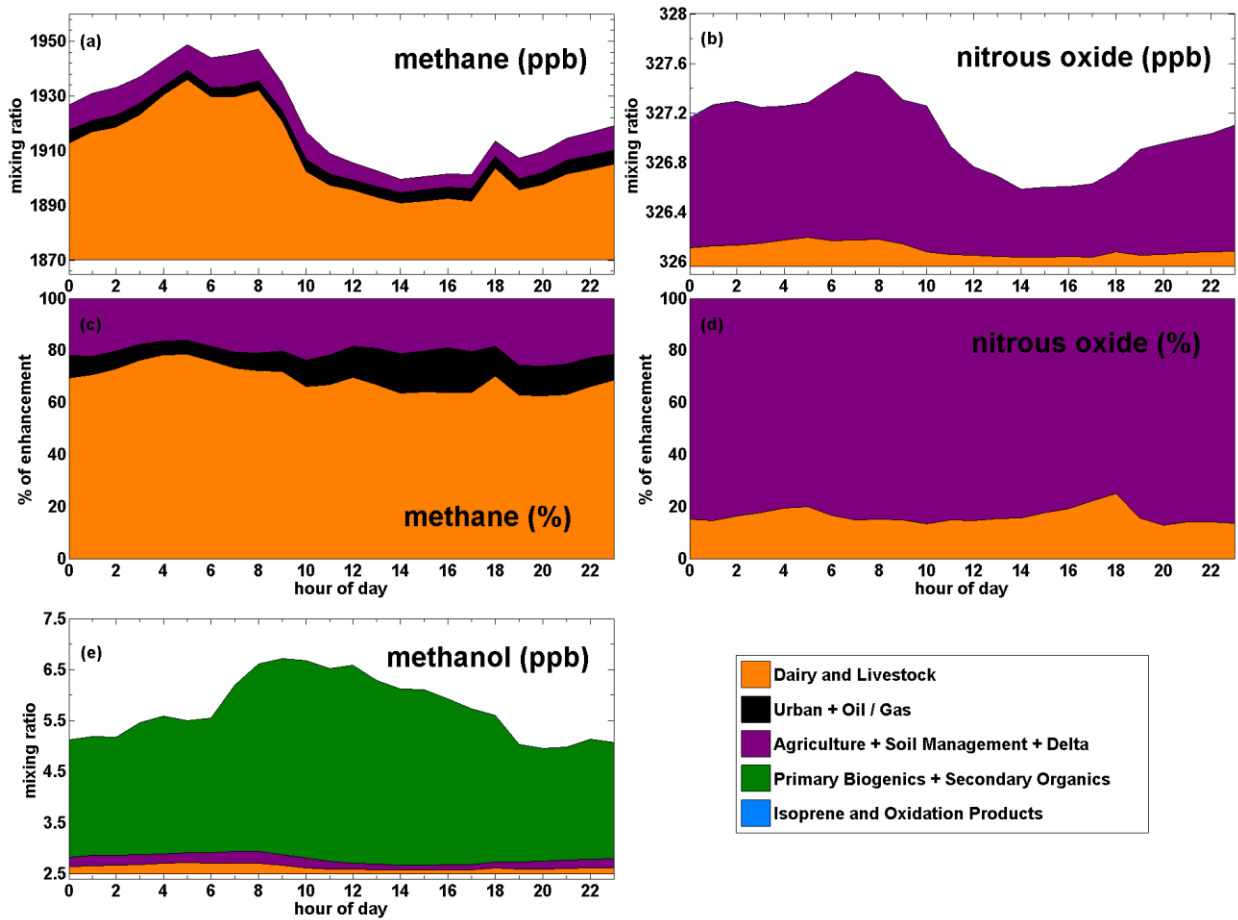
Figure 4. 19. Mean diurnal distribution plots apportioned by PMF generated source factors for summer 2013 period (Jun 1 – Aug 4). The plots include source-wise distribution of methane enhancements (a) in ppb above seasonal minimum and (c) by percentage; source-wise distribution of nitrous oxide enhancements (b) in ppb above seasonal minimum and (d) by percentage, and (e) source-wise distribution of methanol enhancements above seasonal minima. The legend represents the factor source categories of the 6-factor PMF solution for summer 2013.
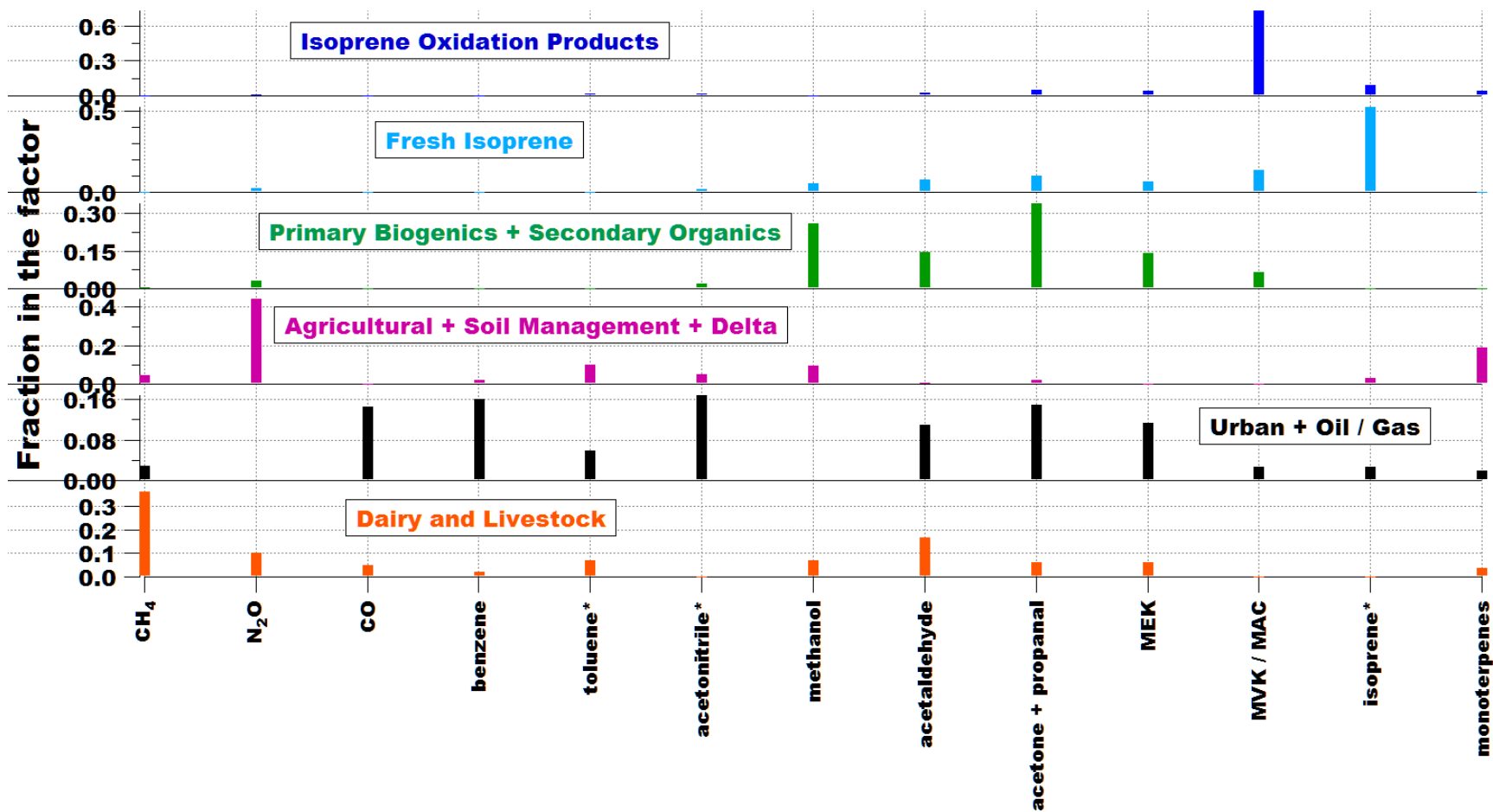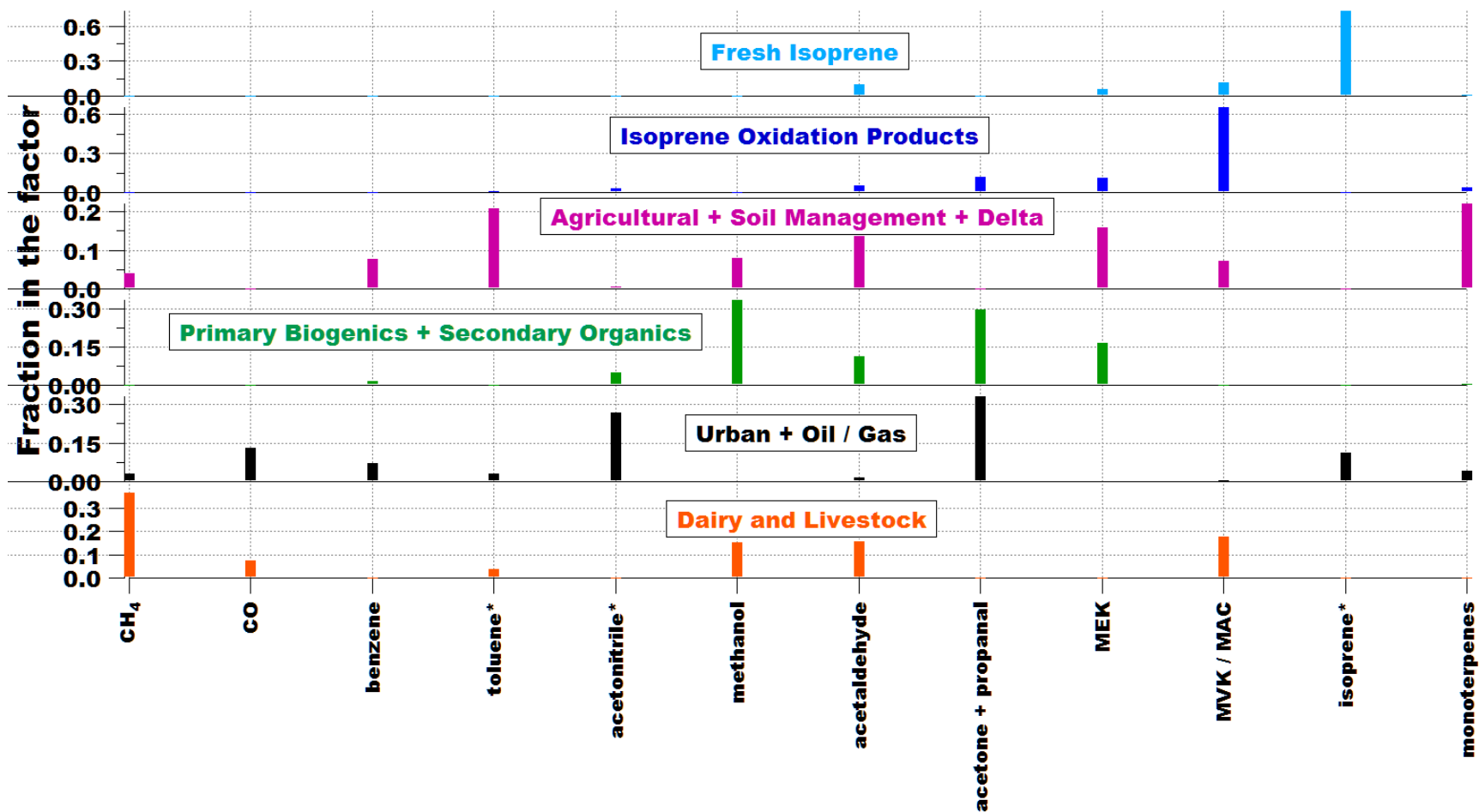
Figure 4. 20. Factor profiles of resolved PMF source factors denoting major source categories influencing the chemical composition of each profile during summer of 2012 (Jun 16 – Aug 31). The sum of the scaled mass fractions of all species adds up to unity for each profile. The VOCs with an asterisk sign may have minor contributions from other VOCs detected at the same *m/z* depending on the season (see text).
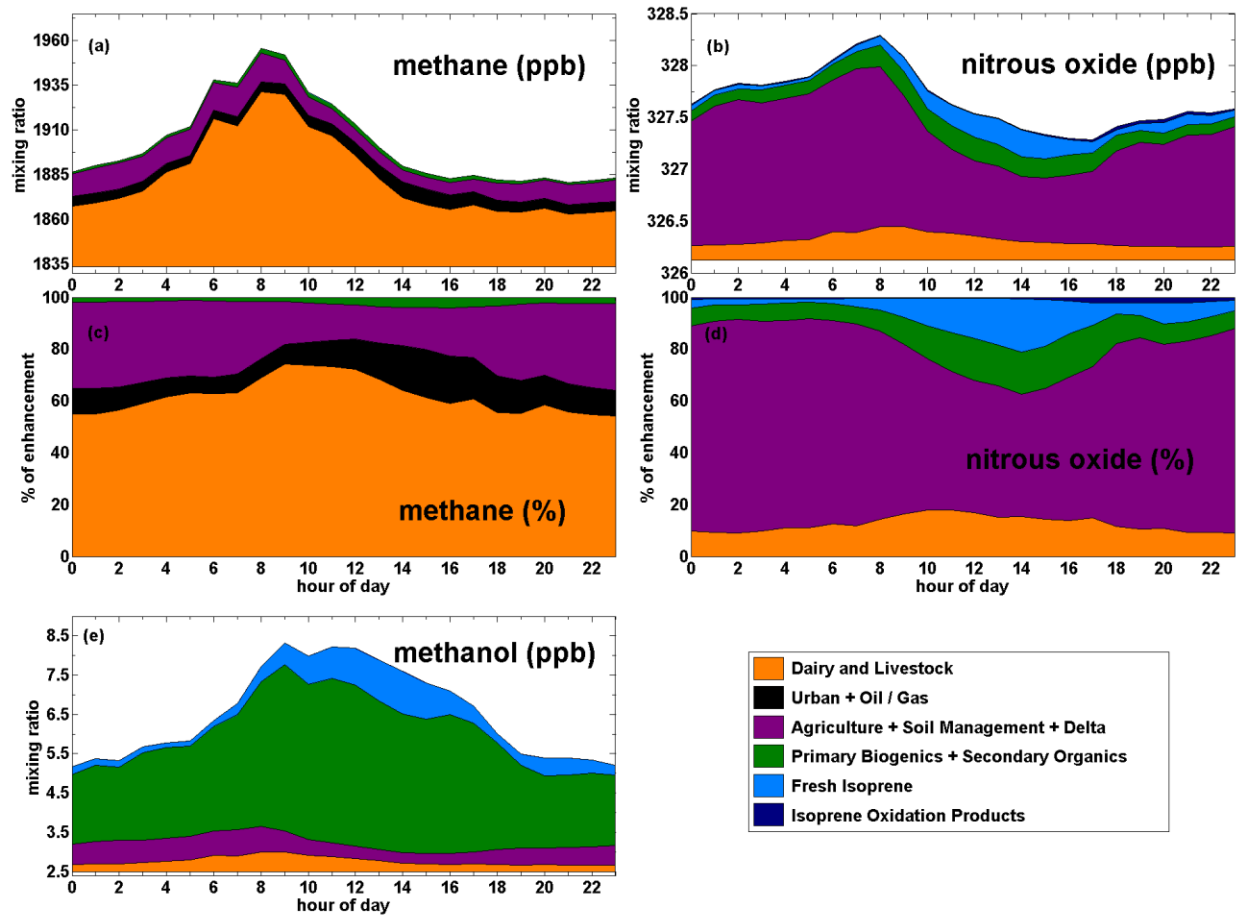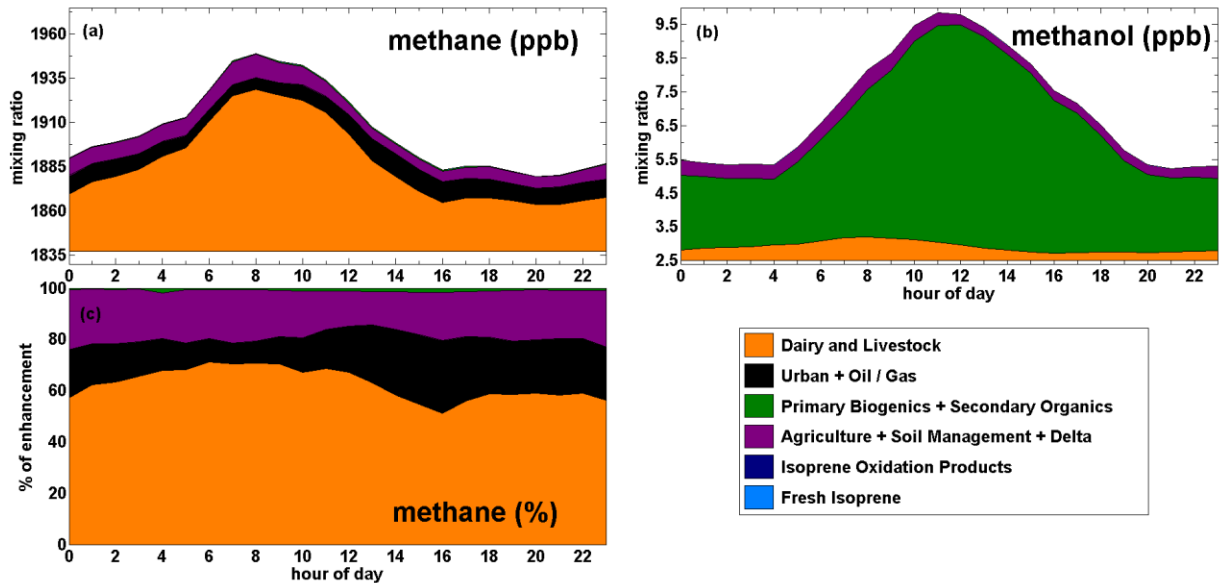
Figure 4. 21. Mean diurnal distribution plots apportioned by PMF generated source factors for summer 2012 period (Jun 16 – Aug 31). The plots include source-wise distribution of methane enhancements (a) in ppb above seasonal minimum and (c) by percentage and (c) source-wise distribution of methanol enhancements above seasonal minima. The legend represents the factor source categories of the 6-factor PMF solution for summer 2012
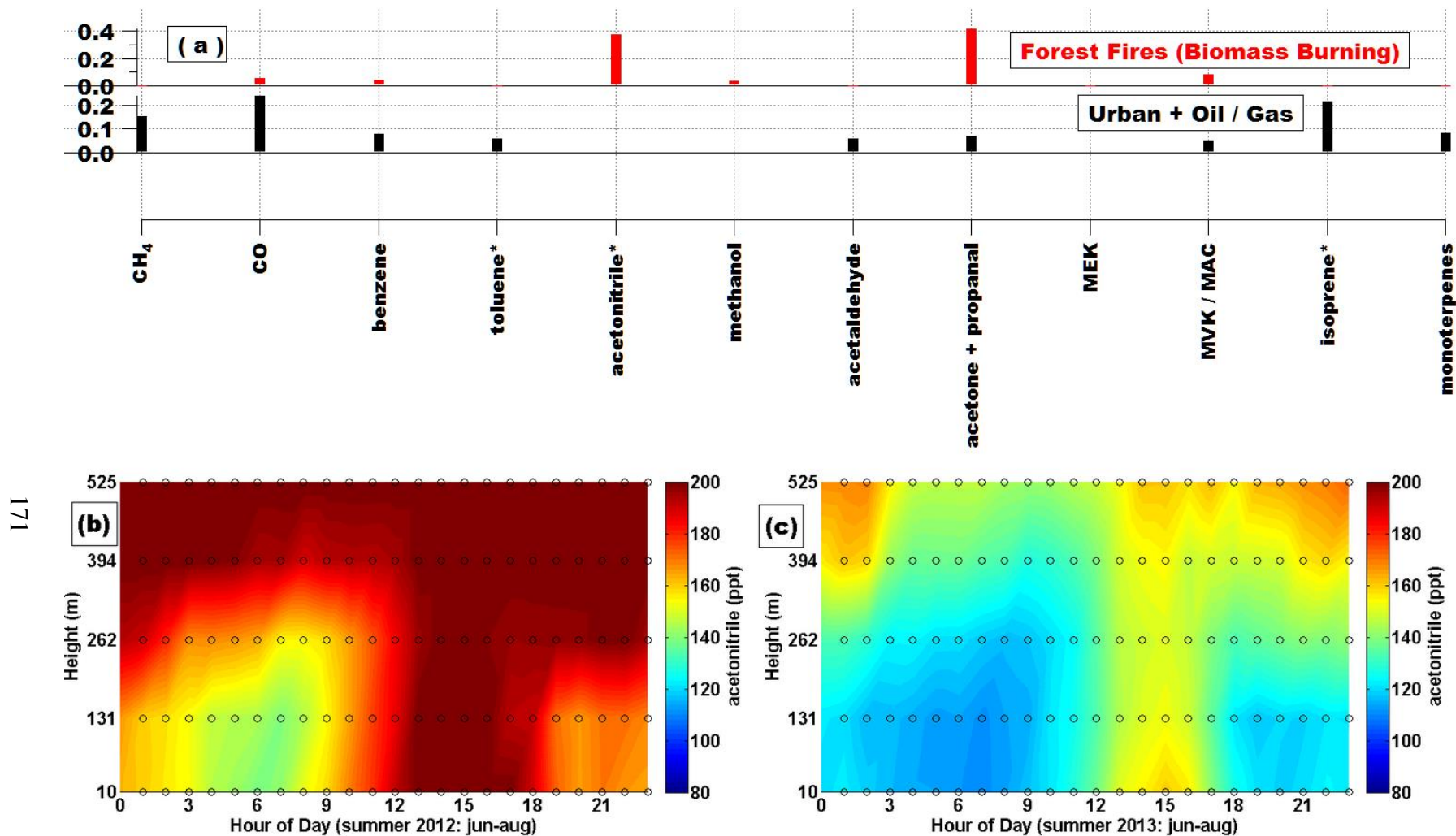
Figure 4. 22. (a) An additional source factor attributed to forest fires results from splitting of the urban + oil / gas factor in a 7-factor PMF solution during summer of 2012; vertical mean diurnal profile of biomass burning tracer acetonitrile during (b) summer of 2012 and (c) summer of 2013 showing accumulation of large emissions in the upper part of the mixed layer from significantly higher forest fire activity in the Sierra Nevada mountains during this period (Jun – Aug) in 2012 versus 2013. The Rush Fire in northeastern California (second largest wildfire in California recorded history) took place in August 2012.
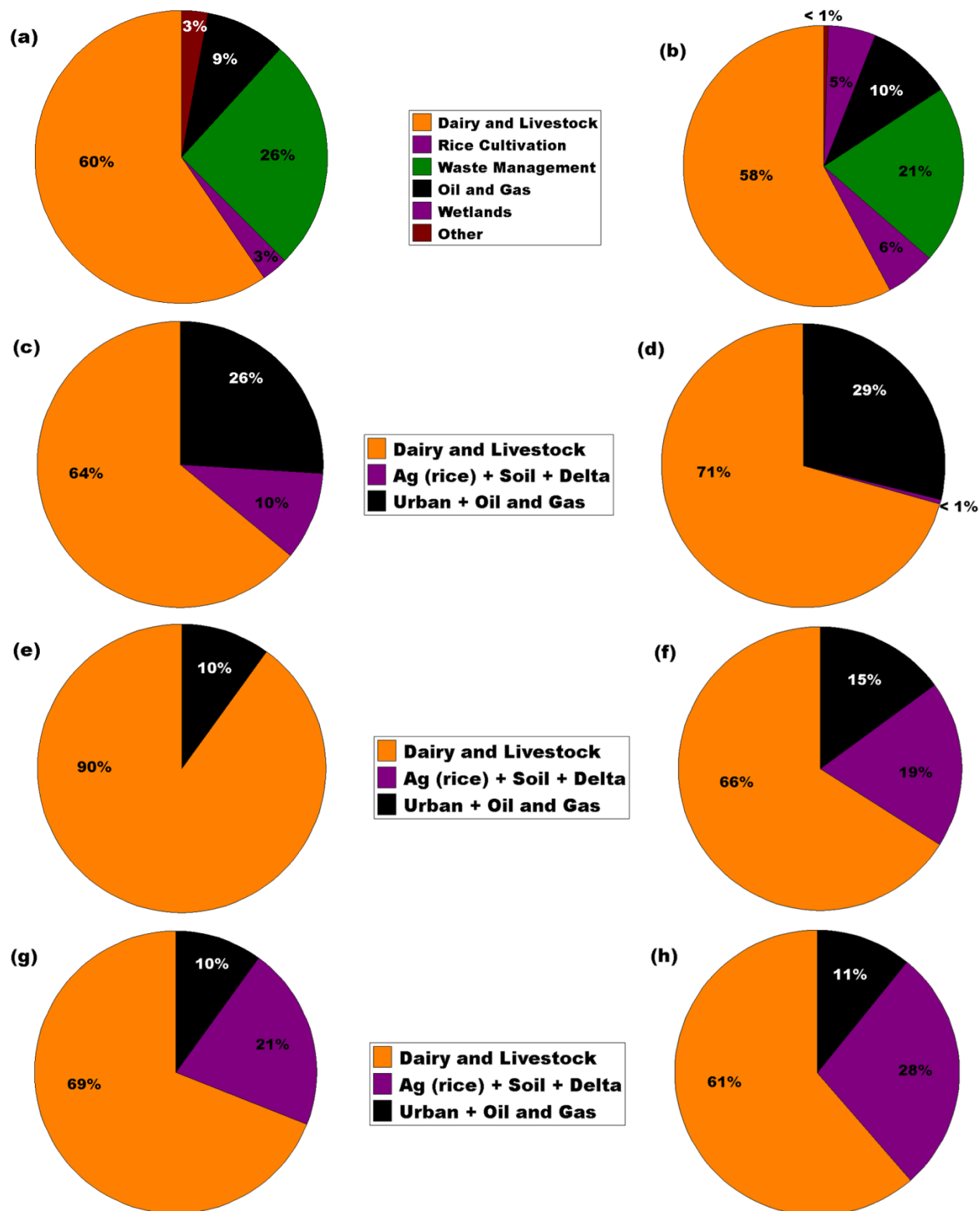
Figure 4. 23. **Pie** charts comparing the distribution of emissions (percentage of total) from CH_4 sources. The pie charts represent (a) 2008 ARB CH_4 inventory, (b) summing of 2008 CALGEM CH_4 emissions from region 6, 7 and 8 (Jeong et al., 2013), PMF-derived source-wise CH_4 emissions distribution at Walnut Grove tower during (c) early fall 2012, (d) late fall 2012, (e) winter, (f) winter-spring 2013, (g) spring 2013, and (h) summer 2013.

172

Figure 4. 24. Pie charts comparing the distribution of emissions (percentage of total) from N_2O sources. The pie charts represent (a) 2012 ARB N_2O inventory, (b) 2008 EDGAR v4.2 N_2O distribution, PMF-derived source-wise N_2O emissions distribution at Walnut Grove tower during (c) late fall 2012, (d) winter, (e) spring 2013, and (f) summer 2013.
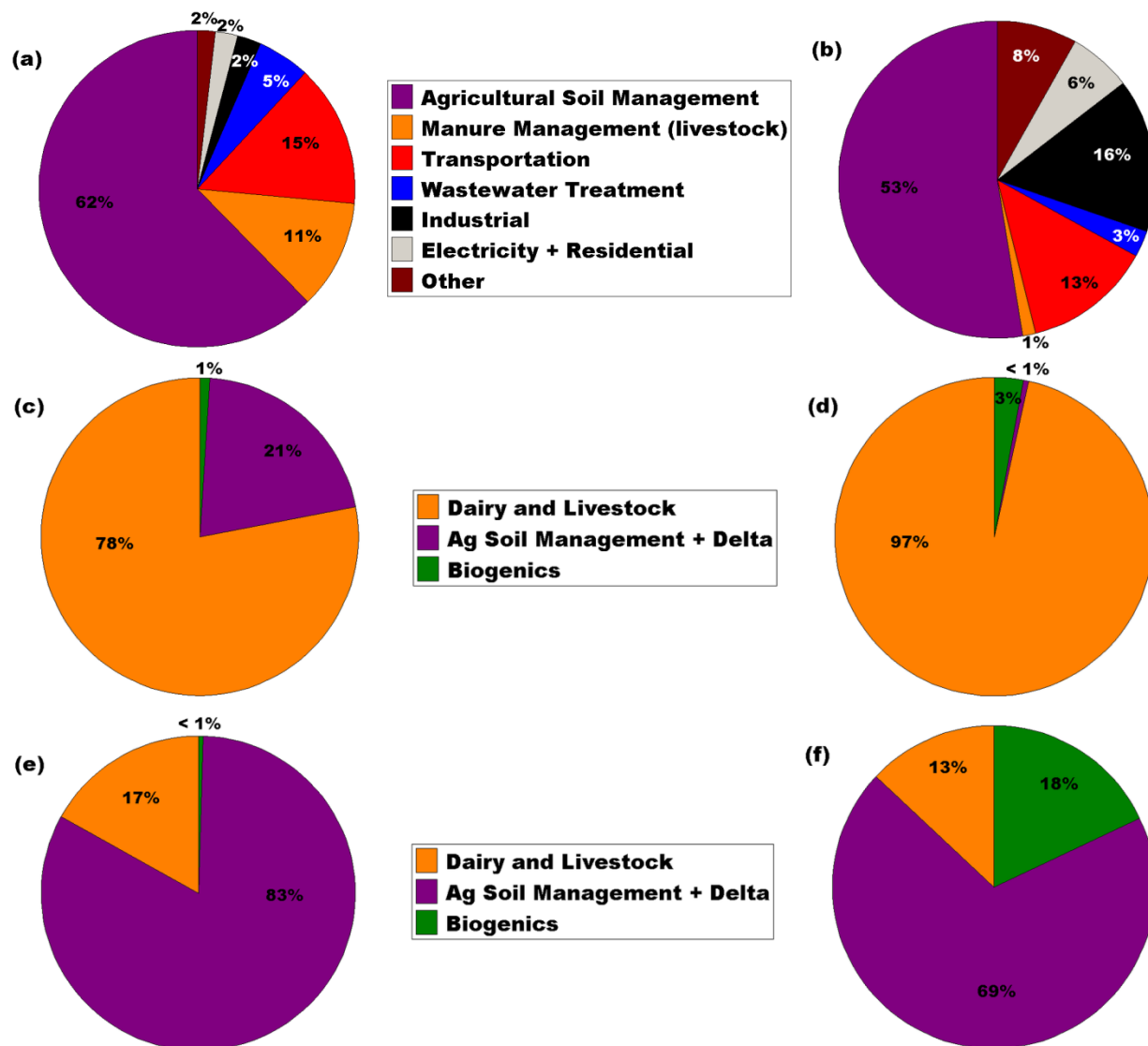
173

Chapter 5: Summary and Recommendations for Future Work

5.1   Summary of this work

This dissertation presents information to improve the regulatory and research community understands of the distribution and strength of CH_4 and N_2O sources, which are two major non-CO_2 greenhouse gases, in and around the Central Valley of California. We use the top-down source apportionment technique of positive matrix factorization (PMF) and the direct flux measurement approach of eddy covariance in the preceding chapters as our analysis tools. We performed measurements at fixed tower sites in two polluted agro-industrial areas; the urban area of Bakersfield in the San Joaquin Valley (CalNex 2010), and a predominantly rural setting at Walnut Grove tall tower near the Sacramento-San Joaquin River Delta (WGC 2012 - 13), over vastly different temporal scales (~ 1 month and 1 year, respectively). We also performed airborne measurements across the Central Valley (CABERNET 2011) covering a larger spatial scale (~ 10,000 km of flight path).

In Chapter 2, mixing ratio measurements were conducted for a month and a half in the urban core of Bakersfield in the summer of 2010 during the CalNex campaign. We use a novel approach of applying PMF on a unified data set containing enhancements of CH_4, N_2O, CO and ~ 50 VOCs representing a broad suite of source markers in order to apportion the major sources of CH_4 and N_2O influencing the observed enhancements. The dairy and livestock source is found to account for the bulk of the diurnal enhancements of both CH_4 (70 – 90 %) as well as N_2O (50 – 60 %) emphasizing the importance of validating emissions reported in the non-CO_2 GHG emissions inventory for these sectors through source-specific measurements. No significant CH_4 is apportioned to the fugitive / evaporative source whose noteworthy origin is the oil / gas operations in and surrounding the urban core. This is potentially due to active CH_4 removal from vented gases and also likely due to the overwhelming prevalence of CH_4 from dairy sources. Most of the remaining N_2O is apportioned to the agricultural and soil management source (~ 20 – 25 %) representing emissions of N_2O from use of fertilizers on intensively cultivated crop lands in the southern San Joaquin Valley. Contributions of N_2O enhancements from the vehicle source are found to be insignificant. This result is in direct contrast to this sector's contribution included in the official California state inventory (~ 18 %), demonstrating a major error in the bottom-up statewide accounting of N_2O emissions.

In Chapter 3, we performed forty hours of airborne mixing ratio measurements of CH_4 along with several VOCs to investigate 'hotspots' of CH_4 emissions. The airborne eddy covariance technique was applied to the measurements to derive, for the first time, spatially resolved airborne CH_4 fluxes over different source regions. The highest enhancements of CH_4 are observed over the dairy and feedlot intensive regions in the San Joaquin Valley with correspondingly high CH_4 fluxes. These fluxes, combined with an areal cowhead density factor derived for this source region, produces a range of CH_4 emission rates over multiple flight runs that are similar but larger than methane emission rates reported in the inventory. Huge

enhancements of CH_4, correlated with those of combustion / fugitive tracers like benzene and toluene, along with significant fluxes are also observed over the largest oil fields in the state in the western part of Kern County during one flight leg. Significant vented / fugitive losses of CH_4 are observed from a large natural gas cogeneration facility which is an insignificant source in the current point-source emissions inventory. Anti-correlation of CH_4 and CO_2 time series along with fluxes of CH_4 from a rice paddy field are observed in the Sacramento Valley. Besides this, enhancements of CH_4 are also observed from several other sources including wetlands, landfills, biomass burning episodes, natural gas fields, and that advected downwind of urban centers, all of which provide a spatial understanding of sources of CH_4 and their relative strengths in and around the Central Valley. We demonstrated that airborne eddy covariance can be an effective technique for direct estimation of landscape level CH_4 fluxes from area sources and can be an important tool in the future verification and validation of the bottom-up inventory.

In Chapter 4, we attempt to understand the spatial and temporal distribution of CH_4 and N_2O sources by conducting year-round measurements from a tall television transmission tower in Walnut Grove at the eastern edge of the Sacramento − San Joaquin River Delta in the Central Valley of California over 2012-13. The mixing ratio measurements are combined with coincident measurements of 10 VOCs and CO serving as potential source markers, and the PMF source-apportionment technique is applied to smaller datasets over narrower time periods representing different seasons. As a result, the CH_4 enhancements are apportioned into three sources: a dairy and livestock source that represents the bulk of the observed enhancements (55 − 90 %); a Delta plus temperature dependent agricultural and soil management source originating from anaerobic releases of CH_4 from wetlands and cycling of flooded / drained agricultural systems (~ 0 − 40 %) whose contributions are virtually non-existent in winters and significant in summers; and finally an urban and oil / gas source accounting for emissions primarily from non-biological industrial activities from upwind gas fields and urban regions (10 − 35 %). N_2O is primarily apportioned to two sources: the first arising from manure management in the dairy and livestock sector and the other originating from fertilizer-use triggered soil emissions of N_2O from agricultural sources in the Delta. The relative proportion of emissions from these two sources is mostly controlled by the timing and extent of the growing season when fertilizers are used on farms. The agriculture source accounts for 80 - 90 % of N_2O emissions during the spring and summer, down to ~ 20 % during the latter part of the fall season while the source is absent in the PMF apportionment during winters, when dairies and livestock are shown to account for most of the observed N_2O enhancements. No N_2O is detected in the urban and oil / gas source even though vehicle emissions of N_2O are expected to get apportioned to this source factor highlighting a significant deviation from the inventory. We conclude that certain CH_4 and N_2O sources display a temporal heterogeneity, and this should be accounted for in the inventory through long term source-specific and top-down measurements. Particularly, CH_4 emissions from wetlands need to be quantified and included in the state inventory while N_2O emissions from the transportation sector should be re-evaluated based on more recent vehicle emission studies.

5.2   Recommendations for future work

In this dissertation, I was able to augment our understanding of the regional distribution of sources of two major greenhouse gases, CH_4 and N_2O, in the Central Valley of California and its

periphery. The Central Valley is one of the most industrialized and high-producing agricultural regions of the world producing ~ 8 % of the nation's agricultural output by value, on less than 1 % of total farmland in the United States (CASR, 2011), thereby rightly earning the nickname of 'nation's vegetable and fruit basket'. The Central Valley also sits on top of rich oil and gas formations that support a vast oil and gas extraction and processing industry. The San Joaquin Valley alone would be ranked fourth in oil production in the nation if it were a state (~ 515,000 barrels of oil per day), while just Kern County has more than 42,000 producing oil wells that account for ~ 68% of the oil produced in California, 10 % of US production, and close to 1 % of total world annual oil production (DOGGR, 2012). What this means is that there are a multitude of significant emissions sources of GHGs and VOCs arising from this extensive agro-industrial complex that are collocated and co-emitting into the same atmospheric boundary layer. Our ability to apportion and resolve these GHG sources, and estimate emissions rates from these sources such that it is representative of the targeted source itself and is 'uncontaminated' by the influence of nearby sources is critical to the success of the 'top-down' measurements and also in the verification and validation of the 'bottom-up' GHG inventory (CARB, 2013). The results from this work suggest that more comprehensive studies are required for improving the 'state of knowledge' regarding CH_4 and N_2O source emission strengths, and raise three main questions that I suggest be investigated further:

1) Given the arbitrary mix of major CH_4 and N_2O emissions sources in the Central Valley, are targeted source-specific and long-term measurements more 'appropriate' than other top-down approaches for the inventory validation process?

2) Does the regulatory community in California have an adequate quantitative understanding of the CH_4 emissions from the Oil and Gas sector? Furthermore, will increased fracking activity significantly change the emissions from this sector?

3) What is the most accurate method to quantify and validate estimates of N_2O emissions from agriculture with all its spatial and temporal complexities?

For the first question, the answer lies in conducting studies and experiments whose results can be 'reasonably and logically' scaled up with limited resources. The technology available for trace gas measurements has improved dramatically in the last decade or so with current availability of GHG instrumentation that are highly sensitive to small changes in backgrounds and provide precise, drift-free automated measurements for long periods and can sample changes in atmospheric constituents at very fast rates (10 Hz or higher). Quite importantly, the power requirements of these instruments have become much more manageable. These instruments provide researchers the opportunity to utilize the short-range inverse dispersion technique, where a backward Lagrangian Stochastic (bLS) atmospheric dispersion model coupled with a Monin-Obukhov similarity theory (MOST) description of near-surface winds can be used to infer source emission rates from upwind and downwind gas concentration measurements (Flesch et al., 2004). Experiments based on this scientific technique are relatively low-budget and not resource-intensive, and have been shown to provide reliable long-term estimates of CH_4, NH_3 and N_2O emissions from a variety of area sources like dairy farms and agricultural fields (McGinn et al., 2006; Turner et al., 2010; Leytem et al., 2011; Ro et al., 2013; VanderZaag et al., 2014). Ground based eddy covariance, using fast-response analyzers, has been demonstrated to be a robust

method to directly measure emissions of CH_4 and N_2O over relatively homogenous area sources e.g. rice paddy and wetlands (Teh et al., 2011; Baldocchi et al., 2012; Hatala et al., 2012; Knox et al., 2014). Both the above mentioned techniques can be applied over complete annual cycles in order to determine unique emission rates representative of different seasons and farm management practices. These methods are more suitable than short-term estimates directly derived from airborne measurements or from inverse dispersion of airborne observations and sparse satellite observations. These direct estimation methods conducted at facility-level spatial resolutions complement the knowledge derived from the regional high spatial resolution (0.1° × 0.1°) long-term multi-tower based WRF-STILT back trajectory analysis (Jeong et al., 2012a, 2012b, 2013) and together, these two methods can be used to constrain the non-CO_2 GHG inventory effectively.

To explore the second question, more comprehensive source specific measurements within or above the oil and gas (O&G) fields of California are recommended. There is a tremendous scarcity of reported data measurements on CH_4 from the O&G sector in California and this is partly due to the long held assumption that fugitive and vented losses of CH_4 from this industry are minor in comparison to other major CH_4 sources in the state. However, recent work in the Southern California region has recognized natural gas distribution losses from the O&G sector to be responsible for much of the CH_4 underestimation in the bottom-up inventory that is observed from top-down measurements (Peischl et al., 2013) in that region. Recent evaluation of the current CARB CH_4 'bottom-up' inventory with a spatially resolved inventory developed using new and measurement-based data, suggests underestimation of CH_4 emissions from the O&G production and extraction sector by 3 to 7 times (Jeong et al., 2014). A major bulk of this industry is located in the Central Valley. Indeed, the airborne CH_4 measurements reported in Chapter 3 point to significant emissions over oil fields and fugitive leaks from natural gas cogeneration plants and production infrastructure. In light of the vast spatial expanse of the O&G source and the random distribution of hundreds, if not thousands of minor point sources, ground based measurement techniques may not be able to provide representative emission estimates for O&G production sector. Airborne measurements combined with a mass balance approach, using data from multiple flight transects upwind and downwind of O&G operations and vertical profiles, can be applied to derive direct CH_4 emissions estimates (Ryerson et al., 2001; Mays et al., 2009; Turnbull et al., 2011; Karion et al., 2013; Peischl et al., 2013). Of course, if high speed CH_4 flux analyzers are available, the airborne eddy covariance approach presented in Chapter 3 and described in Misztal et al. (2014) can be expected to produce representative direct estimates of CH_4 with minimal flux losses. Such airborne measurements, when combined with simultaneous measurements of source marker light alkanes and CO, provide more power to the science of GHG source attribution. I believe that targeted and comprehensive airborne measurements can provide a significantly improved understanding of the 'true' contribution of O&G production sector to the CH_4 inventory.

Finally, from our experience and observations in this dissertation, ground-based eddy covariance from small towers located on farm lands seems to be the most direct and reliable way to estimate N_2O emissions from the agricultural and soil management sector as they provide an integrated picture of whole-ecosystem gas exchange. Up till now, we have seen some accounts of N_2O fluxes measured using a static flux chamber approach but not eddy covariance (e.g. Teh et al., 2011). Modern analyzers capable of providing high frequency continuous measurements of

N_2O have only recently become available, and can be utilized to provide eddy covariance measurements of N_2O from agricultural ecosystems which generally have a homogenous landscape, which is an important requirement for eddy covariance. The current ARB N_2O inventory is based on emission factors from direct and indirect emissions and activity (fertilizer sale) data, with no accounting of different farming practices, narrower fertilizer types, crop and soil types etc. Year-long flux measurements on crop lands with different major crop types (e.g rice, corn, walnuts, etc.) will allow quantification of fluxes from high-impact events and conditions like fertilizer spraying, application of pesticides, tilling, precipitation, flooded agricultural residues, drainage of fields etc. These direct N_2O estimates can provide a wealth of valuable information to verify, validate and improve the inventory and also to assess the agreement with Denitrification-Decomposition (DNDC) and other biogeochemical models.

5.3   References

CARB (2013), California Greenhouse Gas Inventory for 2000-2012 - by IPCC Category. http://www.arb.ca.gov/cc/inventory/data/data.htm. accessesd on September 23, 2014.

CASR (2011), California Agricultural Statistics Crop Report, 2011. created by California Department of Food and Agriculture, Sacramento, CA and United States Department of Agriculture.

DOGGR (2012), 2011 Preliminary report on California oil and gas production statistics, Department of Conservation's Division of Oil, Gas and Geothermal Resources; Publication No. PR03.

Baldocchi, D., Detto, M., Sonnentag, O., Verfaillie, J., Teh, Y. A., Silver, W. and Kelly, N. M.: The challenges of measuring methane fluxes and concentrations over a peatland pasture, Agric. For. Meteorol., 153, 177–187, doi:10.1016/j.agrformet.2011.04.013, 2012.

Flesch, T. K., Wilson, J. D., Harper, L. a., Crenna, B. P. and Sharpe, R. R.: Deducing Ground-to-Air Emissions from Observed Trace Gas Concentrations: A Field Trial, J. Appl. Meteorol., 43(3), 487–502, doi:10.1175/1520-0450(2004)043<0487:DGEFOT>2.0.CO;2, 2004.

Hatala, J. a., Detto, M., Sonnentag, O., Deverel, S. J., Verfaillie, J. and Baldocchi, D. D.: Greenhouse gas (CO2, CH4, H2O) fluxes from drained and flooded agricultural peatlands in the Sacramento-San Joaquin Delta, Agric. Ecosyst. Environ., 150, 1–18, doi:10.1016/j.agee.2012.01.009, 2012.

Jeong, S., Hsu, Y.-K., Andrews, A. E., Bianco, L., Vaca, P., Wilczak, J. M. and Fischer, M. L.: A multitower measurement network estimate of California's methane emissions, J. Geophys. Res. Atmos., 118(19), 11,339–11,351, doi:10.1002/jgrd.50854, 2013.

Jeong, S., Millstein, D. and Fischer, M. L.: Spatially Explicit Methane Emissions from Petroleum Production and the Natural Gas System in California, 2014.

Jeong, S., Zhao, C., Andrews, A. E., Bianco, L., Wilczak, J. M. and Fischer, M. L.: Seasonal variation of CH 4 emissions from central California, J. Geophys. Res., 117(D11), D11306, doi:10.1029/2011JD016896, 2012a.

Jeong, S., Zhao, C., Andrews, A. E., Dlugokencky, E. J., Sweeney, C., Bianco, L., Wilczak, J. M. and Fischer, M. L.: Seasonal variations in N 2 O emissions from central California, Geophys. Res. Lett., 39(16), n/a–n/a, doi:10.1029/2012GL052307, 2012b.

Karion, A., Sweeney, C., Pétron, G., Frost, G., Michael Hardesty, R., Kofler, J., Miller, B. R., Newberger, T., Wolter, S., Banta, R., Brewer, A., Dlugokencky, E., Lang, P., Montzka, S. a., Schnell, R., Tans, P., Trainer, M., Zamora, R. and Conley, S.: Methane emissions estimate from airborne measurements over a western United States natural gas field, Geophys. Res. Lett., 40(16), 4393–4397, doi:10.1002/grl.50811, 2013.

Knox, S. H., Sturtevant, C., Matthes, J. H., Koteen, L., Verfaillie, J. and Baldocchi, D.: Agricultural peatland restoration: effects of land-use change on greenhouse gas (CO2 and CH4) fluxes in the Sacramento-San Joaquin Delta., Glob. Chang. Biol., 1–16, doi:10.1111/gcb.12745, 2014.

Leytem, A. B., Dungan, R. S., Bjorneberg, D. L. and Koehn, A. C.: Greenhouse Gas and Ammonia Emissions from an Open-Freestall Dairy in Southern Idaho, J. Environ. Qual., 42(1), 10–20 [online] Available from: http://www.ncbi.nlm.nih.gov/pubmed/23673734, 2011.

Mays, K. L., Shepson, P. B., Stirm, B. H., Karion, A., Sweeney, C. and Gurney, K. R.: Aircraft-based measurements of the carbon footprint of Indianapolis., Environ. Sci. Technol., 43(20), 7816–23, doi:10.1021/es901326b, 2009.

McGinn, S. M., Flesch, T. K., Harper, L. A. and Beauchemin, K. A.: An Approach for Measuring Methane Emissions from Whole Farms, , 14–20 [online] Available from: https://www.agronomy.org/publications/jeq/abstracts/35/1/14, 2006.

Peischl, J., Ryerson, T. B., Brioude, J., Aikin, K. C., Andrews, a. E., Atlas, E., Blake, D., Daube, B. C., de Gouw, J. a., Dlugokencky, E., Frost, G. J., Gentner, D. R., Gilman, J. B., Goldstein, a. H., Harley, R. a., Holloway, J. S., Kofler, J., Kuster, W. C., Lang, P. M., Novelli, P. C., Santoni, G. W., Trainer, M., Wofsy, S. C. and Parrish, D. D.: Quantifying sources of methane using light alkanes in the Los Angeles basin, California, J. Geophys. Res. Atmos., 118(10), 4974–4990, doi:10.1002/jgrd.50413, 2013.

Ro, K. S., Johnson, M. H., Stone, K. C., Hunt, P. G., Flesch, T. and Todd, R. W.: Measuring gas emissions from animal waste lagoons with an inverse-dispersion technique, Atmos. Environ., 66, 101–106, 2013.

Ryerson, T. B., Trainer, M., Holloway, J. S., Parrish, D. D., Huey, L. G., Sueper, D. T., Frost, G. J., Donnelly, S. G., Schauffler, S., Atlas, E. L., Kuster, W. C., Goldan, P. D., Hu, G., Meagher, J. F. and Fehsenfeld, F. C.: Observations of Ozone Formation in Power Plant Plumes and Implications for Ozone Control Strategies, , 292(x), 719–724, 2001.

Teh, Y. A., Silver, W. L., Sonnentag, O., Detto, M., Kelly, M. and Baldocchi, D. D.: Large Greenhouse Gas Emissions from a Temperate Peatland Pasture, Ecosystems, 14(2), 311–325, doi:10.1007/s10021-011-9411-4, 2011.

Turnbull, J. C., Karion, a., Fischer, M. L., Faloona, I., Guilderson, T., Lehman, S. J., Miller, B. R., Miller, J. B., Montzka, S., Sherwood, T., Saripalli, S., Sweeney, C. and Tans, P. P.: Assessment of fossil fuel carbon dioxide and other anthropogenic trace gas emissions from airborne measurements over Sacramento, California in spring 2009, Atmos. Chem. Phys., 11(2), 705–721, doi:10.5194/acp-11-705-2011, 2011.

Turner, D. A., Edis, R. B., Chen, D., Freney, J. R., Denmead, O. T. and Christie, R.: Determination and mitigation of ammonia loss from urea applied to winter wheat with N-(n-butyl) thiophosphorictriamide, Agric. Ecosyst. Environ., 137(3-4), 261–266, 2010.

VanderZaag, A. C., Flesch, T. K., Desjardins, R. L., Baldé, H. and Wright, T.: Measuring methane emissions from two dairy farms: Seasonal and manure-management effects, Agric. For. Meteorol., 194, 259–267, 2014.